US Army Corps of Engineers

HYDRAULICS LABORATORY

TECHNICAL REPORT HL-89-14

VERIFICATION OF THE HYDRODYNAMIC AND SEDIMENT TRANSPORT HYBRID MODELING SYSTEM FOR CUMBERLAND SOUND AND KINGS BAY NAVIGATION CHANNEL, GEORGIA

by

Mitchell A. Granat, Noble J. Brogdon, John T. Cartwright
William H. McAnally, Jr.

Hydraulics Laboratory

DEPARTMENT OF THE ARMY
Waterways Experiment Station, Corps of Engineers
PO Box 631, Vicksburg, Mississippi 39181-0631

July 1989
Final Report

Prepared for Officer in Charge of Construction
TRIDENT
DEPARTMENT OF THE NAVY
Naval Facilities Engineering Command
St. Marys, Georgia 31558-0768

and

Naval Submarine Base
Kings Bay, Georgia 31547

Destroy this report when no longer needed. Do not return it to the originator.

The findings in this report are not to be construed as an official Department of the Army position unless so designated by other authorized documents.

The contents of this report are not to be used for advertising, publication, or promotional purposes. Citation of trade names does not constitute an official endorsement or approval of the use of such commercial products.

Unclassified

SECURITY CLASSIFICATION OF THIS PAGE

REPORT DOCUMENTATION PAGE

Form Approved OMB No. 0704-0188

1a REPORT SECURITY CLASSIFICATION: Unclassified	1b RESTRICTIVE MARKINGS
2a SECURITY CLASSIFICATION AUTHORITY	3 DISTRIBUTION/AVAILABILITY OF REPORT: Approved for public release; distribution unlimited.
2b DECLASSIFICATION/DOWNGRADING SCHEDULE	
4 PERFORMING ORGANIZATION REPORT NUMBER(S): Technical Report HL-89-14	5 MONITORING ORGANIZATION REPORT NUMBER(S)
6a NAME OF PERFORMING ORGANIZATION: USAEWES Hydraulics Laboratory; 6b OFFICE SYMBOL (If applicable): CEWES-HE-E	7a NAME OF MONITORING ORGANIZATION
6c ADDRESS (City, State, and ZIP Code): PO Box 631 Vicksburg, MS 39181-0631	7b ADDRESS (City, State, and ZIP Code)
8a NAME OF FUNDING/SPONSORING ORGANIZATION: See reverse; 8b OFFICE SYMBOL (If applicable)	9 PROCUREMENT INSTRUMENT IDENTIFICATION NUMBER
8c ADDRESS (City, State, and ZIP Code): See reverse	10 SOURCE OF FUNDING NUMBERS: PROGRAM ELEMENT NO; PROJECT NO.; TASK NO.; WORK UNIT ACCESSION NO.

11 TITLE (Include Security Classification)
Verification of the Hydrodynamic and Sediment Transport Hybrid Modeling System for Cumberland Sound and Kings Bay Navigation Channel, Georgia

12 PERSONAL AUTHOR(S)
Granat, Mitchell A.; Brogdon, Noble J.; Cartwright, John T.; and McAnally, William H., Jr.

13a TYPE OF REPORT	13b TIME COVERED	14 DATE OF REPORT (Year, Month, Day)	15 PAGE COUNT
Final report	FROM _____ TO _____	July 1989	270

16 SUPPLEMENTARY NOTATION
Available from National Technical Information Service, 5285 Port Royal Road, Springfield, VA 22161.

17 COSATI CODES			18 SUBJECT TERMS (Continue on reverse if necessary and identify by block number)	
FIELD	GROUP	SUB-GROUP	Cumberland Sound	Marsh-estuarine circulation
			Hydrodynamics	Model verification
			Kings Bay (Georgia)	Sedimentation

19 ABSTRACT (Continue on reverse if necessary and identify by block number)

A hybrid modeling system (coupled physical and numerical models) was developed to investigate the hydrodynamic and sedimentation processes of Cumberland Sound and the interior Kings Bay navigation channel. The hybrid modeling procedures and the physical and numerical model verifications are described in detail.

The Kings Bay physical model was an accurately scaled fixed-bed concrete model of the Cumberland Sound/Kings Bay estuarine system. The physical model provided the means of assessing three-dimensional hydrodynamic characteristics of Cumberland Sound and Kings Bay. It also provided the boundary forcing conditions for the numerical model and an expanded data base for comparison. Verification of the physical model to reproduce pre-Trident channel field measurements collected during November 1982 and transitional channel conditions measured during January 1985 was demonstrated.

(Continued)

20 DISTRIBUTION/AVAILABILITY OF ABSTRACT	21 ABSTRACT SECURITY CLASSIFICATION
☒ UNCLASSIFIED/UNLIMITED ☐ SAME AS RPT ☐ DTIC USERS	Unclassified
22a NAME OF RESPONSIBLE INDIVIDUAL	22b TELEPHONE (Include Area Code) / 22c OFFICE SYMBOL

DD Form 1473, JUN 86 *Previous editions are obsolete*

SECURITY CLASSIFICATION OF THIS PAGE

Unclassified

BLOCK 8a. NAME OF FUNDING/SPONSORING ORGANIZATION and
BLOCK 8c. ADDRESS (Continued).

Officer in Charge of Construction
TRIDENT
DEPARTMENT OF THE NAVY
Naval Facilities Engineering Command
St. Marys, GA 31558-0768

and

Naval Submarine Base
Kings Bay, GA 31547

19. ABSTRACT (Continued).

The other component of the modeling system was the US Army Corps of Engineers Generalized Computer Program System: Open-Channel Flow and Sedimentation, TABS-2. TABS-2 is a complete depth-averaged finite element numerical modeling system. The numerical hydrodynamic model RMA-2V used physical model-derived St. Marys Inlet water levels and tributary velocity measurements for the boundary forcing conditions for an average tidal cycle. The numerical model was verified to physical model tidal elevations and depth-averaged velocity data for interior locations.

A wetting and drying algorithm was used to numerically model the extensive marsh and intertidal areas of the estuarine system. Marsh-estuarine circulation interaction and prescribed marsh elevation were found to be important in achieving proper hydrodynamic reproduction. Three separate numerical model schematizations or meshes of the Cumberland Sound system were verified as the submarine channel evolved in detail. RMA-2V demonstrated reasonable reproduction of pre-Trident and transitional channel hydrodynamic conditions for the Cumberland Sound/Kings Bay system.

Hydrodynamic results from RMA-2V were used in the numerical sediment transport code STUDH in modeling the interaction of the flow transport and sedimentation on the bed. Both cohesive (clay and silt) and noncohesive (silt and sand) sedimentation were modeled. STUDH was verified through comparisons of model predictions with actual field shoaling rates. Excellent numerical model pre-Trident channel sediment verification was demonstrated. Model predictions for the upper Trident channel turning basin for the transitional channel demonstrated higher shoaling rates than the limited field data. Possible explanations for this difference included low field sediment loads associated with the prolonged east coast drought, the transitional nature of the channel, and the possible need for further model adjustments. The sediment model was developed and verified for long-term average conditions, and additional model adjustments could not be justified based on the limited transitional channel data.

Verification of the hydrodynamic and sediment transport hybrid modeling system for Cumberland Sound and Kings Bay navigation channel has been demonstrated. The developed modeling procedures can be used in carefully designed testing programs to assess potential hydrodynamic and sedimentation impacts associated with submarine plan channel and remedial measure alternatives.

EXECUTIVE SUMMARY

A hybrid modeling system (coupled physical and numerical models) was developed to investigate the hydrodynamic and sedimentation processes of Cumberland Sound and the associated interior Kings Bay navigation channel, to predict long-term average maintenance dredging requirements for planned channel improvements, and to evaluate potential remedial measures. This report describes the hybrid modeling system (Model A) and addresses the physical and numerical model verifications. Subsequent Model A reports address pre- and post-Trident channel predictions and model evaluations of potential remedial measures for areas north of the upper turning basin. A companion numerical model investigation, Model B,* was undertaken to address hydrodynamic and sedimentation processes of the St. Marys Inlet and the offshore ocean entrance channel.

The Kings Bay physical model was a distorted-scale fixed-bed concrete model that reproduced approximately 206 square miles of southeast Georgia and northeast Florida, and about 220 square miles of the adjacent Atlantic Ocean. The model was constructed to linear scale ratios, model to prototype, of 1:100 vertically and 1:1,000 horizontally; the vertical scale in the physical model was stretched 10 times relative to the horizontal scale. This is a typical scaling factor used for estuarine physical models. The Kings Bay physical model was approximately 126 ft long and 108 ft wide and covered an area of about 12,600 square ft. Salinity was maintained at a 1:1 ratio. The vertical and horizontal scales dictated the other scaling factors (time, velocity, discharge) based on Froudian relations. Time, for example, was compressed in the physical model so that one complete ebb and flood semidiurnal tidal cycle (12.42 hr) occurred in 7.452 min on the model.

The physical model was an accurately scaled reproduction of the Cumberland Sound/Kings Bay estuarine system. Verification of the physical model to reproduce observed tide, velocity, and salinity field measurements was undertaken to ensure the reliability of model results. Stainless steel artificial roughness or resistance strips projecting from the molded concrete bed of

---

* S. Rao Vemulakonda, Norman W. Scheffner, Jeffrey A. Earickson, and Lucia W. Chou. 1988 (Apr). "Kings Bay Coastal Processes Numerical Model," Technical Report CERC-88-3, US Army Engineer Waterways Experiment Station, Vicksburg, MS.

the model served as the primary means of adjusting the physical model to reproduce hydrodynamic field conditions.

Two distinct physical model verification efforts were undertaken. The first effort centered around the pre-Trident channel conditions using field data sets collected on 10 and 12 November 1982 and focused on the areas in and south of Kings Bay. This field data collection effort, although conceived as a supplement to the US Geological Survey data collected during November 1981 and July 1982, became the primary data set for physical model verification. The physical model was found to reasonably reproduce the pre-Trident channel field measurements.

The second physical model verification effort centered around the field data set collected on 26 January 1985 and focused on the areas in and north of Kings Bay. This data set was collected during a transitional channel condition with the upper end of Kings Bay already dredged to Trident channel depths. This collection effort was undertaken to verify the velocity and tide conditions north of Kings Bay since hybrid model investigations had indicated the importance of flow characteristics in this portion of the system. Additional roughness strip and geometry adjustments were performed in the physical model areas north of Kings Bay prior to final verification to the transitional channel condition. The physical model was found to reasonably reproduce the transitional channel field condition.

As verified, the physical model can be used to investigate the three-dimensional flow characteristics of the Cumberland Sound/Kings Bay system associated with the long-term average freshwater discharge and average tidal conditions. The physical model can be used to examine alternative plan conditions: geometry in the model can be modified physically to represent the desired new condition and the model rerun to assess the resulting three-dimensional flow characteristics. Comparison of results between two model runs with identical conditions except for the plan modification provides a means of assessing potential hydrodynamic impacts associated with the plan modification.

Another primary task of the physical model was to provide average boundary forcing conditons for the numerical model and to provide an expanded data base for comparison. Briefly, physical model tidal cycle ocean water levels collected at the St. Marys Inlet entrance were used as the numerical model ocean boundary forcing conditions. Depth-averaged physical model tidal cycle

velocity observations collected at the Amelia, Jolly, St. Marys, Crooked, and Cumberland river boundary locations of the numerical model were used as the upstream boundary forcing conditions in the numerical model. Physical model tide and velocity measurements were also collected at selected interior locations throughout the modeled area of interest for numerical model verification.

The numerical modeling system used in this study was the US Army Corps of Engineers Generalized Computer Program System: Open-Channel Flow and Sedimentation, TABS-2. TABS-2 is a collection of preprocessor and postprocessor utility codes and three main finite element two-dimensional depth-averaged computational programs. The finite element method provides a means of obtaining an approximate solution to a system of governing equations (i.e., equations of motion and conservation) by dividing the area of interest into smaller subareas called elements; time-varying partial differential equations are transformed into finite element form and then solved in a global matrix system over the modeled area of interest. The solution is smooth over each element and continuous over the computational area. A wetting and drying algorithm was used in modeling the extensive marsh and intertidal areas of the estuarine system.

The numerical hydrodynamic code RMA-2V used the boundary forcing conditions derived from the physical model to solve the depth-integrated equations of conservation of mass and momentum in two horizontal directions and provided hydrodynamic solutions for water-surface elevations and horizontal velocity components over the entire modeled area of interest. Verification of RMA-2V was accomplished through water-surface elevation and velocity comparisons with corresponding physical model data. Numerical model bottom roughness (Manning's n) and eddy viscosity coefficient assignments based on physical characteristics and marsh elevation schematization provided the necessary means for verifying the numerical model.

Marsh-estuarine circulation interaction was found to be important in achieving proper reproduction of Cumberland Sound and Kings Bay hydrodynamic characteristics. A compromise between tidal reproduction and velocity reproduction was made in achieving the desired agreement between the numerical model and the physical model measurements. A nominal marsh elevation of +4.0 ft mean low water was selected in schematizing the numerical model marsh areas that flooded and dried during the tidal cycle. Higher marsh elevations

increased tidal ranges but resulted in reduced current velocities.

The numerical model (Mesh 1) demonstrated excellent main channel ebb and flood velocity phase and magnitude agreement with the physical model measurements for the pre-Trident channel verification condition. Tributary and secondary channels adjacent to marsh areas demonstrated excellent velocity phase agreement and a slightly reduced numerical model ebb and flood velocity magnitude relative to the physical model measurements. Excellent tidal phase and midtide level agreement was also demonstrated. Numerical model high- and low-water elevations were generally within 0.1 to 0.3 ft of the physical model measurements. A finer resolution of the marsh areas and of the wetting and drying process would improve the local comparison; however, based upon the excellent agreement of the main channel velocity characteristics and the uncertainties of precise marsh elevations, additional revisions were not attempted.

In general, an improved numerical model to physical model agreement in tide and velocity characteristics was achieved during the transitional channel verification. The greatest improvements were in the areas north of Kings Bay, the areas in which additional physical model geometry and roughness adjustments were performed. Both the physical model and the numerical model demonstrated reduced ebb and flood current velocities in the deepened upper Kings Bay relative to the pre-Trident condition.

An additional pre-Trident verification effort was undertaken for the RMA-2V numerical model using the pre-Trident channel physical model data set and the revised numerical schematization (Mesh 4) developed for the upper basin remedial measures testing. The resolution of the original pre-Trident mesh was modified considerably as proposed plan channel revisions and potential remedial measures testing were requested. This third verification effort was undertaken to ensure that the mesh revisions did not alter the hydrodynamic characteristics and to provide an updated data set for plan comparison purposes. Subtle variations in high-water elevations and in localized velocity conditions were identified between the revised mesh and the original mesh. Overall verification of the revised mesh was considered as good as the original verification.

The hydrodynamic results from the RMA-2V verification were used in the numerical sediment transport code STUDH as input information to solve the depth-integrated convection-diffusion equation for a single sediment

constituent. The interaction of the flow (transport) and the bed (sedimentation) was treated in routines that computed source/sink (erosion/deposition) terms over the entire modeled area. Cohesive (clay and silt) and noncohesive (sand and silt) sediments were handled in separate sections of the code.

Verification of STUDH was accomplished through comparison of model predictions with actual field shoaling rates for pre-Trident conditions. An average pre-Trident shoaling rate of 1.2 million cubic yards per year was determined from suitable hydrographic field surveys collected between July 1979 and August 1982. Seasonal extreme values varied from 0.4 million to 2.6 million cubic yards per year. Relatively low shoaling rates, less than 1.0 ft per year, were indicated for the navigation channel in Cumberland Sound, while high shoaling rates, greater than 3.0 ft per year, were indicated for the channel areas within Kings Bay.

Model testing coefficients were based upon the latest field data, laboratory testing analyses, and previous modeling experience, as available. Sediment grain size distribution was the primary adjustment means for noncohesive sedimentation and bed density was the primary adjustment means for cohesive sedimentation. An in situ bed density field effort conducted at Kings Bay during July 1985 indicated that a dry weight bed density of 300 kg/cu m would be an appropriate estimate for cohesive sediment modeling purposes. Prior to this period a dry weight density of 200 kg/cu m was used. Results presented in this report reflect the revised density.

The pre-Trident RMA-2V verification data set was considered to be an approximation of the long-term average hydrodynamic conditions associated with the long-term sedimentation processes affecting the navigation channel through Cumberland Sound and Kings Bay. Several cohesive and noncohesive sediment model tidal cycle runs were performed separately to initialize model sediment concentrations and bed conditions. Results for each sediment type were then extrapolated to provide model predictions for a complete sedimentation year. These results were arithmetically combined to produce a yearly sedimentation rate for comparison to the field data. Excellent pre-Trident numerical model to field sediment verification was demonstrated.

A similar modeling procedure and set of model coefficents were used to examine shoaling rates associated with the January 1985 transitional channel geometry conditions. Field shoaling rates were determined for the recently dredged upper Trident turning basin for the January 1985-January 1986 period.

This area had no previous survey information for determining a shoaling history. Model predictions for the upper basin area indicated higher sedimentation rates than were indicated by the limited field data. Several possible explanations for this difference included low field sediment loads associated with the prolonged east coast drought conditions, the ongoing dredging operations and transitional nature of the channel, and the possible need for further model adjustments. The sediment model was developed and verified for long-term average conditions, and additional model adjustments could not be justified based on the limited available data for this area; additional time and monitoring are required before any other model adjustments can be made with confidence.

Pre-Trident channel model shoaling conditions determined using the revised Mesh 4 schematization and RMA-2V results demonstrated little to no sedimentation impact associated with the increased resolution mesh. Excellent Mesh 4 verification to the pre-Trident shoaling conditions was indicated.

Verification of the hydrodynamic and sediment transport hybrid modeling system for Cumberland Sound and Kings Bay navigation channel has been demonstrated. Mesh 4 and the modeling procedures developed should be used in carefully designed testing programs to assess potential hydrodynamic and sedimentation impacts associated with plan channel and remedial measures testing.

PREFACE

The modeling study reported herein was requested by the Department of the Navy, Officer in Charge of Construction (OICC), Trident, Kings Bay, in a letter to the US Army Engineer Waterways Experiment Station (WES) dated 16 September 1982. WES was requested to undertake a modeling study to examine the hydrodynamic and sedimentation processes of the Kings Bay Submarine Base harbor facilities and channels, to predict long-term average maintenance dredging requirements for planned channel enlargements, and to evaluate possible remedial measures. A two-part model study was developed. Part one, referred to as Model A, was a hybrid model (coupled physical and numerical models) designed to address the interior portion of the system inland of the throat of St. Marys Inlet. The second part, Model B, developed at the Coastal Engineering Research Center, WES, addressed the outer portion seaward from the inlet throat. This report describes the Model A hybrid modeling system developed for Kings Bay and Cumberland Sound and addresses the physical and the numerical model verifications. Subsequent reports address Model A predictions for pre- and post-Trident channel conditions and model evaluations of potential remedial measures.

This study was conducted in the Hydraulics Laboratory of WES under the general supervision of Messrs. H. B. Simmons and F. A. Herrmann, Jr., former and present Chiefs of the Hydraulics Laboratory, respectively; R. A. Sager, Assistant Chief of the Hydraulics Laboratory; W. H. McAnally, Chief of the Estuaries Division (ED); W. D. Martin, Chief of the Estuarine Engineering Branch (EEB), ED; R. A. Boland and J. V. Letter, former and present Chiefs of the Estuarine Simulation Branch (ESB), ED; and M. A. Granat, EEB, Project Manager. Mr. N. J. Brogdon, Jr., ESB, was Project Engineer for the physical model and Mr. Granat was Project Engineer for the numerical models. Ms. B. P. Donnell, ESB, assisted during the early stages of the numerical modeling. Ms. C. J. Coleman, Estuarine Processes Branch, and Mr. D. M. Stewart, EEB, assisted as numerical model technicans during several stages of this investigation. Physical model technicians who assisted throughout the investigation included Messrs. J. T. Cartwright, J. S. Ashley, C. R. Holmes, D. M. White, and J. Cessna, ESB. Mr. D. H. Terrell of Instrumentation Services Division, WES, was in charge of physical model instrumentation. Contract monitoring for

the study was provided by Messrs. George Carpenter, John Randall, and Brian Smith, OICC, Trident.

This report was prepared by Messrs. Granat, Brogdon, Cartwright, and McAnally. Mrs. Marsha C. Gay, Information Technology Laboratory, WES, edited this report. A special acknowledgement is given to Ms. B. P. Donnell and Messrs. S. A. Adamec and D. P. Bach, Estuaries Division TABS modeling consultants, who continuously provided valuable support throughout the conduct of the numerical modeling efforts.

COL Dwayne G. Lee, EN, is the Commander and Director of WES. Dr. Robert W. Whalin is the Technical Director.

CONTENTS

CONVERSION FACTORS, NON-SI TO SI (METRIC) UNITS OF MEASUREMENT

Non-SI units of measurement used in this report can be converted to SI (metric) units as follows:

Multiply	By	To Obtain
acre-feet	1233.482	cubic metres
cubic feet	0.02831685	cubic metres
cubic yards	0.7645549	cubic metres
degrees (angle)	0.01745329	radians
degrees Fahrenheit	*	Celsius degrees or Kelvins
feet	0.3048	metres
gallons	3.785412	cubic decimetres
inches	25.4	millimetres
miles (US nautical)	1.852	kilometres
miles (US statute)	1.609344	kilometres
ounces (fluid)	0.029577353	cubic decimetres
pounds (force)	4.448222	newtons
pounds (force)-second per square foot	47.88026	pascals-second
pounds (mass) per cubic foot	16.018463	kilograms per cubic metre
pounds (mass) per square foot	4.882428	kilograms per square metre
square feet	0.09290304	square metres
square miles	2.589988	square kilometres

* To obtain Celsius (C) temperature readings from Fahrenheit (F) readings, use the following formula: $C = (5/9)(F - 32)$. To obtain Kelvin (K) readings, use: $K = (5/9)(f - 32) + 273.15$.

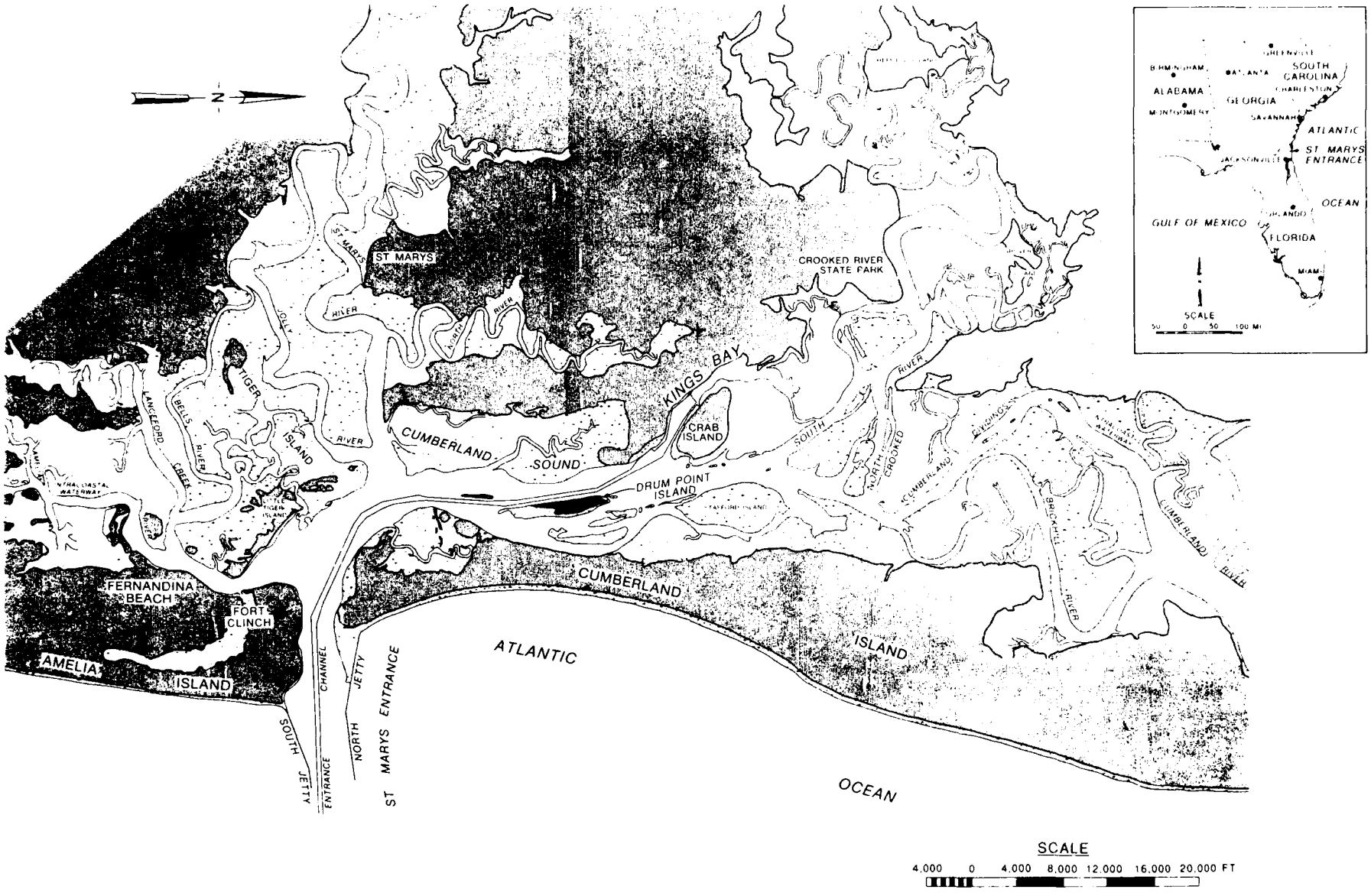

Figure 1. General study area location map

VERIFICATION OF THE HYDRODYNAMIC AND SEDIMENT TRANSPORT HYBRID MODELING SYSTEM FOR CUMBERLAND SOUND AND KINGS BAY NAVIGATION CHANNEL, GEORGIA

PART I: INTRODUCTION

Background

1. The original Kings Bay facility, located adjacent to Cumberland Sound in southeast Georgia, was designed and developed as an emergency Army Munitions Operation Transportation facility in the late 1950's. Initial channel depths were authorized at 32 ft* mean low water.** The facility was never placed into operational use and was in a standby mobilization status with channel depths of about 32 ft maintained on an "as time and money permitted" basis. Figure 1 shows the general Cumberland Sound and Kings Bay area.

2. An Environmental Impact Statement prepared in June 1976 for a one-time maintenance dredging operation indicated that approximately 1.7 million cubic yards of material would have to be removed from the turning basin and Kings Bay channel area. The last previous recorded maintenance dredging took place in 1970. Dredging records from this period are limited or not available and cannot be used to assess annual shoaling rates.

3. In July 1978, ownership of the Kings Bay facility was transferred to the Department of the Navy for use as a Naval submarine base for Poseidon class submarines. Between July 1978 and July 1979, approximately 8.6 million cubic yards of material were removed for facility expansion. Major channel realignment, channel widening, and channel deepening were performed. The lower entrance channels were authorized at depths of 38 to 40 ft and a width of 400 ft. The remaining interior approach channels were authorized at a depth of 34 ft and a width of 300 ft. Kings Bay was authorized at a 37-ft depth.

---

* A table of factors for converting non-SI to SI (metric) units is presented on page 11.

** All depths and elevations (el) described in this report refer to local mean low water (mlw), which is 2.75 ft below National Geodetic Vertical Datum (NGVD).

4. The total length of the interior Poseidon channel, from the throat of St. Marys entrance adjacent to Fort Clinch to the end of the main docking facility, was about 7 n.m. The narrowest point between land masses within Kings Bay was about 1,000 ft and occurred at the entrance to the submarine base. The channel width widened from about 650 ft at the entrance to about 1,200 ft at the downstream end of the main docking facility. At this location, a 643-ft-long Poseidon submarine support tender was usually anchored perpendicular to the channel. A floating dry dock was located parallel to the channel about 0.5 n.m. downstream from the Kings Bay entrance. Details of the submarine channel are shown in Figures 11-13 and discussed in paragraphs 69-74.

5. The most recent basic plan channel conditions incorporated in the model testing program included widening the approach channel to 500 ft and deepening it to 46 ft; deepening Kings Bay to 48 ft; some additional widening within Kings Bay and at some of the lower channel bends; relocating the Poseidon tender from perpendicular to the channel at Kings Bay to parallel to the channel above the floating dry dock; extending Kings Bay another nautical mile to the northwest to include a small boat facility, a Trident dry dock, and an upper turning basin; and building a magnetic silencing facility adjacent to the submarine channel across from Drum Point Island. Approximately 25.5 million cubic yards of material will be removed to accomplish this planned interior channel expansion. The modeling efforts did not address the lower Kings Bay turning basin or the St. Marys Inlet turning and sediment basins, which were designed subsequent to model testing.

Objectives

6. The primary objectives of the modeling study were to predict average currents and long-term average maintenance dredging requirements for enlarged channel and port facilities for the submarine base, to develop and evaluate remedial measures that might reduce sedimentation without adversely affecting ship handling, and to enhance base operational readiness. Another primary goal of the entire study effort was to maintain a fast-track pace to provide the Navy with results on priority tasks while maintaining the required flexibility to adapt to project design changes. Model results were provided to the Navy in memorandum format as they became available.

Scope

7. The modeling study included many different tasks and subtasks. Some of the final design plans for channel expansion evolved during the 7 years of construction and during model testing. The models were updated, in a timely fashion, as additional information was obtained. This report describes the hybrid modeling system (coupled physical and numerical models) and the procedures developed to investigate the hydrodynamic and sediment transport processes associated with the Naval Submarine Base, Kings Bay, GA, and the Cumberland Sound access channel between Kings Bay and the ocean entrance at St. Marys Inlet. The main focus of this report is to address the verification of the models. Subsequent reports address model predictions for pre- and post-Trident channel conditions and model evaluations of potential remedial measures.

PART II: THE PROTOTYPE

Description

8. The Naval Submarine Base, Kings Bay, is located in southeast Georgia, about 9.6 n.m. north of the St. Marys Inlet entrance jetties at the Atlantic Ocean. The base is within the Cumberland Sound estuarine system, which includes extensive salt marshes and sand flats (shaded areas on Figure 1) typical of the Sea Island system of southeast Georgia. The mean tidal range at the ocean entrance between Amelia Island, in the State of Florida, and Cumberland Island, in the State of Georgia, is 5.8 ft. Maximum spring tidal ranges can exceed 8.0 ft in the interior portions of the estuary.

9. The primary source of fresh water for the Cumberland Sound estuarine system is the St. Marys River. The river originates in the Okefenokee Swamp, approximately 120 n.m. upstream from Cumberland Sound, and enters the sound about 5.5 n.m. south of the Kings Bay entrance. The St. Marys drainage basin includes about 1,478 square miles of swampland and coastal plain. The long-term average freshwater discharge at the mouth of the river is about 1,500 cfs. Freshet discharges as high as 18,000 cfs have been recorded. Suspended sediment loads within the St. Marys River are generally low.

10. The Crooked River, located approximately 2 n.m. north of Kings Bay, is the second largest contributor of fresh water to the Cumberland Sound system. This river is much smaller than the St. Marys and consists of a drainage basin of about 90 square miles with an average freshwater discharge of about 100 cfs. The total fresh water entering Cumberland Sound from the remaining drainage basins is estimated to be less than the Crooked River flow.

11. The relatively low average total freshwater discharge into Cumberland Sound and the relatively high tidal range and associated strong current velocities generally maintain the sound as a well-mixed estuarine system. Salinity within the sound and Kings Bay is generally vertically and laterally homogeneous. Longitudinally, salinity within the sound is only slightly reduced from the ocean entrance conditions. Salinity in Kings Bay typically varies from about 26 to 32 ppt during the year.

12. Sedimentation within Cumberland Sound, including Kings Bay, is not the result of localized flocculation (geochemistry associated with a freshwater-saltwater interface). Long-term hydrodynamic processes, including

ebb and flood circulation cells and reduced current velocities within Kings Bay, are primarily responsible for transporting already flocculated clay sediments and causing the high sedimentation rates at Kings Bay.

Hydrodynamic Field Data

13. Hydraulics and sediment field measurements of the Cumberland Sound/Kings Bay area were obtained for verification of the models used in this investigation. The data were obtained in field surveys conducted in 1982 and 1985 and from hydrographic surveys previously conducted by the US Army Engineer District, Savannah, and US Army Engineer District, Jacksonville.

14. The hydraulic data collection program is described in the following paragraphs. The equipment and techniques used are described in Appendix A, and the data are presented in Appendices B and C.

Hydraulic data collection, 1982

15. The November 1982 survey by the US Army Engineer Waterways Experiment Station (WES) was designed only to supplement the primary data collection program by the US Geological Survey (USGS), which occurred in November 1981 and July 1982 (Radtke 1985). The USGS data proved to be unsatisfactory for complete model verification use, and the November 1982 data served as the primary data for initial verification. Selected information from the USGS field efforts was used to supplement the November 1982 data for the pre-Trident verification efforts. These field efforts (USGS and WES) focused on Kings Bay and the Cumberland Sound areas to the south.

16. During the WES 1982 survey, the harbor in Kings Bay and channel in Cumberland Sound were in the pre-Trident facility condition as described in paragraphs 3 and 4. Wind conditions during the survey period were generally light (5-12 mph) with winds from the northeast on 10 November and from the southwest on 12 November. Air temperatures were seasonal with morning temperatures around 45° F and afternoon temperatures around 65° F.

17. Water levels, current velocities, salinities, and suspended sediments were measured in an intensive survey on 10 and 12 November, 1982. Data sampling locations are shown in Figure 2.

18. Water levels were measured at the 11 tide gage locations shown in Figure 2 using Fisher and Porter Model 1550 gages. Water level was recorded

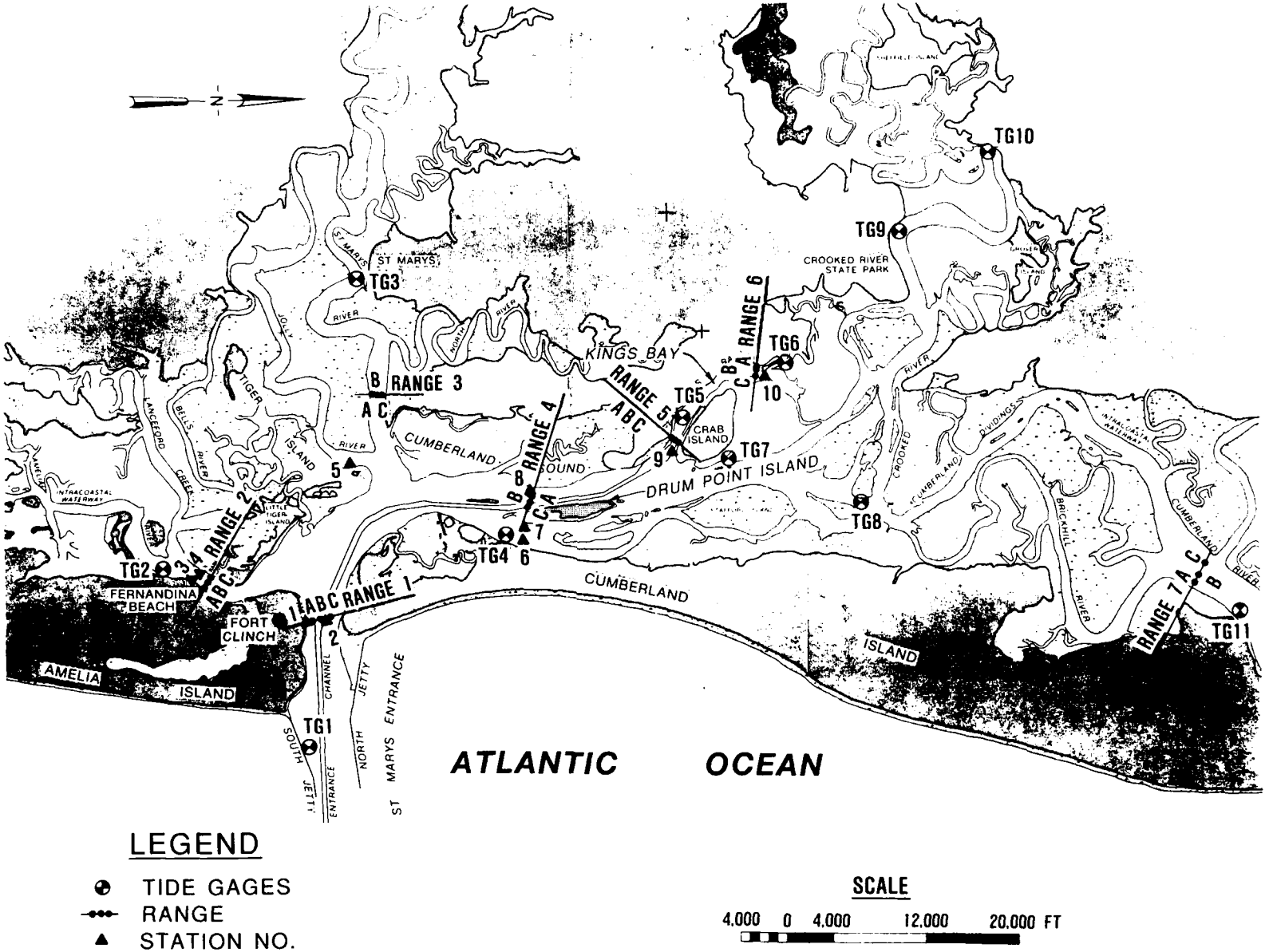

Figure 2. November 1982 field data sampling location map

at 15-min intervals during the survey and for approximately 3 weeks prior to 10 November.

19. Current velocities (speed and direction) were measured with ENDECO Model 174, moored, recording meters (numeric stations, Figure 2) and from boats with over-the-side equipment (alphanumeric stations, Figure 2). The moored meters sampled the middepth current velocity at a 2-min interval at the stations shown in Figure 2 for approximately the same period as the tide measurements.

20. Over-the-side measurement equipment was used to measure current velocities and collect water samples at 21 stations on 7 ranges as shown in Figure 2. Measurements were taken at three depths at each station where depth permitted: 2 ft below the surface, middepth, and 3 ft above the bottom. On 10 November, stations on ranges 1-4 were measured at approximately 1-hr intervals for approximately 13 continuous daylight hours. On 12 November, stations on ranges 4-7 were measured at approximately 1-hr intervals for approximately 13 continuous daylight hours. By measuring velocities at range 4 on both days and at moored meter stations and tides throughout the survey period, the two 13-hr periods could be related to each other, more nearly satisfying the need for synoptic data.

Hydraulic data collection, 1985

21. In January 1985 a second verification data collection effort was performed to provide information in areas not covered by the prior efforts and to show how the system behaved with some of the Trident channel constructed. At the time of the survey, the upper end of Kings Bay had been dredged to Trident depths (48 ft), but the approach channel in Cumberland Sound and the lower end of Kings Bay (including the tender perpendicular to the channel) were still at pre-Trident conditions. This field effort centered around Kings Bay and the areas to the north and northwest.

22. The survey consisted of measurements at 23 stations as shown in Figure 3. Stations 1A, 1B, and 1C (adjacent to and west of Drum Point Island) were approximately at the same locations as the range 4 over-the-side stations monitored during the November 1982 survey. All measurements taken during the 1985 collection were taken with the over-the-side equipment, using the same methods and intervals as the November 1982 survey, except that water samples for salinity and suspended sediments were not collected.

23. The date of the survey was selected to coincide with a predicted

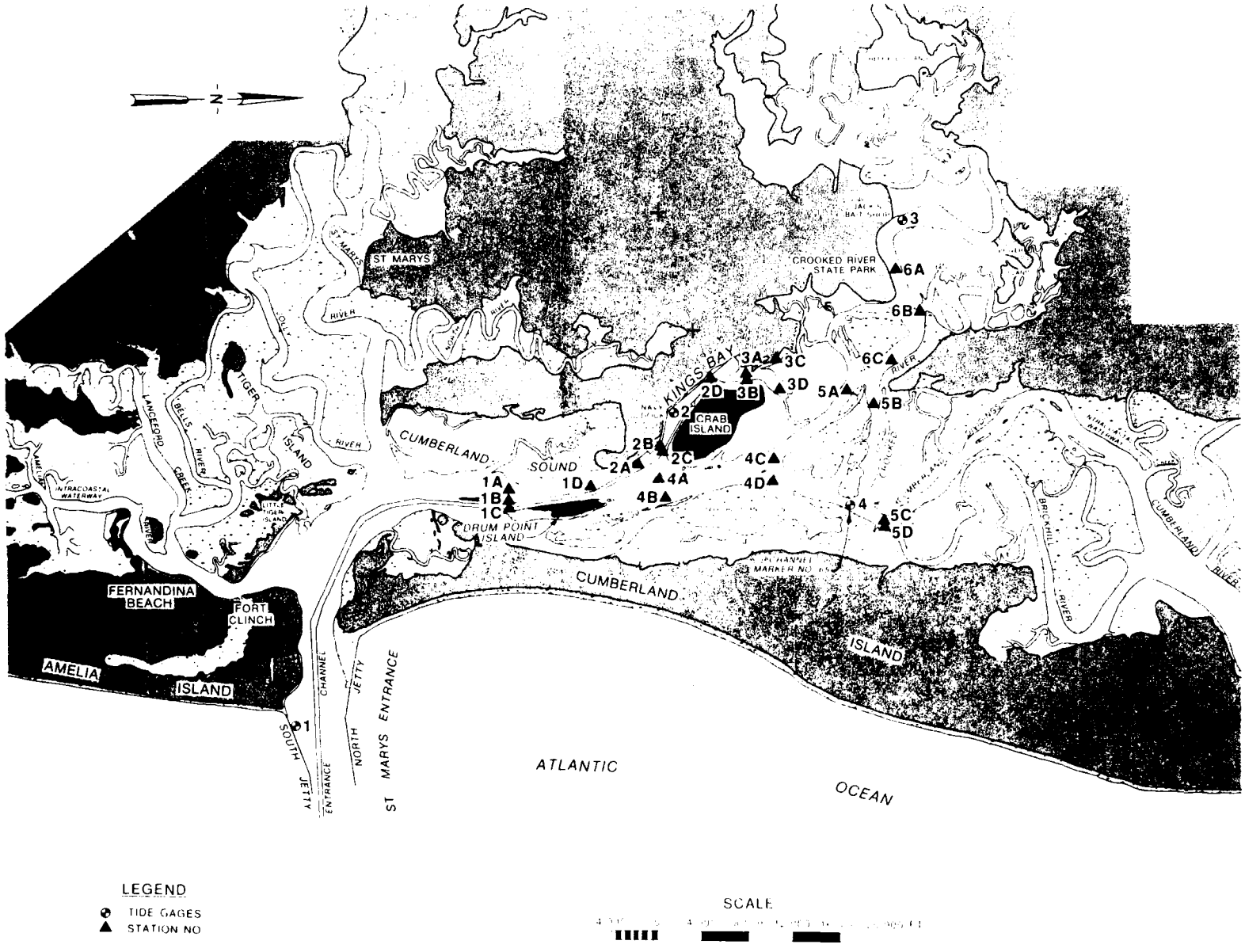

Figure 3. January 1985 field data sampling location map

semidiurnal tide similar to that recorded during the November 1982 survey. A strong (20-30 mph) wind blew from the northwest for several days prior to and including the morning of the survey on the 26th. This caused a distortion of the normal tide water levels and phases, preventing a near-duplication of the 1982 survey conditions. Temperatures during the survey period were below normal with a morning low of 7° F and an afternoon temperature around 35° F. This was not a desirable situation for collecting field data for model verification, but the survey could not be postponed because of project schedule demands.

Sediment Field Data

24. Sediment samples were also collected at the bed surface during each of the field exercises. These samples were brought back to the laboratory for grain size distribution analyses.

25. Ideally, long-term (5-10 years) hydrographic (bathymetric) records associated with a particular project condition should be used in filtering and reducing the general natural variability in sedimentation rates. In the case of Kings Bay and Cumberland Sound, such long-term records were not available. As stated in paragraph 2, little to no shoaling data existed prior to the Navy's acquisition of Kings Bay in 1978. The channel associated with Kings Bay has been in a transitional expansion state since that time.

26. Condition, examination, or pre- and post-dredging hydrographic surveys have been collected by Savannah District on at least a three-times-a-year basis since 1978. These surveys covered the submarine channel and generally extended only a few hundred feet on either side of the channel prism line. A special, approximately monthly, survey interval was undertaken by Savannah District between January 1985 and September 1985 to collect sedimentation data for the recently dredged Trident channel above the Poseidon Kings Bay operational area. This area had no previous survey information for determining a shoaling history.

Pre-Trident channel shoaling data set

27. Channel depths from suitable hydrographic surveys were compared to obtain shoaling rate information for verification of the Kings Bay numerical sediment model. Surveys immediately following dredging periods were avoided to reduce the impact of initial channel adjustment. Briefly, an array

processing system was developed that compared irregularly spaced input survey depth data between two surveys and reduced them into measurements of depth and volume change. The channel areas were subdivided into separate zones for analysis purposes.

28. Two years of successive survey data (July 1979-June 1981) were analyzed to obtain estimates of average infill rates for the channel areas below Drum Point Island. Due to dredging operations, 3 years of discontinuous survey data (July 1979-August 1982) were analyzed for the channel areas adjacent to and north of Drum Point Island. Yearly average and extreme high and low shoaling rates were determined for zones corresponding to the numerical model schematization of the pre-Trident channel areas. Based on these analysis periods the average pre-Trident shoaling rate was determined to be about 1.2 million cubic yards per year; seasonal extreme values varied from 0.4 million cubic yards per year to 2.6 million cubic yards per year. These shoaling rate assessments, by zone, are presented in Part VI, "Verification of the Numerical Sediment Transport Model, STUDH." Sediment types (cohesive and noncohesive) could not be determined from the available information. The obtained shoaling rate estimates were in general agreement with Savannah District dredging records.

In situ bed density measurements

29. An additional field site visit was made by personnel of WES and Sediment Dynamics International, LTD, during July 1985 to examine the in situ bed density of the cohesive sediments depositing in Kings Bay. A SIRAD (Sediment Instrumentation Research and Development) B.S.G.1 Backscatter Gamma Density Gage was used aboard a Savannah District survey vessel during this survey. The findings indicated that 300 kg/cu m* would be an appropriate estimate for characterizing the freshly deposited cohesive sediments in the numerical model (Salkield 1985). As described in Part VI, 200 kg/cu m was used prior to this survey information for initial model predictions. Since the numerical model sediment code, STUDH, uses mass in the transport equations, adjustments to previous model predictions (cubic yards per year and feet per year) can easily be made (multiply initial cohesive sedimentation predictions by 200/300) to account for this revised bed density. Results

* Because the sediment model is formulated in metric units, all associated model coefficients will also be described in metric units.

presented in this report have been adjusted accordingly, except where otherwise indicated.

PART III: THE KINGS BAY MODELING SYSTEM

Introduction to Modeling

30. Solutions to coastal hydraulics problems are principally obtained by use of four primary methods: field observations, analytical solutions, numerical models, and physical models. Any of these four may be the best single approach for solving a particular problem. Choosing between them requires knowledge of the phenomena that are important to the problem and an understanding of the strengths and weaknesses of the solution methods.

Field observations

31. Field (prototype) data collection and analysis serve both as an important aspect of the other solution methods and as an independent method. Alone, field data show the estuary as it behaved under a specific set of conditions prior to and at the time of measurement. By skillful scheduling of data collection, careful analysis, and luck, one can obtain estimates of the separate effects of various physical phenomena such as tides, river discharge, and wind. Field data can reveal problem areas and define the magnitude of problems and can, to a limited extent, be used to estimate the estuary's response to different conditions of tide and river discharge. They can also be used in an attempt to identify changes caused by a modification to the estuary. Field data are an indispensable element in verification of numerical and physical models; they are used by the modeler to adjust the model and show that the model results are reliable.

32. Obtaining sufficient temporal and spatial data coverage in the field is a formidable and expensive task; therefore, available field data are often too sparse to describe an estuary in any but the most general terms. Those not intimately familiar with data collection and analysis often overestimate the accuracy and reliability of the data.

Analytical solution methods

33. Analytical solutions are recognized as a separate solution method, but they must be carefully defined in order to distinguish them from numerical models. Analytical solutions are those in which answers are obtained by use of mathematical expressions. These expressions or equations describe physical phenomena in mathematical terms and thus may be considered to be mathematical models of physical reality. For example, Manning's equation is a simple

analytical model of the complex process of energy losses in open-channel flows. A more rigorous and complete analytical model of the losses is included in the turbulent version of the Navier-Stokes equations, the Reynolds equations.

34. Analytical models usually combine complex, poorly understood phenomena into coefficients that are determined empirically. Manning's roughness coefficient, for instance, combines the various effects of energy dissipation into a single parameter. The degree of simplification of the analytical model dictates how it is solved. For example, Manning's equation can be solved directly, whereas the Reynolds equations must be simplified and solved by numerical methods.

35. If a calculation can be solved by substituting values of the independent variables into the equation (a closed form solution), then the solution method is analytical. The calculation may be performed by hand or by computer, but the solution is still an analytical one.

36. The analytical solution method has advantages of speed and simplicity, but it cannot provide many details. In estuaries, analytical solutions can be used for gross representations of tidal propagation and average cross-sectional velocities in simple geometries. Details of flow cannot be predicted. The usefulness of analytical solutions declines with increasing complexity of geometry or increasing detail of results desired.

Numerical modeling

37. Numerical modeling employs special computational methods, such as iteration and approximation, to solve mathematical expressions that do not have closed form solutions. A numerical model thus applies numerical (computational) analysis to solve mathematical expressions that describe the physical phenomena. The distinction between analytical solutions obtained by computer calculations and numerical modeling solutions may become blurred. In this report, the computer programs used to solve the governing equations are referred to as generalized computer programs or codes. When the codes are combined with a geometric schematization (mesh or grid) and specified parameters representing a particular estuary, the combination is called a model.

38. Numerical models are generally classified by the number of spatial dimensions over which variables are permitted to change. Thus in a one-dimensional flow model, currents are averaged over two dimensions (usually width and depth) and vary only in one direction (usually longitudinally).

Two-dimensional models average variables over one spatial dimension, either over depth (a vertically averaged horizontal model) or width (a laterally averaged vertical model). Three-dimensional models solve equations accounting for variation of the variables in all three spatial dimensions (vertical, lateral, and longitudinal).

39. Time is a fourth dimension considered in modeling. Steady-state numerical models solve the governing equations for a single condition or distinct time. A time-varying model solves the governing equations over time and for any varying prescribed conditions and periods desired.

40. Numerical modeling provides much more detailed results than analytical methods and may be substantially more accurate, but it does so at the expense of time and money. Model run costs and computer memory requirements increase with increased resolution, dimensionality, and simulation time. Models of sufficient detail may require very large computers to solve the large systems of equations and store results. However, once a numerical model has been formulated and verified for a given area, it can quickly provide predictions for different conditions. Numerical models are capable of simulating some processes that cannot be handled in any other way.

Physical modeling

41. Physical scale models have been used for many years to solve coastal hydraulic problems. Careful observance of appropriate scaling requirements permits the physical modeler to obtain reliable solutions to problems that often can be solved no other way. A physical model provides a very succinct three-dimensional visual picture of the entire area of interest over the simulation time. It can provide insight into physical processes that otherwise would be very difficult to observe and illustrate.

42. Physical hydraulic models of estuaries can reproduce tides and other long waves; some aspects of short-period wind waves; longshore currents; freshwater flows; pollutant discharges; some aspects of sedimentation; and three-dimensional variations in currents, salinity, density, and pollutant concentration. Present practice does not include simulation of water-surface setup and currents due to wind. Applicability of model laws and choice of model scales are dependent on which of these phenomena are of interest. Conflicts in similitude requirements for the various phenomena usually force the modeler to neglect similitude of some phenomena in order to more accurately reproduce the dominant processes of the situation. For example, correct

modeling of tides and currents often requires that a model have different scales for vertical and horizontal dimensions. This geometric distortion permits accurate reproduction of estuarine flows and is a common and acceptable practice; but it does not permit optimum modeling of short-period waves, which requires an undistorted-scale model for simultaneous reproduction of refraction and diffraction.

Hybrid modeling

43. The preceding paragraphs have described the four principal solution methods and some of their advantages and disadvantages. In practice, two or more methods are used jointly, with each method being applied to that portion of the problem for which it is best suited. For example, field data are usually used to define the most important processes and verify that a model adequately predicts hydrodynamic conditions in an estuary. Combining two or more methods in simple ways has been common practice for many years. Combining physical modeling and numerical modeling to provide results not possible any other way is termed a hybrid solution; combining them in a closely coupled fashion that permits feedback between the models is termed an integrated hybrid solution.

44. Judicious selection of solution methods in a hybrid approach can greatly improve accuracy, reliability, and detail of the results. By devising means to combine results from several methods, the modeler can include effects of many phenomena that previously were neglected or poorly modeled. Examples of processes that are good candidates for hybrid modeling are (a) sediment transport and flow hydrodynamics or (b) tidal flows and short-period waves. In the first case, hydrodynamics drives the sediment transport process, and in a carefully designed study, the feedback from the bed change to hydrodynamics is minimal. In the second case, the interaction of the two processes is often dominated by one or the other such that they can be analyzed as independent events and the results combined. Processes that have a strong feedback loop, such as hydrodynamics of freshwater-saltwater interaction, are not suitable for separation in the hybrid approach and consequently should be analyzed together.

Modeling limitations

45. Any solution method or model is an approximation of the prototype. Each has its own set of limitations, simplifications, and underlying assumptions. Results obtained from any technique must always be considered as

approximate solutions to the given set of conditions. A verification process is required to demonstrate the degree of reasonableness for all predictions. The degree of sophistication of the technique and the resulting verification are offset by time and cost constraints.

46. Many approximations, simplifications, and assumptions have been made in the present hybrid approach, and only some of them are explicitly stated in this report. Each approximation, simplification, and assumption can be arguably justified as necessary or desirable, but the net result must be considered only an approximation to a very complex system and its processes. The authors believe that the hybrid method developed here was the most advanced modeling method available at the time the work was performed; but in comparison to the complex interaction of processes in Kings Bay, it was still simple.

The Physical Model

Physical model description

47. The limits of the Kings Bay physical model, shown in Figure 4, reproduced approximately 206 square miles of the prototype area including about 14 miles of the St. Marys River (to about 7 miles upstream from the town of St. Marys); the Jolly River; about 6 miles of the Amelia River; all of Cumberland Sound and Kings Bay; about 13 miles of the Crooked River (lower south and north forks) upstream to Sheffield Island; about 9 miles of the Cumberland Dividings and River to Terrapin Point; the extensive system of smaller channels, creeks, and marsh areas that affect tidal action throughout the modeled area; and about 220 square miles of the Atlantic Ocean from about 5 miles south and about 14 miles north of the respective St. Marys Inlet jetties. Prototype contours within 4 miles of the ends of the jetties were reproduced to scale (to about the 45-ft depth contour); the remaining ocean area, the ocean boundary, was molded at a flat 100-ft elevation. St. Andrew Sound Inlet, located about 17 n.m. north of the St. Marys Inlet, was about 3 n.m. beyond the northern limit of the model. In the interior, the Cumberland Sound and St. Andrew estuarine systems are connected by a system of small rivers, sloughs, and marsh. Propagation of tidal flows through the St. Andrew system was simulated with an artificial labyrinth system opening to the model ocean. This labyrinth system was adjusted so that hydrodynamic conditions in the

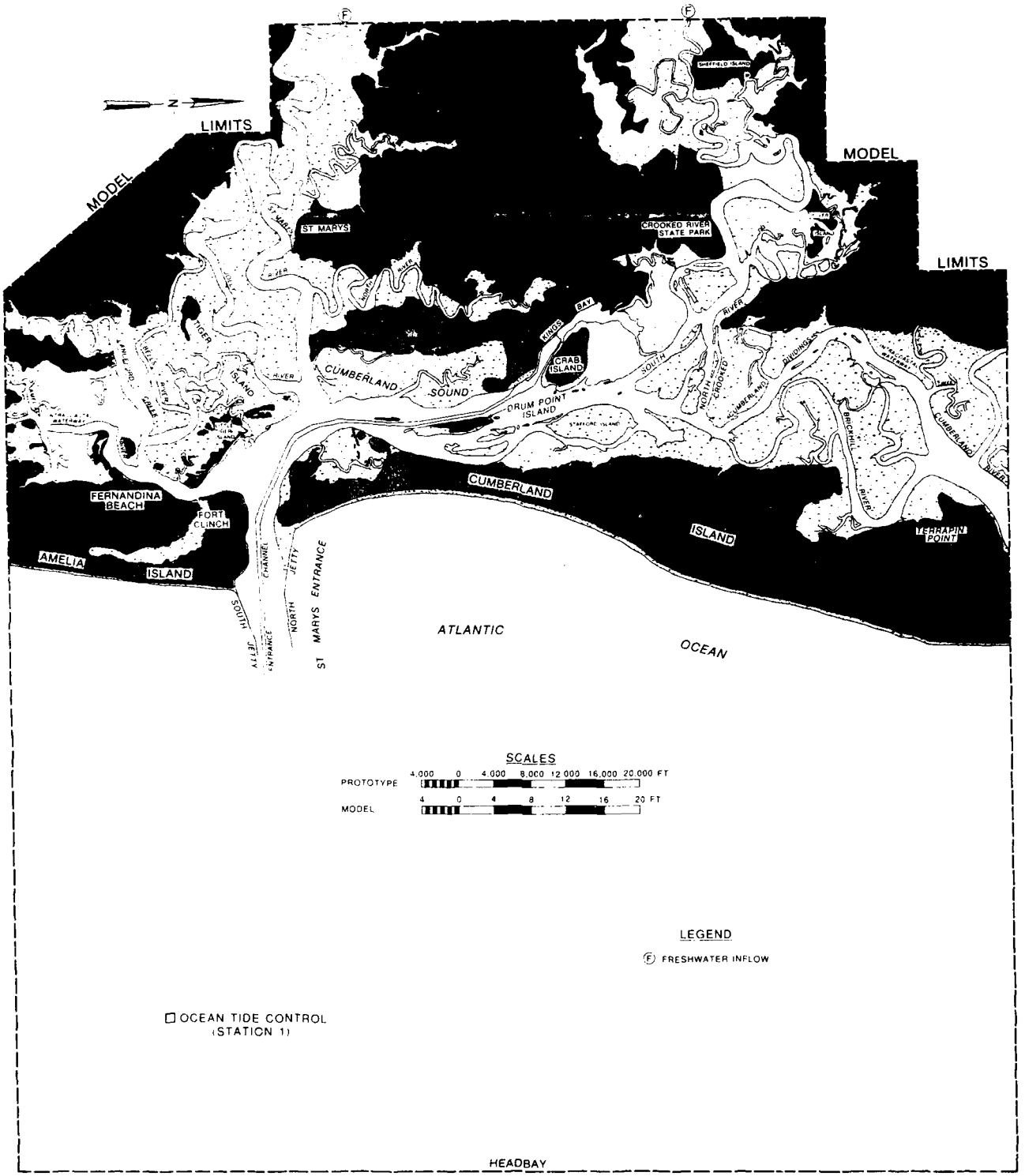

Figure 4. Physical model limits

study area were reproduced to an acceptable degree.

48. The model was constructed to linear scale ratios, model to prototype, of 1:100 vertically and 1:1,000 horizontally. From these basic ratios the following ratios were computed by Froudian relations:

Characteristic	Ratio
Slope	10:1
Velocity	1:10
Time	1:100
Discharge	1:1,000,000
Volume	1:100,000,000
Area (cross-section)	1:100,000
Area (horizontal)	1:1,000,000

The salinity ratio in the model was 1:1. One prototype tidal cycle (semidiurnal) of 12.42 hr was reproduced in the model in 7.452 min. Horizontal grid coordinates of the model were based on the Georgia coordinate system, and vertical control was based on local mean low water datum. The model was approximately 126 ft long and 108 ft wide and covered an area of about 12,600 sq ft. It was completely enclosed to protect it and its appurtenances from the weather, and to permit uninterrupted operation.

49. The model was a fixed-bed type, molded to most recent prototype hydrographic surveys. The entrance and Fernandina Beach channel survey was conducted by Jacksonville District during 1982. The channel survey beginning inside the entrance (adjacent to Fort Clinch) and extending into Kings Bay proper was conducted by Savannah District during July 1982. These survey data covered the channel and generally only a few hundred feet on either side of the channel prism line. Recent hydrographic survey data for the areas outside of the channel were not generally available. The most recent (1983) National Ocean Survey (NOS) bathymetric charts were used for these areas; in some instances, the most recent survey data presented on these charts date back to data collected in 1934-1935. Hydrographic information used for model construction of adjacent beaches was collected in 1974.

50. Artificial roughness is used in geometrically distorted models to properly scale energy losses, to enhance mixing, and to properly distribute flow. Permanent artificial roughness in the Kings Bay model consisted of 1/2-in.-wide metal strips placed in water depths greater than -2.0 ft, and

cut off at mean low water elevation. The tidal flats and marsh areas were initially molded in at +1.0 ft and roughened by raking the surface during construction. During the verification process it was discovered that these elevations should have been closer to +4.0 to +5.0 ft. These areas were raised by fixing a thin layer of pea gravel in place with a mixture of cement and sand.

Model appurtenances

51. The model was equipped with the necessary appurtenances to reproduce and measure all pertinent phenomena such as tidal elevations, salinity, current velocities, freshwater inflows, and dispersion characteristics. Apparatus used in connection with the reproduction and measurement of these phenomena included a mechanical tide generator and recorder, tide gages, conductivity meters, water sample collection apparatus, current velocity meters, and freshwater measuring weirs. This equipment is described in detail in the following paragraphs.

52. Tides in the model were reproduced by a tide generator (Figure 5) located in the model ocean. The tide generator maintained a differential between a pumped inflow of salt water (supply) to the model ocean and a gate-controlled gravity return flow to the supply sump (elevation lower than the ocean) as required to produce the desired water levels at the tide control station. The tide generator was equipped with a continuous tide recorder so that the accuracy of the tide reproduction could be checked visually at any time. Continuous read-out data from a water-level detector located at the tide control station were also recorded on a digital logger and a strip chart recorder, where visual checks for accuracy could be made at any time during operation. During the physical model verification phases, the south jetty tide station was used as the control station. For the base and plan tests, the control tide station was changed to the offshore ocean tide control (Figure 4) to avoid potential plan geometry impacts.

53. Water-surface elevations throughout the model were measured manually. Permanently mounted and temporary point gages were used for manual measurement of tidal elevations. These gages were graduated with a vernier scale to 0.001 ft (0.1 ft prototype). A high-precision automatic water-level detector (Figure 6) designed and built at WES was used to obtain a continuous record of water-surface elevations at the ocean tide control station. This unit had a displacement range of 0.5 ft, accuracy of 0.003 in., resolution of

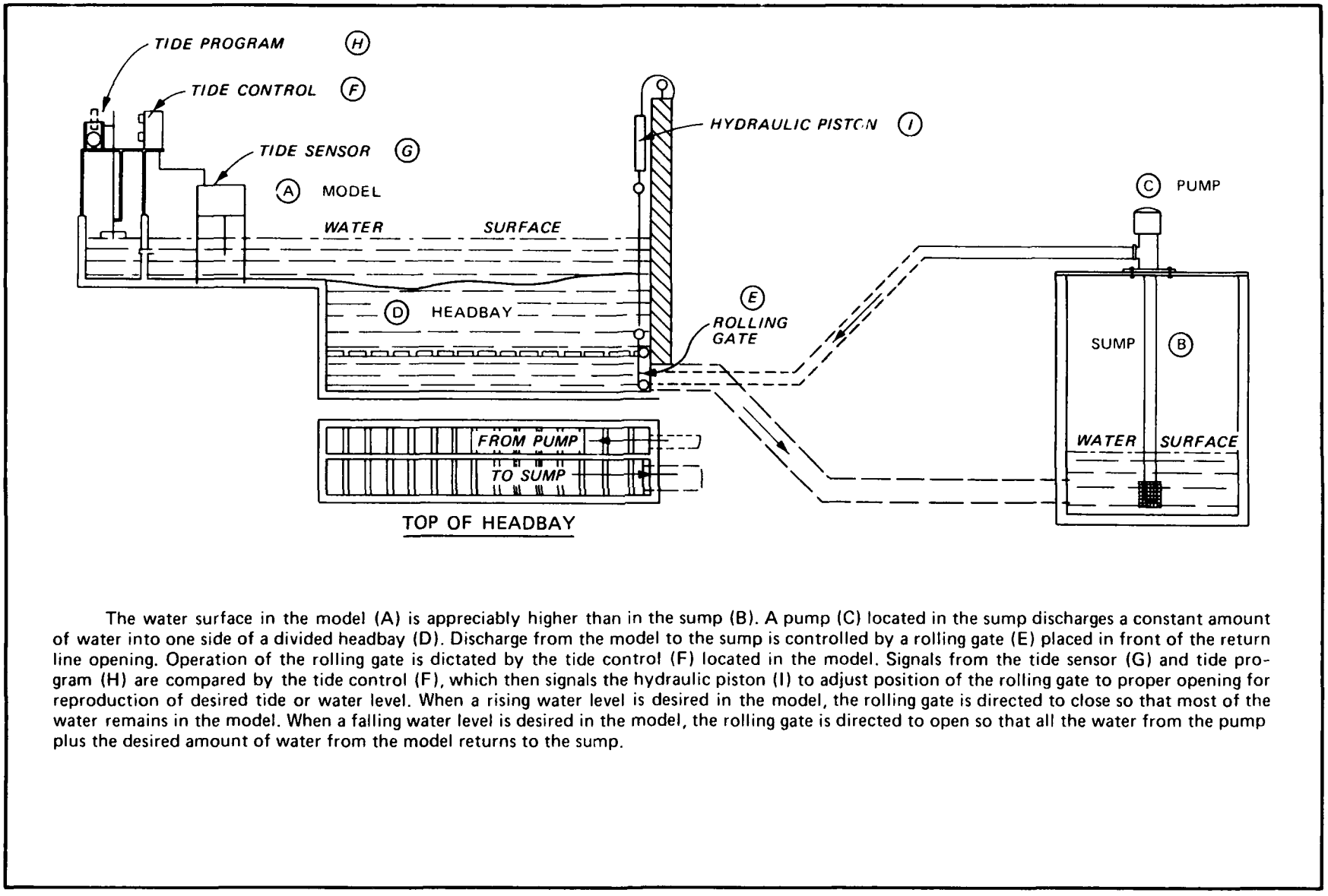

The water surface in the model (A) is appreciably higher than in the sump (B). A pump (C) located in the sump discharges a constant amount of water into one side of a divided headbay (D). Discharge from the model to the sump is controlled by a rolling gate (E) placed in front of the return line opening. Operation of the rolling gate is dictated by the tide control (F) located in the model. Signals from the tide sensor (G) and tide program (H) are compared by the tide control (F), which then signals the hydraulic piston (I) to adjust position of the rolling gate to proper opening for reproduction of desired tide or water level. When a rising water level is desired in the model, the rolling gate is directed to close so that most of the water remains in the model. When a falling water level is desired in the model, the rolling gate is directed to open so that all the water from the pump plus the desired amount of water from the model returns to the sump.

Figure 5. Physical model tide generator

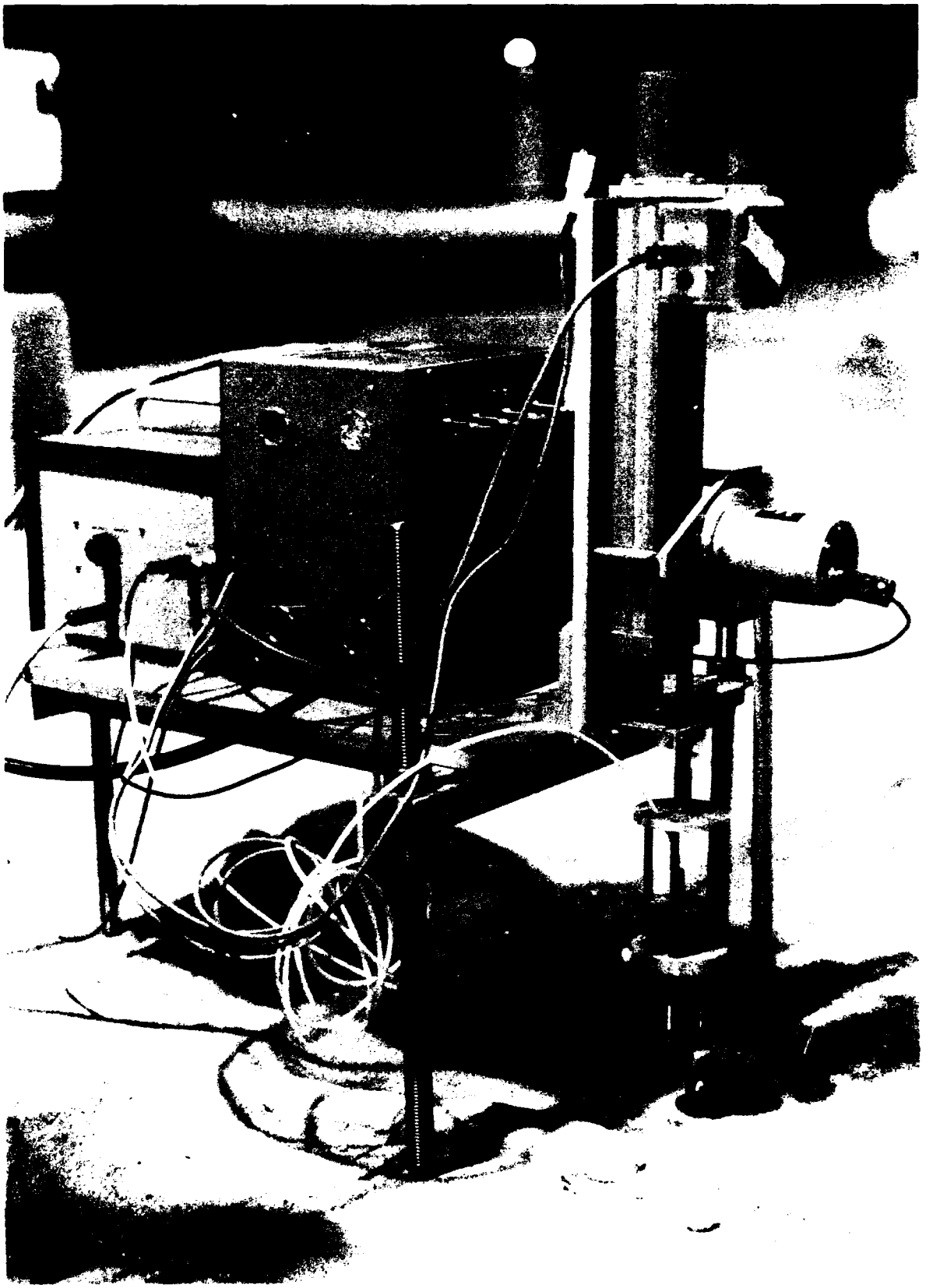

Figure 6. Physical model automatic water-level detector

0.005 in., and a temperature range of 32° to 110° F.

54. The detector used an air capacitance system consisting of a stainless steel probe, a servosystem, and a capacitance transducer. The servomechanism used a precision slide table and stepping motor to maintain a fixed capacitance between the water surface and the probe faceplate. The movement of the slide table and probe were measured by a potentiometer producing an analog voltage converted to a signal that was recorded on strip chart or digital recorder and converted to an elevation.

55. Fresh water was introduced into the model at the St. Marys and Crooked River boundaries. Measuring weirs were used to maintain desired discharges at each boundary. To maintain constant volume balance in the model, skimming weirs located in the offshore ocean area were used to remove similar volumes of diluted surface water. A constant ocean salinity was maintained by adding salt brine to the supply sump. The brine solution was obtained by passing supply sump water over rock salt stored in a Lixator adjacent to the sump. The rate of brine introduction was carefully monitored to ensure a constant source salinity in the supply sump throughout the testing period.

56. During the 1982-1983 pre-Trident verification phase of testing only, salinity throughout the model was determined by collection of water samples and conductivity measurements. Figure 7 illustrates a typical vacuum water sampling system. Electrical conductivity measurements and conversion to salinity concentration were performed in the laboratory. Figure 8 shows the conductivity cell.

57. Current speed measurements were obtained with miniature Price-type current meters (Figure 9). Each meter had five cups constructed of a lightweight plastic 0.04 ft (4 ft prototype) in diameter that were mounted on a thin horizontal wheel 0.08 ft (80 ft prototype) in diameter. The center of the cups were 0.05 ft (5 ft prototype) from the bottom of the frame. The meters were calibrated frequently and were capable of measuring speeds as low as 0.03 fps (0.3 fps prototype). Current directions were obtained using a very lightweight vane (Figure 10) that pivoted with the current. Direction was read in tens of degrees.

58. Photographs were taken during the initial plan testing condition and composite mosaics were made to document surface current patterns and for possible later comparison and evaluation of proposed remedial measures. The mosaics and/or individual photographs also provided a means for current

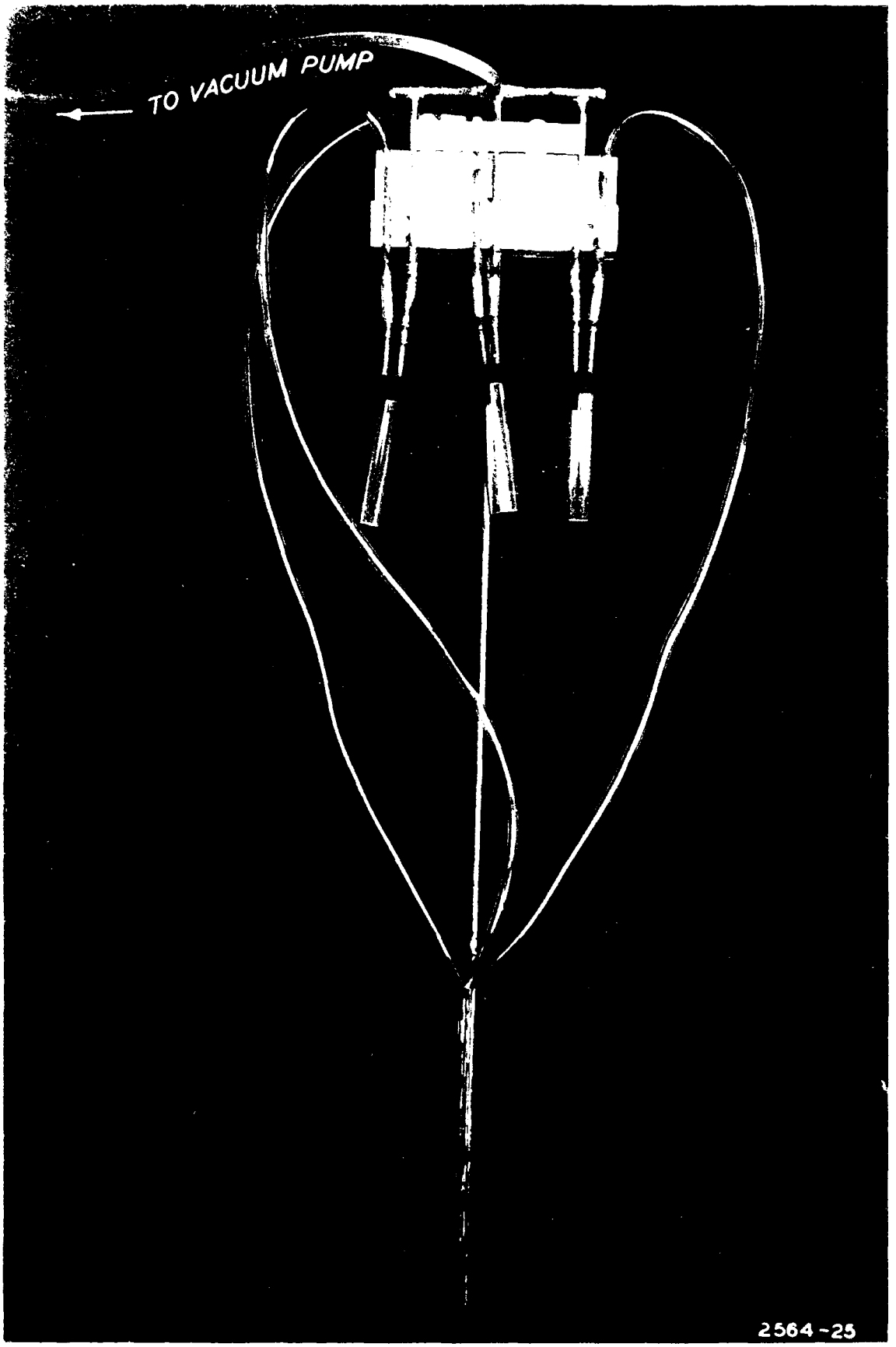

Figure 1. Vertical model water sampling system.

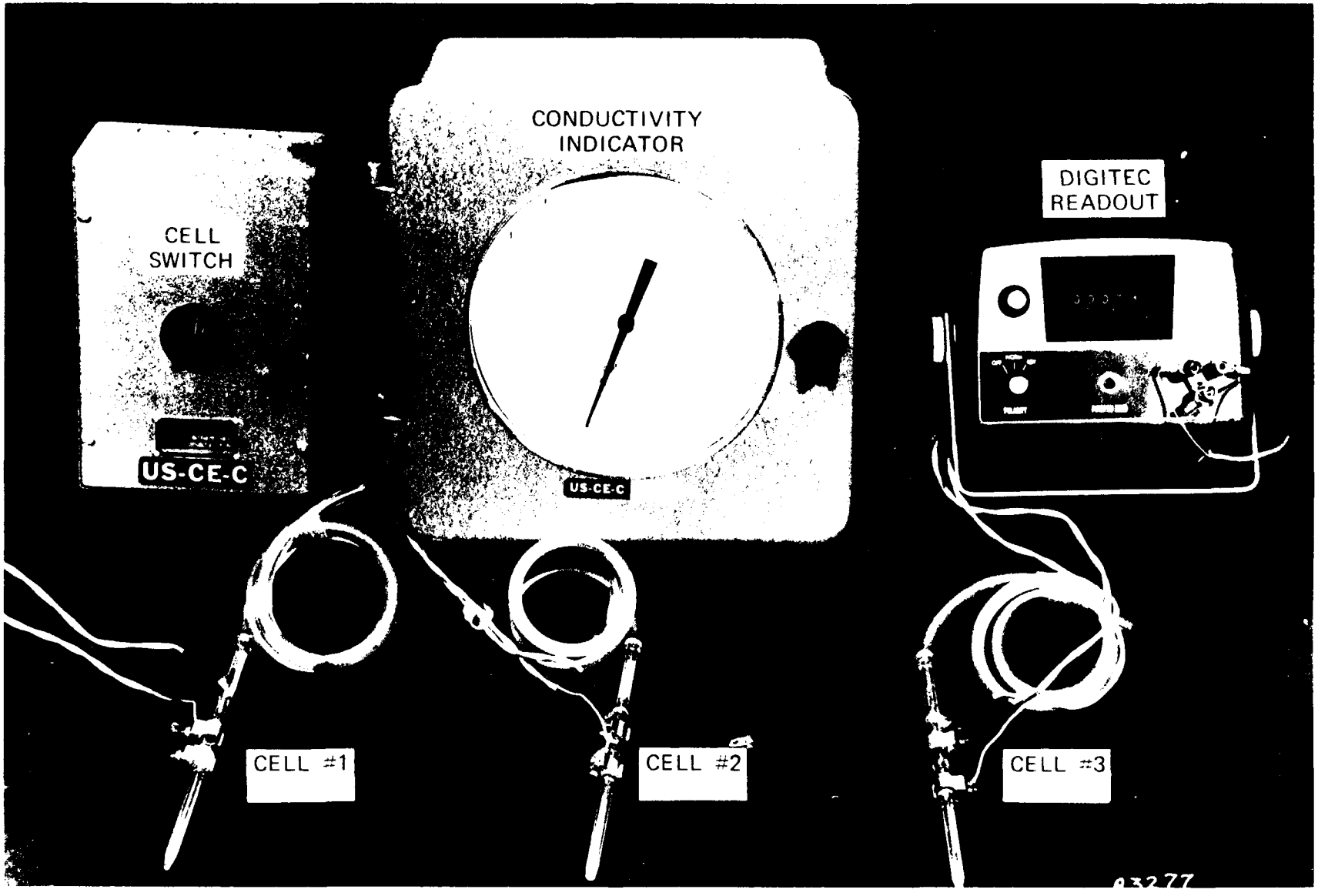

Figure 8. Physical model conductivity sampling apparatus

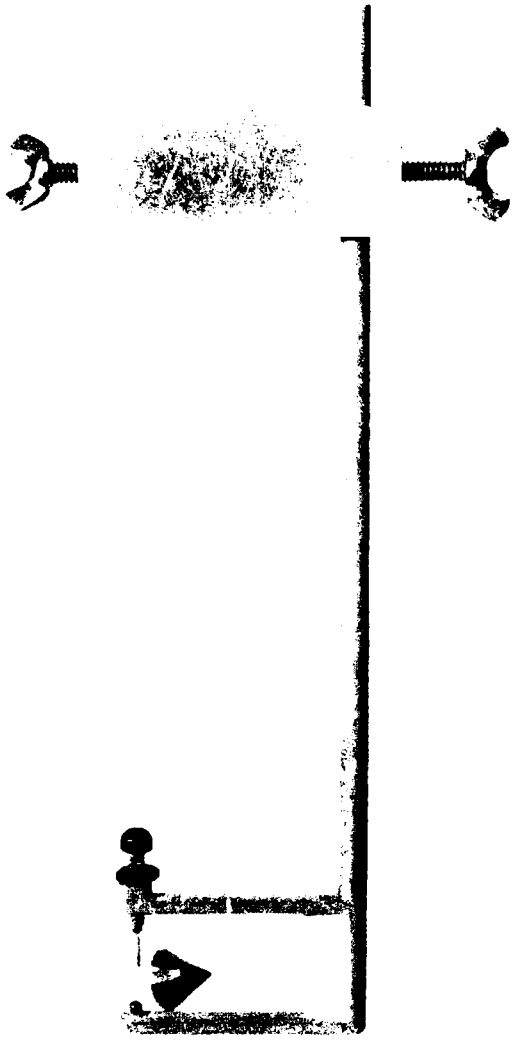

Figure 9. Physical model miniature Price-type current meter

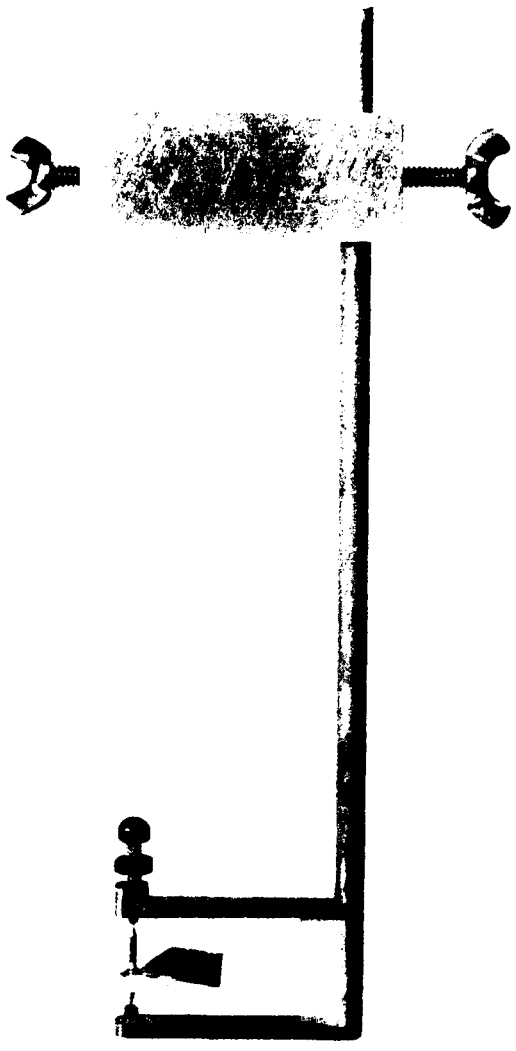

Figure 10. Physical model current direction vane

velocity analysis, especially in areas too shallow for measurements with the velocity meter. The mosaics were prepared from time-exposure photographs of confetti floating on the water's surface. A bright light that flashed immediately prior to closing of the camera lens resulted in a bright spot near the end of each confetti streak, indicating the direction of flow. Current velocities could be determined from the photographs by measuring the total length of the confetti streaks and comparing the lengths with the velocity scale presented in the mosaic or photograph. These mosaics are on file at Officer in Charge of Construction (OICC) and WES.

Accuracy of measurements

59. Point measurements of tidal elevations in the model were made with gages graduated to 0.001 ft (0.1 ft prototype) and were generally read to the nearest 0.0005 ft. Limitations of the current velocity meters used in the model should be considered in making comparisons between model and prototype velocity data. The center line of the meter cup was about 0.05 ft above the bottom of the frame; therefore, bottom velocity measurements in the model were obtained at a point comparable to 5.0 ft above the bottom in the prototype, instead of 3.0 ft as in the prototype metering program. The model velocities were determined by counting the number of revolutions in a 10-sec interval (which represented a period of about 17 min in the prototype), as compared with a 1-min observation in the prototype. The horizontal spread of the entire meter cup wheel was about 0.11 ft in the model, representing about 110 ft in the prototype, as compared with less than 1.0 ft for the prototype meter. Thus the distortion of area (model to prototype) resulted in comparison of prototype point velocities with model velocities for a much larger area. The same was true for the vertical area since the height of the meter cup was about 0.04 ft (4.0 ft prototype) as compared with only a few inches for the prototype meter.

60. The only model salinity measurements requested and analyzed were collected during the 1982-1983 pre-Trident verification effort. These measurements were made with a conductivity meter and were considered to be accurate within 0.5 ppt in the higher salinity range and 0.2 ppt in the lower range. The model samples were collected 2 ft above the bottom, middepth, and just below the surface with a fixed-multidepth sampler (Figure 7). The elevations of the model samples were relative to mean low water and did not vary with the tide as did the prototype surface and middepth samples. Model water

samples were simultaneously drawn into separate vials from the three elevations by means of a vacuum system. Similar to the model velocity data, the model salinity data also represented an average over a much larger prototype area, since the vacuum sampling system used in the model drew the sample from a radius of about 1/2 to 1 in. (8 vertical feet and 80 horizontal feet prototype).

The Numerical Modeling System, TABS-2

61. The numerical modeling system used in this study was Open Channel Flow and Sedimentation, TABS-2 (Thomas and McAnally 1985). TABS-2 is a collection of preprocessor and postprocessor utility codes and three main finite element computational programs. It is a two-dimensional depth-averaged modeling system. Briefly, hydrodynamic results (water-surface elevations and velocity components) from the physical model were used for input boundary forcing conditions and for verification of the numerical hydrodynamic model. Water-surface elevation and velocity solutions from this model were then used as input information in the sediment model for sediment transport and sedimentation predictions.

The finite element method

62. A brief and simplified discussion of the finite element method (FEM) is provided; for a more complete and thorough treatment see Zienkiewicz (1971), Desai (1979), or Baker (1983). The FEM is a means for obtaining an approximate solution to a system of governing equations by making certain assumptions about the form of the solution. The partial differential equations are transformed into finite element form and then solved in a global matrix system over the entire area of interest.

63. The FEM employs piecewise approximations over a number of discrete elements. The result is a large set of simultaneous equations in matrix form. The present codes execute the solution by means of a front-type solver that assembles a portion of the matrix and solves it before assembling the next portion of the matrix. The efficiency of this front solver is largely independent of bandwidth and does not require as much care in formation of the computational mesh as do traditional solvers.

64. Dependent variables (i.e., water-surface elevation, velocity, or sediment concentration) are approximated over each element by continuous

functions that interpolate in terms of unknown point (node) values of the variables. An error, defined as the deviation of the approximate solution from the correct solution, is minimized by the Galerkin method of weighted residuals. The residual, the total error between the approximate and correct solutions, is weighted by a function that is identical with the interpolating function. In the TABS-2 system these shape functions are quadratic for flow and concentration and linear for depth.

65. When boundary forcing conditions are imposed, a set of solvable simultaneous equations is created. The solution is smooth over each element and continuous over the computational network. In the flow model (RMA-2V), derivatives in time are replaced by nonlinear finite difference approximation. The solution is fully implicit and the set of simultaneous equations is solved by full Gaussian elimination, with the nonlinear terms solved by Newton-Raphson iteration. Time-stepping in the sediment code (STUDH) is performed by a Crank-Nicholson finite difference approach with a weighting factor (THETA) of 0.66.

The finite element computational network

66. The first and one of the most important steps in the numerical modeling effort was the development of the computational network or mesh. This was a geometric schematization of the entire modeled area of interest. It was composed of interconnected quadrilateral or triangular zones (elements). The corners of these elements (corner nodes) were precisely located in a fixed coordinate system and assigned a representative bed surface elevation. Midside nodes were also established between each corner node. These midside and corner nodes were the computational points in the numerical codes.

67. Several guidelines must be considered in the development of any mesh. Resolution of a problem area improves with an increase in the number of nodes and elements; but computational time, output, and overall costs also increase. A careful compromise must be achieved. Resolution must be great enough to describe the geometry and flow while maintaining a reasonable (low) number of computational points. Interior nodal points must be carefully selected to avoid sharp gradients in depth and in dependent variables (i.e., velocity or concentration), and the resulting elements must be geometrically well-structured triangles or quadrilaterals avoiding convex quadrilaterals

(boomerang-shaped) and sharp needlelike shapes. The external boundary of the mesh should be continuous and smooth.

68. An advantage of the finite element method is the ability to use randomly and irregularly spaced (in the X-Y plane) computational points. Internal and external curve-sided elements can also be used. These capabilities allow a better schematization of complex geometries while keeping the number of computational points to a minimum. Another important advantage is that increased resolution across a specific problem area or modification to an existing geometry or configuration is possible with a minimum amount of mesh refinement.

The Kings Bay computational meshes

69. A complication in the development of the Kings Bay mesh was the extensive marsh and sand flat areas that flooded and dried during each tidal cycle. A wetting and drying algorithm for these areas was developed and incorporated into both numerical models (King, Granat, and Ariathurai 1986). This routine used the sediment bed surface elevation and the water-surface elevation, as predicted during the actual model run, to determine when during the tidal cycle a specific area either dried (the water depth became too small to effectively contribute to total flow) or flooded. If the water-surface elevation during a time-step was predicted to go below a specified depth (DSET) at any node of a computational element, the entire element was deleted from the computational network for that time-step. The routine checked the predicted water depth at each time-step and restored previously dried elements to the computational network when the bed in the entire element was predicted to be a specified depth below the surface of the water (DSETD). The algorithm created new external and internal boundaries as wetting and drying occurred. The wetting and drying process required extra care during mesh development to ensure adequate resolution during periods of lower water levels, to avoid stranded pools of water, and to minimize numerical shock (instability) during the wetting and drying procedure. An associated TABS-2 postprocessor code tracked the computational mesh wetting and drying process. Time series plots of either wetted or dried elements could be obtained.

70. Ideally all testing should be conducted using the same basic resolution mesh and consistent model coefficient assignments. Through the course of this modeling project, several meshes were developed and tested as additional information was obtained and as plan channel revisions and

alternatives were requested. Every effort was made to maintain a valid testing program while adapting to new information and project design changes in a timely fashion. The three primary meshes related to model verification are summarized in Table 1 and discussed in the following paragraphs.

71. Figure 11 illustrates the finite element mesh (Mesh 1) used during the first phase of hydrodynamic and sediment testing, which included the original 1982-1983 pre-Trident channel verification and the initial plan (Plan 1) testing. The shaded areas on this figure indicate those elements that flooded and dried during the tidal cycle. This mesh consisted of 2,382 nodes and 791 elements and incorporated the revised schematization for the anticipated Trident plan channel requested by OICC through February 1984. Figure 11b shows the detail of the base and plan navigation channel. Plan revisions included the colocation of the Poseidon floating dry dock and tender and the associated relocation of the magnetic silencing facility to the north. Channel depths from the Savannah District November 1982 examination survey were used in the schematization for the verification (pre-Trident channel base) testing condition. This basic mesh, with some revisions, was used during the second phase of testing, which centered around examining several alternative routes for the Atlantic Intracoastal Waterway (AIWW). Several reports describing these investigations may be found in Granat 1987a and Granat 1987b.

72. Figure 12 illustrates the revised mesh for the final preferred AIWW alternative examined (alternate Route C), the mesh used during the 1985-1986 transitional channel verification effort. This mesh maintained the same horizontal schematization for the pre-Trident channel area used during the 1982-1983 verification effort, but also incorporated the revised schematization required for the OICC-requested Trident plan channel revisions through January 1985. These revisions, shown in detail in Figure 12b, included (a) plan channel widening to the northeast of the first bend inside Cumberland Sound, (b) better schematization of the areas east of and including Drum Point Island based on a Savannah District August 1985 condition survey, (c) relocation of the magnetic silencing facility to the northeast associated with the anticipated AIWW relocation, (d) smoothing of the transition between the magnetic silencing facility and the waterfront docking area west of the Poseidon floating dry dock, (e) extension of the waterfront docking area to the northwest, widening the entrance to Kings Bay, (f) gradual widening of lower Kings Bay along the west side between the marginal wharf and the small boat facility,

and (g) squaring off the corner of the upper turning basin adjacent to the Trident dry dock.

73. The submarine channel geometry (depth) condition schematized for the 1985-1986 transitional channel verification effort was based on the Savannah District January 1985 examination survey. This mesh consisted of 885 elements and 2,611 computational nodes. This same mesh with various alternative channel depth schematizations was used during phase 3 testing to examine submarine channel advance maintenance dredging as a means of selecting the channel depths that would minimize maintenance dredging requirements.

74. Figure 13 illustrates the revised mesh (Mesh 4) developed prior to and in anticipation of phase 4 testing, which involved examining potential upper basin remedial measures. The mesh developed during the 1985-1986 verification was the starting point for the additional revisions that increased mesh resolution in the areas north and west of Kings Bay. The remedial measures requiring the additional resolution, shown in Figure 13b, included (a) a tide gate barrier above the planned turning basin, (b) a sediment trap below the tide gate but above the turning basin, and (c) additional channelization from the upper end of Kings Bay into the south fork of the Crooked River through either Marianna Creek or the back channel around Big Crab Island. The geometry (depth) schematized during the Mesh 4 verification effort included the November 1982 depth conditions everywhere except for the area east of and including Drum Point Island, which included the August 1985 revised depth conditions. This revised mesh consisted of 1,118 elements and 3,224 nodes. A previous node depth assignment error resulting in an anomalous hole north of the channel across from Fort Clinch was also corrected prior to Mesh 4 testing.

The hydrodynamic numerical model, RMA-2V

75. The first main numerical model program, A Two-Dimensional Model for Free Surface Flows, RMA-2V, is a finite element solution of the Reynolds form of the Navier-Stokes equations for turbulent flows. It solves the depth-integrated equations of conservation of mass and momentum in two horizontal directions and provides hydrodynamic solutions for water-surface elevations

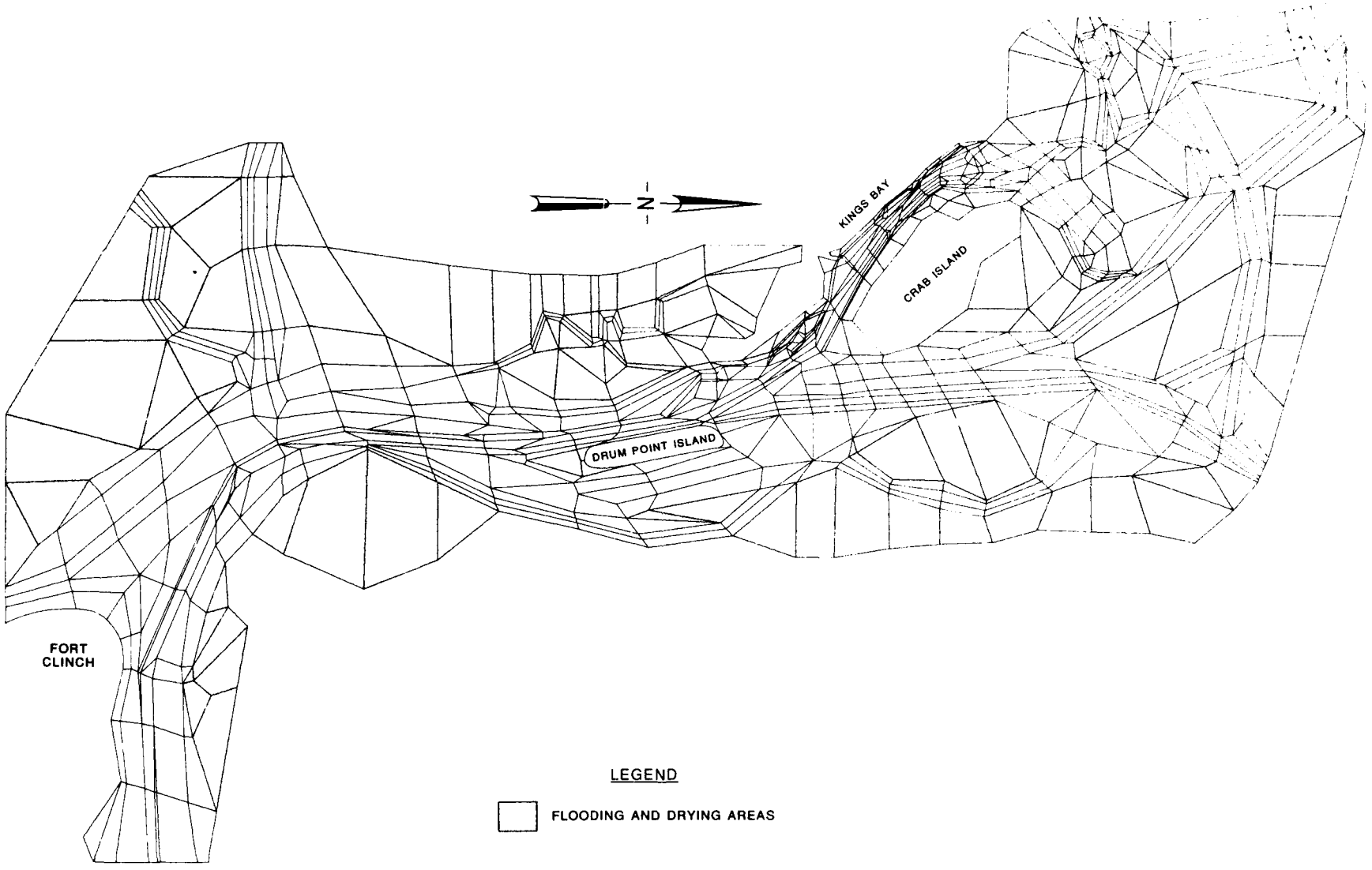

a. Complete computational area

Figure 11. Numerical model Mesh 1 (Continued)

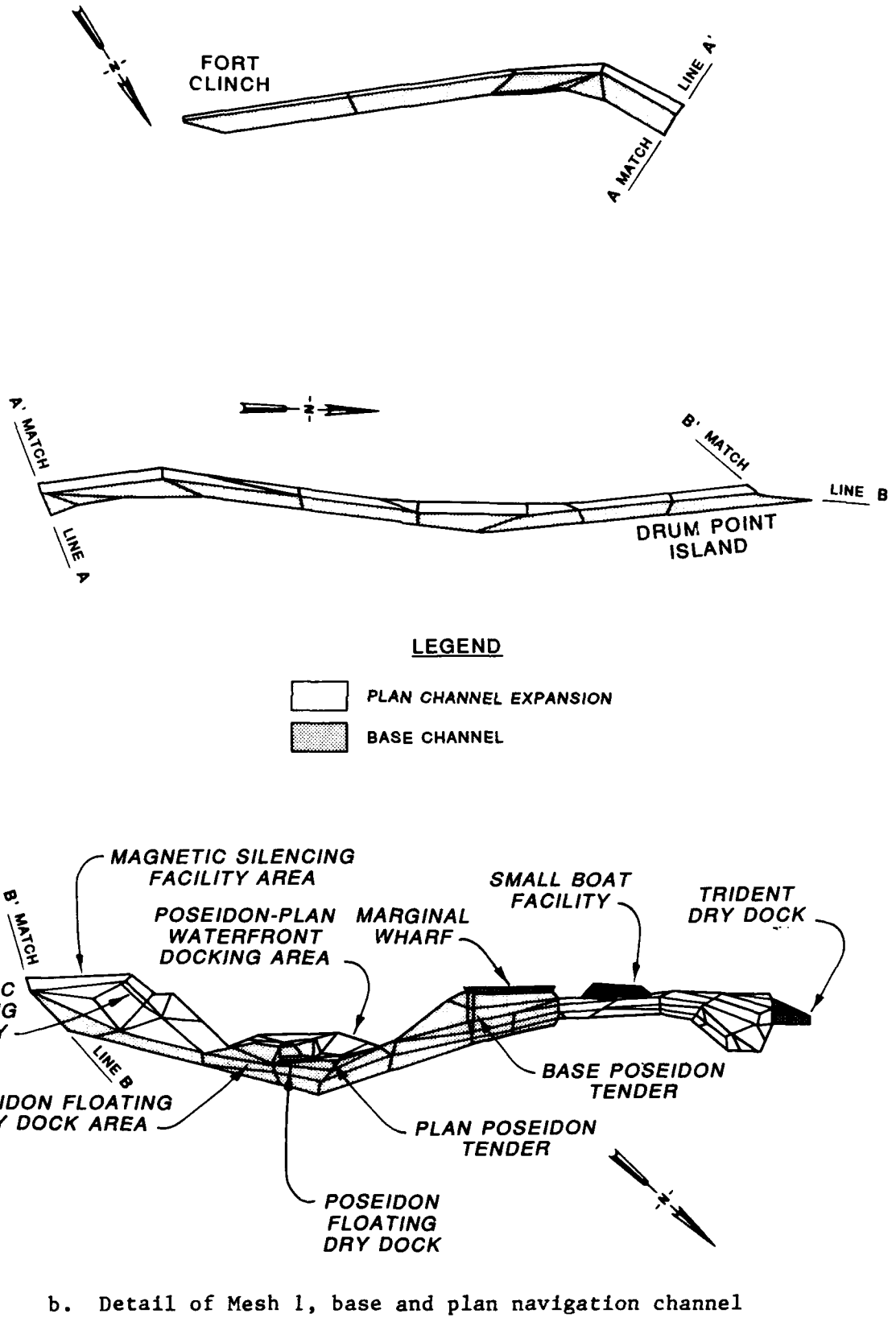

b. Detail of Mesh 1, base and plan navigation channel

Figure 11. (Concluded)

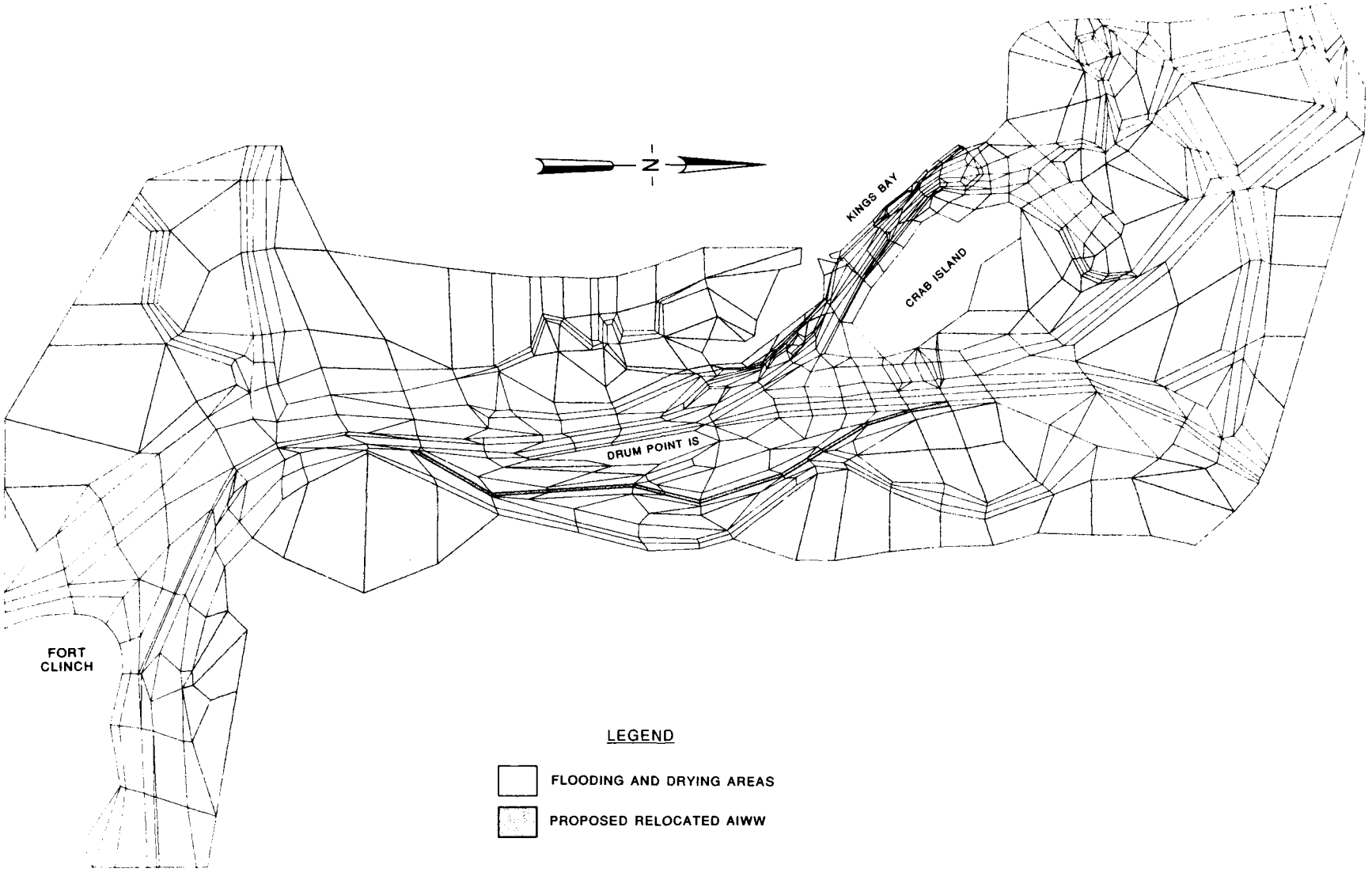

a. Complete computational area

Figure 12. Numerical model transitional channel mesh (Continued)

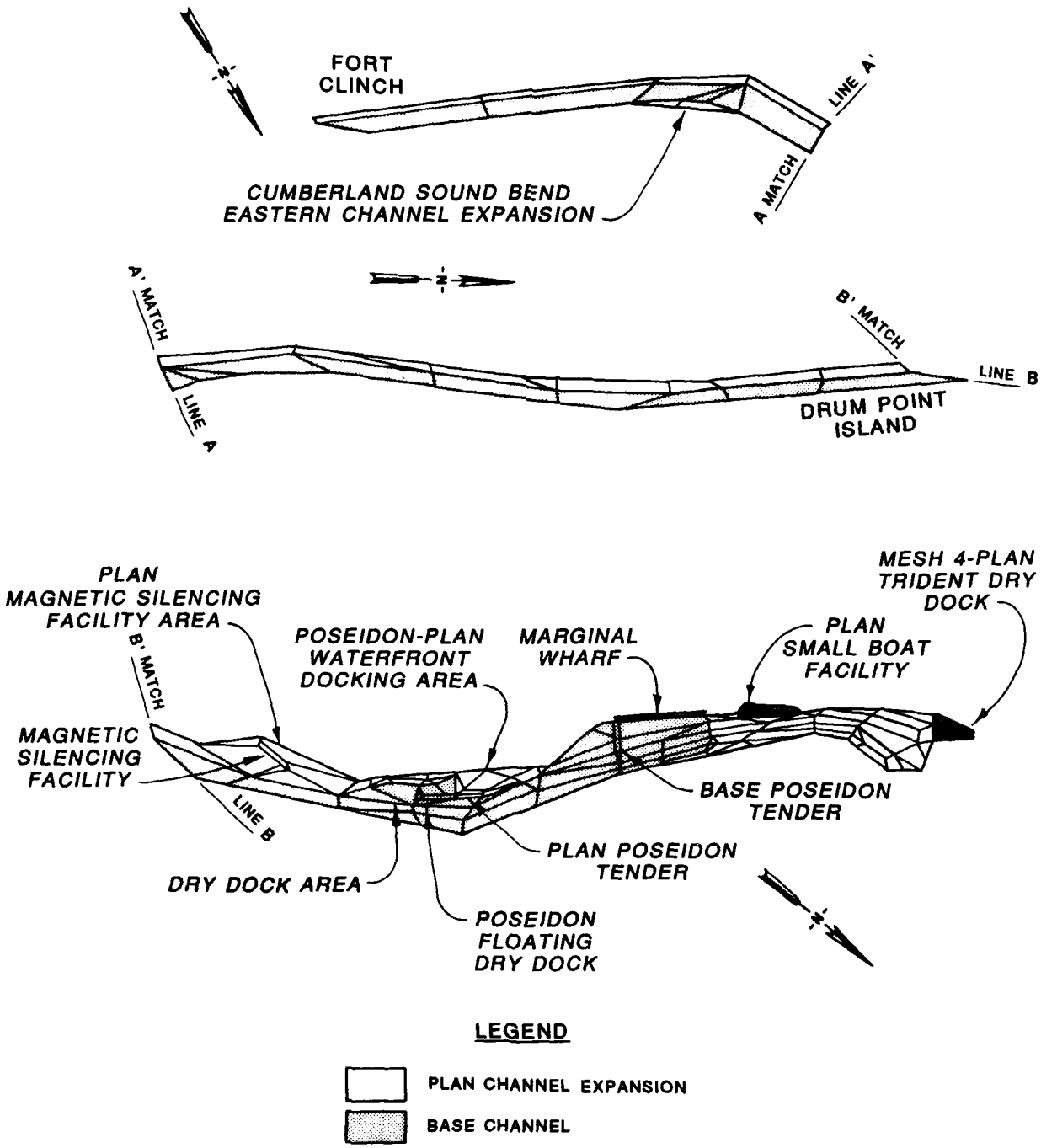

b. Detail of transitional channel mesh, base and plan navigation channel

Figure 12. (Concluded)

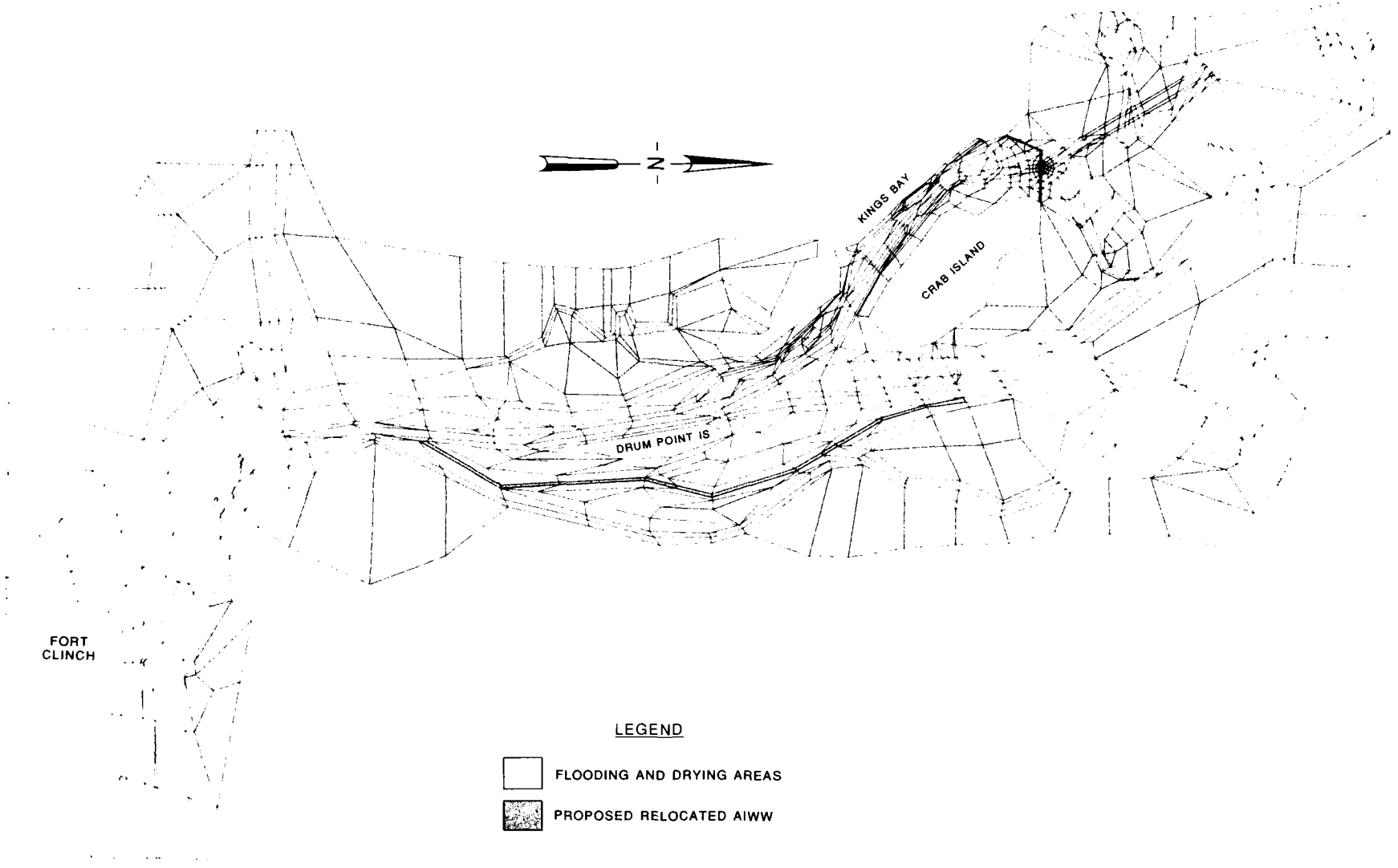

a. Complete computational area

Figure 13. Numerical model Mesh 4 (Continued)

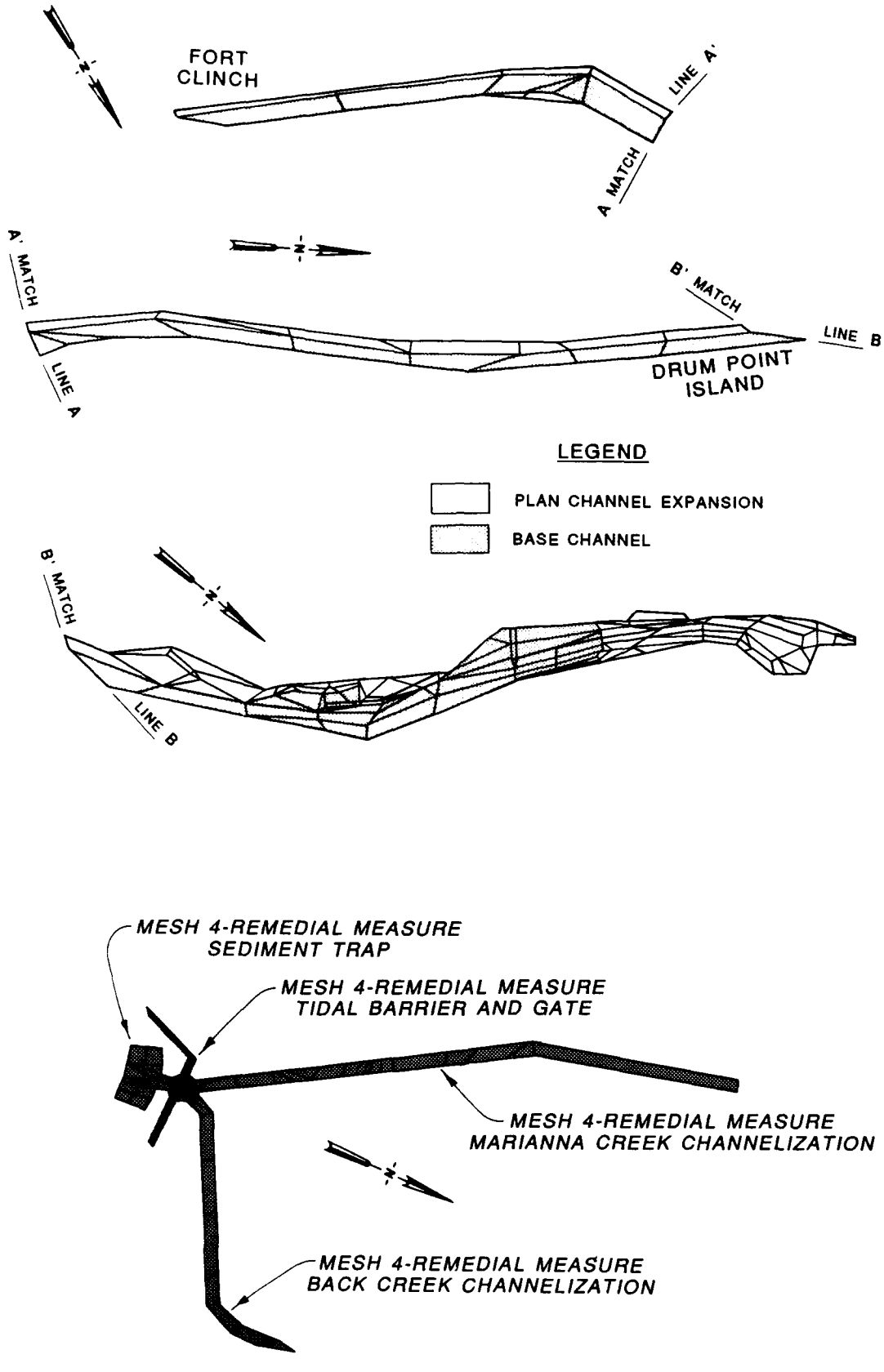

b. Detail of Mesh 4, base and plan navigation channel and potential remedial measures

Figure 13. (Concluded)

and horizontal velocity components. The form of the solved equations is as follows:

$$h\frac{\partial u}{\partial t} + hu\frac{\partial u}{\partial x} + hv\frac{\partial u}{\partial y} - \frac{h}{\rho}\left(\varepsilon_{xx}\frac{\partial^2 u}{\partial x^2} + \varepsilon_{xy}\frac{\partial^2 u}{\partial y^2}\right) + gh\left(\frac{\partial a}{\partial x} + \frac{\partial h}{\partial x}\right)$$

$$+ \frac{gun^2}{\left(1.486h^{1/6}\right)^2}\left(u^2 + v^2\right)^{1/2} - \zeta V_a^2 \cos\psi - 2h\omega v \sin\phi = 0 \qquad (1)$$

$$h\frac{\partial v}{\partial t} + hu\frac{\partial v}{\partial x} + hv\frac{\partial v}{\partial y} - \frac{h}{\rho}\left(\varepsilon_{yx}\frac{\partial^2 v}{\partial x^2} + \varepsilon_{yy}\frac{\partial^2 v}{\partial y^2}\right) + gh\left(\frac{\partial a}{\partial y} + \frac{\partial h}{\partial y}\right)$$

$$+ \frac{gvn^2}{\left(1.486h^{1/6}\right)^2}\left(u^2 + v^2\right)^{1/2} - \zeta V_a^2 \sin\psi + 2\omega hu \sin\phi = 0 \qquad (2)$$

$$\frac{\partial h}{\partial t} + h\left(\frac{\partial u}{\partial x} + \frac{\partial v}{\partial y}\right) + u\frac{\partial h}{\partial x} + v\frac{\partial h}{\partial y} = 0 \qquad (3)$$

where

h = depth

u,v = velocities in the Cartesian directions

x,y,t = Cartesian coordinates and time

ρ = density

ε = eddy viscosity coefficient, for xx = normal direction on x-axis surface; yy = normal direction on y-axis surface; xy and yx = shear direction on each surface

g = acceleration due to gravity

a = elevation of bottom

n = Manning's n value

1.486 = conversion from SI (metric) to non-SI units

ζ = empirical wind shear coefficient

V_a = wind speed

ψ = wind direction

ω = rate of earth's angular rotation

ϕ = local latitude

76. The original code, RMA-2, was developed by Norton, King, and Orlob (1973) of Water Resources Engineers, for the US Army Engineer District, Walla Walla. Enhancements to the original code were made by Norton and King (1977) of Resource Management Associates, and by the WES Hydraulics Laboratory (Thomas and McAnally 1985). The present version of the code, RMA-2V, was formulated in terms of velocity and was streamlined for vector processing. Manning's n roughness coefficients were used in simulating bottom friction, and eddy viscosity coefficients were used in defining turbulent exchanges. Boundary conditions were specified as water level, velocity, or discharge; and external or side boundaries were treated as either slip (parallel flow) or static (stagnation point, zero velocity). As will be discussed in the verification section, specified marsh area elevation was found to be an important variable that influenced hydrodynamic results.

The sediment model, STUDH

77. The second main program, Sediment Transport in Unsteady 2-Dimensional Flows, Horizontal Plane, STUDH, uses the finite element approach in solving the depth-integrated convection-diffusion equation in two horizontal dimensions for a single sediment constituent. The basic form of the convection-diffusion equation is

$$\frac{\partial C}{\partial t} + u\frac{\partial C}{\partial x} + v\frac{\partial C}{\partial y} = \frac{\partial}{\partial x}\left(D_x \frac{\partial C}{\partial x}\right) + \frac{\partial}{\partial y}\left(D_y \frac{\partial C}{\partial y}\right) + \alpha_1 C + \alpha_2 = 0 \qquad (4)$$

where

C = concentration of sediment

u = depth-integrated velocity in x-direction

v = depth-integrated velocity in y-direction

D_x = dispersion coefficient in x-direction

D_y = dispersion coefficient in y-direction

α_1 = coefficient of concentration-dependent source/sink term

α_2 = coefficient of source/sink term

The source/sink terms were computed in routines that treated the interaction of the flow and the bed. Separate sections of the code handled computations for cohesive (clay and silt) and noncohesive (sand and silt) materials.

78. The original program was developed by Dr. Ranjan Ariathurai under the direction of Dr. R. B. Krone at the University of California, Davis, CA

(UCD). The basic program was extended under the US Army Corps of Engineers Dredged Material Research Program, resulting in the generalized computer program SEDIMENT II (Ariathurai, MacArthur, and Krone 1977). Major revisions to this program were performed by personnel of the WES Hydraulics Laboratory and Dr. Ariathurai, Resource Management Associates, under the US Army Corps of Engineers research program, Improvement of Operations and Maintenance Techniques, culminating in the present version of STUDH, which was applicable for both cohesive and noncohesive sediments (Thomas and McAnally 1985).

79. For noncohesive sediments, the supply of sediment to or from the bed was controlled by the transport potential of the flow and the availability of material in transport or on the bed. The potential sand transport capacity for the specified flow condition was calculated using a transport power (work rate) formulation developed by Ackers and White (1973). Briefly, it is based upon a dimensionless grain size and a sediment mobility parameter. The Manning shear stress equation

$$u_* = \frac{(\bar{u}n)\sqrt{g}}{CME\ (h)^{1/6}} \tag{5}$$

where

u_* = shear velocity

$\bar{u}$ = mean flow velocity

n = Manning's roughness value (assigned)

CME = coefficient of 1 for SI (metric) units and 1.486 for non-SI units

h = water depth

was used for computing bed shear stress, τ_b, using

$$\tau_b = \rho(u_*)^2 \tag{6}$$

where ρ is the water density.

80. The total load transport function of Ackers and White provided a potential sediment concentration G_p. This value was the depth-averaged concentration of sediment that would occur under the given hydrodynamic conditions (determined in RMA-2V) if an equilibrium transport rate was reached with an unlimited supply of sediment. The rate of sediment deposition (or erosion) was then computed as

$$R = \frac{G_p - C}{t_c} \tag{7}$$

where

R = rate (depositional if $C > G_p$ or erosional if $C < G_p$)

G_p = potential concentration

C = actual concentration

t_c = time constant

81. The finite element approach was used in solving the convection-diffusion equation for the entire computational network. The major input coefficients used in the noncohesive modeling included sediment grain characteristics (size, shape, specific gravity, settling velocity), bed roughness (Manning's n) values, and effective diffusion.

82. For cohesive sediments, the smooth-wall log velocity profile

$$\frac{\bar{u}}{u_*} = 5.75 \log \left(3.32 \frac{u_* h}{\nu} \right) \tag{8}$$

where ν is the kinematic viscosity of water, was used to calculate the bed shear stress. Deposition rates were calculated with the equations of Krone (1962):

$$S = \begin{cases} -\frac{2V_s}{h} C \left(1 - \frac{\tau_b}{\tau_d} \right) & \text{for } C < C_c \quad (9) \\ -\frac{2V_s}{hC_c^{4/3}} C^{5/3} \left(1 - \frac{\tau_b}{\tau_d} \right) & \text{for } C > C_c \quad (10) \end{cases}$$

where

S = source term

V_s = fall velocity of a sediment particle

h = flow depth

C = sediment concentration in water column

τ_d = critical shear stress for deposition

C_c = critical concentration = 300 mg/ℓ

Erosion rates were computed by Ariathurai's simplification (Ariathurai, MacArthur, and Krone 1977) of Partheniades' (1962) results for particle by particle erosion:

$$S = \frac{P}{h}\left(\frac{\tau_b}{\tau_e} - 1\right) \quad \text{for } \tau_b > \tau_e \tag{11}$$

where

P = erosion rate constant

τ_e = critical shear stress for erosion

83. Mass failure of a bed layer was possible when the bed shear stress, τ_b, exceeded the bulk shear strength τ_s of the layer. The erosion rate source term is

$$S = \frac{T_L \rho_L}{h\Delta t} \quad for \quad \tau_b > \tau_s \tag{12}$$

where

T_L = thickness of the failed layer

ρ_L = density of the failed layer

Δt = time interval over which failure occurs

84. The major input coefficients used in the cohesive sediment code included the critical shear stress for deposition, the particle settling velocity, the critical shear stress for particle erosion, the erosion rate constant, the bed structure, the density and bulk shear strength of each bed layer, and the effective diffusion.

PART IV: VERIFICATION OF THE PHYSICAL MODEL

Prototype Surveys

85. Two WES field surveys were undertaken in the prototype to obtain hydrodynamic and salinity data for use in verifying the Kings Bay physical model. The first survey, conducted on 10 and 12 November 1982, focused on Kings Bay and those areas to the south. The second survey was conducted on 26 January 1985 and focused on the areas west and north of Drum Point Island, including Kings Bay. These surveys are described in Part II. Selected data from a third survey collected by the USGS on 14 July 1982 (Radtke 1985) were also used in the verification process.

Verification Procedures

86. The pre-Trident channel verification of the physical model (1982-1983) was accomplished in three stages (tide, velocity, and salinity). The freshwater discharge for the November 1982 verification was 1,000 cfs for the St. Marys River and 100 cfs for the Crooked River. Hydraulic verification ensured that tidal elevations and current velocities were in proper agreement with the prototype (the natural system). Salinity verification ensured that salinity phenomena in the model corresponded to those of the prototype for similar conditions of tide, ocean salinity, and freshwater discharge.

87. During hydraulic verification of the tides, tide generator operation and model roughness amount and distribution were adjusted in such a manner that the tides generated in the model ocean would accurately reproduce prototype tidal phase (time of arrival) and water-surface elevations throughout the model.

88. Verification of current velocities was accomplished by reproducing each of the two tidal conditions (10 and 12 November) in turn and adjusting the model roughness distribution (while retaining the total amount of roughness from the initial tidal adjustment) until current velocities at each metering station were reproduced in the model to an acceptable accuracy while maintaining acceptable tidal reproduction. This procedure involved switching back and forth from tidal adjustment to current adjustment and from one

prototype condition to the other until the optimum correspondence was achieved between model and prototype results.

89. Verification of salinities in the model required maintaining proper salinity in the model ocean and accurately reproducing prototype currents and mixing conditions. The latter reproduction was accomplished without any redistribution of roughness as developed in the velocity verification process.

90. The model operation procedures and roughness distribution developed during these verification steps were used in initial plan channel testing. A similar procedure, involving some additional roughness and geometry adjustments in the areas north of Kings Bay, was used to establish the conditions for the 1985 transitional channel verification process and in all subsequent testing.

1982 Pre-Trident Verification

Tidal verification

91. The objective of the physical model tidal verification was to obtain an accurate reproduction of prototype tidal elevations and phases throughout the model. Prototype tidal data from nine recording tide gages (Figure 14) were available to verify the accuracy of the model tidal adjustment to the 1982 data.

92. Comparison of model and prototype tidal data for the two primary tide conditions reproduced in the model for the November 1982 period are presented in Plates B1-B6. These plates show tidal elevations for the 10 November 1982 (Plates B1-B3) and 12 November 1982 (Plates B4-B6) tidal conditions at the nine tide gage locations: St. Marys entrance south jetty (station 1; this was the tide control station during verification), Fernandina Beach Marina (station 2), St. Marys River City Dock (station 3), Cumberland Island (station 4), Lower Kings Bay Dock (station 5), Marianna Creek (station 6), northern Cumberland Sound (station 8), Crooked River State Park (station 9), and Upper Crooked River (station 10).

93. Model-to-prototype verification showed that tidal elevations, tidal ranges, and tidal phases for the 10 November 1982 conditions were in good agreement. The greatest discrepancy observed during the low-water period occurred at stations 3 and 10, St. Marys River and Upper Crooked River, respectively. Each of these stations was located in an area of the model

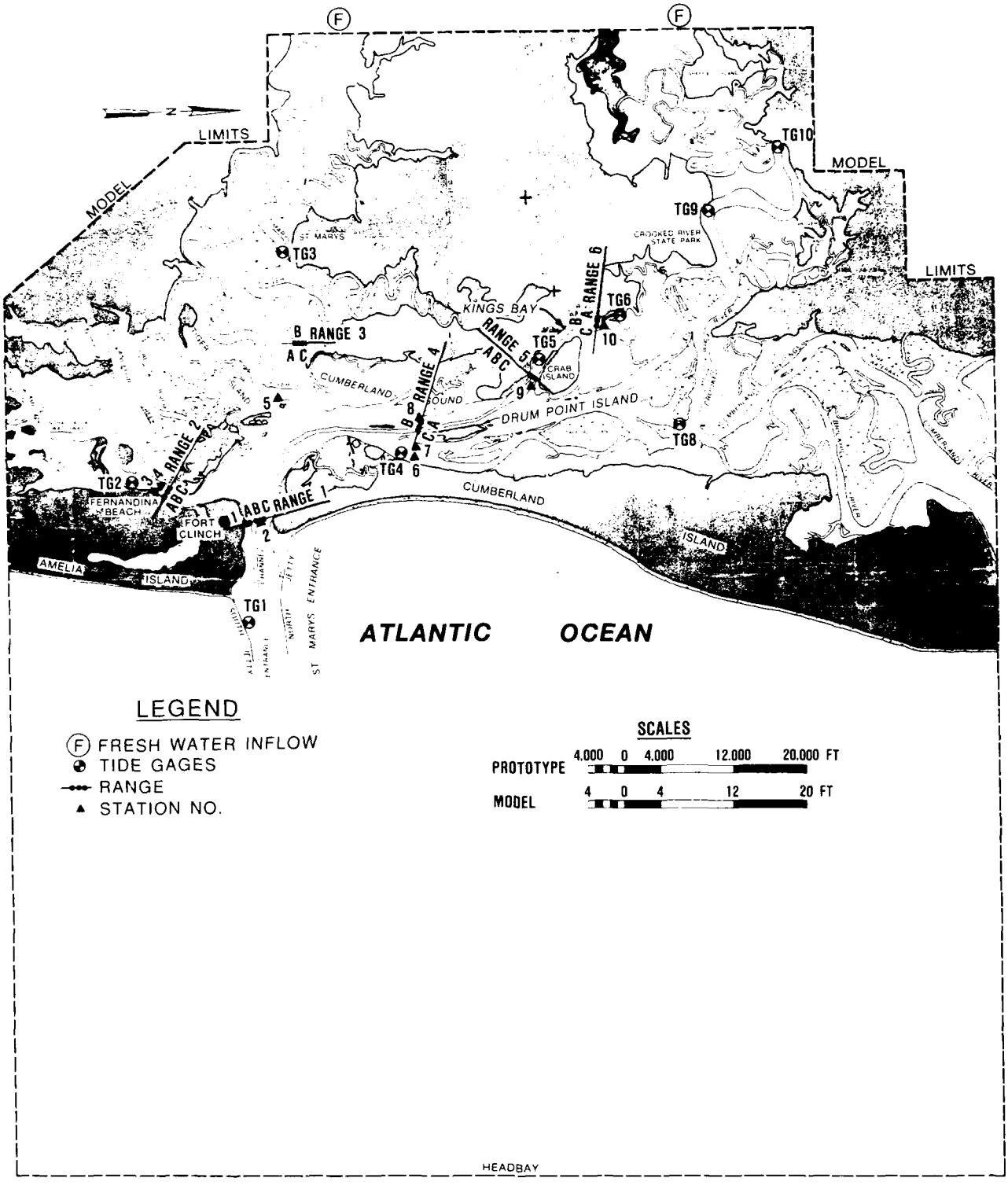

Figure 14. Pre-Trident November 1982 verification station location map

which was molded to old bathymetric data (1934-1935). The greatest discrepancy in phase and high-water elevation occurred at station 8, located in northern Cumberland Sound near the confluence of the Crooked River and Cumberland Dividings. Tide ranges throughout the model were slightly less than that in the prototype.

94. Model and prototype tidal elevations, tidal ranges, and tidal phases for the 12 November 1982 period were in good agreement. As observed with the 10 November 1982 period, stations 3, 8, and 10 showed the greatest discrepancy between model and prototype. Tide ranges observed throughout the model were again generally slightly less than the prototype for this period.

Current velocity verification

95. The objective of the current velocity verification was to obtain an accurate reproduction of prototype current velocities and flow distributions (lateral, vertical, and longitudinal) throughout the model. Prototype current velocity data were available at 16 stations on 6 ranges for the 10 November 1982 condition and at 9 stations on 3 ranges for the 12 November 1982 condition. Locations of comparison stations are shown in Figure 14.

96. Comparisons of model and prototype current velocities for all stations on each prototype survey date are shown in Plates B7-B28. Surface, middepth, and bottom measurements were generally taken at 1-hr intervals in the field and at 30-min intervals in the model. Model data curves represent averaged data from three identical model runs. These averaged data points were plotted and smooth curves were drawn through the points. The overall agreement between prototype and model is considered to be very satisfactory.

97. The 10 November and 12 November 1982 data collection periods will be discussed separately because prototype conditions on those two days were different and different stations were monitored. Stations monitored on 10 November were south of Kings Bay and included stations 1A, 1B, 1C, 2A, 2B, 2C, 3, 3A, 3B, 3C, 4A, 4B, 4C, 5, 6, and 7. Stations monitored on 12 November were west and north of Drum Point Island and included stations 4A, 4B, 4C, 5A, 5B, 5C, 6A, 6B, and 6C. Alphanumeric stations were over-the-side observations and numeric stations were long-term middepth observations.

98. 10 November 1982. Data at range 1 (Plates B7-B9), across St. Marys Inlet, show excellent agreement between model and prototype. Missing prototype velocity values were the result of excessive wire angles (horizontal current meter displacement) associated with high current velocities.

Interpolating between available points, it appears that the model was reproducing the maximum prototype ebb currents to an acceptable degree. Bottom maximum ebb currents in the model appear to have been slightly higher than prototype.

99. At range 2 (Plates B10-B12), located in the Amelia River, model maximum flood current velocities were generally higher than prototype. Due to a meter malfunction, no prototype over-the-side maximum ebb current velocity data were obtained at this range. Endeco current meter data collected at station 3 (Plate B13), also located in Amelia River about 1,500 ft upstream from range 2, showed that the model was reproducing maximum ebb currents fairly well and that maximum flood currents were lower than those observed in the prototype.

100. In the St. Marys River (range 3), model maximum ebb and flood current velocities (Plates B14-B16) were generally higher than observed in the prototype. Ebb velocity differences were more numerous than flood differences. The greatest differences occurred at the bottom depths. As discussed in paragraphs 49 and 93, these differences may be associated with localized geometry differences between the model (based on 1934-1935 bathymetric data) and the 1982 field conditions.

101. Station 5 (Plate B17), located in the mouth of the Jolly River, showed excellent agreement between model and prototype. Maximum flood currents were generally higher in the model than observed in the prototype. Maximum ebb current velocities showed excellent agreement.

102. Range 4 data consisted of stations 4A, 4B, and 4C, located on the west side of Drum Point Island, and stations 6 and 7, located on the east side of Drum Point Island. Plates B18-B20 and B21 and B22, respectively, demonstrated that the model was reproducing current velocities and phases properly at this critical Cumberland Sound cross section.

103. 12 November 1982. Stations 4A, 4B, and 4C (Plates B23-B25) were also monitored on 12 November. Model current velocities at these stations were again in very close agreement with the prototype. Station 4A demonstrated the best agreement, as maximum current velocities and phase were extremely close to the prototype measurements. Model current velocities at station 4B were in good agreement; however, maximum ebb and flood current velocities at the surface and middepth were slightly lower than prototype. Bottom depth current velocities at station 4B were in excellent agreement with

the prototype. Station 4C followed the same trend as was observed at 4B, as maximum current velocities at the surface and middepth were lower than prototype. The bottom depth current velocities were in excellent agreement. At each station, model velocity phase was in excellent agreement with that observed in the prototype. No prototype data were available at stations 6 and 7 for the 12 November 1982 sampling period.

104. As the 12 November 1982 verification progressed, the low prototype current velocity data at range 5, across the entrance to Kings Bay, appeared to be inconsistent with other measurements and possibly in error because of meter malfunction (Plates B26-B28). Verification of this critical range was demonstrated with model velocity comparisons to an earlier prototype field exercise conducted by USGS on 14 July 1982 (Radtke 1985). The data were not synoptic with the other field data used for verification, which severely limited their usefulness, but they served to confirm that the model was behaving correctly at the entrance to Kings Bay.

105. Model tide reproduction of the 14 July 1982 water levels at tide stations 1 and 5 are shown in Plates B29 and B30. For velocity comparison, model station 5A corresponded to USGS station numbered boat 5, model station 5B to USGS Boat 3, and model station 5C to USGS boat 1. The comparison of USGS prototype current velocity data and model data is shown in Plates B31-B33. These data show that the model was reproducing currents correctly at this critical location. Phase and maximum currents were in excellent agreement with the 14 July 1982 data.

106. Current velocities measured at range 6 (Plates B34-B36), located above the Poseidon Kings Bay operational area, showed excellent agreement with the prototype data collected on 12 November. Slack periods were in good agreement as were maximum current velocities at this range. In most instances, range 6 model currents were slightly less than those observed in the prototype.

Salinity verification

107. The objective of the model salinity verification was to demonstrate an accurate reproduction of vertical, lateral, and longitudinal distributions of prototype salinities throughout the model. Salinity observations were made hourly in the prototype and in the model. Averaged data from two identical model tests were plotted versus time and smooth curves drawn through the points. Comparison of prototype and model data is shown in

Plates B37-B57. As previously stated, no additional model roughness adjustments were made for salinity verification. The agreement demonstrated between model and prototype data is considered good.

108. 10 November 1982. Salinity data for this period were available at ranges 1, 2, 3, and 4. These data are presented in Plates B37-B48. Comparison of model and prototype salinities at range 1, in St. Marys Inlet (Plates B37-B39), shows that the model salinity values were slightly higher than prototype. Model salinity values observed at range 2, in Amelia River (Plates B40-B42), were slightly lower than prototype during periods of maximum intrusion (high-water slack) and very close to prototype values at periods of low-water slack. Comparison of model and prototype salinity values at range 3, located in the St. Marys River (Plates B43-B45), showed that the model high-water slack salinities were slightly higher than prototype while low-water slack salinities values were slightly lower than prototype. No significant differences were noted in regard to depth nor from one station to another on this range. Salinities observed in the model at range 4 across Cumberland Sound, south of Kings Bay (Plates B46-B48), were generally higher than prototype throughout the tidal cycle.

109. 12 November 1982. Prototype salinity data for this verification period were available at ranges 4, 5, and 6 and are presented with model data in Plates B49-B57. Model salinities at range 4 (Plates B49-B51), as with the 10 November data set, were generally higher than the prototype throughout the tidal cycle. Model salinities at ranges 5 and 6 (Plates B52-B57) were generally very close to the observed prototype values. The greatest difference at either of these ranges occurred at station 5A (Plate B52), where model salinities were slightly higher than those in the prototype for the 12 November 1982 period.

1985 Transitional Period Verification

110. Following model verification to the 1982 pre-Trident channel prototype data set and a period of hybrid model plan testing, it was determined, primarily from test results and model observations, that the flow characteristics north of Kings Bay had a major influence on hydrodynamic and sedimentation processes within Kings Bay and the adjacent areas. An additional hydrodynamic verification effort was, therefore, undertaken for this area of the

model. No additional effort was made to verify salinity conditions.

111. As described in paragraph 85 and Part II of this report, the field survey was carried out on 26 January 1985. The meteorological conditions prior to and during this field effort were far from ideal for a verification data set (i.e., wind effects are not reproducible in the physical model); however, critical time schedules and contracts required that the effort be undertaken. The meteorological influences on the field data should be considered when comparing model and prototype data.

112. Prior to the initiation of the January 1985 transitional channel model verification, the model geometry for Kings Bay and the navigation channel was revised to reflect Savannah District January 1985 bathymetric conditions. These conditions included the recently dredged 48-ft-deep upper Trident basin located above the Poseidon Kings Bay operational area. The procedure followed during this verification period was very similar to that followed during the November 1982 verification period; however, care was taken to leave intact the existing roughness south of Kings Bay (the area previously verified to November 1982 prototype data). As the verification effort progressed, additional bathymetric (geometry) changes in the channels north of Kings Bay and additional roughness adjustments in northern Cumberland Sound, Cumberland Dividings, Cumberland River, and Crooked River were made to achieve the final verification. These revisions, made necessary by bathymetric changes in the prototype since the available hydrographic maps were prepared (i.e., 1935), were based on more recent information obtained from aerial photographs and small boat surveys. The St. Andrew labyrinth system discussed in paragraph 47 was also adjusted to improve hydrodynamic conditions reproduced for the 1985 transitional channel data set.

Tidal verification

113. Prototype tidal data from four recording tide stations were available for model verification to the 1985 field conditions (Figure 15). Comparison of model and prototype tide data are presented in Plates C1 and C2. These plates show model and prototype tidal elevations at station 1 (St. Marys entrance, south jetty; same location as 1982 verification), station 2 (lower Kings Bay dock; station 5 during the 1982 verification), station 3 (Crooked River State Park; station 9 during 1982 verification), and station 4 (northern Cumberland Sound; station 8 during 1982 verification). These data show that

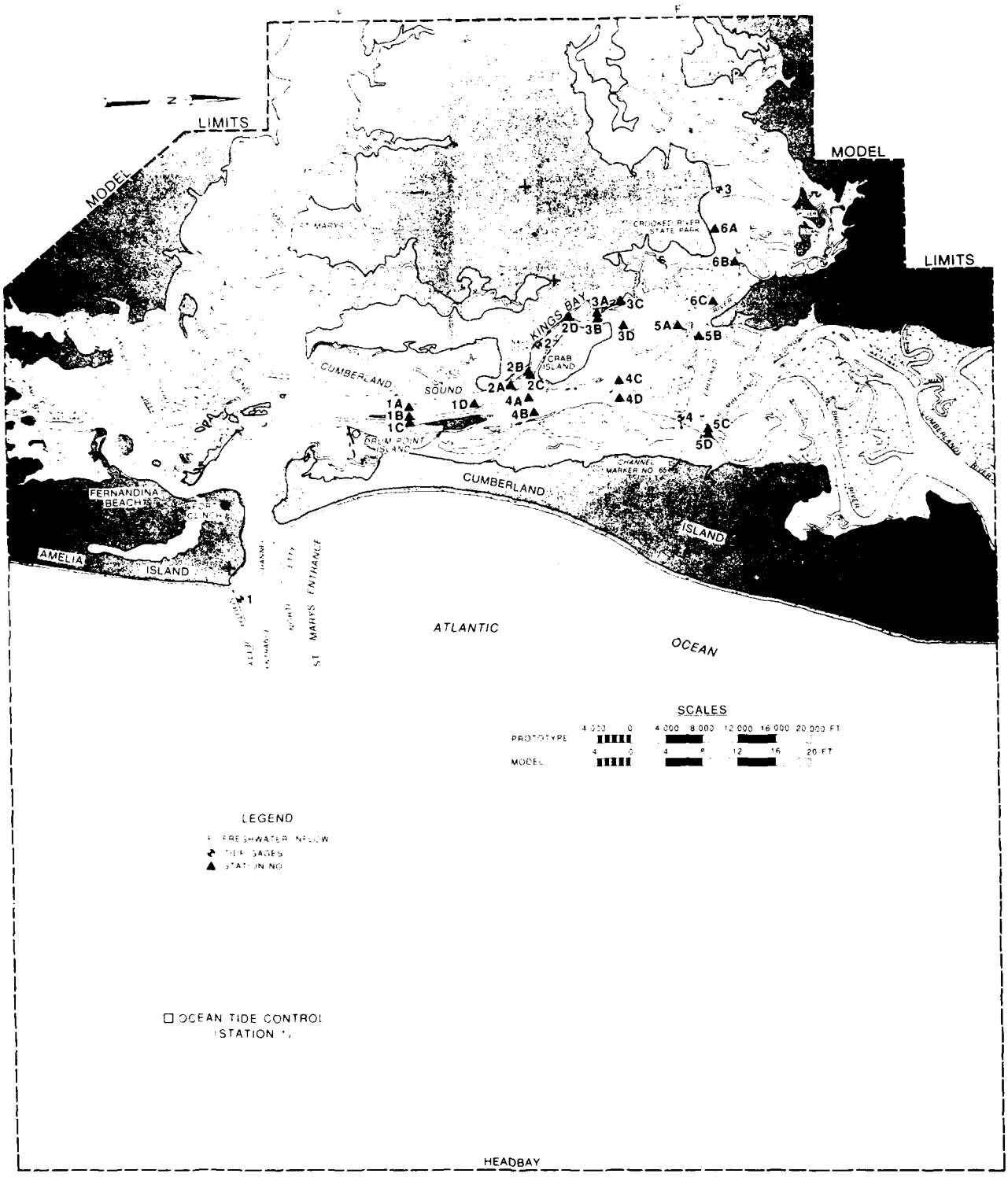

Figure 15. Verification station location map, transitional channel, January 1985 survey

the model reproduction of tidal elevations, tidal ranges, and tidal phases were in good agreement with the prototype.

114. The St. Marys entrance south jetty tide station (station 1) was, again, the control tide station for this verification effort. As shown in Plate C1, model reproduction of the prototype high and low waters was excellent; however, there appeared to be about a 15-min phase shift (later time of arrival) for the physical model data.

115. Tidal reproduction at the lower Kings Bay dock tide station (station 2, Figure 15) showed good agreement with prototype tide range and extremes; however, these water-surface elevations occurred about 30 min later in the model than in the prototype (Plate C1).

116. At station 3, adjacent to Crooked River State Park (Figure 15), the model was accurately reproducing low-water elevations; however, the high-water elevation in the model was about 0.25 ft lower than prototype observations, resulting in a tidal range 0.25 ft too small (Plate C1). The phase of high- and low-water elevations was in good agreement.

117. Station 4 data, from northern Cumberland Sound near the confluence of Crooked River and Cumberland Dividings (Figure 15), indicated that the model was accurately reproducing low-water elevation, but was about 0.1 ft lower than prototype at high water (Plate C2). The model phase at this station, like that of station 2, was about 30 min later than that of the prototype.

Current velocity verification

118. Prototype current velocity data were available at 23 field stations west and north of Drum Point Island (including Kings Bay) for model verification to the 1985 field conditions (Figure 15). As shown in Plates C3-C25, the agreement obtained for the January 1985 prototype data set and the model data set is considered to be very satisfactory especially considering the unfavorable meteorological conditions existing during the prototype survey period.

119. Model data at stations 1A, 1B, 1C, and 1D, west of Drum Point Island (Figure 15), show good agreement with the prototype (Plates C3-C6). Maximum current velocities observed in the model were slightly (less than 1 fps) higher than prototype observations. The arrival times of slack waters at stations 1A, 1B, 1C, and 1D were in excellent agreement with the prototype data. The greatest discrepancy occurred at stations 1A and 1B, where

station 1A slack before ebb occurred about 0.5 to 1.0 hr later than observed in the prototype, while slack before flood at station 1B occurred about 0.5 to 1.0 hr later than prototype. Slack periods at other stations on range 1 were in good agreement with the prototype.

120. Stations 2A, 2B, 2C, and 2D were located in Kings Bay (Figure 15). These data (Plates C7-C10) show that the model and prototype in this area were in good agreement. Maximum flood and ebb current velocities at station 2A were in excellent agreement, while model slack-water arrival times were generally about 0.5 to 1.0 hr later than observed in the prototype. Maximum current velocities at station 2B were generally less than observed prototype current velocities, particularly at surface and middepth elevations. Slack periods at this station, like those of station 2A, occurred later in the model than observed in the prototype. The difference between model and prototype ranged from about 0.5 hr at the surface to about 2.0 hr at the bottom. Maximum current velocity observations at station 2C were in good agreement with the prototype. Slack periods at station 2C, particularly slack before flood, occurred about 1.0 hr later in the model. Maximum current velocities at station 2D were slightly lower in the model than the prototype, and like stations 2A, 2B, and 2C, the slack-water arrival times were slightly later than in the prototype.

121. Stations 3A and 3B were located in the upper Trident basin and 3C and 3D were located in the small channels immediately north of the basin (Figure 15). Maximum flood current velocities observed in the model at stations 3A and 3B (Plates C11 and C12) were slightly lower than prototype observations. However, maximum ebb current velocities in the model were generally about 2.0 fps higher than prototype observations at these two stations, particularly at the surface and middepth elevations. As previously noted for stations located in the immediate vicinity and south of the basin, stations 3A and 3B likewise had late arrival times of slack waters by about 1.0 hr. Maximum current velocities at stations 3C and 3D (Plates C13 and C14) were higher in the model than were prototype observations. Maximum flood and ebb current velocities at stations 3C and 3D were about 1.0 fps higher than prototype. Again, model slack periods at these two stations were about 1.0 hr later than prototype.

122. Stations 4A, 4B, 4C, and 4D, located in Cumberland Sound in the vicinity of Stafford Island (Figure 15), had maximum flood current velocities

slightly lower than prototype, while maximum ebb current velocities were either only slightly greater than prototype or in excellent agreement. The difference between model and prototype maximum currents was generally less than 1.0 fps. Slack periods in the model were generally later than in the prototype, particularly slack before flood. Model and prototype data at stations 4A, 4B, 4C, and 4D are compared in Plates C15-C18.

123. Stations 5A and 5B were located in the south and north branches of the Crooked River, respectively. Stations 5C and 5D were located at the confluence of Cumberland Dividings and the Crooked River (Figure 15). Comparisons of model and prototype data are shown in Plates C19-C22. Maximum flood current velocities at station 5A were lower than those of the prototype by about 1.0 fps at the surface and middepth and about 0.5 fps lower at the bottom depth. Maximum ebb current velocities at station 5A were slightly higher than prototype velocities. The phase of slack periods at station 5A was in excellent agreement with that of the prototype. Current velocities and phase at station 5B were both in excellent agreement with those of the prototype.

124. Maximum flood current velocities at station 5C were in good agreement with those of the prototype, while maximum ebb current velocities were greater than prototype velocities. Slack periods at station 5C generally occurred about 1.0 hr earlier in the model. Maximum current velocities at station 5D were in excellent agreement with the prototype. Prototype data at station 5D were available for only about 7 hr of the cycle; however, model data were in good agreement with the existing prototype data. The slack before flood in the model occurred slightly earlier than the prototype data indicated.

125. Comparison of model and prototype current velocity observations for stations 6A, 6B, and 6C are shown in Plates C23-C25. These stations were located in the north branch of the Crooked River (Figure 15). Both maximum flood and ebb current velocities at station 6A were higher than prototype velocities, generally by about 0.5 fps. Slack before flood occurred later in the model than in the prototype. Slack before ebb was in excellent agreement with the prototype. Maximum current velocities, both in the flood and ebb directions, at station 6B were slightly lower in the model. Times of slack periods were in excellent agreement with the prototype at station 6B. Maximum flood current velocities at station 6C in the model were in excellent agreement with the prototype, while maximum ebb current velocities were generally

slightly lower than prototype observations. Times of occurrence of slack periods at station 6C were also in excellent agreement.

Physical Model Verification Conclusion

126. Agreement between model and prototype phenomena, as evidenced by the comparison of model and prototype tide, current velocity, and salinity data, has been demonstrated. The model is considered to be sufficiently similar to its prototype to be used confidently in assessing three-dimensional (lateral, longitudinal, and vertical) effects of proposed plans on hydrodynamic processes. The physical model is also ideally suited for providing boundary forcing conditions and interior data bases for numerical modeling purposes.

PART V: VERIFICATION OF THE NUMERICAL HYDRODYNAMIC MODEL, RMA-2V

Verification Approach

127. Hydrodynamic verification of RMA-2V was accomplished with numerical bottom roughness (Manning's n) and eddy viscosity coefficient assignments and marsh elevation schematization adjustments through comparison of numerical model water-surface elevation and velocity data with corresponding physical model data. The physical model and numerical model are based on different sets of underlying approximations and assumptions, and the ability of each model to produce comparable results using realistic coefficients and approximations enhances confidence in each model's verification.

128. This approach of using the physical model data for numerical model comparison purposes allowed a more detailed verification than would be possible using available prototype data. Once the physical model was verified to reproduce available prototype data, verification of the numerical model to an expanded physical model data set was undertaken. The physical model control tide station was changed from the south jetty to the offshore ocean tide control to reduce potential impacts associated with plan channel alternatives.

129. A separate set of physical model boundary forcing conditions and sampling locations was used. Figure 16 illustrates the sampling locations selected for numerical model verification and testing purposes. A long-term average freshwater discharge of 1,000 cfs for the St. Marys River and 100 cfs for the Crooked River was introduced at the physical model boundaries for these two tributaries. A 5.7-ft mean range tide (+6.2 ft high water to +0.5 ft low water) was generated at the physical model ocean tide control (station 1, Figure 16) for numerical model pre-Trident channel verification testing conditions. This tide produced a +5.90- to +0.25-ft tide at the physical model St. Marys Inlet tide station (station 2, Figure 16). This tide was used as the numerical model ocean tidal boundary forcing condition.

130. Data sampling began in the physical model once the verified model reached a stabilized salinity distribution (the same salinity from tidal cycle to tidal cycle) with the new boundary conditions. Half-hourly (every 18 sec in the model) water-surface elevations were measured for three replicate tidal cycles at the nine physical model tide stations. Current speed and direction observations were also taken half-hourly for three replicate tidal cycles at

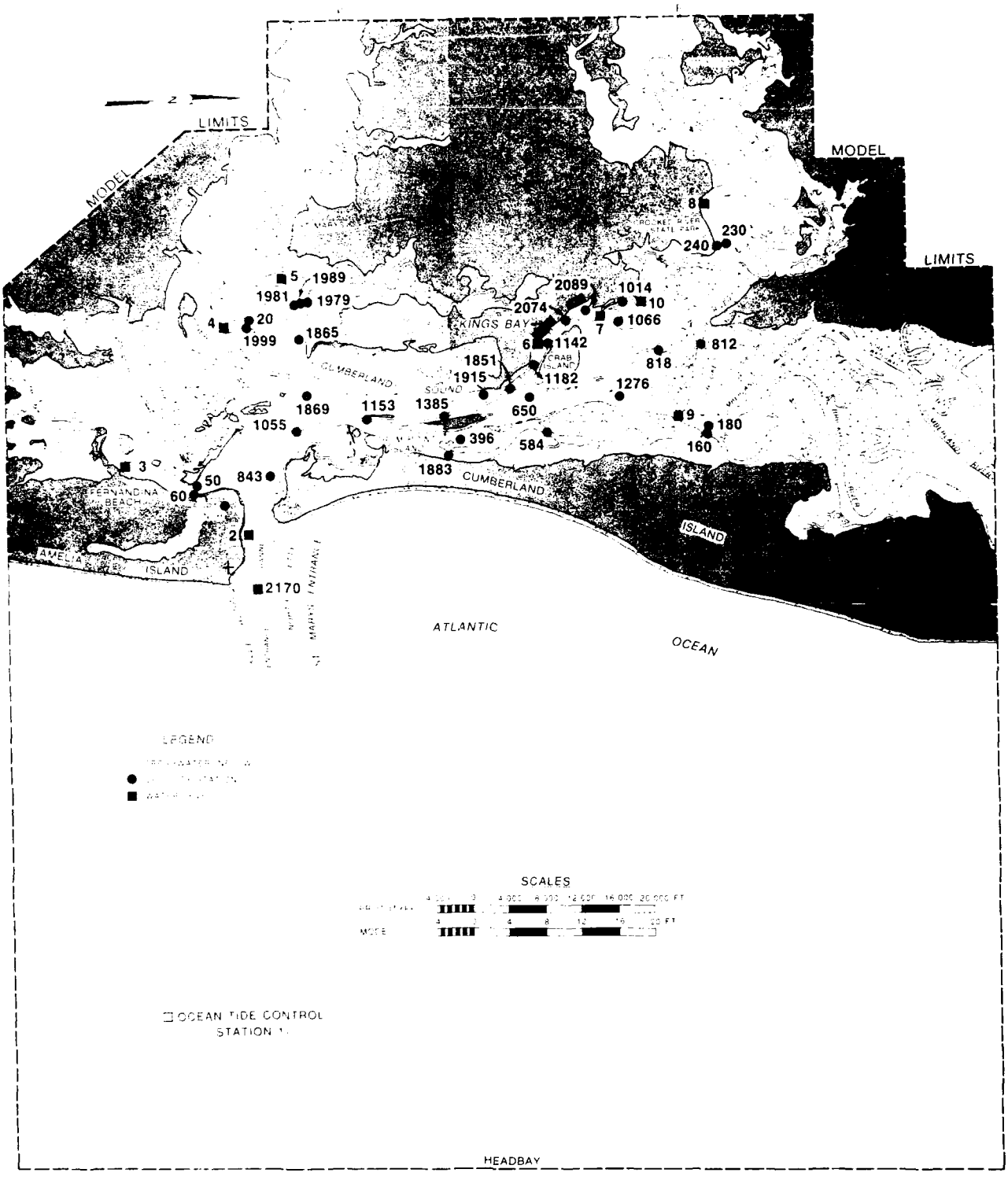

Figure 16. Numerical model verification, base, and plan testing station location map

the 36 velocity stations (21 interior stations and 15 boundary stations). For each station, these data were averaged to produce one complete tidal cycle of tide and velocity information. The velocity data were then depth-averaged by Rieman sum to produce a compatible data set for numerical model verification use.

Preliminary Testing

131. Early stages of numerical model verification used prototype data for comparison and preliminary (unverified) physical model velocity data for tributary boundary forcing conditions and water-surface elevations for the ocean boundary forcing condition. This approach allowed concurrent development of both models (physical and numerical).

132. Numerical model sensitivity tests of wetting and drying demonstrated marsh-estuarine circulation hydrodynamic interactions. Artificially lowering the surface elevations of the marsh areas (i.e., bed elevations set at -2.0 ft) so that they stayed wet during the entire tidal cycle generally increased ebb and flood current velocities while reducing tidal range, relative to similar model runs with marsh elevations from +2.5 to +5.0 ft. Lower marsh elevations caused both tide and velocity peaks to arrive later. Adjustment of marsh elevations (within reasonable limits) was justified in that actual elevations were not known and that the mesh wetting and drying computation method requires flexibility in depth assignment to preserve water mass and momentum.

133. Several model runs with various Manning's n roughness values, eddy viscosity coefficients, and various marsh elevations were examined. A marsh elevation of +4.0 ft was selected as the nominal elevation for optimum tide and velocity reproduction. Higher marsh elevations generally tended to reduce current velocity and increase tidal range (King, Granat, and Ariathurai 1986). The higher marsh elevations resulted in a reduced tidal prism and an associated reduced current velocity; the increased tidal range may be the result of reduced frictional loss associated with a decreased period of marsh inundation. Table 2 provides a summary of the selected verification roughness values and eddy viscosity coefficients assigned to the various types of elements. Minimal reclassification of element type was undertaken prior to the

final Mesh 1 verification run. Similar coefficient values were used for all of the final numerical model runs (pre-Trident Mesh 1 verification, transitional channel verification, pre-Trident Mesh 4 verification, and all plan testing). The water depth below which a node was considered dry by RMA-2V (DSET; paragraph 69) was set at 0.1 ft. The water depth at which a dry node was considered to become wet again by RMA-2V (DSETD; paragraph 69) was set at 0.25 ft.

134. The nine element types established during mesh development were based on physical characteristics. Open-water interior areas were assigned element types 1, 2, or 3 depending on their characteristics. Turbulent exchange coefficients, in units of pounds-second per square foot, were set at 100 for the open-water areas; and the Manning's n value varied from 0.015 for maintained "smooth" channel areas, 0.020 for other large open-water areas, and 0.025 for the smaller channel and creek areas that led into marsh areas. Main marsh areas that flooded and dried during each tidal cycle were assigned an element type 4 with a turbulent exchange coefficient of 200 and an n value of 0.050. Secondary marsh and sand flat areas were assigned an element type 5 with an exchange coefficient of 170 and an n value of 0.040. A type 6 element, with an exchange coefficient of 150 and an n value of 0.030, characterized transitional areas between open-water and marsh zones. The ocean entrance area was characterized as a type 7 element with a turbulent exchange coefficient of 500 and a Manning's n value of 0.020. The Kings Bay marginal wharf was assigned an element type 8 with an exchange coefficient of 300 and an n value of 0.030. Element type 9 was used to characterize the elements associated with the Poseidon tender and floating dry dock. The actual water depth at each node location associated with the tender and dry dock was used to schematize the geometry condition. The Manning's n value was increased to 0.030 and the turbulent exchange coefficient was reduced to 70 in an attempt to reproduce flow blockage and shear associated with each vessel.

Pre-Trident Mesh 1 Verification

135. Pre-Trident Mesh 1 verification efforts were undertaken during 1982 and 1983. Once the verified physical model was stabilized to the testing conditions, the final physical model data set was collected for deriving the numerical model verification boundary forcing conditions and for numerical

model-physical model comparisons. The averaged half-hour physical model ocean water levels for St. Marys Inlet (station 2, Figure 16) were used as the tidal boundary forcing conditions (input data) across the ocean boundary of the numerical model. The physical model half-hour depth-averaged velocity data for each of the tributary systems were used as upstream velocity boundary forcing conditions, linearly distributed across each tributary boundary.

136. Time in the physical and numerical models was referenced to the moon's transit over the 81st meridian. The same 12.42-hr tidal cycle was repeatedly generated in each model. The numerical model was run for 15.5 hr (hours 8.0-23.5) using the physical model derived boundary forcing conditions to obtain water-surface elevation and velocity data for the entire mesh area. Numerical model hour 13.0, the first time-step of the second tidal cycle, corresponded to hour 0.58 of the first tidal cycle. Hour 8 was chosen as the numerical model starting point since it was close to high water and all marsh areas were inundated (i.e., wet, below the surface of the water). The first 3 hr of the model run were necessary for model spin-up to eliminate initial transients.

Pre-Trident Mesh 1 tidal verification

137. Plate D1a illustrates the physical model tide generated at the ocean control tide station (station 1, Figure 16) and Plate D1b illustrates the physical model derived tidal boundary forcing condition generated at the numerical model ocean boundary. Node 2170 data are representative of this tidal condition. Numerical model to physical model time-history water-surface elevation comparisons are illustrated in Plates D2-D5. Excellent phase (time of arrival) agreement was indicated at all stations. The largest variation occurred at the St. Marys dock tide gage (station 5, Figure 16 and Plate D3) where falling water levels in the numerical model occurred about 15 min earlier than in the physical model. This difference is within the physical model detection limits.

138. Figure 17 summarizes the physical model and numerical model comparisons for high- and low-water elevations and the midtide level for each of the tide stations. Station 1 was the offshore ocean tide control for the physical model; the compared numerical model data (node 2170) represent the input boundary forcing conditions prescribed for the numerical model ocean boundary. The numerical model and physical model data are for different locations and should not be directly evaluated. These data are provided for

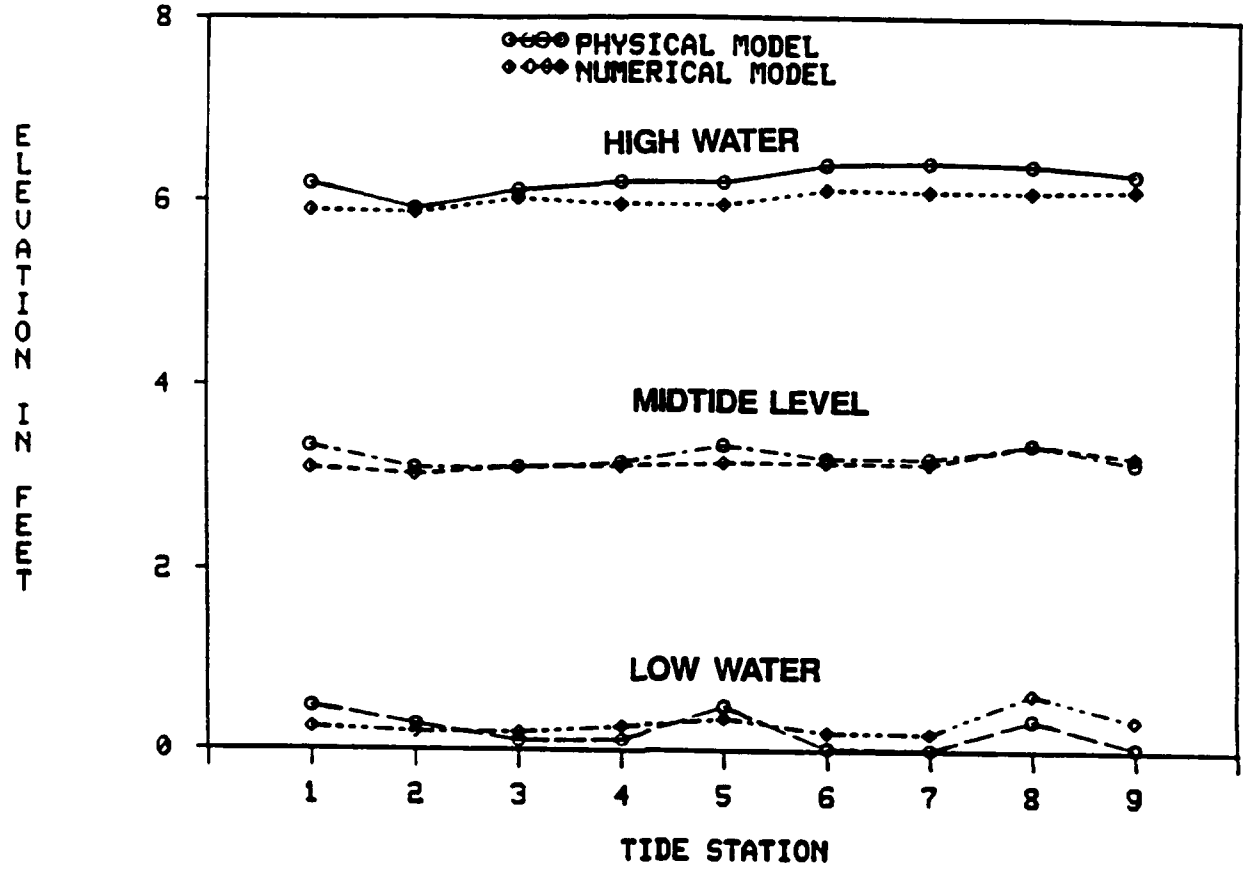

PHYSICAL AND NUMERICAL MODEL TIDE STATIONS

Physical Model	Location	Numerical Model Node
1	Physical model ocean tide control/ numerical model ocean boundary	2170
2	St. Marys Inlet	1939
3	Amelia River	60
4	Jolly River	1999
5	St. Marys City Dock	1989
6	Lower Kings Bay	1150
7	Marianna Creek	2227
8	Crooked River State Park	240
9	Northern Cumberland Sound	780

Figure 17. Pre-Trident Mesh 1 tidal verification summary

comparisons to later testing conditions. The numerical model data are for the inlet area and the physical model data are for the offshore ocean (Figure 16).

139. The largest physical model to numerical model midtide level difference occurred at station 5 in St. Marys River. The elevated midtide level of the physical model data for St. Marys River was not observed in the numerical model (i.e., the numerical model demonstrated a reduced midtidal level associated with a lower high and lower low water) indicating an overall increased ebb flow efficiency in the numerical model of St. Marys River. This tide difference may be associated with the absence of a density (salinity) gradient in the depth-averaged numerical model. It may also be associated with the marsh-estuarine circulation interactions previously described or with geometric schematization differences. Numerical model and physical model midtide levels at the other stations were in excellent agreement, with all differences less than 0.1 ft.

140. Tidal ranges in the numerical model were reduced relative to physical model ranges. As described in paragraphs 132 and 133, tidal agreement was sacrificed for improved velocity agreement. Numerical model water levels were generally within 0.1-0.3 ft of physical model levels. This was in reasonable agreement considering the 0.1-ft confidence of the physical model measurements and the numerical model schematization of the marsh zones. The tidal range differences were usually associated with reduced numerical model high-water elevations and elevated low-water elevations relative to the physical model measurements. In general, a closer numerical model to physical model tide agreement was achieved with an elevated marsh surface elevation of +4.5 ft; however, velocity agreement was negatively affected under this condition.

Pre-Trident Mesh 1 velocity verification

141. Numerical model to physical model velocity comparisons are illustrated in Plates D6-D16. Main channel stations progressing from the entrance channel upstream to the upper turning basin are presented first (Plates D6-D10), followed by tributary and secondary channels progressing from south to north. Velocity phase (time of occurrence of ebb and flood velocity) was generally in excellent agreement at all stations. Flood velocity phase in the numerical model appeared to lag behind the physical model data during the lower water level periods (elevations less than +4.0 ft) when the numerical model marshes were dry. Numerical model flood velocity phase tended to be in

better agreement with the physical model during the higher water level periods when the marshes were inundated.

142. Figure 18 presents physical and numerical model maximum flood and ebb summary values for each of the velocity sampling stations. Numerical model and physical model velocity magnitudes were generally in excellent agreement for the main channel stations; the greatest variations existed during the early stages of the flood cycle (Plates D6-D16). Numerical model velocities were somewhat lower than the physical model velocities during the period of the flood cycle when the extensive marsh areas in the numerical model were dry. This variation was not surprising considering the marsh-estuarine circulation hydrodynamic interactions previously discussed. A finer resolution of the marsh areas and of the wetting and drying process would improve the comparisons, but was not warranted in light of the lack of precise elevation and hydrodynamic data for the marsh zones.

143. Numerical model to physical model velocity magnitude comparisons were considered reasonable for the tributary and secondary channels. These stations were generally located adjacent to marsh zones and were more directly influenced by marsh hydrodynamics. As with the channel stations, finer resolution of the wetting and drying processes over the marsh areas would improve the comparisons; however, the additional computation was not pursued because of the overall acceptable velocity agreement and distances of these stations away from the immediate areas of interest, i.e., the main channel.

144. Stations 1883, 584, 818, 1014, 1066, and 812 (Figures 16 and 18 and Plates D12-D15) are examples of stations with marsh zones on each side. Numerical model ebb and flood velocities were generally lower than those of the physical model with flood velocity differences generally greater than ebb velocity differences. Shallow depths at stations 1066 and 812 (6 and 8 ft, respectively) may also contribute to the higher physical model velocities at these two stations; the missing values for physical model station 1066 (Plate D15) result from insufficient water depth for physical model measurements. It should be recalled that prototype velocity field measurements were not available for the areas above Kings Bay during the 1982-1983 verification period and that based on information collected for the 1985 transitional channel verification period, additional physical model geometry and roughness adjustments were performed in this area for the later verification.

145. The two St. Marys River stations (stations 1865 and 1869,

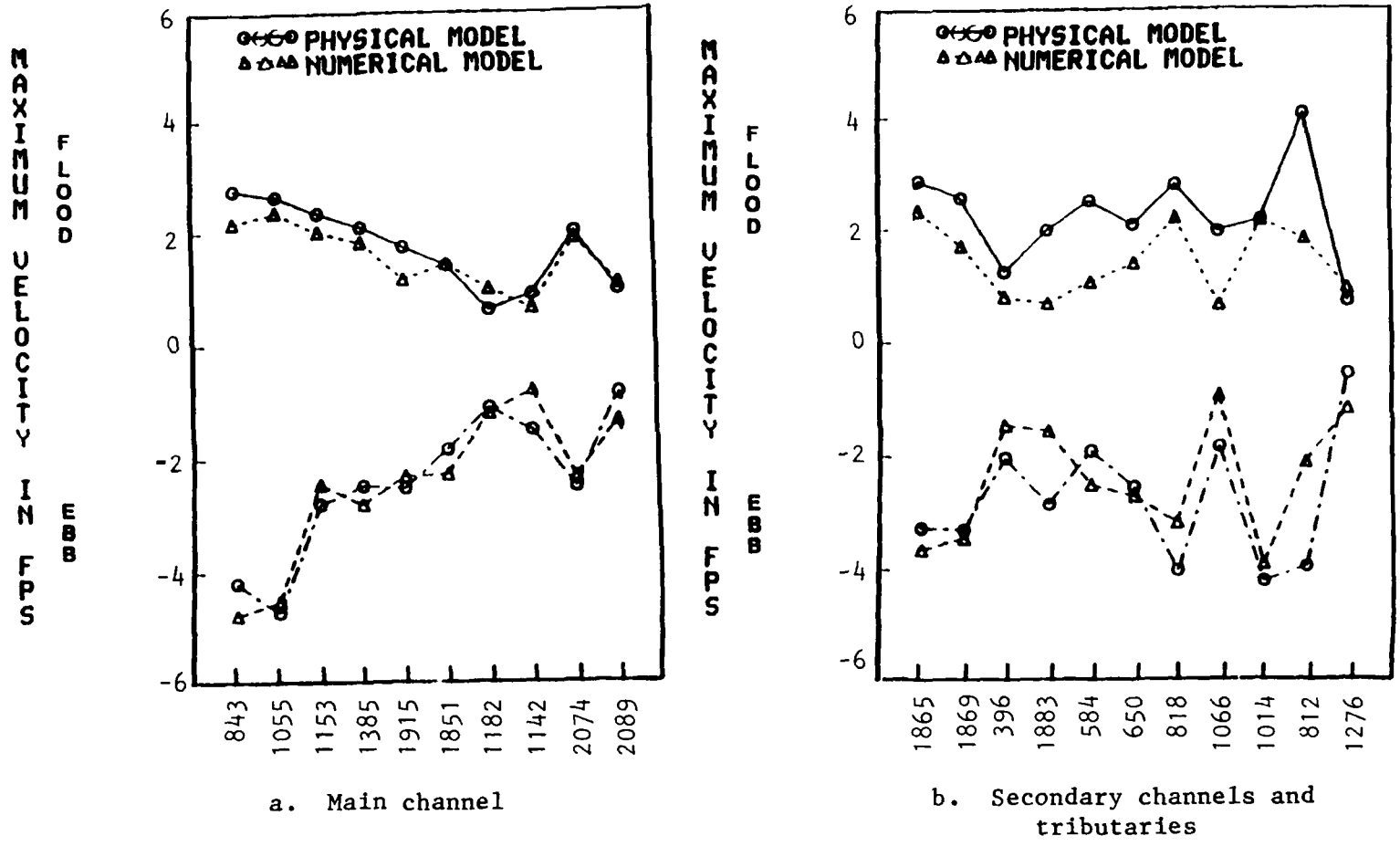

a. Main channel

b. Secondary channels and tributaries

Figure 18. Pre-Trident Mesh 1 velocity verification summary

Plate D11) indicated reduced numerical model flood and increased numerical model ebb velocities (increased ebb dominance) relative to the physical model data. As with the tide data, these differences may be associated with the depth-averaged nature of the numerical model (i.e., no vertical density gradient) or with differences in the geometric schematization.

Transitional Channel Verification

146. Transitional channel verification efforts were undertaken during 1985 and 1986. The physical model geometry conditions tested during this verification effort included channel depths as indicated on the Savannah District January 1985 examination survey as well as updated bathymetric information and roughness adjustments for the areas north of Kings Bay (see paragraphs 21 and 112). The January 1985 geometry condition included the recently dredged 48-ft-deep upper Trident basin, located above the Poseidon Kings Bay operational area. The numerical model geometry conditions included the January 1985 channel depths, a better schematization of the areas east of and including Drum Point Island based on the Savannah District August 1985 condition survey (this information was made available after the physical model transitional channel verification), and the revised numerical model schematization required to incorporate plan channel revisions through January 1985, including the relocated magnetic silencing facility associated with the potential AIWW relocation (see paragraphs 72 and 73).

147. Sampling, data reduction, and modeling procedures (physical and numerical) followed during this verification effort were similar to those during the Mesh 1 verification. A separate set of physical model observations was undertaken for deriving numerical model boundary forcing conditions and for verification purposes after the physical model was verified to the 1985 conditions. The physical model ocean tide control (station 1, Figure 16) was again used as the physical model control tide station. The same physical model ocean tide condition as used during the pre-Trident verification (+6.2 to +0.5 ft) was desired; however, a tide with a slightly increased high- and low-water elevation (+6.3 to 0.55 ft), range (5.75 ft instead of 5.7 ft), and tidal plane was generated at the ocean tide control. The physical model ocean tidal plane was elevated about 0.1 ft (3.45 ft instead of 3.35 ft) higher than the pre-Trident channel condition. This ocean tide resulted in a +6.0- to

+0.4-ft tide at station 2 in St. Marys Inlet instead of a +5.90- to +0.25-ft tide as produced during the pre-Trident condition. The resulting boundary forcing condition differences complicate the comparisons between transitional channel and pre-Trident channel verifications. Geometry, roughness, and mesh schematization differences add to the complexity of comparisons between the two verification periods.

Transitional channel tidal verification

148. Plate E1a provides a comparison between the tides generated at the physical model ocean tide control during the transitional channel verification and the pre-Trident channel verification. A slight phase shift with a later time of arrival and a slightly elevated tidal plane are indicated for the physical model transitional channel condition relative to the pre-Trident condition. Plate E1b provides a comparison of the resulting physical model derived ocean tidal boundary forcing conditions used in the numerical model for the two verification efforts. The phase shift and elevated tidal plane indicated at the physical model ocean tide control for the transitional channel boundary condition relative to the pre-Trident condition is increased at the St. Marys Inlet numerical model ocean boundary.

149. Plates E2-E5 illustrate the numerical model to physical model time-history water-surface elevations at the interior tide stations for the transitional channel verification. A similar phase shift and increased tidal plane are also demonstrated at the interior stations relative to the pre-Trident conditions (Plates D2-D5). The effect of the inundation of the marsh in the physical model and the numerical model data is clearly evidenced in the reduced rate of elevation change at water-level elevations above 4.0 ft. The numerical model data demonstrate greatest variations from the physical model during the inundation (i.e., at elevations greater than 4.0 ft). This variation results from the reduced geometric marsh resolution schematized in the numerical model as compared to the physical model. In general, numerical model tidal phase was about 15 min later than physical model tidal phase at most locations; stations 4 and 5 in the Jolly and St. Marys rivers were exceptions with equal phase but slightly elevated physical model plane.

150. Figure 19 summarizes the numerical model and physical model comparisons for high- and low-water elevation and midtide level for each transitional channel tide station. Station 1 represents the ocean tide boundary control station for each model. Because the geographic location was different

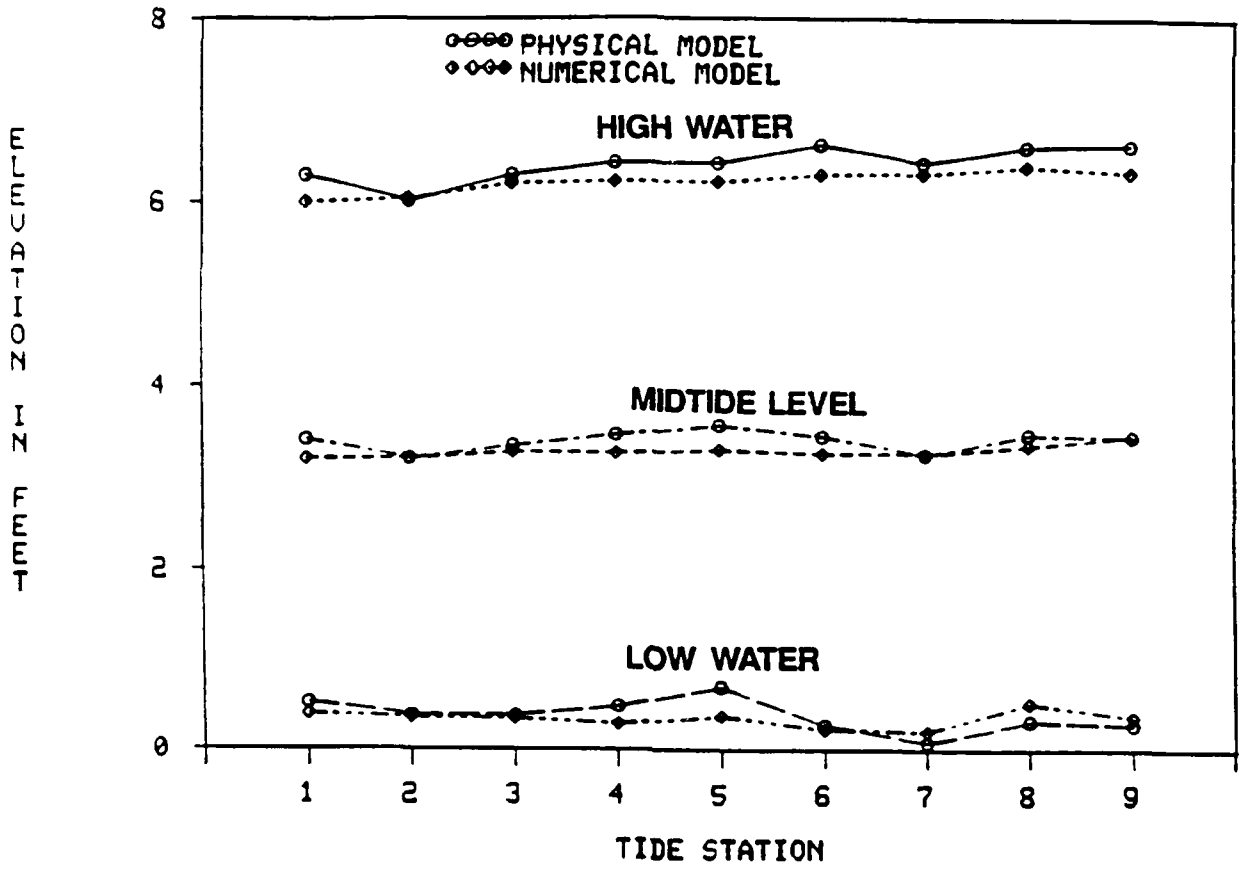

PHYSICAL AND NUMERICAL MODEL TIDE STATIONS

Physical Model	Location	Numerical Model Node
1	Physical model ocean tide control/ numerical model ocean boundary	2170
2	St. Marys Inlet	1939
3	Amelia River	60
4	Jolly River	1999
5	St. Marys City Dock	1989
6	Lower Kings Bay	1150
7	Marianna Creek	2227
8	Crooked River State Park	240
9	Northern Cumberland Sound	780

Figure 19. Transitional channel tidal verification summary

for each model (paragraph 138 and Figure 16), the illustrated tidal boundary forcing conditions should not be directly evaluated. As addressed in paragraphs 147-149, the boundary conditions and the resulting tide elevations at the interior stations for both the physical and numerical models were generally increased during the transitional channel verification testing relative to the pre-Trident channel verification.

151. Interior transitional channel high-water elevations generally increased about 0.2 ft compared with pre-Trident elevations (some or all of this increase may be associated with the previously described boundary forcing condition differences). The relative differences between the numerical model and physical model high-water elevations were about the same for the two verification conditions (Figures 17 and 19). Station 7, above Kings Bay in Marianna Creek, was an exception, illustrating closer numerical model and physical model agreement (i.e., the physical model transitional channel high-water elevation was not elevated relative to the pre-Trident condition, and the numerical model elevation was raised resulting in closer numerical model to physical model agreement).

152. Physical model transitional channel low-water elevations were also generally elevated about 0.2 ft; stations 7 and 8 (Marianna Creek and Crooked River State Park) were exceptions, demonstrating little change compared to pre-Trident conditions. Numerical model transitional channel interior low-water elevations usually remained unchanged from pre-Trident conditions (St. Marys Inlet and Amelia River stations 2 and 3 were exceptions, with elevated low waters), generally resulting in closer numerical model and physical model low-water elevation agreement (Figures 17 and 19). The Jolly and St. Marys River stations 4 and 5 illustrated increased numerical model and physical model transitional channel low-water differences associated with elevated physical model low-water elevations. These differences are thought to be associated with the absence of a numerical model vertical density gradient.

153. As previously stated, the transitional channel tidal planes in both the numerical model and the physical model were elevated relative to the pre-Trident testing. Stations 4 and 5 in the Jolly and St. Marys rivers exhibited the largest numerical model to physical model plane differences (Figure 19); the physical model tidal plane was 0.20 ft and 0.25 ft, respectively, above the numerical model plane at these two stations. The transitional channel tidal plane difference indicated at Kings Bay (station 6) is associated

with an elevated physical model high-water elevation relative to the numerical model.

154. In general, the model adjustments made prior to the final transitional channel verification improved the numerical model to physical model correspondence for tidal characteristics. The greatest improvements were in low-water elevations and tidal range for stations above Kings Bay, the area in which most of the adjustments were performed.

Transitional channel
velocity verification

155. Numerical model transitional channel velocity boundary forcing conditions are compared to numerical model pre-Trident boundary forcing conditions in Plates E6-E11. Data from each tributary are presented in a clockwise order from Amelia River in the south to Cumberland Dividings in the north. The velocity boundary forcing condition variations may be associated with physical model boundary control differences (see paragraph 147), physical model geometry and roughness modifications between the two verification conditions (see paragraph 146), and/or localized noise in the physical model data. Station 1981, on the south side of the St. Marys River (Plate E8), provides an excellent example of localized noise. An eddy circulation pattern existed at this station during the transitional channel testing (also during the plan channel testing), producing an early flood direction flow during hours 13.5-15.5. This eddy pattern was not evident during the pre-Trident channel testing period. As previously discussed, boundary forcing condition variations complicate comparisons between the two verification efforts.

156. Transitional channel numerical model to physical model time-history velocity comparisons are illustrated in Plates E12-E22. As in the pre-Trident comparisons, main channel stations progressing from the entrance channel upstream to the upper Kings Bay turning basin are presented first (Plates E12-E16), followed by tributary and secondary channels from south to north. As described in paragraph 146, geometry and roughness distribution differences between the two verification periods and between the physical model and the numerical model (i.e., revised numerical model transitional channel geometry adjacent to and including Drum Point Island) also need to be considered in evaluating the comparisons. During the mesh reschematization for transitional channel testing, numerical model station 1915 (Plate E14), was moved about 350 ft to the northeast in the planned revised vicinity of the

magnetic silencing facility. The physical model station was not moved.

157. Figure 20 presents physical model and numerical model transitional channel maximum flood and ebb summary values for each of the velocity sampling stations. Velocity magnitude trends between the two verification periods (Figures 18 and 20) were generally in close agreement. The most noticeable difference between these two conditions was for the upper end of Kings Bay; stations 2074 and 2089 demonstrated reduced transitional channel physical and numerical model flood and ebb velocities associated with the deepened turning basin. Physical model transitional channel flood velocity at station 812 (north fork of Crooked River) was also reduced, resulting in closer numerical model and physical model velocity agreement; physical model ebb velocity remained much greater than the numerical model ebb velocity at this station.

158. In general, numerical model and physical model transitional channel flood velocities tended to be in somewhat closer agreement than did the pre-Trident comparisons. Numerical model to physical model flood and ebb velocity agreement was improved at station 1066, the small back channel from Kings Bay to the south fork of Crooked River. Station 818, the lower south fork of Crooked River, was the only station demonstrating increased numerical model to physical model flood velocity differences. This difference was the result of reduced numerical model transitional channel flood velocity relative to the physical model and to the numerical model pre-Trident condition.

159. Maximum ebb velocity agreement at most transitional channel stations was generally as good as the pre-Trident conditions with some exceptions. Numerical model ebb velocities within the main channel between Drum Point Island and the Poseidon operational area (stations 1385 to 1182) generally were increased relative to the pre-Trident condition. Physical model velocities generally did not demonstrate this trend of increased velocity, resulting in increased physical model to numerical model differences. As addressed in the following section (Mesh 4 verification), [illegible] the apparent increased numerical model ebb velocity was associated with the revised mesh schematization of the area adjacent to Drum Point Island. The other station demonstrating increased numerical model to physical model differences was station 1883, located east of Drum Point Island. This increased difference was associated with an increased physical model ebb velocity.

160. In summary, numerical model and physical model flood velocities

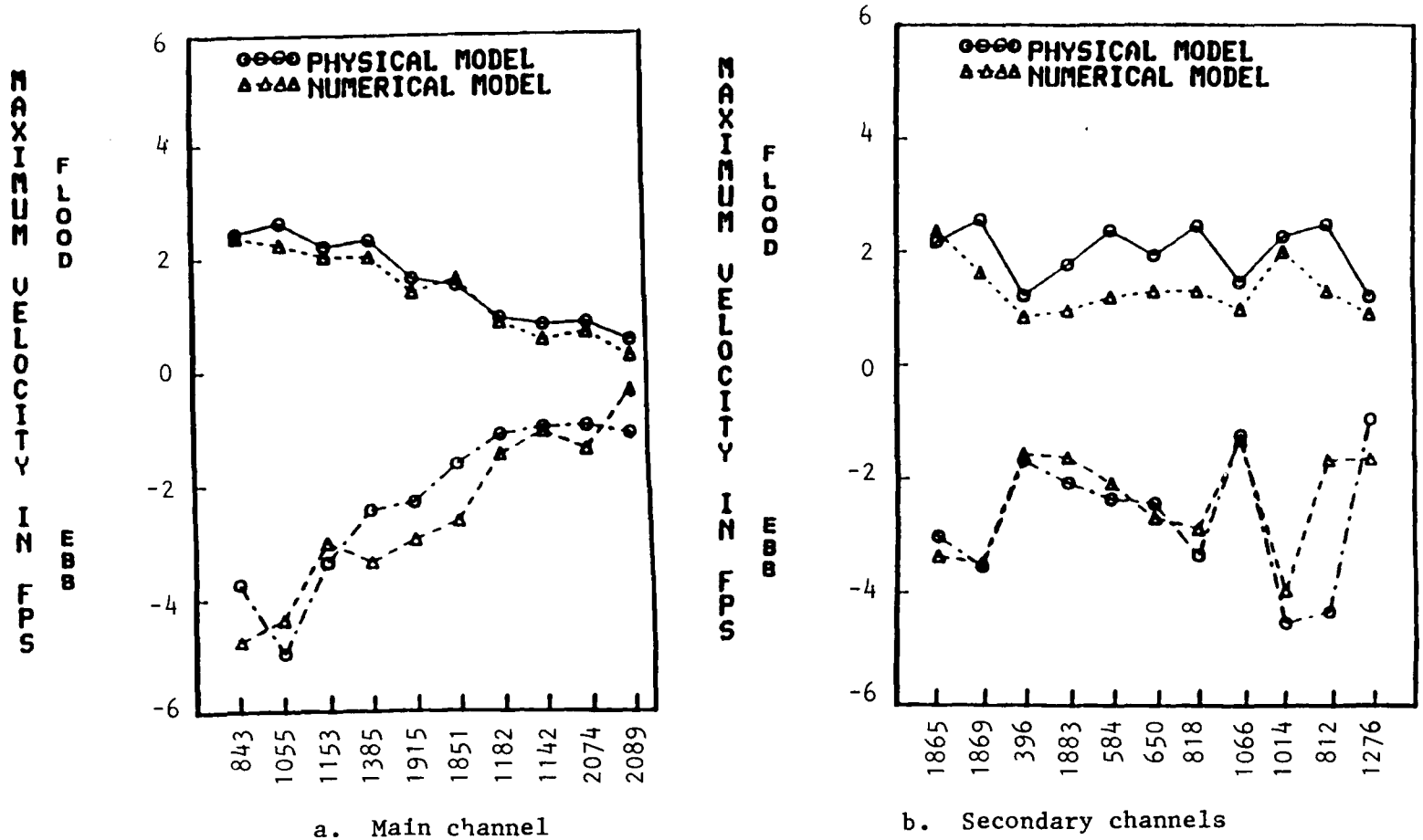

a. Main channel

b. Secondary channels

Figure 20. Transitional channel velocity verification summary

for the transitional channel verification period were generally in closer agreement than for the pre-Trident verification period. Ebb velocities for the secondary channel stations were also generally in better agreement. Main channel ebb velocities between lower Kings Bay and Drum Point Island indicated increased physical model and numerical model differences for the transitional verification period. Some of this increase was associated with the revised numerical model schematization adjacent to Drum Point Island resulting in increased numerical model ebb velocities. Relative to pre-Trident conditions, both the physical and the numerical models demonstrated reduced ebb and flood current velocities in the deepened upper Kings Bay (stations 2074 and 2089).

Pre-Trident Mesh 4 Verification

161. An additional numerical model pre-Trident hydrodynamic verification was undertaken with the basic revised mesh created for the plan channel upper basin remedial measures testing, to detect hydrodynamic variations associated with the revisions and increased resolution of Mesh 4. The numerical model mesh geometry (channel depths and element types) was revised back to pre-Trident channel conditions prior to the hydrodynamic model run. To allow proper reproduction of the wetting and drying process, an adjustment to the basic plan mesh was required adjacent to the marsh area northwest of the Poseidon floating dry dock. This revision involved reschematizing five small elements into six elements and adding one additional node. The same boundary conditions derived from the pre-Trident physical model (1983) were again used as the Mesh 4 numerical model boundary forcing conditions.

Pre-Trident Mesh 4 tidal verification

162. Plate D1 illustrates the physical model and numerical model ocean tidal boundary forcing conditions. Plates F1-F4 present the interior pre-Trident physical model and pre-Trident Mesh 4 numerical model water-surface elevation time-history comparisons for comparable stations. Excellent numerical model to physical model tidal phase was indicated at all stations. No detectable tidal phase differences were indicated when comparing Mesh 1 and Mesh 4 numerical model conditions (Plates D2-D5 and F1-F4).

163. Figure 21 summarizes the pre-Trident high- and low-water elevation comparisons for the physical model, the numerical model Mesh 4, and the numerical model Mesh 1 data. As in Figures 17 and 19, physical model station 1

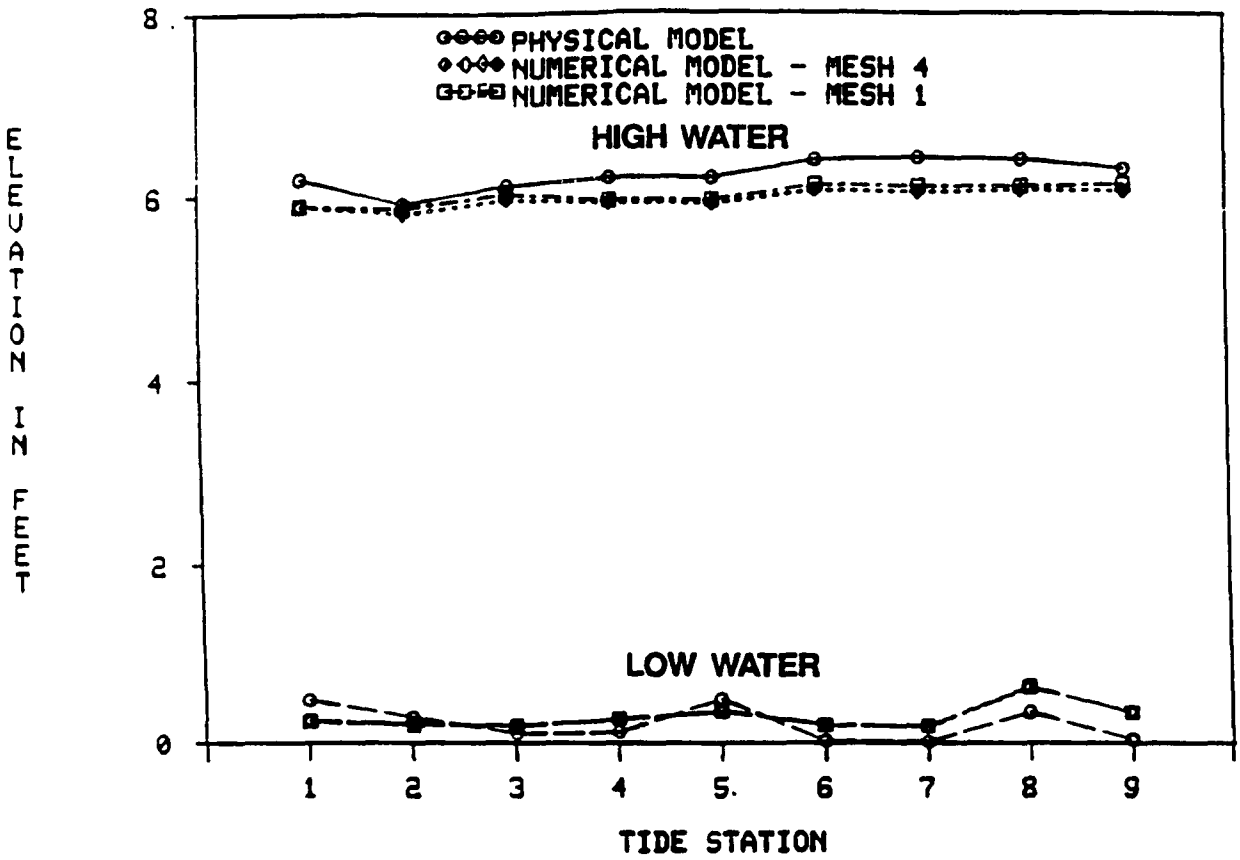

PHYSICAL AND NUMERICAL MODEL TIDE STATIONS

Physical Model	Location	Numerical Model Node
1	Physical model ocean tide control/ numerical model ocean boundary	2170
2	St. Marys Inlet	1939
3	Amelia River	60
4	Jolly River	1999
5	St. Marys City Dock	1989
6	Lower Kings Bay	1150
7	Marianna Creek	2227
8	Crooked River State Park	240
9	Northern Cumberland Sound	780

Figure 21. Pre-Trident Mesh 4 tidal verification summary.

(the offshore tide control) and numerical model St. Marys Inlet boundary node 2170 are at different locations, and their data should not be directly evaluated. These data are the respective tidal boundary forcing conditions for each model and can be compared from test to test. The numerical model boundary forcing conditions for Mesh 4 and Mesh 1 were identical. Resulting low-water elevations at the interior tide stations did not vary between the two meshes. A trend of slightly reduced Mesh 4 numerical model high-water elevation, relative to Mesh 1 elevations, is indicated at the interior stations. The Mesh 4 high-water elevations were reduced between 0.04 and 0.07 ft relative to the Mesh 1 condition. This very subtle variation is the result of the described mesh revisions.

Pre-Trident Mesh 4
velocity verification

164. The pre-Trident velocity boundary forcing conditions used during Mesh 1 verification (Plates E6-E11) were again used for the Mesh 4 verification. Plates F5-F15 illustrate resulting velocity time-history comparisons between the pre-Trident Mesh 4 numerical model data and the pre-Trident physical model data. Main channel stations progressing from the entrance channel upstream to the upper Kings Bay turning basin are again presented first (Plates F5-F9), followed by the tributary and secondary channel stations from south to north. Although there were some subtle velocity variations between the Mesh 4 results and the Mesh 1 results, overall Mesh 4 velocity verification is considered to be as good as the original Mesh 1 verification.

165. Figure 22 illustrates the maximum flood and ebb velocities for the pre-Trident physical model, numerical model Mesh 4, and numerical model Mesh 1 conditions. The subtle velocity variations between the two numerical model meshes are clearly summarized in this illustration. The greatest Mesh 4 to Mesh 1 variation was about 0.6 fps at station 1915 during the ebb cycle. As previously discussed, this station was shifted to the northeast during the mesh revision associated with the relocation of the magnetic silencing facility, so some of the Mesh 4 velocity increase may be explained by the difference in location. Stations 1153 and 1385, downstream of station 1915, and station 1851, upstream of station 1915, however, also demonstrated increased ebb velocity for Mesh 4 relative to Mesh 1. Station 584, east of Stafford Island, was another station that demonstrated large Mesh 4 to Mesh 1 ebb velocity variations. This station was in the area of revised geometry, based on

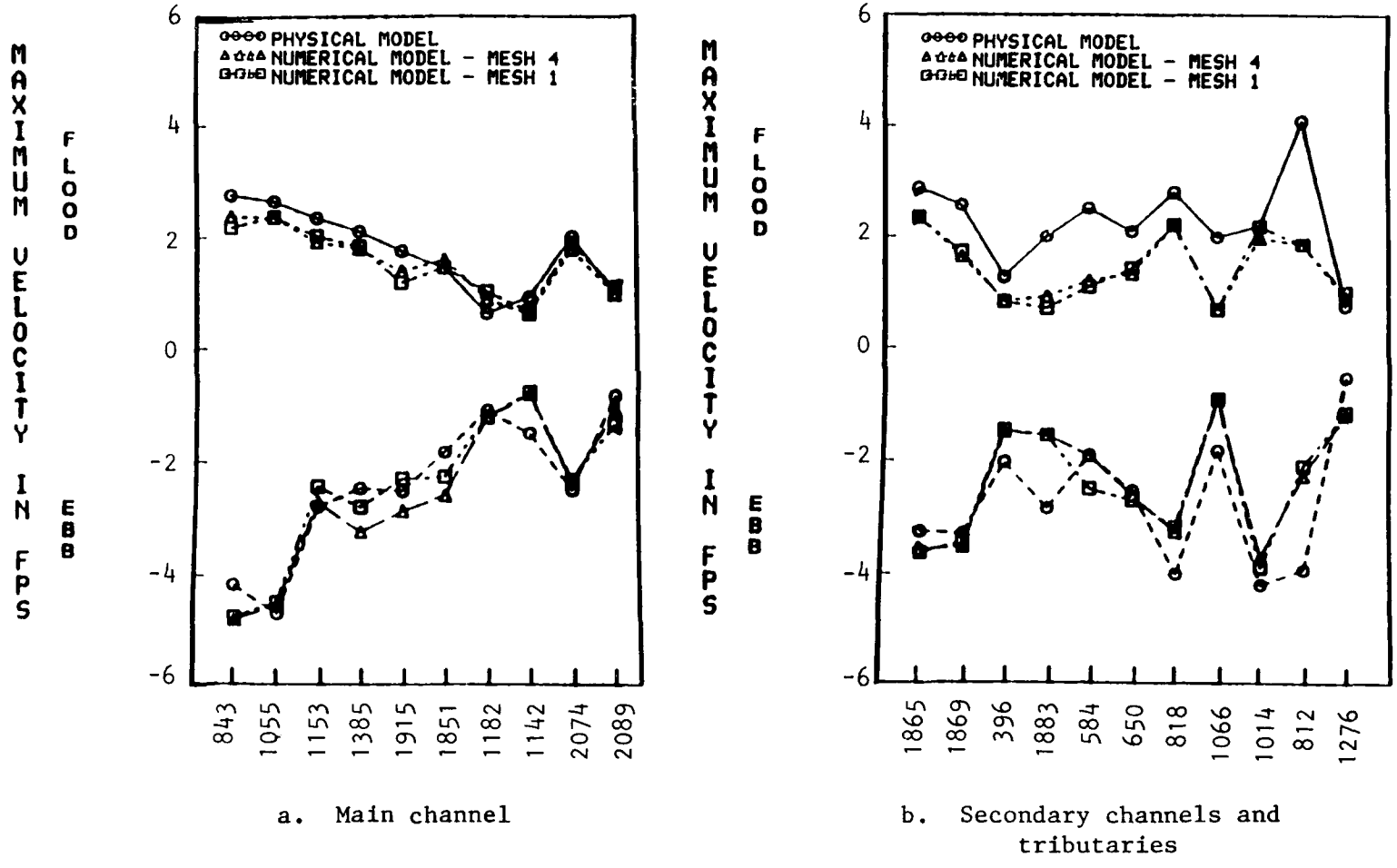

a. Main channel

b. Secondary channels and tributaries

Figure 22. Pre-Trident Mesh 4 velocity verification summary

the August 1985 condition survey (see paragraph 72). The fact that the other stations demonstrated close velocity agreement between Mesh 4 and Mesh 1 conditions indicated that mesh refinements had only localized hydrodynamic influence.

166. The numerical model velocity differences between Mesh 4 and Mesh 1 for stations 1385, 1915, 1851, and 1153 were smaller than the differences between the physical model and numerical model for the transitional channel condition. Station 1182, in lower Kings Bay, did not demonstrate any ebb velocity change between Mesh 4 and Mesh 1 and indicated excellent agreement with the physical model.

RMA-2V Verification Conclusion

167. In summary, the RMA-2V numerical model has been verified to reasonably reproduce pre-Trident and transitional channel hydrodynamic conditions. Marsh-estuarine circulation interaction was found to be important in achieving proper reproduction of Cumberland Sound and Kings Bay hydrodynamic characteristics. Application of a wetting and drying algorithm was used in obtaining the desired reproduction. The numerical model was found to be sensitive to prescribed marsh elevation. A compromise between tidal reproduction and velocity reproduction was made in achieving the desired hydrodynamic agreements. A numerical model marsh elevation of +4.0 ft was selected as the nominal elevation for final testing purposes. A closer tidal agreement was achieved with a marsh elevation of +4.5 ft; however, velocity was negatively affected under this condition. Excellent main channel velocity reproduction was demonstrated during the pre-Trident channel verification. Tributary and secondary channel velocity reproduction was considered acceptable. Velocity and tidal agreement was generally improved during the transitional channel verification. Localized hydrodynamic variations resulting from mesh modifications required for plan channel revisions were identified. These variations demonstrate the importance of consistent mesh resolution between tests for proper comparison and interpretation.

PART VI: VERIFICATION OF THE NUMERICAL SEDIMENT TRANSPORT MODEL, STUDH

Verification Approach

168. Long-term (numbers of years) prototype shoaling records with a nearly constant depth channel should be used for a sediment verification. Unfortunately, these records were not available for the Cumberland Sound-Kings Bay system. The channel has been undergoing modification since the Navy took over ownership in 1978, and prior bathymetric surveys are scant.

169. Sediment verification of STUDH was accomplished through several separate but complementary stages. Numerical model hydrodynamic data from each of the RMA-2V verification data sets were used as input data for sediment model computations for each of the conditions examined (i.e., Mesh 1 pre-Trident channel, transitional channel, and Mesh 4 pre-Trident channel). Each of these data sets was considered to be an approximation of the long-term hydrodynamic conditions associated with the long-term sedimentation processes affecting Cumberland Sound and Kings Bay for each condition.

170. As discussed in the following sections, for each of the verification efforts, several cohesive and noncohesive sediment model tidal cycle runs were performed separately taking advantage of hot-start capabilities (using output data from previous runs as initial conditions in following runs) to initialize model sediment concentration and bed conditions. Results for each sediment type were then extrapolated to simulate a complete sedimentation year. These results were arithmetically combined to produce a yearly total sedimentation rate for comparison to each other and to available prototype data.

Cohesive sedimentation

171. Three separate tidal cycle runs were performed in determining cohesive sedimentation rates. Table 3 provides summary values for the various sediment coefficients used in each of these runs. Critical shear stresses were based upon previous laboratory experiments on sediments from nearby areas, boundary and initial concentrations were based upon field data, and other coefficients were based upon previous modeling experience. The following coefficients were maintained for each run: Crank-Nicholson THETA was 0.66; the critical shear stress for deposition was 0.05 N/sq m; the erosion rate constant was 0.002 kg/sq m/sec; particle specific gravity was 2.65;

effective diffusion was 50 sq m/sec; boundary inflow sediment concentration was 0.10 kg/cu m; and for computational stability, a zero settling velocity was maintained along the exterior boundary.

172. During the 1982-1983 pre-Trident verification effort and all of phase 2 AIWW testing, the numerical model cohesive bed sediments were characterized with a dry weight bed density of 200 kg/cu m. During the later stages of phase 3 depth optimization testing and all subsequent testing, including the 1985-1986 transitional channel verification and Mesh 4 pre-Trident testing, the dry weight density for the cohesive sediments was increased to 300 kg/cu m. This adjustment was based on the field in situ bed density measurements conducted at Kings Bay during July 1985 (see paragraph 29). Since STUDH predictions for cohesive sediments were based upon mass considerations, cohesive sedimentation predictions for any of the earlier conditions examined can easily be adjusted for volume or shoaling rate computations. Except where otherwise indicated, results presented in this report reflect the revised bed density, i.e., 300 kg/cu m.

173. The cohesive sediment bed was initialized as a noneroding layer (99 N/sq m for the critical shear stress for particle erosion) at the beginning of the first (cold-start) tidal cycle run. An initial suspended sediment concentration of 0.10 kg/cu m was uniformly assigned throughout the computational mesh and allowed to deposit hydrodynamically as a cohesive bed with a critical shear stress for particle erosion of 0.15 N/sq m during this tidal cycle run. A particle settling velocity of 0.0006 m/sec was uniformly assigned throughout the interior portions of the mesh. A complete tidal cycle was run to create a realistic bed structure throughout the mesh.

174. A second tidal cycle was then run (bed layer hot start) using the deposited bed from the first cycle as its initial bed condition. A suspended sediment concentration of 0.10 kg/cu m was again uniformly assigned throughout the computational mesh. The particle settling velocity was reduced to 0.0003 m/sec and the critical shear stress for particle erosion was reduced to 0.12 N/sq m for another complete tidal cycle run. This run generated realistic sediment concentrations throughout the mesh.

175. A third, and final, tidal cycle (bed layer and concentration hot start) was run using the deposited bed and the concentration field at the end of the second cycle as the initial conditions for this tidal cycle run. The particle settling velocity (0.0003 m/sec) and critical shear stress for

particle erosion (0.12 N/sq m) were maintained as in the second run. Bed change results during this tidal cycle run were then extrapolated to simulate an average cohesive sedimentation year.

176. The cohesive sediment coefficients provided in Table 3 were used during each of the final verification and testing efforts. The same modeling procedure (i.e., cold start, bed layer hot start, and bed layer and concentration hot start) was also followed during each effort.

Noncohesive sedimentation

177. Table 4 summarizes the coefficients used for noncohesive sedimentation modeling. The following values were maintained throughout each of the runs: Crank-Nicholson THETA was 0.66; particle specific gravity was 2.65; particle shape factor was 0.70; length factor for deposition was 0.50 times depth; length factor for erosion was 10 times depth; effective diffusion was 250 sq m/sec; boundary inflow sediment concentration was 0.01 kg/cu m; and for computational stability, a zero settling velocity was maintained along the exterior boundary. Based on available prototype bottom sediment samples, shoaling history, and current velocity, three different sediment grain size specifications (fine, medium, and coarse median grain size distributions and corresponding settling velocities) were used to characterize the bed sediments. The noncohesive sediment distribution was adjusted for each of the verification efforts as new schematization and information were available. The specific distribution used for each effort will be illustrated in subsequent sections.

178. The same basic modeling procedures were followed during each effort. During the initial cold-start tidal cycle run, the bed was initialized with an unlimited depth of sediment (actually 10 m of available sediment) and a suspended sediment concentration of 0.01 kg/cu m was uniformly assigned throughout the computational mesh. A 30-day internal extrapolation was performed followed by another tidal cycle run (hot-start extrapolation). The primary purpose of this run-extrapolate-run procedure was to stabilize the concentration field to the prescribed hydrodynamic conditions. The resulting concentration field at the end of this tidal cycle run was used as the initial concentration field for a final tidal cycle run (concentration hot start). Bed change results from this run were then extrapolated to an average noncohesive sedimentation year.

Total sedimentation

179. As previously addressed, the field shoaling information could not be reduced to cohesive and noncohesive components. Extrapolation results from the numerical model cohesive and noncohesive sedimentation predictions were arithmetically combined for comparison to the available prototype data. Figure 23 is a schematic drawing of the pre-Trident channel sedimentation zones used in the verification analysis. During the 1985 field efforts, channel sediment bed sampling confirmed the general location of the cohesive-noncohesive transition zone predicted by the numerical model; cohesive sediments were confined to the vicinity of the floating dry dock and areas to the north and northwest in Kings Bay (zones 14A, 15, 15A, 16, 17, and 18).

Pre-Trident Mesh 1 Verification

180. Figure 24 illustrates the general distribution of the three noncohesive sediment types used during the pre-Trident Mesh 1 verification effort. Preliminary grain size distributions were selected using size analyses of bottom grab samples as a general guide. Some adjustments of size distribution were performed prior to the final verification runs. The inlet throat area was assigned a coarse-grained (0.70-mm) sand with a particle settling velocity of 0.090 m/sec and a Manning's n value of 0.025. The St. Marys River area into Cumberland Sound and to the inlet throat area was characterized with a medium-grained (0.35-mm) sand with a settling velocity of 0.045 m/sec. The Cumberland Dividings entrance area (northeast portion of the study area) was also characterized with this medium-grained sand. All other areas of the computational mesh were characterized with a fine-grained (0.125-mm) sand with a settling velocity of 0.0105 m/sec. With the exception of a few major channel bend areas, a 0.020 Manning's n value was assigned all interior areas. Manning's n values of 0.010 and 0.015 were assigned to the major channel bend area in lower Cumberland Sound and 0.010 was assigned to the channel bend area leading into Kings Bay.

181. High numerical model and field sedimentation rates are indicated for the Kings Bay area; largest rates occur in the vicinity of the floating dry dock. Figure 25 illustrates the resulting total sedimentation (cohesive and noncohesive) numerical model-to-prototype shoaling rate comparison along the navigation channel. Zones 14A and 15A, associated with the floating dry

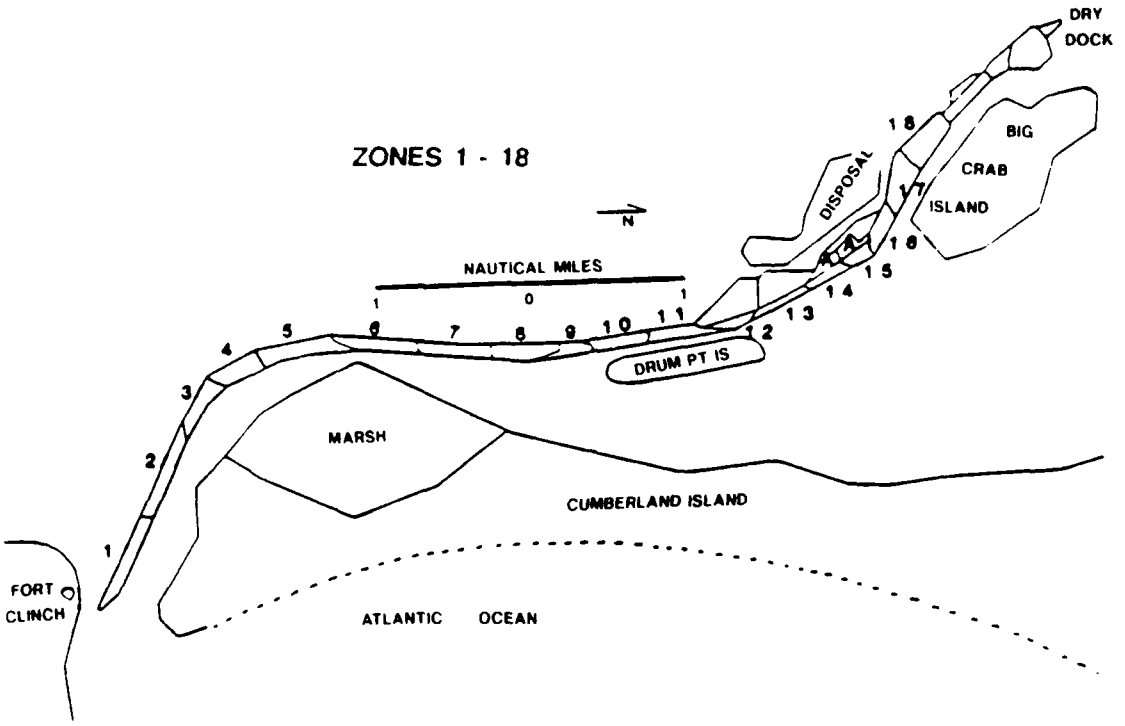

Figure 23. Pre-Trident channel sediment zones used in verification

dock adjacent to the main channel, are plotted separately, to the right of zone 18 (the end of the Poseidon channel). Numerical model results are illustrated for both the 200- and the 300-kg/cu m bed density cohesive sediment conditions. In general, numerical model predictions with the less dense cohesive sediment component (i.e., 200 kg/cu m) resulted in larger rates of deposition (1.46 million cubic yards per year) relative to the average prototype condition (1.2 million cubic yards per year), while predictions with the more dense cohesive characterization resulted in reduced sedimentation (1.05 million cubic yards per year) relative to the field conditions. With the exception of the floating dry dock area (zone 15A), model predictions fell within the range of the field observations.

182. Figure 25 also indicates the noncohesive component of the numerical model prediction for the Kings Bay zones; as illustrated, cohesive sediments account for most of the deposition in the Kings Bay area. Channel sedimentation south of the Kings Bay area (zones 1-14) is basically noncohesive material. Although not shown in Figure 25, the numerical model predicted little sedimentation (i.e., about 1 ft/yr or less) in the proposed upper Trident basin for the pre-Trident channel (depth) condition.

183. Excellent numerical model to prototype sediment verification is

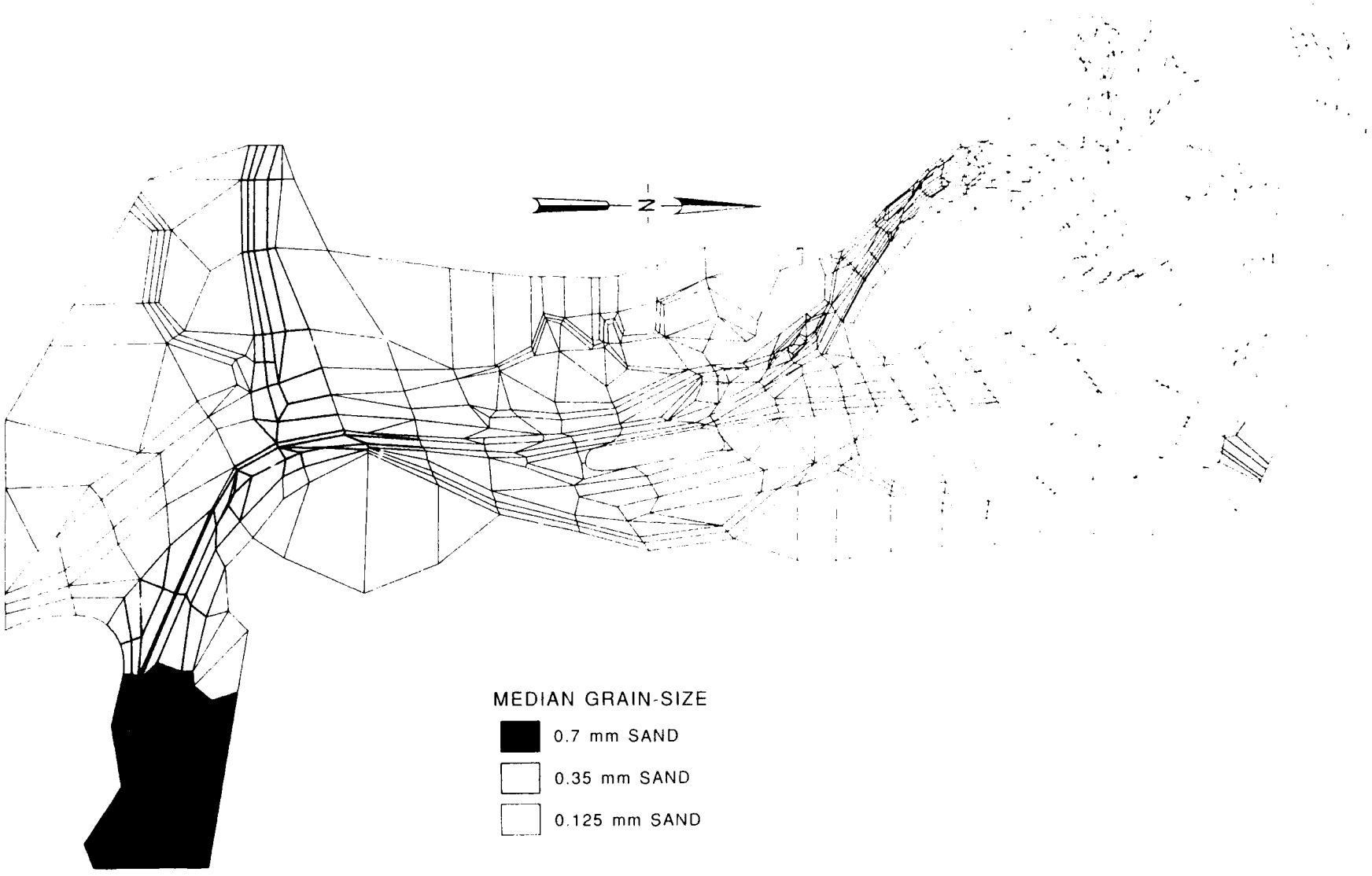

Figure 24. Pre-Trident Mesh 1 noncohesive sediment grain size distribution

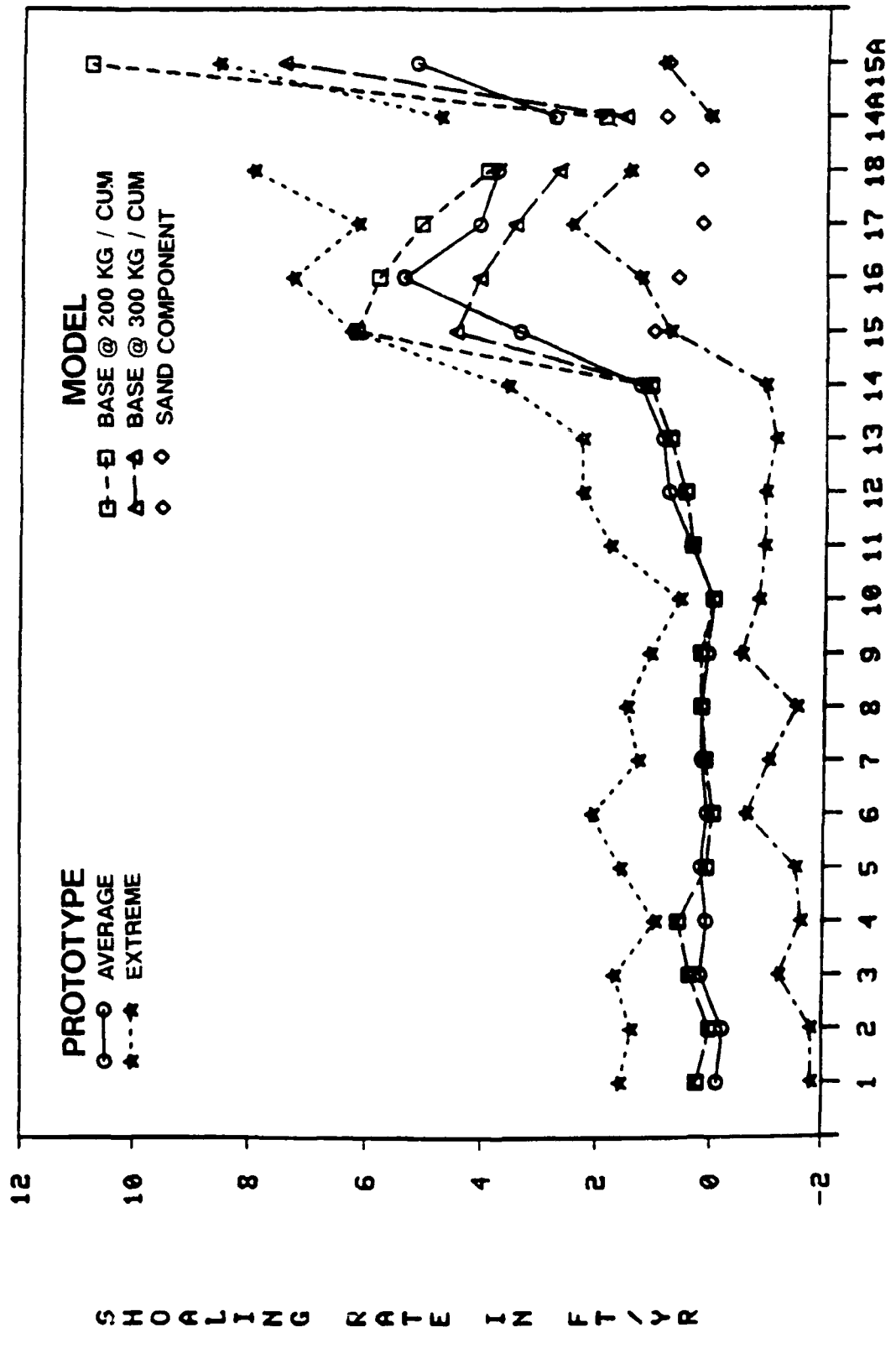

Figure 25. Pre-Trident Mesh 1 sediment verification

demonstrated. Main channel numerical model maximum sedimentation occurred slightly downstream from the prototype maximum, i.e., zone 15 in the numerical model and zone 16 in the field. The largest numerical model-to-prototype variation occurred within the small zone of the floating dry dock. Field surveying within this zone was difficult and sometimes incomplete due to the presence of the floating dry dock. Confidence in shoaling rates within this zone is lower than the other channel areas.

Transitional Channel Verification

184. Several STUDH numerical model runs with different noncohesive sediment grain size distributions were performed during the transitional channel verification effort. Initial runs were conducted using the same sediment characterization as during the Mesh 1 verification effort. As previously discussed, the upper Trident basin area had no previous dredging (shoaling) history. Results from the upper basin field shoaling analysis task for the recently dredged Trident basin (January 1985-January 1986 survey comparisons) indicated a moderate sedimentation rate, on the order of 2 to 3 ft per year, for the basin area. The initial numerical model cohesive and noncohesive sedimentation predictions for the transitional channel were greater, each on the order of 5 ft per year, for the upper Trident Kings Bay turning basin. Based upon information from additional sediment samples and the initial sedimentation predictions, the noncohesive sediments for the shallow channel areas above the Kings Bay facility were assigned medium grain size sediment characteristics. This adjustment reduced the noncohesive sedimentation predictions for the turning basin.

185. Additional noncohesive sensitivity testing was conducted in preparation for the upper basin remedial measures testing. Results from these tests indicated the desirability also to increase the noncohesive sediment grain size for the lower south fork of the Crooked River down into Cumberland Sound to the transition with the submarine channel. This adjustment was based on additional sediment samples and an analysis of model-predicted bed shear stress for this area.

186. Figure 26 illustrates the final selected areas for additional sediment coarsening for the final transitional channel verification and plan testing conditions. These two new areas were assigned the sediment

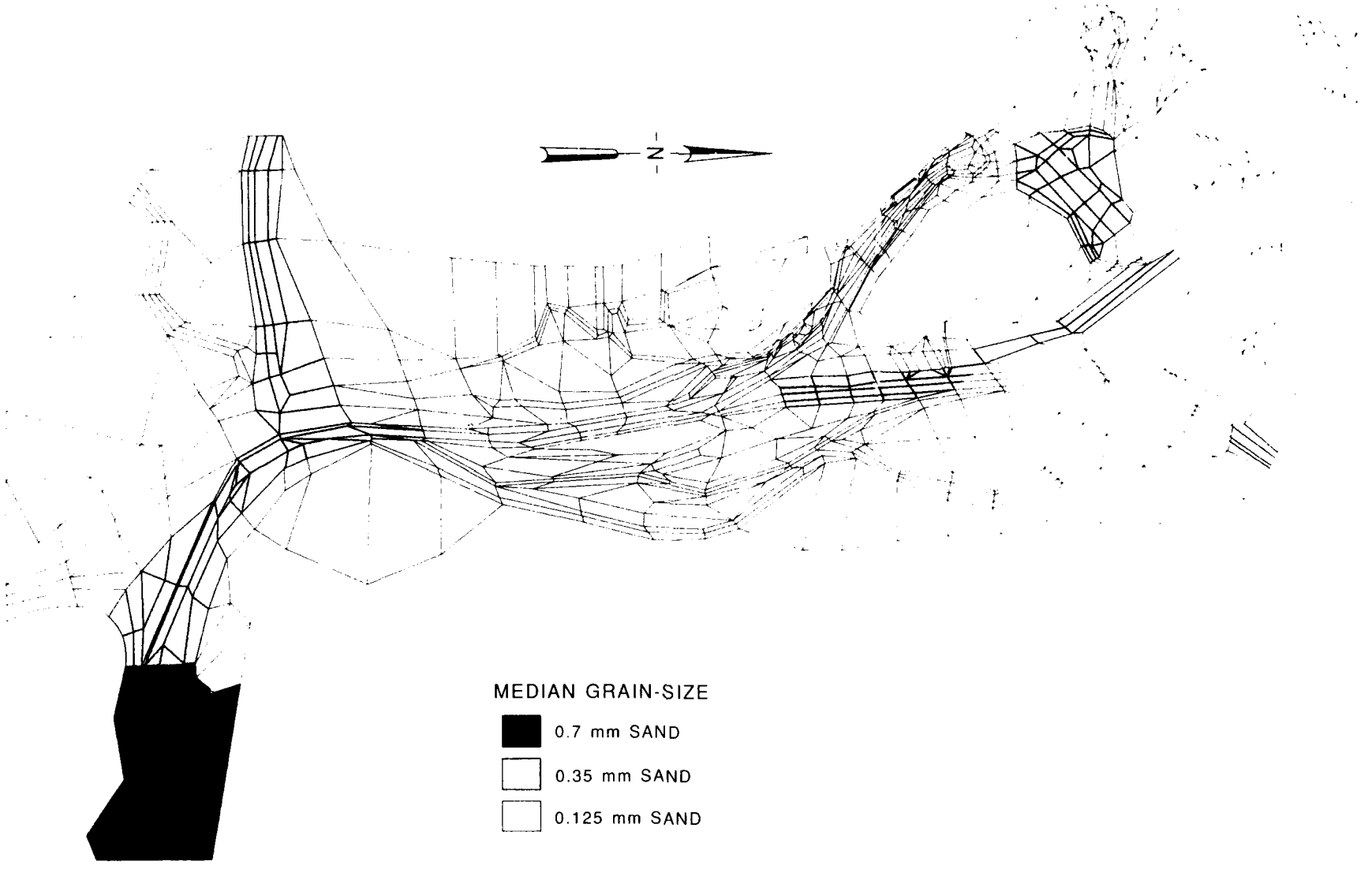

Figure 26. Transitional channel noncohesive sediment grain size distribution

characteristics of medium-grained (0.35-mm) sand. The sediment grain size distribution and associated characteristics of the other areas were maintained as in the pre-Trident Mesh 1 verification.

187. Figure 27 illustrates the numerical model sediment predictions for the transitional channel conditions compared to the pre-Trident field data and the numerical model pre-Trident Mesh 1 verification data set. The numerical model predictions for the deepened upper Trident area (zones 19-21) are also presented. Small to no changes are indicated in the low shoaling areas below zone 15 comparing pre-Trident and transitional channel numerical model predictions; reduced sedimentation is predicted for the transitional channel condition for the lower Kings Bay area (zones 14A-17). High shoaling rates are predicted for the deepened upper Trident basin.

188. Numerical model predictions indicate that the reduced transitional channel velocity and resulting sedimentation changes associated with the deepened upper Trident basin created an efficient sediment trap in the upper Trident Kings Bay area, moving the high deposition areas upstream above the Poseidon operational area. The reduced transitional channel deposition in the lower Kings Bay Poseidon operational area, relative to the pre-Trident condition, demonstrates the need for careful extrapolation of results from one set of conditions to another.

189. As discussed previously, the coarsened grain-size distribution indicated in Figure 26 reduced the amount of noncohesive deposition, but predicted total shoaling rates in the upper turning basin were still much greater than the limited available data indicated. Additional adjustments to further reduce model sedimentation predictions (cohesive and/or noncohesive) were not pursued due to the limited field data and the following additional considerations.

190. During the past several years, including the 1985-1986 period, the entire east coast has been receiving less than normal amounts of rainfall. Corps Districts up and down the coast have been reporting less than average sedimentation problems. Limited numerical model sensitivity testing indicated that reduced cohesive sediment concentration boundary conditions (associated with reduced freshwater discharge) resulted in reduced model sedimentation rates. Since modeling predictions are for long-term average conditions, however, further adjustments of model coefficients to reproduce less than average environmental conditions seemed unwarranted.

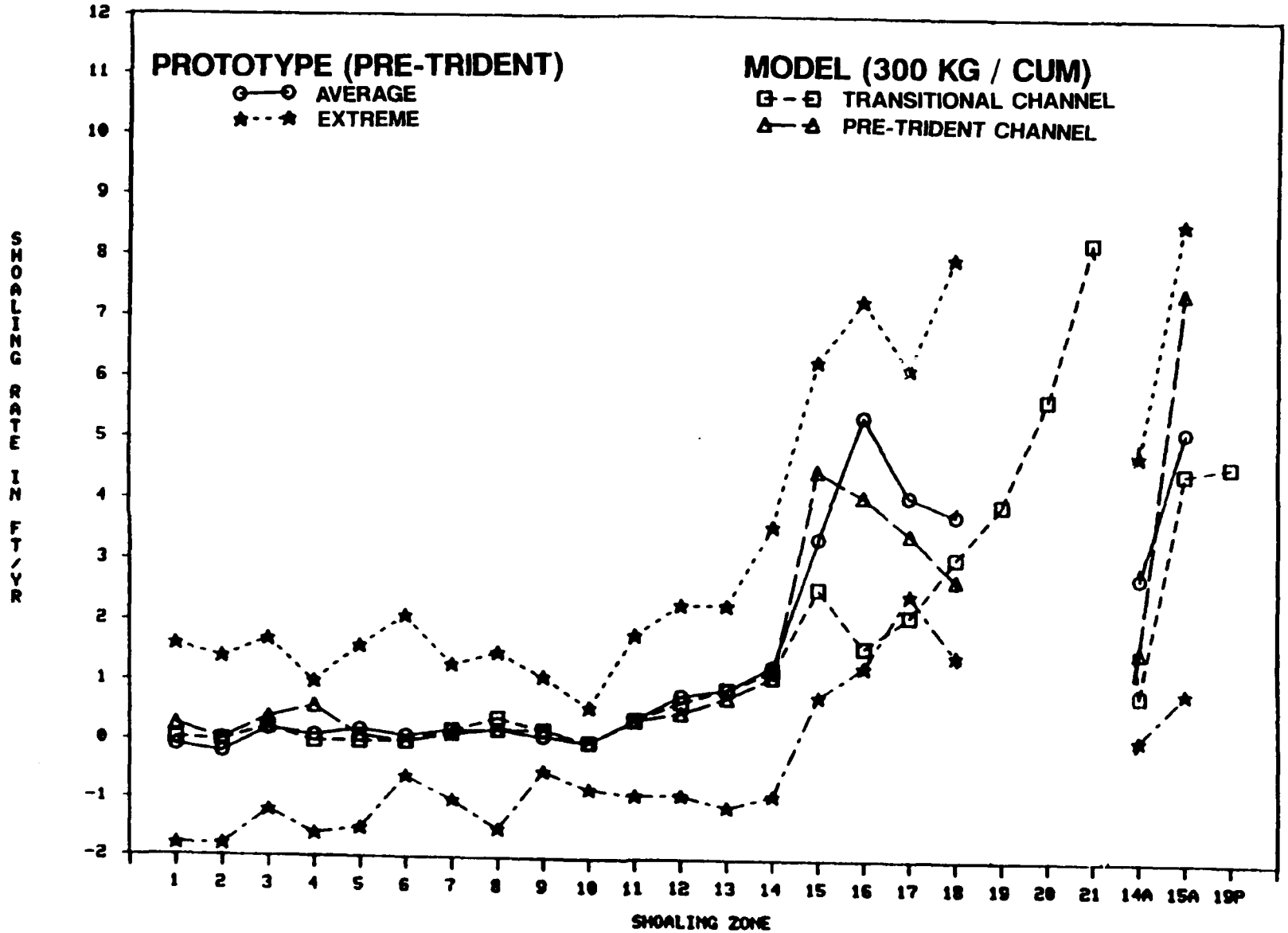

Figure 27. Transitional channel sediment verification

191. Numerical model schematization of the Poseidon tender across the channel at the downstream end of the Kings Bay marginal wharf is another possible explanation for the apparent differences in model and field shoaling rates for the upper end of Kings Bay. As discussed in paragraph 134, the tender was schematized in the hydrodynamic model by simply increasing the Manning's n roughness value (from 0.015 to 0.030) and reducing the turbulent exchange coefficients (from 100 to 70) for the elements representing the tender. The actual water depth at the tender was used to schematize the geometry conditions. The channel cross-sectional area displaced by the tender in its orientation, perpendicular to the channel (across about 50 percent of the channel), was not truly reproduced in the model. Based upon the available pre-Trident shoaling and hydrodynamic information, this schematization appeared reasonable. However, based upon the 1985-1986 transitional channel sedimentation data, the tender schematization may underestimate the blockage of sediment transport and, therefore, overestimate the shoaling rates associated with the transitional channel hydrodynamic and sedimentation processes. This schematization of the tender, however, is reasonable for the plan channel condition with the tender parallel to the channel.

192. A third explanation for the model-to-prototype variation in transitional channel shoaling in the upper Trident basin involves the ongoing Trident channel expansion construction dredging. As previously discussed, the hydrodynamic and sedimentation processes of Kings Bay and Cumberland Sound are in a transitional state, and extrapolating results for one set of long-term average conditions (fixed geometry, i.e., pre-Trident or completed Trident, and average physical environmental conditions) to a set of different conditions has its limitations. As will be shown in the base-to-plan comparison report (Granat and Brogdon, in preparation), the completed plan channel sedimentation distribution is very much different from the indicated transitional channel distribution. High rates of sedimentation were again indicated for the lower end of Kings Bay along with a 1- to 2-ft reduction in sedimentation for the upper basin, comparing numerical model transitional channel predictions with completed Trident plan channel predictions.

193. Any combination of these three possible explanations may help contribute to the differences in predicted numerical model transitional channel sedimentation and the limited field data. The need for further model adjustments, i.e., potential sediment armoring reducing the availability of source

material, cannot be ruled out. However, at this time, sufficient data are not available to justify further model refinements. Additional time and field monitoring will help resolve this question.

Mesh 4 Sedimentation Investigations

194. Pre-Trident channel sedimentation runs were performed with the basic Mesh 4 schematization to ensure that the increased mesh resolution had no negative impacts on channel sedimentation predictions and model verification. These runs were performed after the completion of the upper basin remedial measures testing program. A minor mesh refinement was required (see paragraph 161) in the plan channel waterfront docking area, west of the Poseidon dry dock area, of Mesh 4 (increasing the number of nodes and elements by one) to allow proper flooding and drying to occur when the geometry was revised back to pre-Trident geometry conditions. The revised pre-Trident Mesh 4 contained 1,118 elements and 3,224 nodes compared with 791 elements and 2,382 nodes for the pre-Trident Mesh 1 schematization.

195. The presented sensitivity runs used the Mesh 4 RMA-2V hydrodynamic conditions generated using the pre-Trident physical model hydrodynamic boundary forcing conditions and the revised noncohesive sediment distribution determined during the transitional channel verification period. Figure 28 illustrates this sediment distribution for the coarsened areas above Kings Bay for this testing effort. After testing was completed, it was discovered that node 2669, in Marianna Creek, was inadvertently left uncoarsened during all Mesh 4 testing.

196. Figure 29 illustrates the Mesh 4 pre-Trident numerical model sediment predictions compared with the Mesh 1 predictions at a dry weight density of 300 kg/cu m and the prototype pre-Trident field shoaling rates. The sand component for zones 15 and above are also illustrated for each numerical model prediction. As shown, subtle changes are indicated by a comparison of Mesh 4 predictions with Mesh 1 predictions. In the high shoaling zones of Kings Bay, the Mesh 4 predictions are generally slightly reduced from Mesh 1 predictions. On a total volume shoaling basis, the Mesh 4 sedimentation prediction is within 93 percent of the Mesh 1 prediction. Mesh 4 cohesive and noncohesive deposition is reduced relative to Mesh 1 sedimentation. As expected with the increased grain size distribution of the Mesh 4 characterization, the san

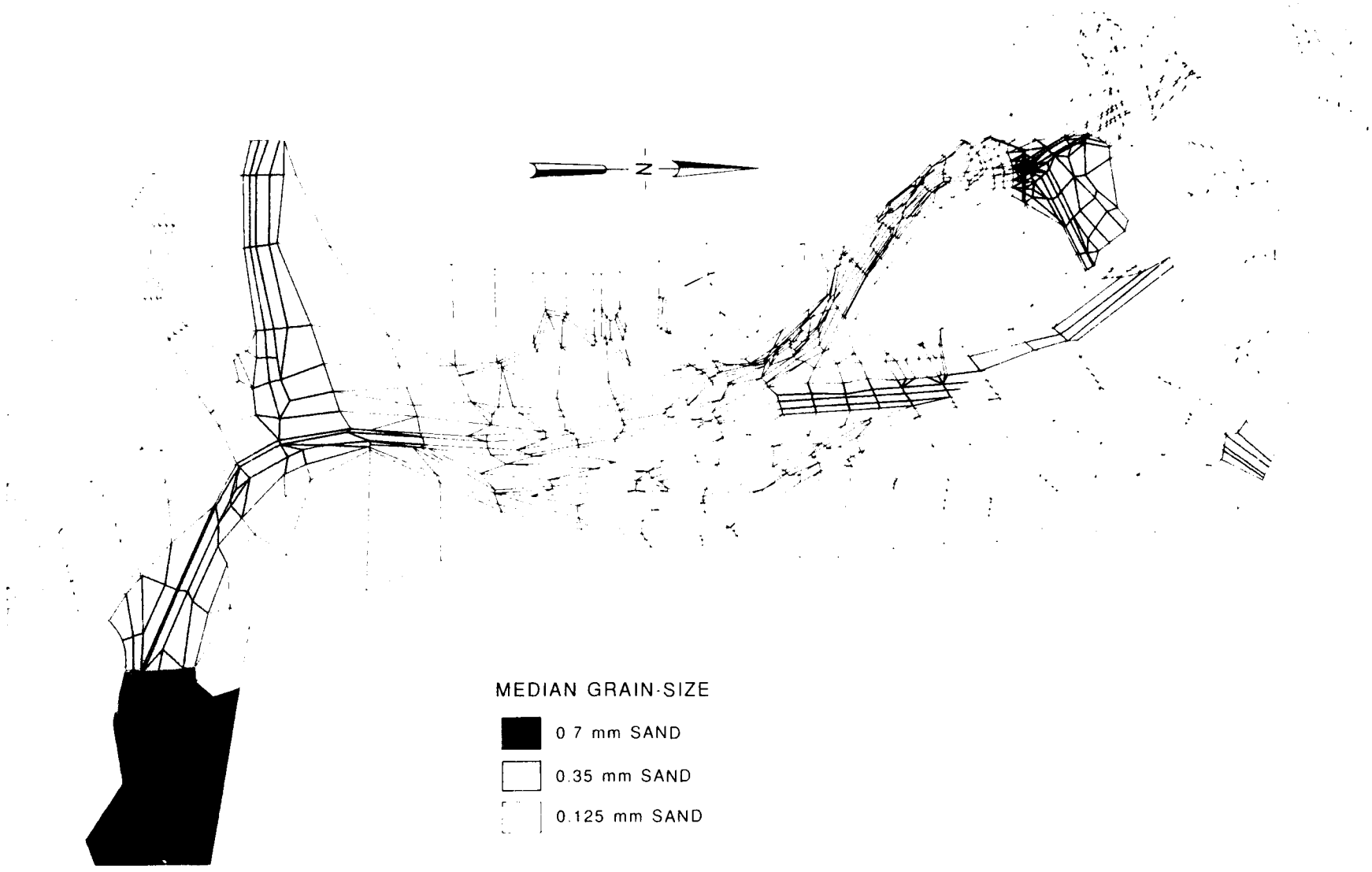

Figure 28. Pre-Trident Mesh 4 noncohesive sediment grain size distribution

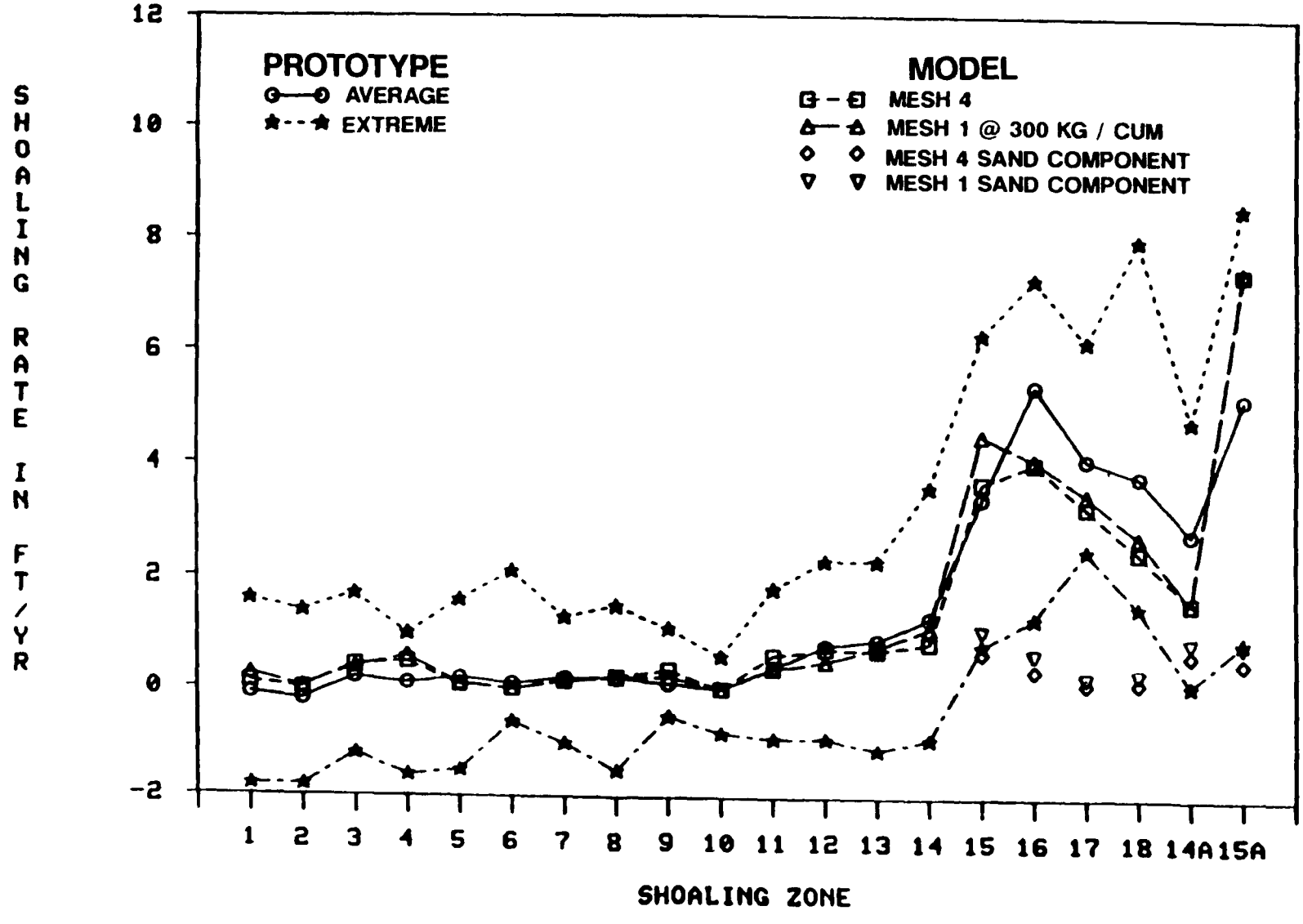

Figure 29. Pre-Trident Mesh 4 sediment verification

component predictions varied the most; overall Mesh 4 sand deposition was about 80 percent of Mesh 1 prediction. Cohesive deposition predictions varied by less than 3 percent.

197. The presented results indicate little to no verification impact associated with the revised schematization of Mesh 4. Largest Mesh 4 to Mesh 1 variations were associated with the increased noncohesive grain size characterization of the areas above Kings Bays. Zone 15 demonstrated the greatest variation, with reduced Mesh 4 sedimentation relative to Mesh 1 conditions. Excellent verification of the numerical model Mesh 4 prediction is indicated compared to the pre-Trident prototype shoaling records. The Mesh 4 pre-Trident model predictions should be used in Mesh 4 plan and remedial measures model comparisons.

STUDH Verification Conclusion

198. The numerical model STUDH has been verified to reproduce long-term average sedimentation processes for the pre-Trident Cumberland Sound/Kings Bay submarine channel by using both the cohesive and noncohesive capabilities of the sedimentation code. Relatively low noncohesive shoaling rates were computed for the lower channel areas below the Kings Bay facility. High shoaling rates, mostly cohesive sediments, were computed for the Poseidon floating dry dock area and the facility areas to the northwest.

199. Model predictions for a transitional period indicated higher rates of sedimentation than indicated in a limited field data set for the recently dredged upper Trident Basin. Several possible explanations for this difference included the prolonged east coast drought with less than normal sediment loads and reduced maintenance dredging requirements reported from east coast Corps Districts; the schematization approach used for the Poseidon tender in its orientation perpendicular to the channel; the transitional nature of the channel and its associated circulation; and/or the potential need for additional model adjustments, i.e., sediment armoring. At present, additional time and monitoring are required before any other model adjustments can be made with confidence.

200. Little to no sediment verification impact was indicated as a result of the increased mesh resolution associated with the revised schematization required for future plan and remedial measures testing. The

Mesh 4 model predictions should be used in plan channel and remedial measures comparisons.

PART VII: SUMMARY AND CONCLUSIONS

201. A hybrid modeling system was developed to investigate hydrodynamic and sedimentation processes of the Cumberland Sound/Kings Bay estuarine system. A fixed-bed physical model was constructed to examine the three-dimensional hydrodynamic and salinity characteristics. Verification of the physical model to reproduce pre-Trident channel field measurements collected during November 1982 and transitional channel conditions measured during January 1985 has been demonstrated. The model can be remolded to test any desired plan channel or remedial measure under consideration to assess potential three-dimensional hydrodynamic or salinity impacts. The physical model was also used to develop boundary forcing conditions and to provide an expanded data set for numerical modeling purposes.

202. The other component of the hybrid modeling system was the US Army Corps of Engineers depth-averaged TABS-2 finite element numerical modeling system. The numerical hydrodynamic model RMA-2V used physical model-derived St. Marys Inlet water levels and tributary velocity measurements for the boundary forcing conditions for an average tidal cycle. The numerical model was verified to physical model tidal elevations and depth-averaged velocity data for interior locations. A wetting and drying algorithm was used in modeling the extensive marsh and sand flat areas of the Cumberland Sound system. Marsh-estuarine circulation interaction was found to be important in achieving the proper hydrodynamic reproduction. The numerical model was found to be sensitive to prescribed marsh elevation. RMA-2V reasonably reproduced pre-Trident and transitional channel hydrodynamic conditions of the Cumberland Sound/Kings Bay system.

203. Hydrodynamic results from the RMA-2V verification were used in the numerical sediment transport code STUDH in modeling the interaction of flow transport and sedimentation on the bed. Both cohesive (clay and silt) and noncohesive (silt and sand) sedimentation was modeled. Verification of STUDH was accomplished through comparison of model predictions with actual field shoaling rates determined from the pre-Trident channel.

204. The RMA-2V verification data set was considered to be an approximation to the long-term average hydrodynamic conditions associated with the long-term sedimentation processes affecting the navigation channel through Cumberland Sound and Kings Bay. Excellent verification to the pre-Trident

field shoaling rate was demonstrated. Model predictions for the upper Kings Bay turning basin for a transitional channel condition indicated higher shoaling rates than indicated by a limited field data set. Several possible explanations for this variation included the prolonged east coast drought and associated reduced sedimentation, the schematization of the Poseidon tender in its orientation perpendicular to the channel, and the transitional nature of the channel. The sediment model has been verified for long-term average conditions. Additional time and monitoring are required before any other model adjustments can be made with confidence.

205. Verification of the hydrodynamic and sediment transport hybrid modeling system has been demonstrated. The latest revised and verified mesh (Mesh 4) and the modeling procedures developed should be used in carefully designed testing programs to assess potential hydrodynamic and sedimentation impacts associated with plan channel and remedial measures testing.

REFERENCES

Ackers, P., and White, W. R. 1973. "Sediment Transport: New Approach and Analysis," Journal of the Hydraulics Division, American Society of Civil Engineers, Vol 99, No. HY11, pp 2041-2060.

Ariathurai, C. R., MacArthur, R. C., and Krone, R. B. 1977 (Oct). "Mathematical Model of Estuarial Sediment Transport," Technical Report D-77-12, US Army Engineer Waterways Experiment Station, Vicksburg, MS.

Baker, A. J. 1983. Finite Element Computational Fluid Mechanics, McGraw-Hill, London.

Desai, C. S. 1979. Elementary Finite Element Method, Prentice Hall, Englewood Cliffs, NJ.

Granat, M. A. 1987a (May). "Application of the TABS-2 Numerical Modeling System for the Evaluation of Advance Maintenance Dredging," Proceedings of San Francisco District Navigation Workshop, San Francisco District, Corps of Engineers, pp 238-267.

_____. 1987b (Aug). "Numerical Model Evaluation of Advance Maintenance," Proceedings, National Conference on Hydraulic Engineering, American Society of Civil Engineers, pp 321-326.

Granat, Mitchell A., and Brogdon, Noble J. "Cumberland Sound and Kings Bay Pre-Trident and Basic Trident Channel Hydrodynamic and Sediment Transport Hybrid Modeling" (in preparation), US Army Engineer Waterways Experiment Station, Vicksburg, MS.

King, I. P., Granat, M. A., and Ariathurai, C. R. 1986 (Aug). "An Inundation Algorithm for Finite Element Hydrodynamic and Sediment Transport Modeling," Proceedings, Third International Symposium on River Sedimentation, Vol III, River Sedimentation, S. Y. Wang, H. W. Shen, L. Z. Ding, ed., School of Engineering, University of Mississippi, University, MS, pp 1583-1593.

Krone, R. B. 1962 (Jun). "Flume Studies of Transport of Sediment in Estuarial Shoaling Processes," Final Report, Hydraulics Engineering Research Laboratory, University of California, Berkeley, CA.

Norton, W. R., and King, I. P. 1977 (Feb). "Operating Instructions for Computer Program RMA-2," Resource Management Associates, Lafayette, CA.

Norton, W. R., King, I. P., and Orlob, G. T. 1973. "A Finite Element Model for Lower Granite Reservoir," prepared for US Army Engineer District, Walla, Walla, Walla Walla, WA, by Water Resources Engineers, Walnut Creek, CA.

Partheniades, E. 1962. "A Study of Erosion and Deposition of Cohesive Soils in Salt Water," Ph.D. Dissertation, University of California, Berkeley, CA.

Radtke, D. B. 1985. "Sediment Sources and Transport in Kings Bay and Vicinity, Georgia and Florida, July 8-16, 1982," US Geological Survey Professional Paper 1347, US Government Printing Office, Washington, DC.

Salkield, A. P. 1985 (Aug). "In-situ Sediment Density Measurements Kings Bay, Georgia, July 1985," Sediment Dynamics International, Ltd., Moline, IL.

Thomas, W. A., and McAnally, W. H., Jr. 1985 (Aug). "User's Manual for the Generalized Computer Program System: Open-Channel Flow and Sedimentation, TABS-2; Main Text and Appendices A through O," Instruction Report HL-85-1, US Army Engineer Waterways Experiment Station, Vicksburg, MS.

Zienkiewicz, O. C. 1971. The Finite Element Method in Engineering Science, McGraw-Hill, London.

Table 1

Numerical Model Verification Mesh Summary

Mesh	Number of Nodes	Number of Elements	Geometric Schematization: Feature	Geometric Schematization: Condition Being Schematized	Date of Depth Survey	Physical Model-Derived Boundary Forcing Condition: Date Generated	Physical Model-Derived Boundary Forcing Condition: H/L, ft* Sta 1	Physical Model-Derived Boundary Forcing Condition: H/L, ft* Sta 2
Mesh 1	2,382	791	Submarine Channel	Feb 1984	Nov 1982	Aug 1983	+6.2/+0.5	+5.9/+0.25
			AIWW	Existing	Nov 1982			
Transitional Channel	2,611	885	Submarine Channel	Jan 1985	Jan 1985	Sep 1986	+6.3/+0.55	+6.0/+0.4
			AIWW	Alternate Route C	Aug 1985			
Mesh 4	3,224	1,118	Submarine Channel	May 1985	Nov 1982	Aug 1983	+6.2/+0.5	+5.9/+0.25
			AIWW	Alternate Route C	Aug 1985			
			Northwest of Kings Bay	Potential Remedial Measures	Aug 1985			

* H = high-water elevation; L = low-water elevation

Table 2

RMA2-V Hydrodynamic Coefficients

Type	Description	Turbulent Exchange Coefficient lb-sec/sq ft	Manning's n
1	Small channel	100	0.025
2	Normal channel	100	0.020
3	Smooth channel	100	0.015
4	Main marsh	200	0.050
5	Secondary marsh	170	0.040
6	Marsh/channel transition	150	0.030
7	Ocean	500	0.020
8	Dock facility	300	0.030
9	Dry dock/tender	70	0.030

Table 3

Cohesive Sedimentation Coefficients

Coefficient	Cycle 1	Cycle 2	Cycle 3
Crank-Nicholson THETA	0.66	0.66	0.66
Critical shear stress deposition, N/sq m	0.05	0.05	0.05
Dry weight density of freshly deposited layer, kg/cu m*	300	300	300
Particle specific gravity	2.65	2.65	2.65
Erosion rate constant, kg/sq m/sec	0.002	0.002	0.002
Effective diffusion, sq m/sec	50	50	50
Boundary inflow sediment concentration, kg/cu m	0.10	0.10	0.10
Exterior boundary particle settling velocity, m/sec	0.0	0.0	0.0
Interior boundary particle settling velocity, m/sec	0.0006	0.0003	0.0003
Critical shear stress particle erosion, N/sq m	0.15	0.12	0.12
Sediment bed initialization	non-eroding	hot start cycle 1	hot start cycle 2
Initialization of suspended sediment concentration	0.10	0.10	hot start cycle 2

* Prior to the 1985-1986 transitional channel verification period, 200 kg/cu m was used. Revised bed density based upon Kings Bay in situ bed density measurements taken during July 1985.

Table 4

Noncohesive Sedimentation Coefficients

Crank-Nicholson THETA	0.66
Particle specific gravity	2.65
Particle shape factor	0.70
Length factor for deposition (times depth)	0.50
Length factor for erosion (times depth)	10.0
Effective diffusion, sq m/sec	250
Boundary inflow sediment concentration, kg/cu m	0.01
Median sediment grain size D_{50}, mm	
Coarse sand	0.70
Medium sand	0.35
Fine sand	0.125
Particle settling velocity, m/sec	
Coarse sand	0.090
Medium sand	0.045
Fine sand	0.0105
Manning's n value	
Ocean	0.025
Channel bend at lower Cumberland Sound	0.015
Channel bend at Kings Bay entrance	0.010
All other areas	0.020

APPENDIX A: FIELD DATA COLLECTION EQUIPMENT AND METHODS

Tidal Elevations

1. Tidal elevations were measured by a system consisting of a stilling well-contained float that is connected to a recording device by a wire rope. The recorders were Fischer and Porter Company Type 1550 punched tape level recorders. They record elevations to the nearest 0.01 ft and have a range of 100 ft. A timer activates the recording mechanism every 15 min, and the float elevation at that time is punched on 16-channel, foil-backed paper tapes. The float is a 3-in.-diam aluminum cylinder, and the stilling well is a 4-in.-diam plastic pipe. Water level in the stilling well responds to water levels outside the well by flow through a 15-ft-long, 3/8-in.-diam copper tube. The tube's outer end is protected against clogging by a cylindrical copper filter.

2. Vertical control for the tide gage assemblies is arbitrary. The 15-ft-long tube used as the stilling well port is designed to minimize short-period oscillations and to cause the well to respond linearly to fluctuations in the outside water level. Response characteristics of the tide wells have been determined by drainage tests.* Figure A1 shows the derived amplitude and phase response characteristics of the tide wells. It can be seen that amplitude decreases sharply in less than 50 min and is less than 10 percent for periods under 1 min. The half-amplitude period is 9 min, while the amplitude response is essentially unity and phase lag approaches zero at tidal periods.

3. Initial synchronization of the tide recorder timer is within ±5 sec of the National Bureau of Standards (NBS) time standard. Bench tests of the timers have shown them to exhibit negligible error for individual readings over a 1-hr period. Gage time is generally accurate to ±2 min per month, except for occasional malfunctions that can cause large time errors. In practice, gage and NBS times are recorded when tapes are removed so that timing errors can be identified.

4. Relative accuracy is affected by temperature of the water, float, and wire, plus salinity changes of the water inside the well. Relative accuracy is considered to be within 0.1 ft.

---

* W. H. McAnally, Jr. 1979. "Water Level Measuring by Estuaries Division, Hydraulics Laboratory," Memorandum for Record, US Army Engineer Waterways Experiment Station, Vicksburg, MS.

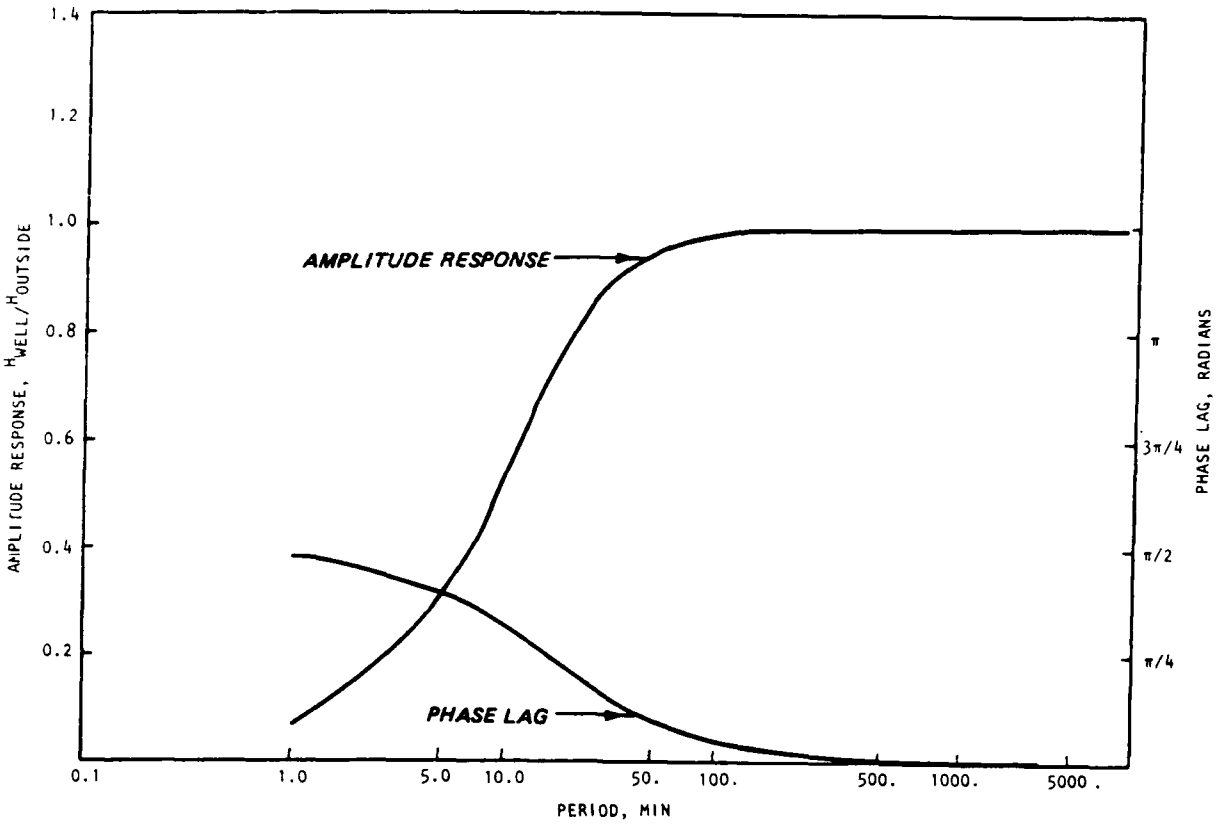

Figure A1. Response characteristics of standard tide well port used in field data collection

Over-the-Side-Equipment

5. The equipment used to obtain discrete samples from a boat consists of a current meter, direction indicator, and weight, each suspended by a wire rope, plus remote readout devices and a support frame. The assembly (Figure A2) is mounted on a boat that moves from station to station collecting data. The current meter is a vertical-axis cup type (Gurley Model 665) with remote, direct-reading speed indicator. The direction indicator consists of a remote-reading magnesyn compass mounted just above the current meter in a waterproof cylindrical housing. Suspended below the meter is a finned, streamlined weight (fish) that holds the sensors in a vertical attitude facing into the flow. The sensor assembly is supported by a 1/8-in. wire rope from a portable support frame that is equipped with a winch to raise and lower the assembly. An indicator on the winch shows the sensor's depth below the water's surface. Water samples are taken at the depth of measurement by pumping through a 3/8-in. plastic tube with tip mounted just below the current

meter and pointed into the flow. A small pump on board the boat pumps the water through a bimetal thermometer and into sample bottles. The pumping rate is 2.8 gpm for a 3-ft lift.

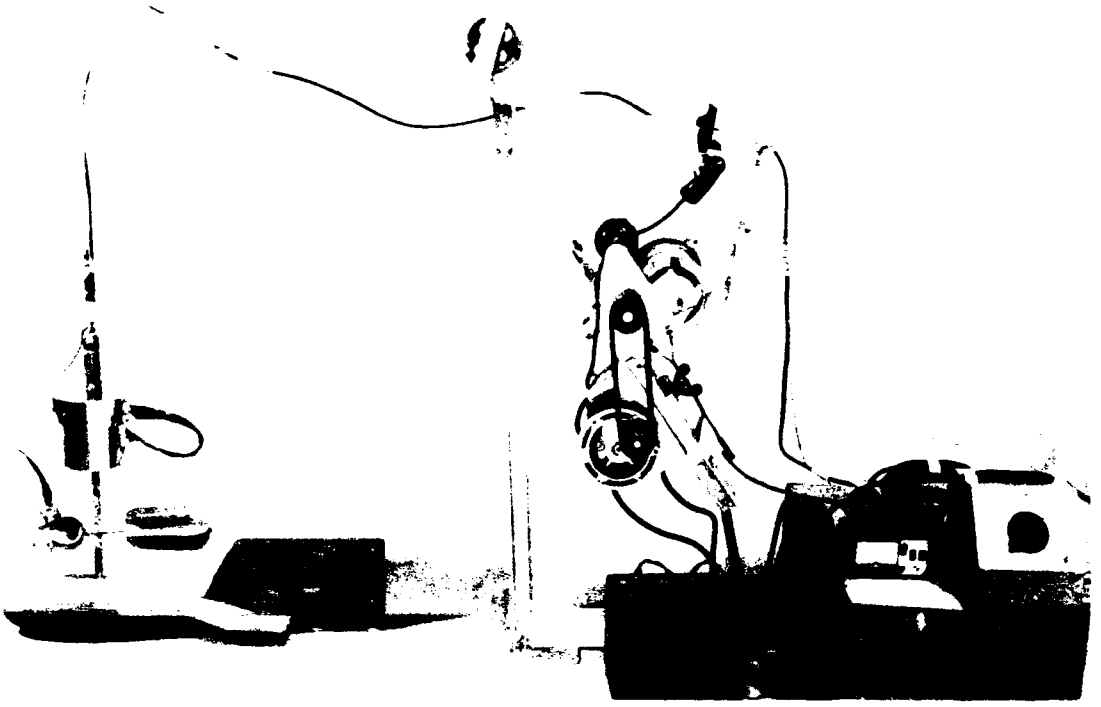

Figure A2. Over-the-side-assembly

6. The Gurley current meter has a threshold speed of less than 0.2 fps and 75° F to give the correct current speed to within +3 to -5 percent for speeds of 1 to 7 fps and ±0.1 fps for speeds less than 1 fps.* Error due to temperature change is approximately 0.05 percent per degree Fahrenheit deviation from 75° F. At flow speeds greater than 3 fps, readings near the surface tend to be somewhat low due to sensor inclination. Accuracy of the direction indicator is within 10 deg at speeds greater than 0.5 fps, but strong wave action moving the boat can cause temporary errors greater than this. Accuracy of the in-line thermometer is approximately ±2° F.

7. Water samples to be used for suspended sediment measurements were placed in 8-oz plastic bottles.

8. Salinities of discrete water samples were measured in the laboratory,

* W. H. McAnally, Jr. 1979. "Calibration Check of Harbor Entrance Branch Prototype Current Measurement Equipment," Memorandum for Record, US Army Engineer Waterways Experiment Station, Vicksburg, MS.

using a Beckman Model RA5 salinometer with automatic temperature compensation. The salinometer was calibrated with standard seawater and was accurate to within ±0.2 ppt.

Recording Current Meters

9. The self-contained recording current meters used for longer term measurements were Environmental Devices Corporation (ENDECO) Type 174 meters. The meter (Figure A3) floats horizontally at the end of a tether, measuring current speed with ducted impeller and direction with an internal compass. The ENDECO 174 also measures temperature with a thermilinear thermistor and conductivity with an induction-type probe. Data are recorded on cartridge-loaded, endless-loop, magnetic tape. Threshold speed is less than 0.08 fps, maximum speed of the unit used was 8.44 fps, and stated speed accuracy was ±3 percent of full scale. The manufacturer states that direction accuracy is ±7.2 deg above 0.08 fps. Time accuracy is ±4 sec per day. A typical tethering arrangement is shown in Figure A4.

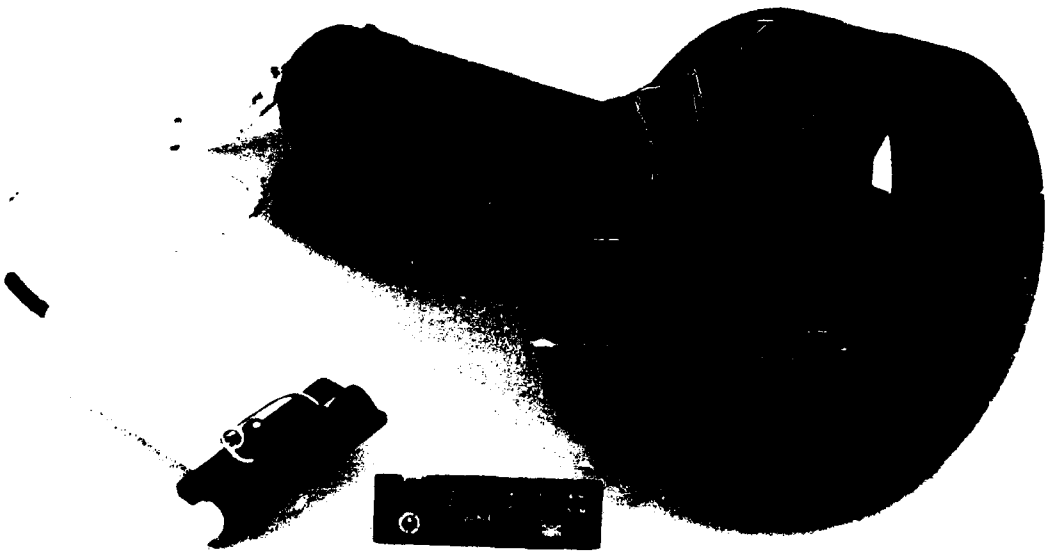

Figure A3. ENDECO 174 meter

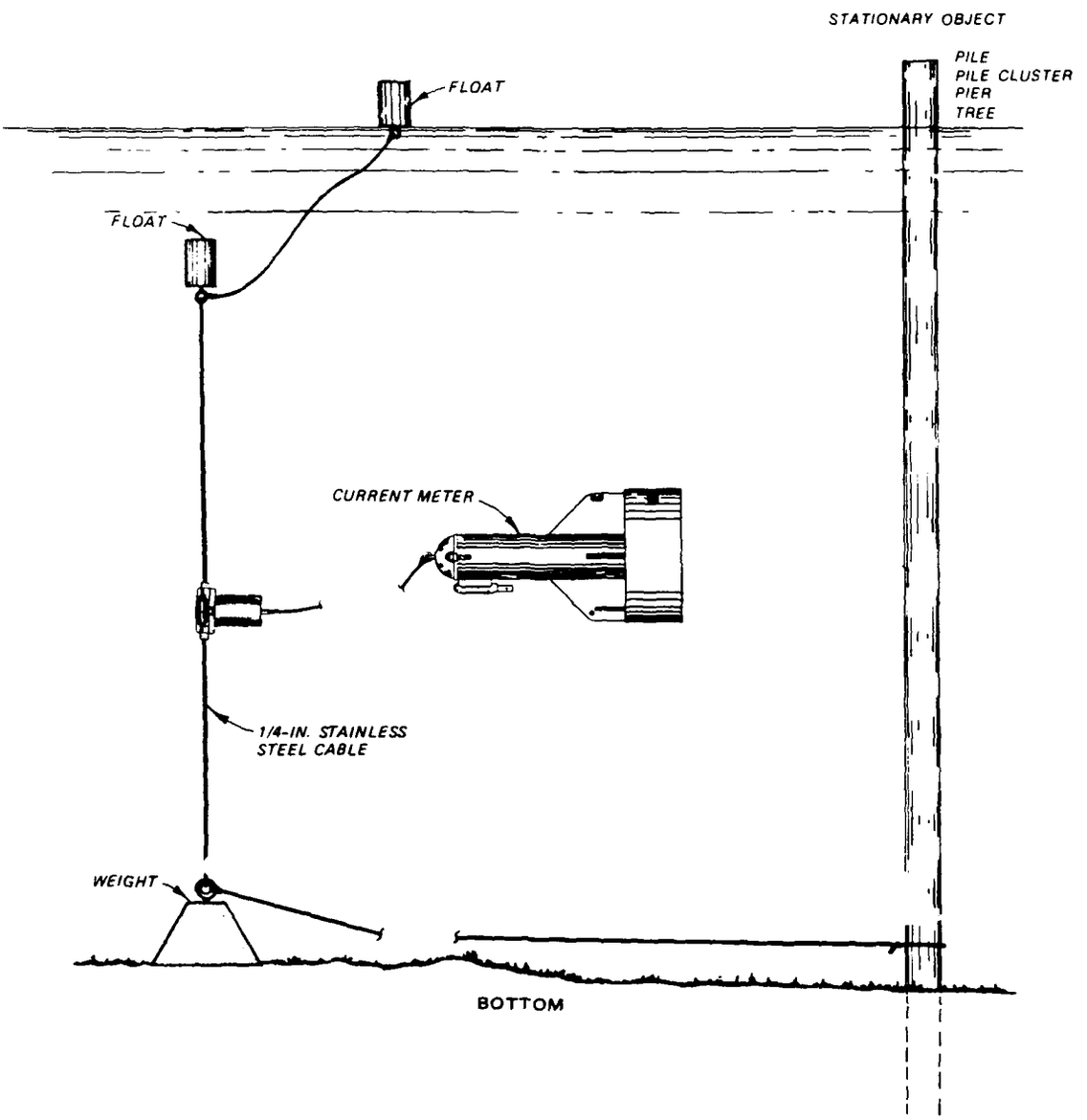

Figure A4. Model 174 tethering arrangement

APPENDIX B: PHYSICAL MODEL PRE-TRIDENT CHANNEL VERIFICATION

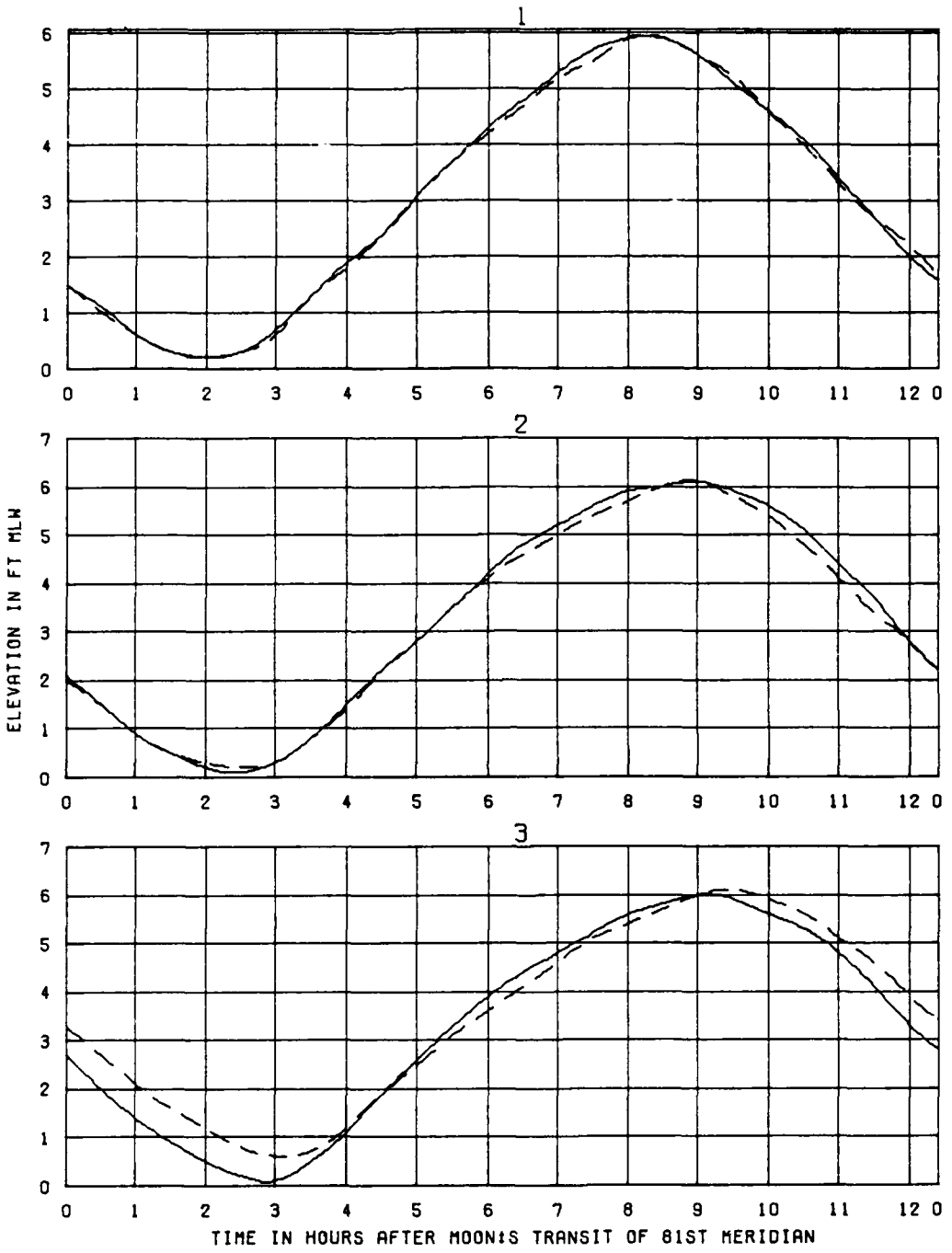

TEST CONDITIONS

TIDE RANGE AT GAGE 1	5.8 FT
OCEAN SALINITY(TOTAL SALT)	32.5 PPT
FRESHWATER INFLOW	1100 CFS

LEGEND
PROTOTYPE ———
MODEL — — —

KINGS BAY MODEL

VERIFICATION OF TIDE HEIGHTS FOR 11-10-82 TIDE

STATIONS
1. 2. AND 3

PLATE B1

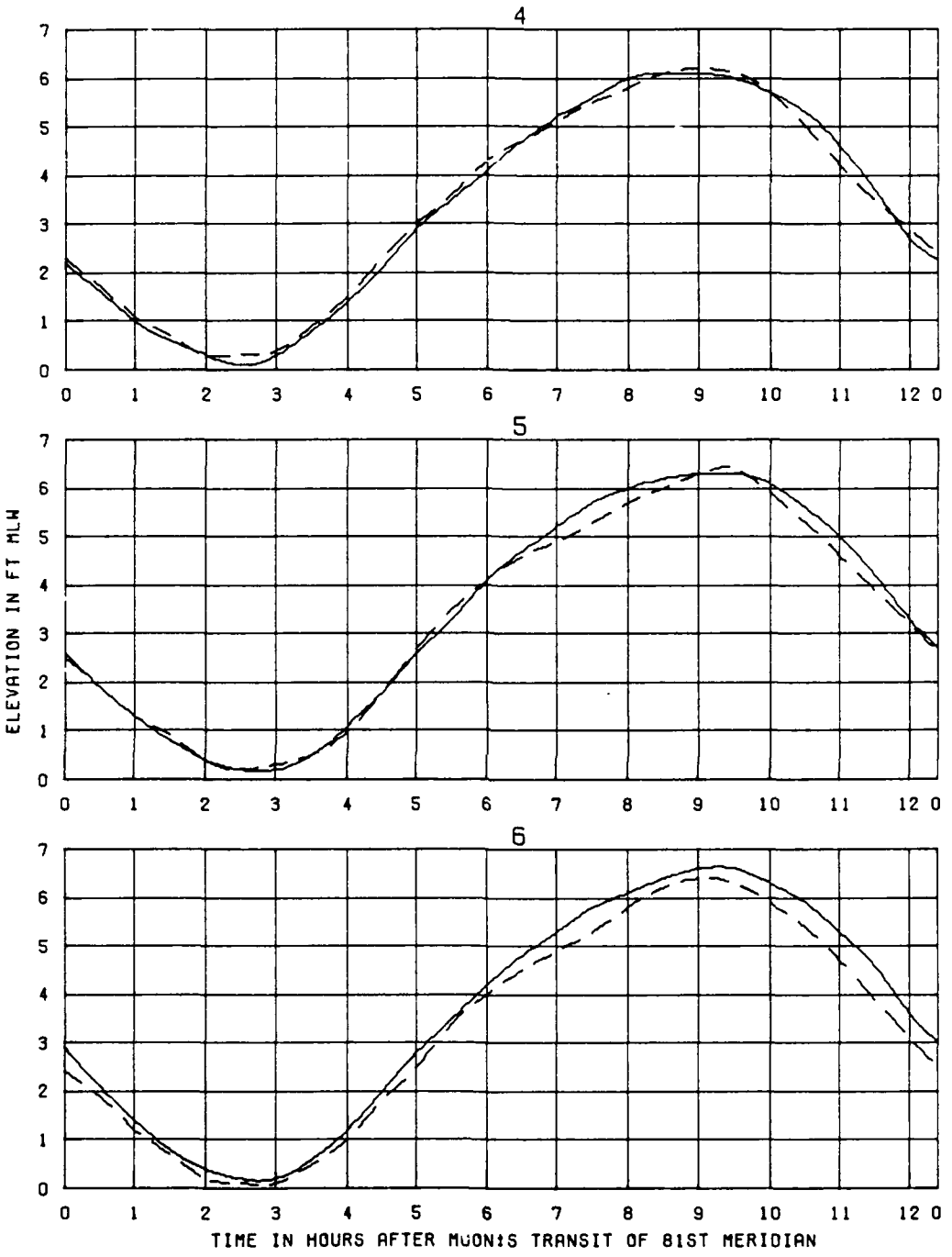

TEST CONDITIONS

TIDE RANGE AT GAGE 1	5.8 FT
OCEAN SALINITY(TOTAL SALT)	32.5 PPT
FRESHWATER INFLOW	1100 CFS

LEGEND
PROTOTYPE ———
MODEL — — —

KINGS BAY MODEL

VERIFICATION OF TIDE HEIGHTS FOR 11-10-82 TIDE

STATIONS
4, 5, AND 6

PLATE B2

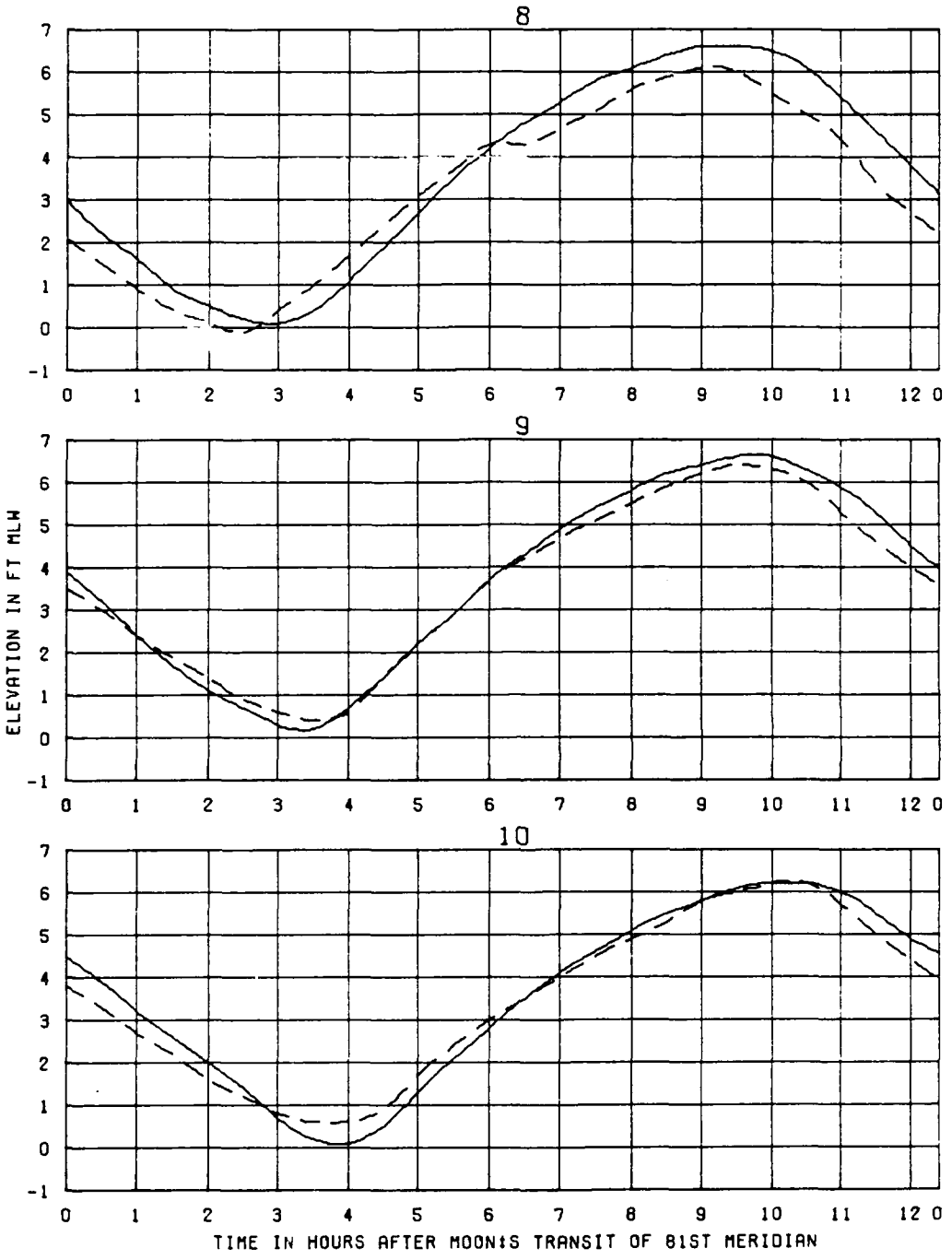

TEST CONDITIONS

TIDE RANGE AT GAGE 1	5.8 FT
OCEAN SALINITY(TOTAL SALT)	32.5 PPT
FRESHWATER INFLOW	1100 CFS

LEGEND
PROTOTYPE ———
MODEL — — —

KINGS BAY MODEL

VERIFICATION OF TIDE HEIGHTS FOR 11-10-82 TIDE

STATIONS
8. 9. AND 10

PLATE B3

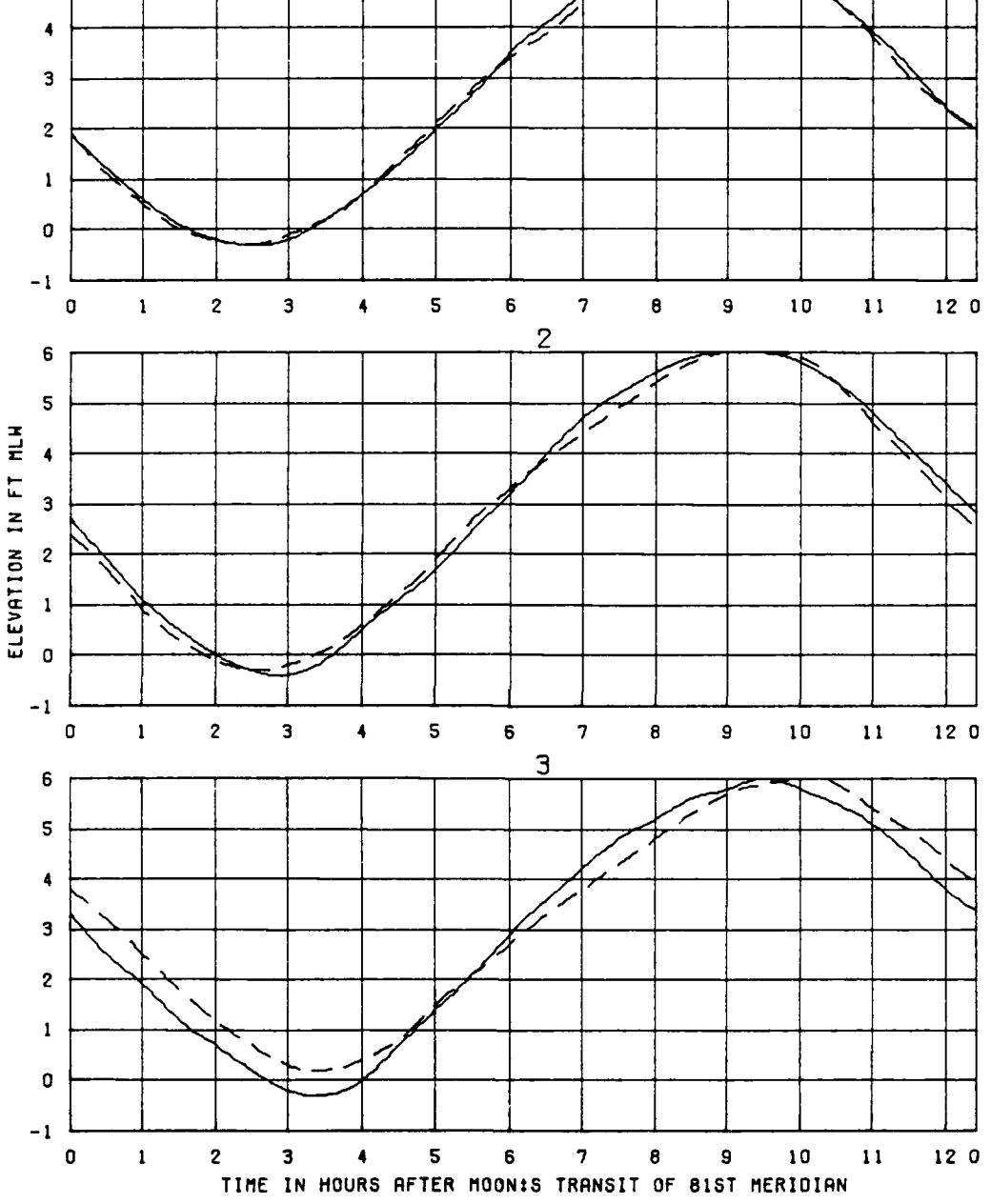

TEST CONDITIONS

TIDE RANGE AT GAGE 1	6.2 FT
OCEAN SALINITY(TOTAL SALT)	32.5 PPT
FRESHWATER INFLOW	1100 CFS

LEGEND
PROTOTYPE ———
MODEL — — —

KINGS BAY MODEL

VERIFICATION OF TIDE HEIGHTS FOR 11-12-82 TIDE

STATIONS
1, 2, AND 3

PLATE B4

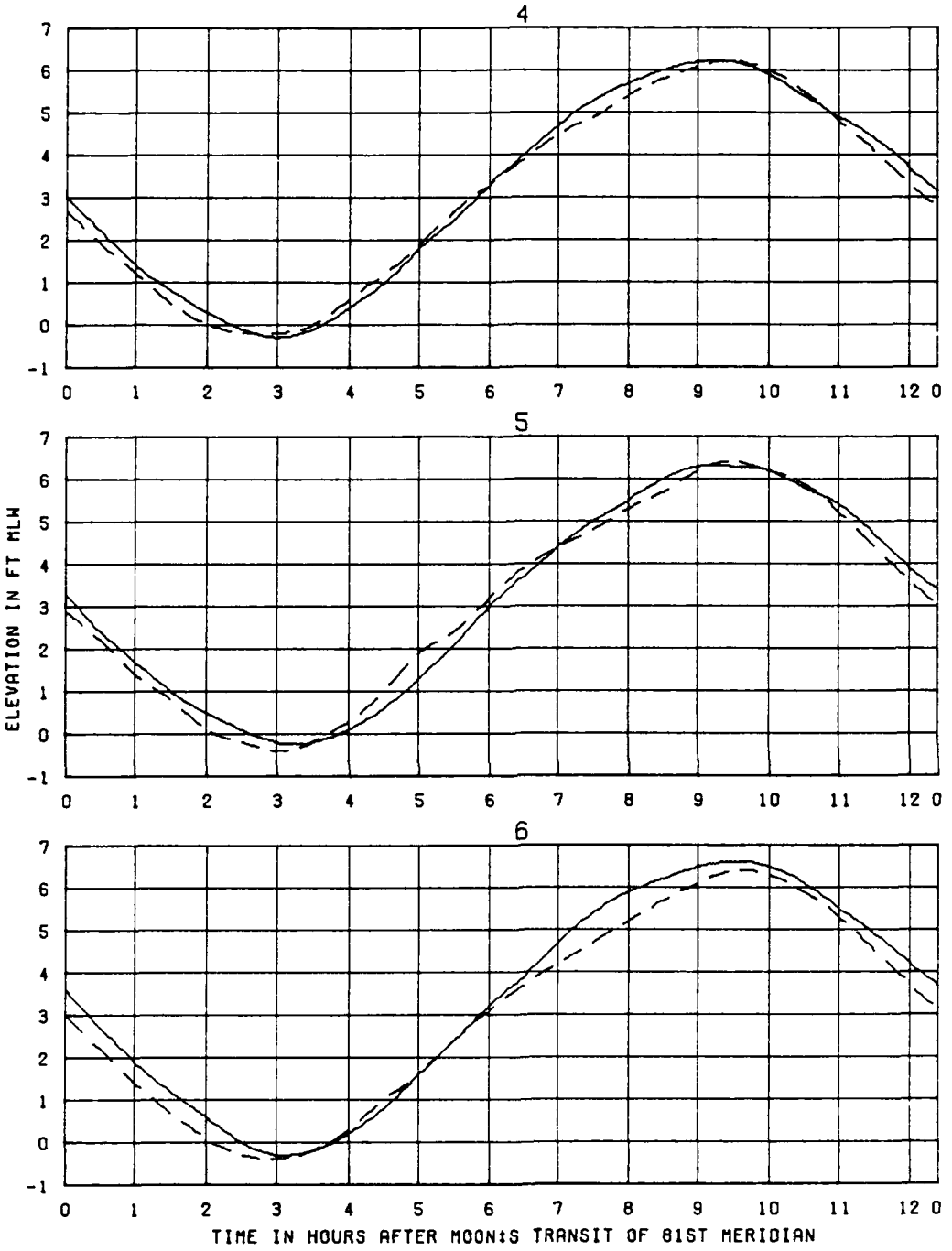

TEST CONDITIONS

TIDE RANGE AT GAGE 1	6.2 FT
OCEAN SALINITY(TOTAL SALT)	32.5 PPT
FRESHWATER INFLOW	1100 CFS

LEGEND
PROTOTYPE ———
MODEL — — —

KINGS BAY MODEL

VERIFICATION OF TIDE HEIGHTS FOR 11-12-82 TIDE

STATIONS
4, 5, AND 6

PLATE B5

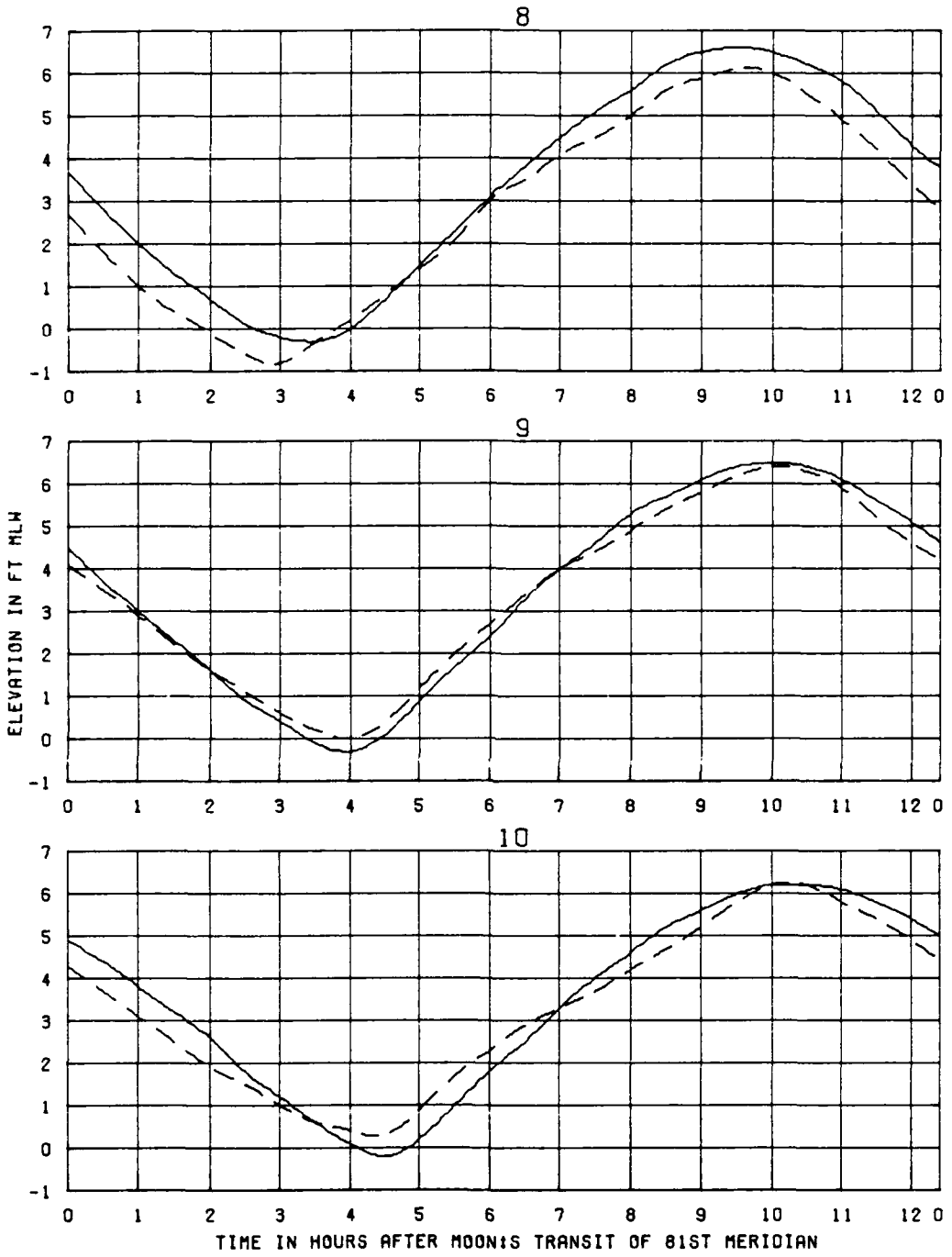

TEST CONDITIONS	
TIDE RANGE AT GAGE 1	6.2 FT
OCEAN SALINITY(TOTAL SALT)	32.5 PPT
FRESHWATER INFLOW	1100 CFS

LEGEND
PROTOTYPE ———
MODEL — — —

KINGS BAY MODEL

VERIFICATION OF TIDE HEIGHTS FOR 11-12-82 TIDE

STATIONS 8, 9, AND 10

PLATE B6

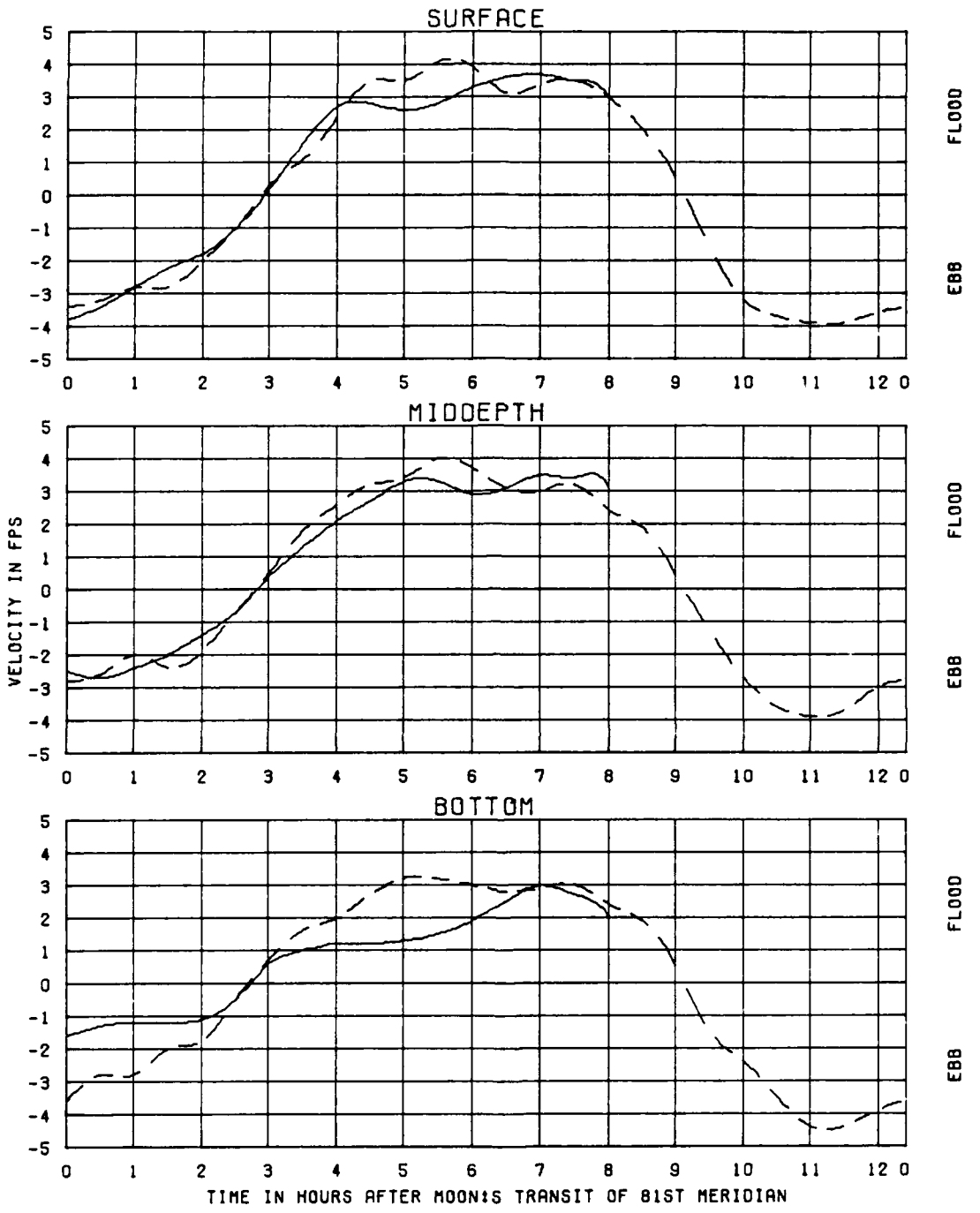

TEST CONDITIONS

TIDE RANGE AT GAGE 1	5.8 FT
OCEAN SALINITY(TOTAL SALT)	32.5 PPT
FRESHWATER INFLOW	1100 CFS

LEGEND

PROTOTYPE ———

MODEL — — —

KINGS BAY MODEL

VERIFICATION OF VELOCITIES FOR 11-10-82 TIDE

STATION 1A

PLATE B7

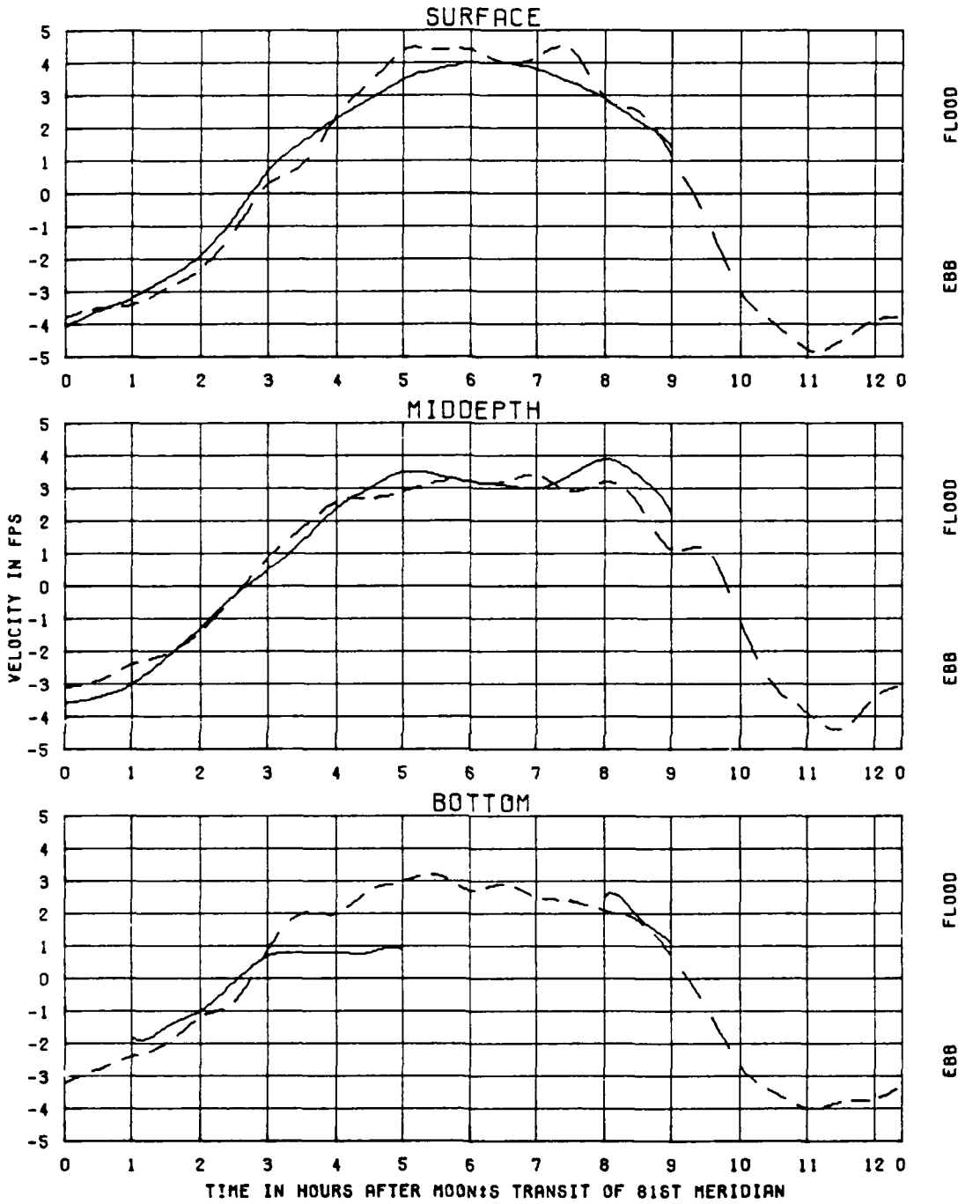

TEST CONDITIONS

TIDE RANGE AT GAGE 1	5.8 FT
OCEAN SALINITY(TOTAL SALT)	32.5 PPT
FRESHWATER INFLOW	1100 CFS

LEGEND
PROTOTYPE ———
MODEL — — —

KINGS BAY MODEL

VERIFICATION OF VELOCITIES FOR 11-10-82 TIDE

STATION
1B

PLATE B8

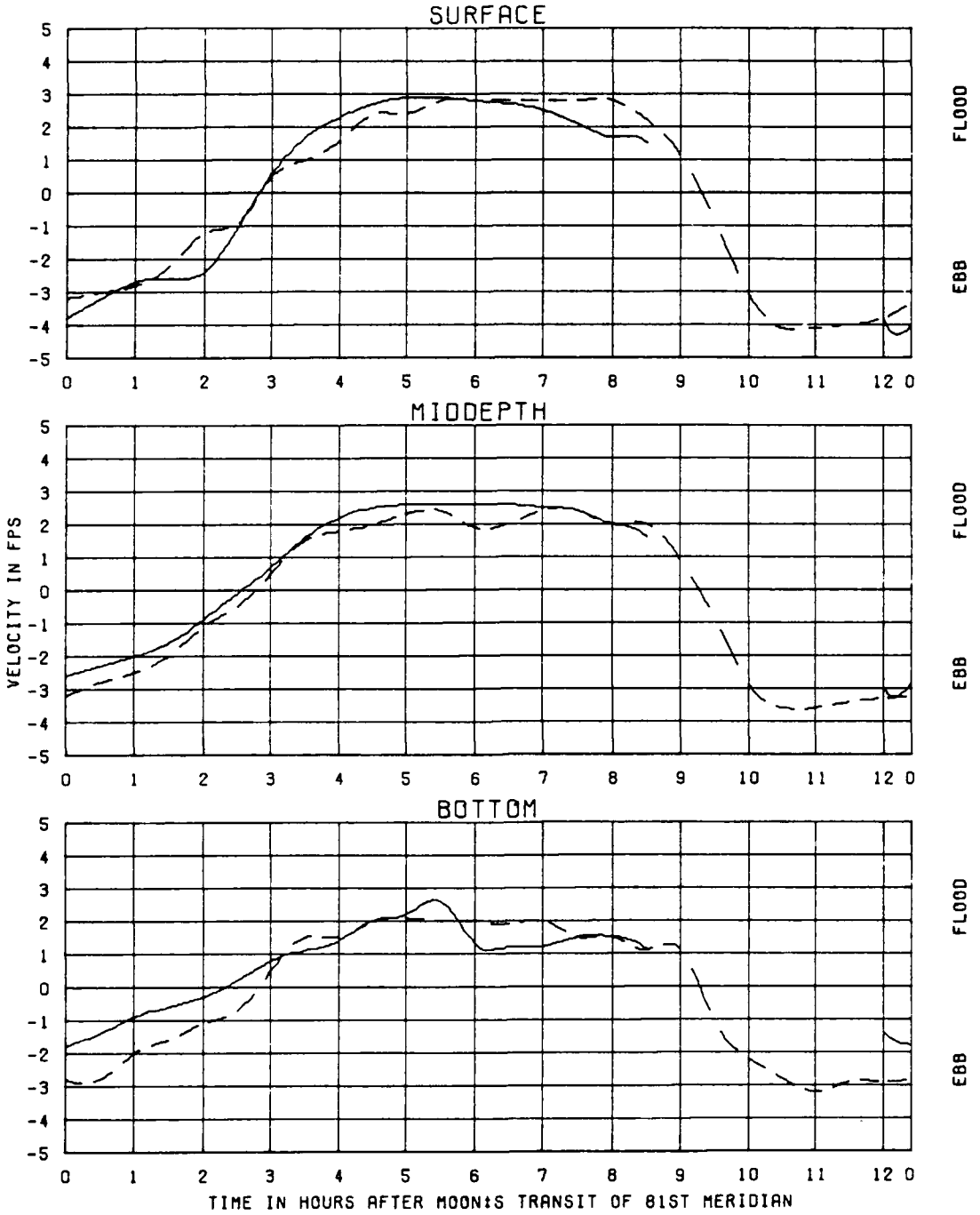

TEST CONDITIONS

TIDE RANGE AT GAGE 1	5.8 FT
OCEAN SALINITY(TOTAL SALT)	32.5 PPT
FRESHWATER INFLOW	1100 CFS

LEGEND
PROTOTYPE ———
MODEL — — —

KINGS BAY MODEL

VERIFICATION OF VELOCITIES FOR 11-10-82 TIDE

STATION
1C

PLATE 89

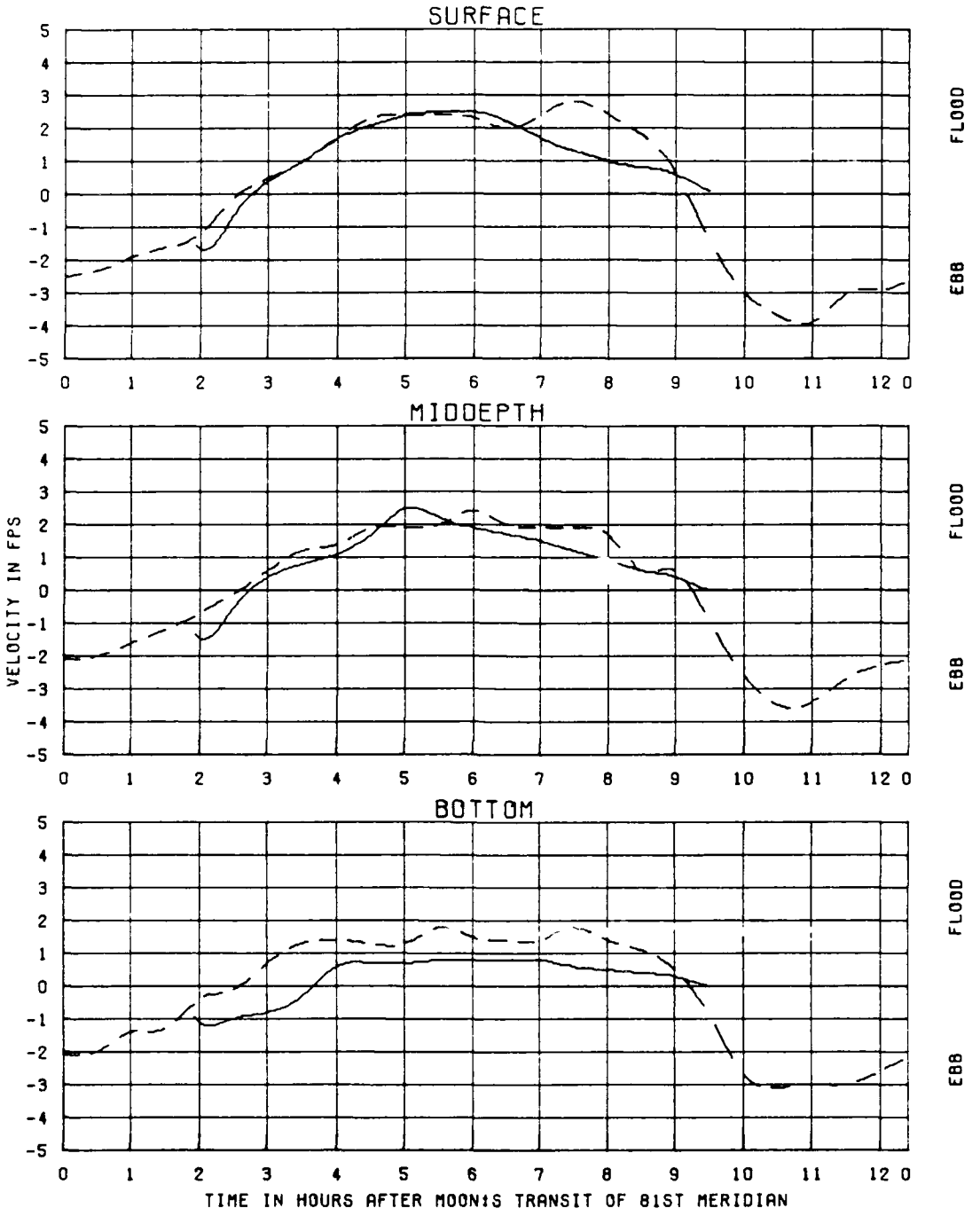

TEST CONDITIONS

TIDE RANGE AT GAGE 1	5.8 FT
OCEAN SALINITY(TOTAL SALT)	32.5 PPT
FRESHWATER INFLOW	1100 CFS

KINGS BAY MODEL

VERIFICATION OF VELOCITIES FOR 11-10-82 TIDE

STATION 2A

LEGEND
PROTOTYPE ———
MODEL — — —

PLATE B10

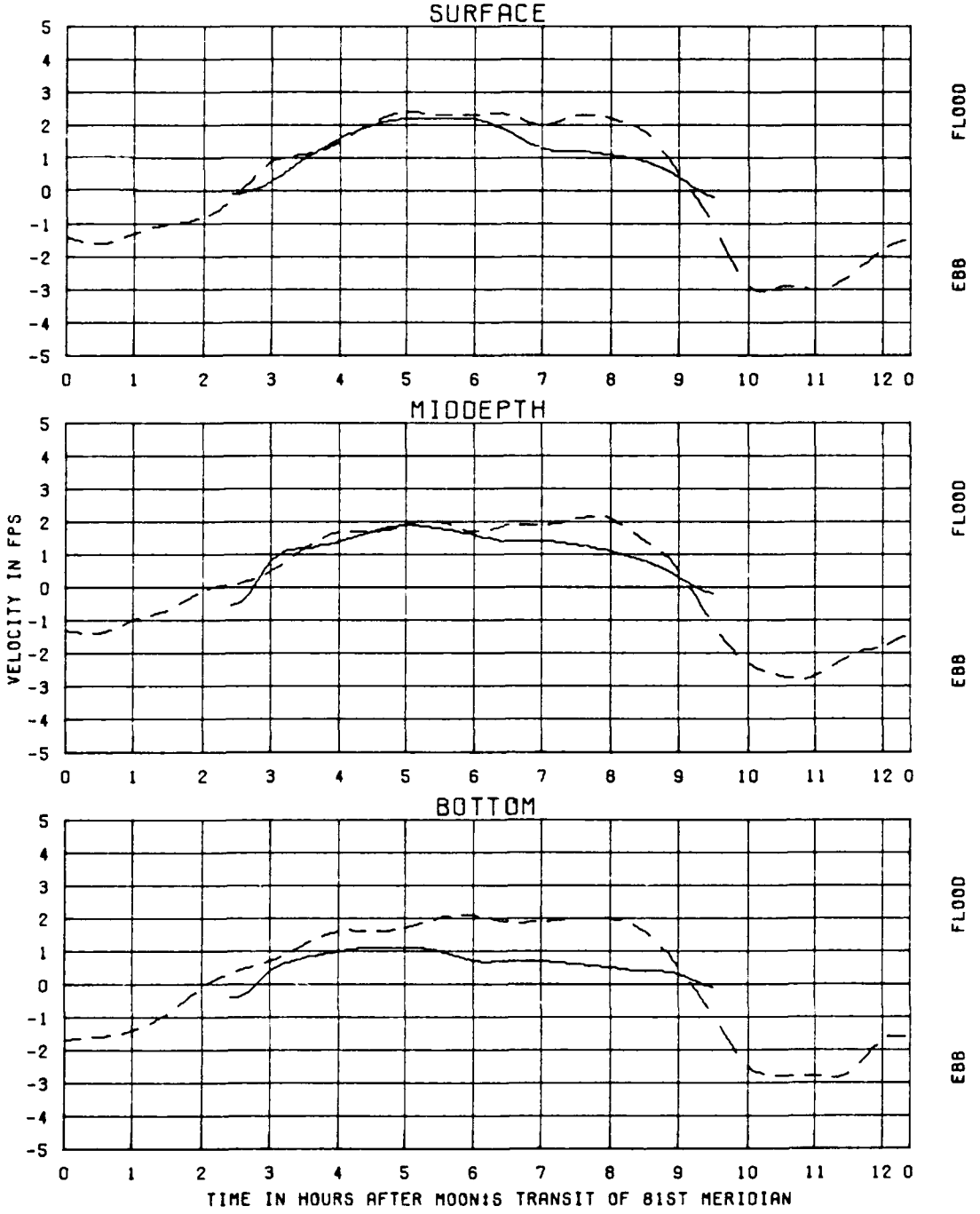

TEST CONDITIONS

TIDE RANGE AT GAGE 1	5.8 FT
OCEAN SALINITY(TOTAL SALT)	32.5 PPT
FRESHWATER INFLOW	1100 CFS

LEGEND
PROTOTYPE ———
MODEL — — —

KINGS BAY MODEL

VERIFICATION OF VELOCITIES FOR 11-10-82 TIDE

STATION
28

PLATE B11

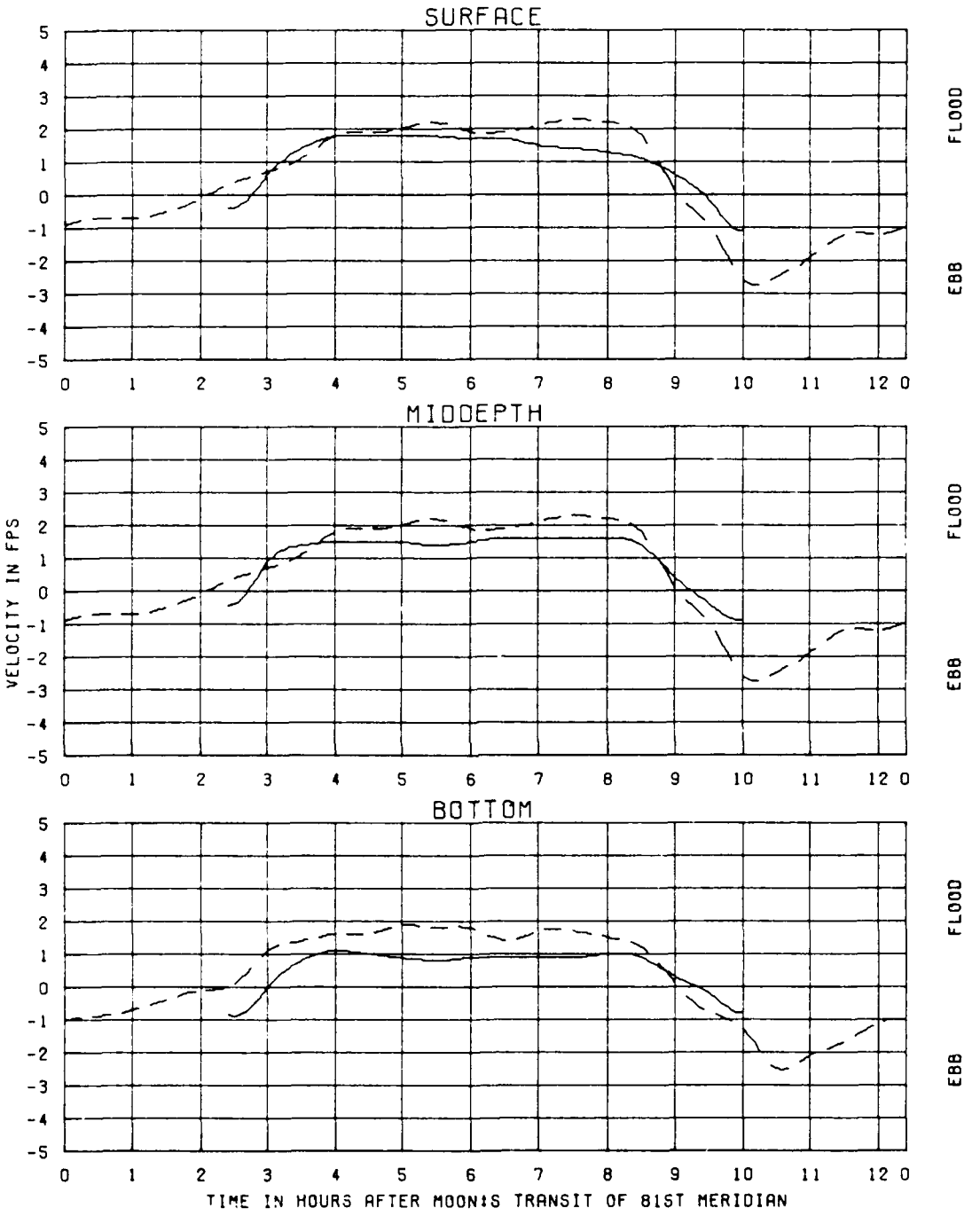

TEST CONDITIONS

TIDE RANGE AT GAGE 1	5.8 FT
OCEAN SALINITY(TOTAL SALT)	32.5 PPT
FRESHWATER INFLOW	1100 CFS

LEGEND
PROTOTYPE ———
MODEL — — —

KINGS BAY MODEL

VERIFICATION OF VELOCITIES FOR 11-10-82 TIDE

STATION
2C

PLATE B12

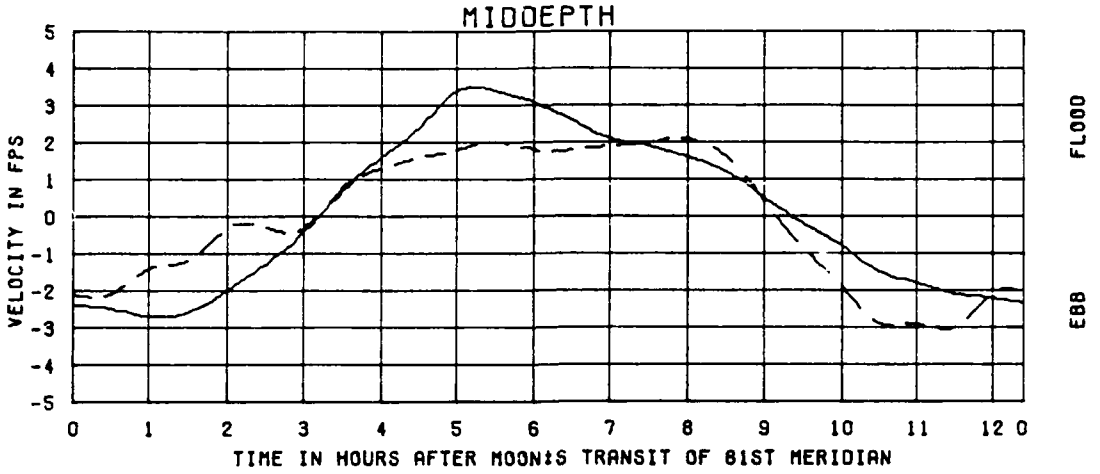

TEST CONDITIONS

TIDE RANGE AT GAGE 1	5.8 FT
OCEAN SALINITY(TOTAL SALT)	32.5 PPT
FRESHWATER INFLOW	1100 CFS

LEGEND

PROTOTYPE ———

MODEL — — —

KINGS BAY MODEL

VERIFICATION OF VELOCITIES FOR 11-10-82 TIDE

STATION 3

PLATE B13

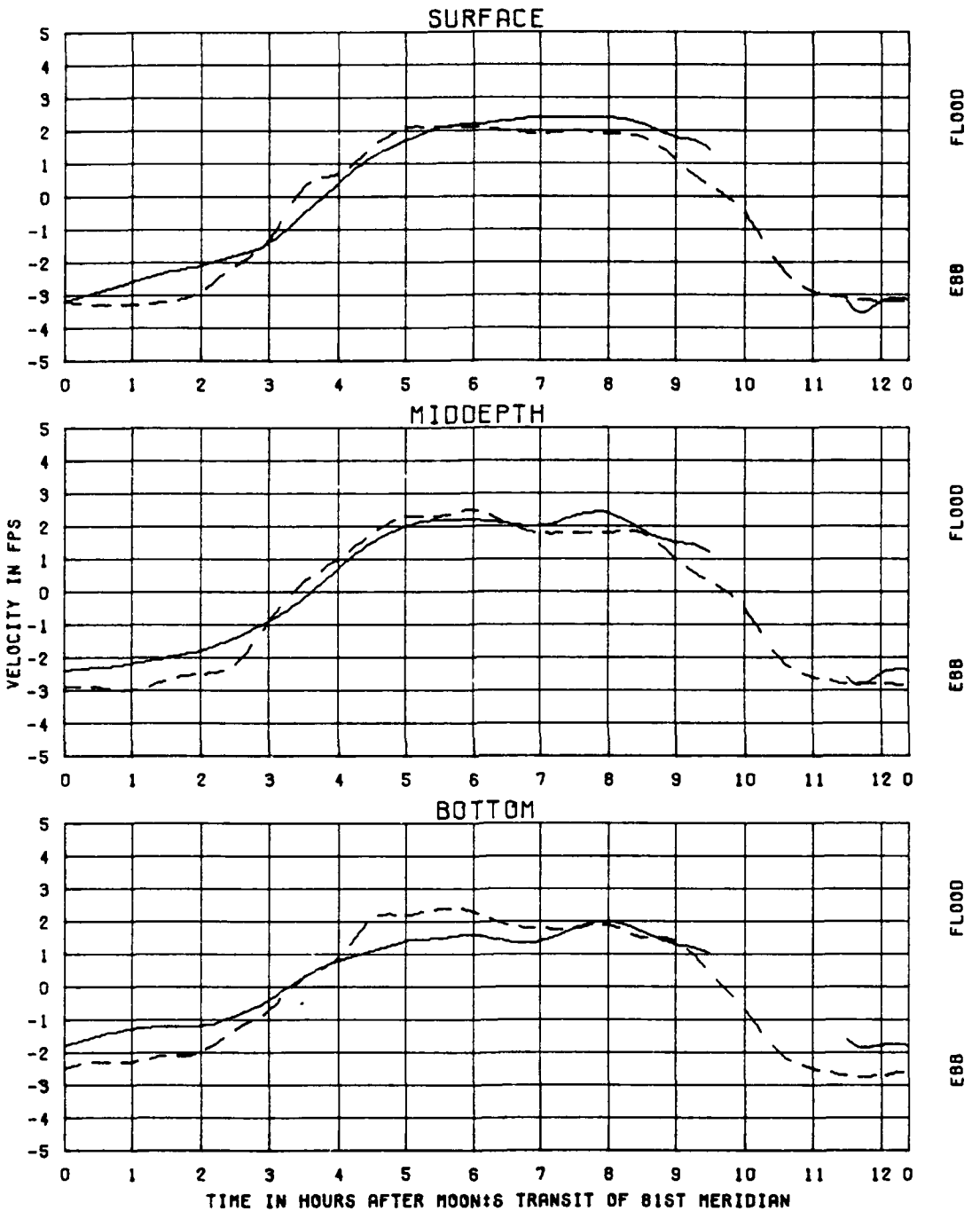

TEST CONDITIONS

TIDE RANGE AT GAGE 1	5.8 FT
OCEAN SALINITY(TOTAL SALT)	32.5 PPT
FRESHWATER INFLOW	1100 CFS

LEGEND
PROTOTYPE ———
MODEL — — —

KINGS BAY MODEL

VERIFICATION OF VELOCITIES FOR 11-10-82 TIDE

STATION 3A

PLATE B14

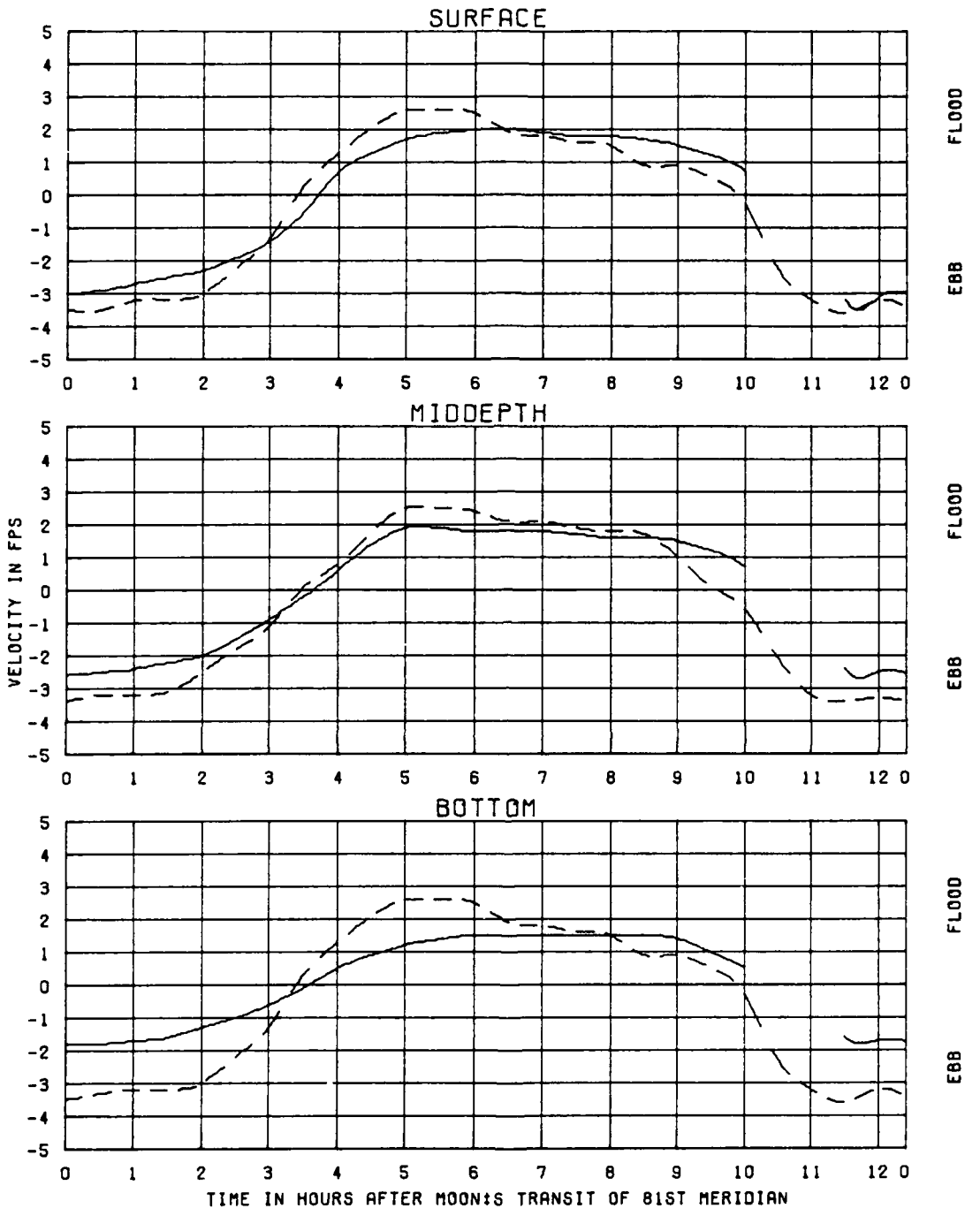

TEST CONDITIONS

TIDE RANGE AT GAGE 1	5.8 FT
OCEAN SALINITY(TOTAL SALT)	32.5 PPT
FRESHWATER INFLOW	1100 CFS

LEGEND
PROTOTYPE ———
MODEL — — —

KINGS BAY MODEL

VERIFICATION OF VELOCITIES FOR 11-10-82 TIDE

STATION 38

PLATE B15

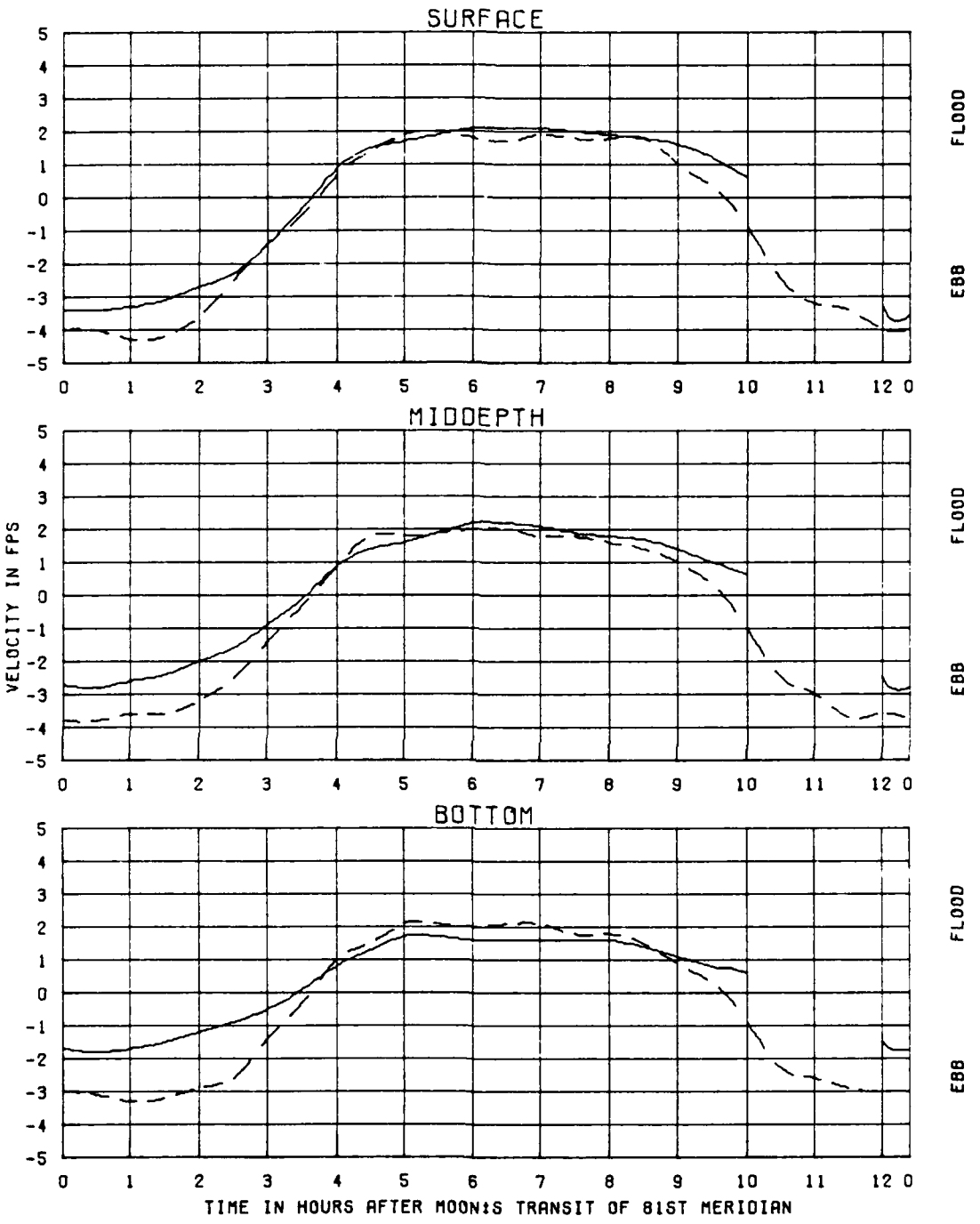

TEST CONDITIONS

TIDE RANGE AT GAGE 1	5.8 FT
OCEAN SALINITY(TOTAL SALT)	32.5 PPT
FRESHWATER INFLOW	1100 CFS

LEGEND
PROTOTYPE ———
MODEL — — —

KINGS BAY MODEL

VERIFICATION OF VELOCITIES FOR 11-10-82 TIDE

STATION
3C

PLATE B16

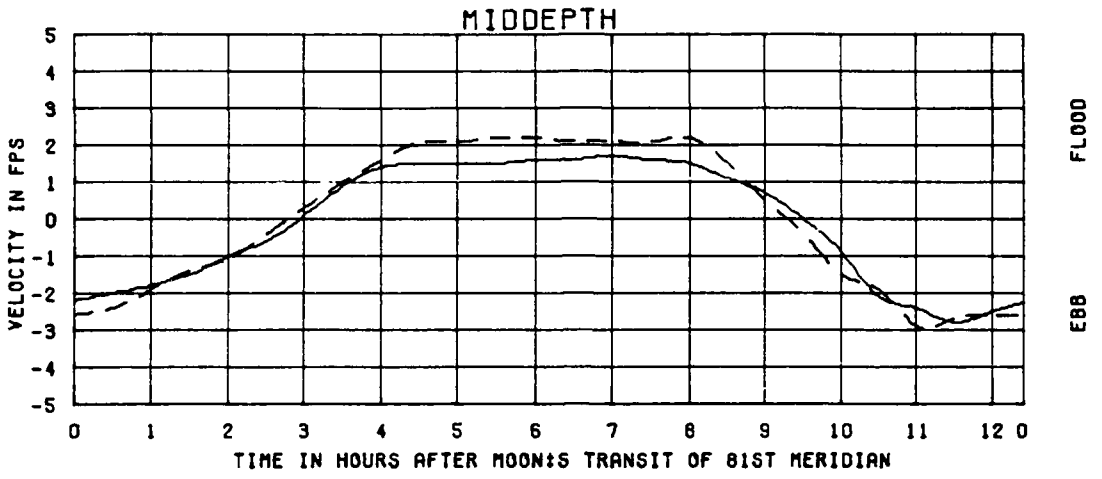

TEST CONDITIONS

TIDE RANGE AT GAGE 1	5.8 FT
OCEAN SALINITY(TOTAL SALT)	32.5 PPT
FRESHWATER INFLOW	1100 CFS

LEGEND

PROTOTYPE ———

MODEL — — —

KINGS BAY MODEL

VERIFICATION OF VELOCITIES FOR 11-10-82 TIDE

STATION 5

PLATE B17

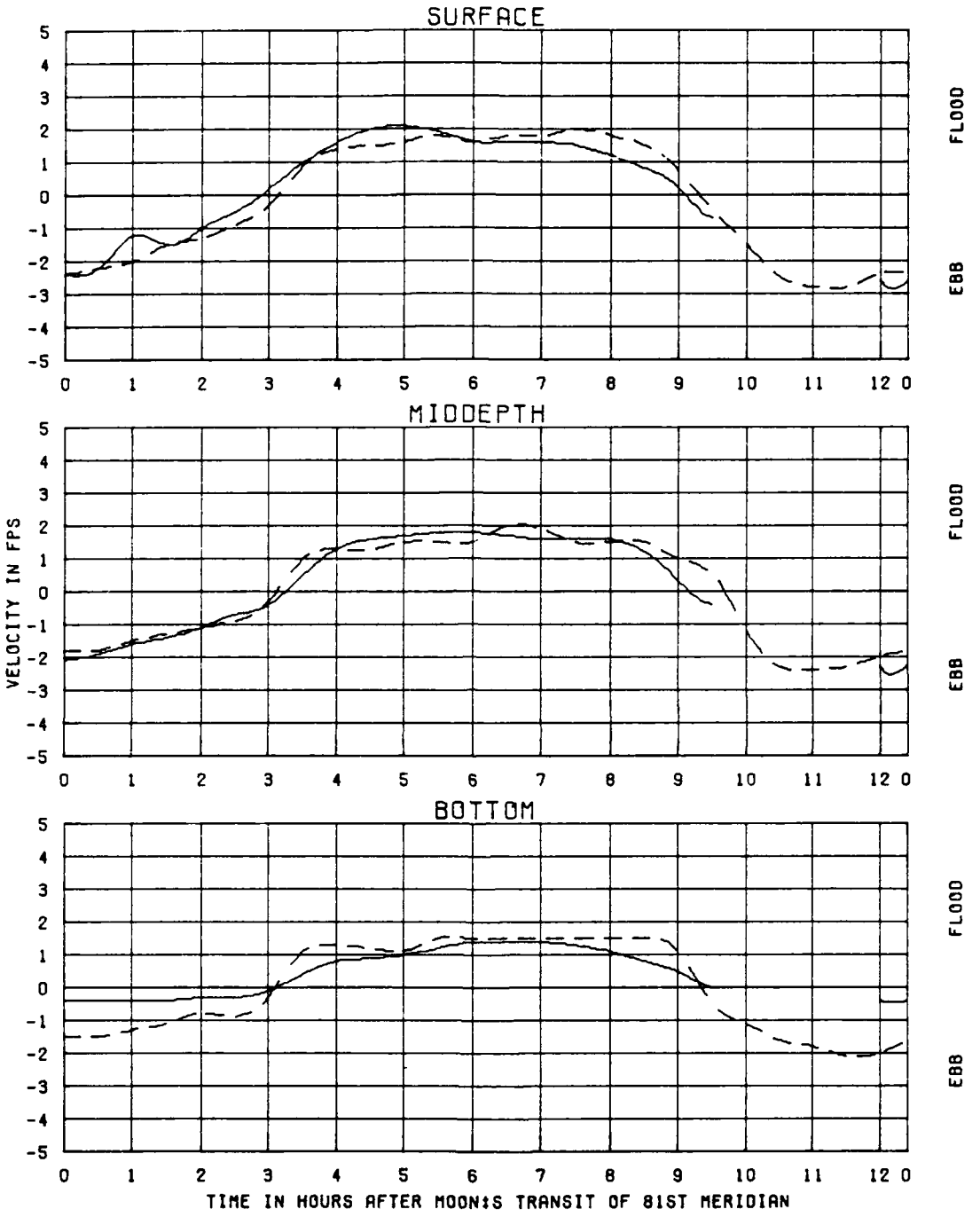

TEST CONDITIONS

TIDE RANGE AT GAGE 1	5.8 FT
OCEAN SALINITY(TOTAL SALT)	32.5 PPT
FRESHWATER INFLOW	1100 CFS

LEGEND
PROTOTYPE ———
MODEL — — —

KINGS BAY MODEL

VERIFICATION OF VELOCITIES FOR 11-10-82 TIDE

STATION
4A

PLATE B18

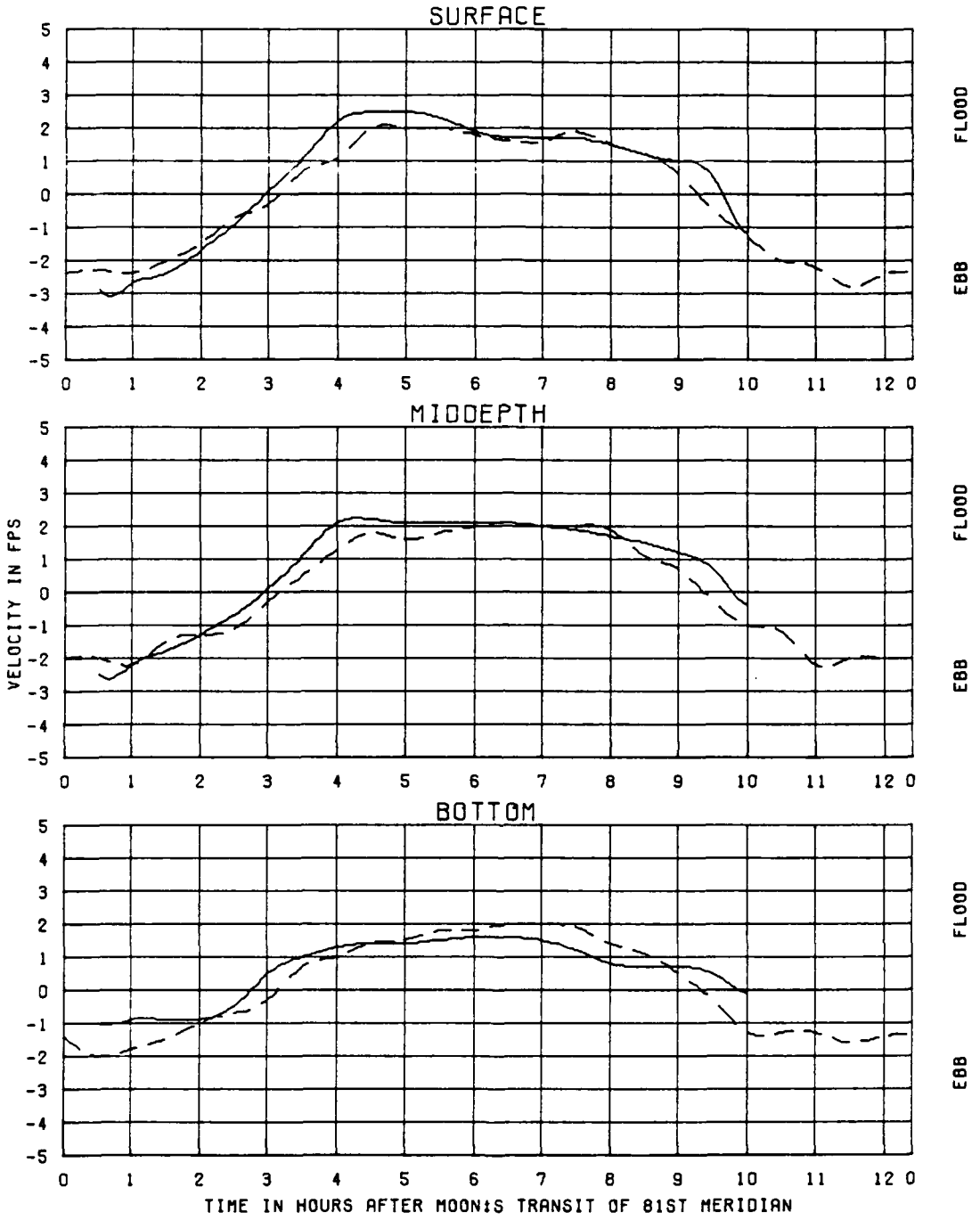

TEST CONDITIONS

TIDE RANGE AT GAGE 1	5.8 FT
OCEAN SALINITY(TOTAL SALT)	32.5 PPT
FRESHWATER INFLOW	1100 CFS

LEGEND
PROTOTYPE ———
MODEL — — —

KINGS BAY MODEL

VERIFICATION OF VELOCITIES FOR 11-10-82 TIDE

STATION 4B

PLATE B19

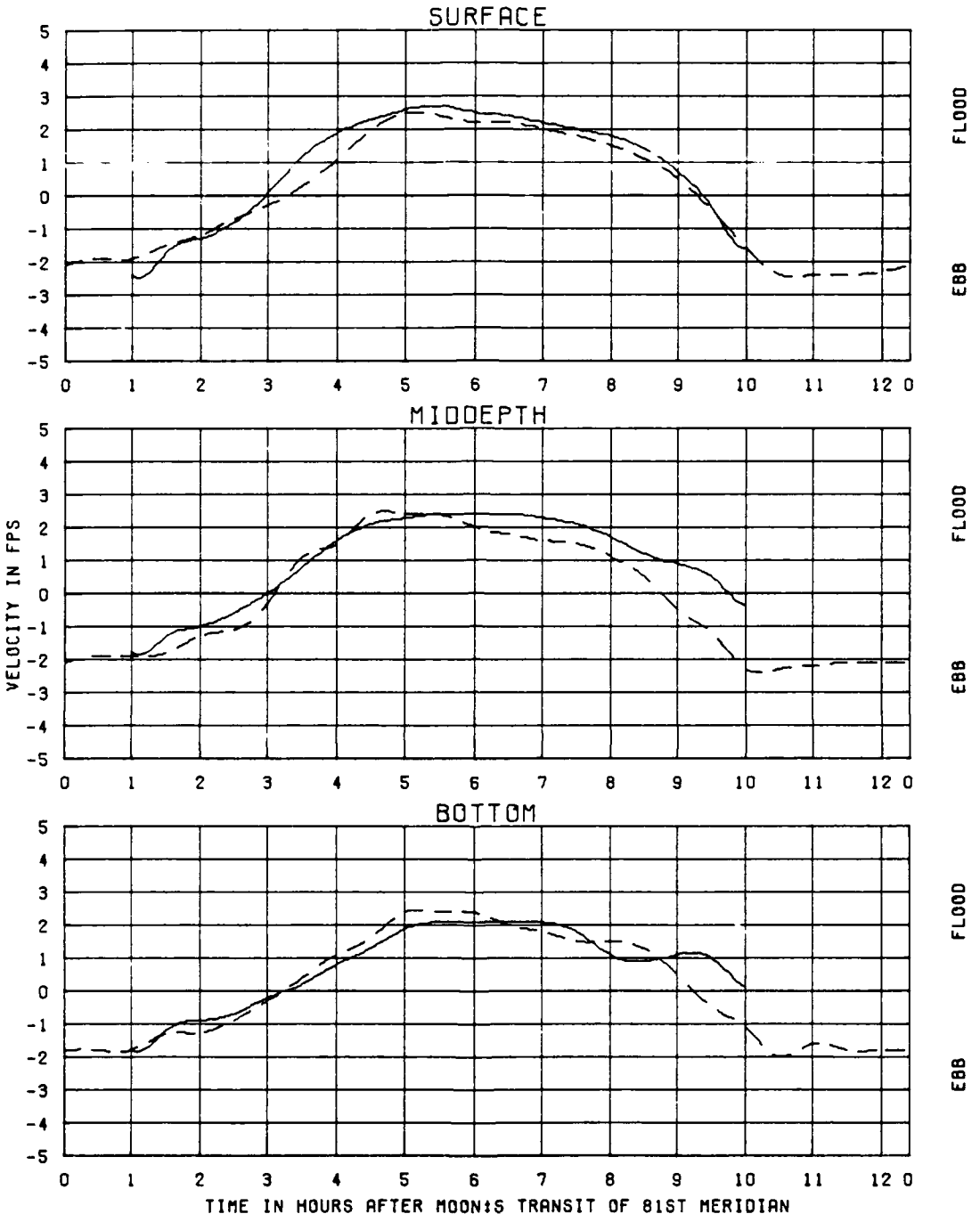

TEST CONDITIONS

TIDE RANGE AT GAGE 1	5.8 FT
OCEAN SALINITY(TOTAL SALT)	32.5 PPT
FRESHWATER INFLOW	1100 CFS

LEGEND
PROTOTYPE ———
MODEL — — —

KINGS BAY MODEL

VERIFICATION OF VELOCITIES FOR 11-10-82 TIDE

STATION
4C

PLATE B20

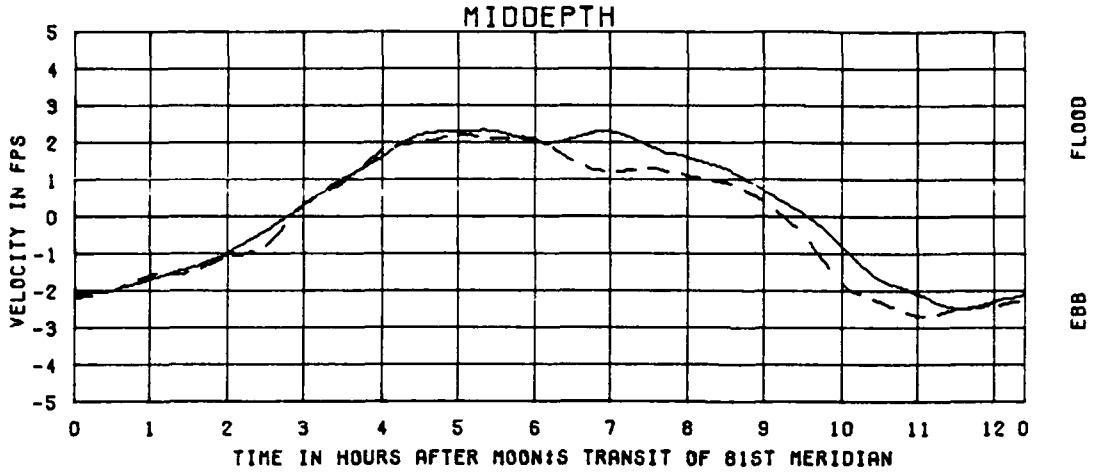

TEST CONDITIONS	
TIDE RANGE AT GAGE 1	5.8 FT
OCEAN SALINITY(TOTAL SALT)	32.5 PPT
FRESHWATER INFLOW	1100 CFS

LEGEND
PROTOTYPE ———
MODEL — — —

KINGS BAY MODEL

VERIFICATION OF
VELOCITIES
FOR 11-10-82 TIDE
STATION
6

PLATE B21

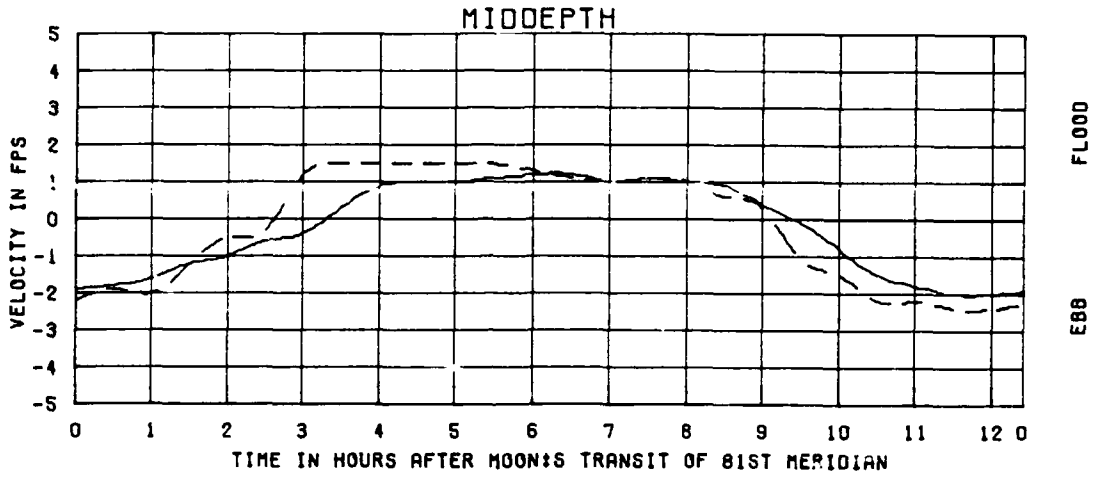

TEST CONDITIONS

TIDE RANGE AT GAGE 1	5.8 FT
OCEAN SALINITY(TOTAL SALT)	32.5 PPT
FRESHWATER INFLOW	1100 CFS

LEGEND

PROTOTYPE ———

MODEL — — —

KINGS BAY MODEL

VERIFICATION OF VELOCITIES FOR 11-10-82 TIDE

STATION 7

PLATE B22

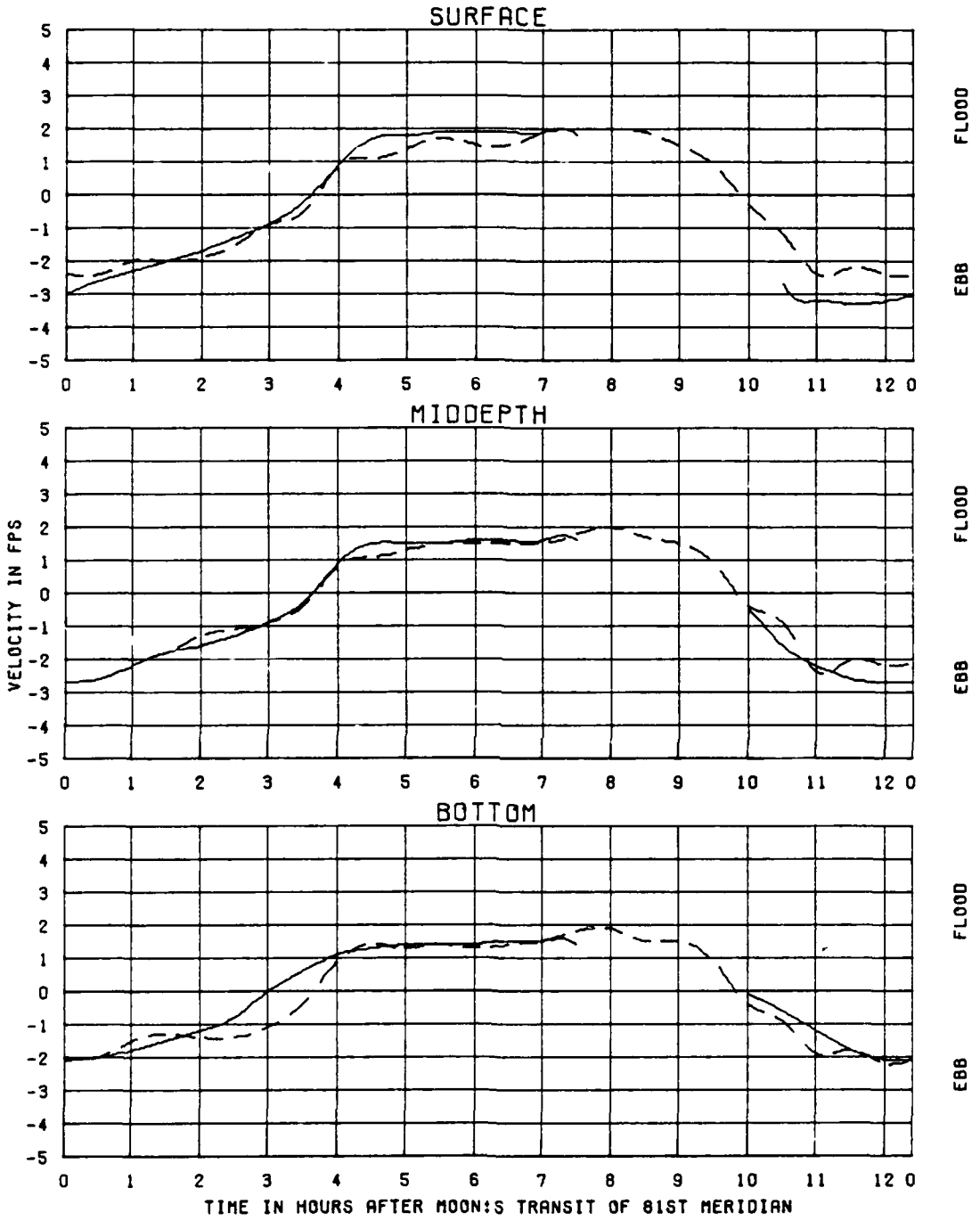

TEST CONDITIONS

TIDE RANGE AT GAGE 1	6.2 FT
OCEAN SALINITY(TOTAL SALT)	32.5 PPT
FRESHWATER INFLOW	1100 CFS

LEGEND
PROTOTYPE ———
MODEL — — —

KINGS BAY MODEL

VERIFICATION OF VELOCITIES FOR 11-12-82 TIDE

STATION
4A

PLATE B23

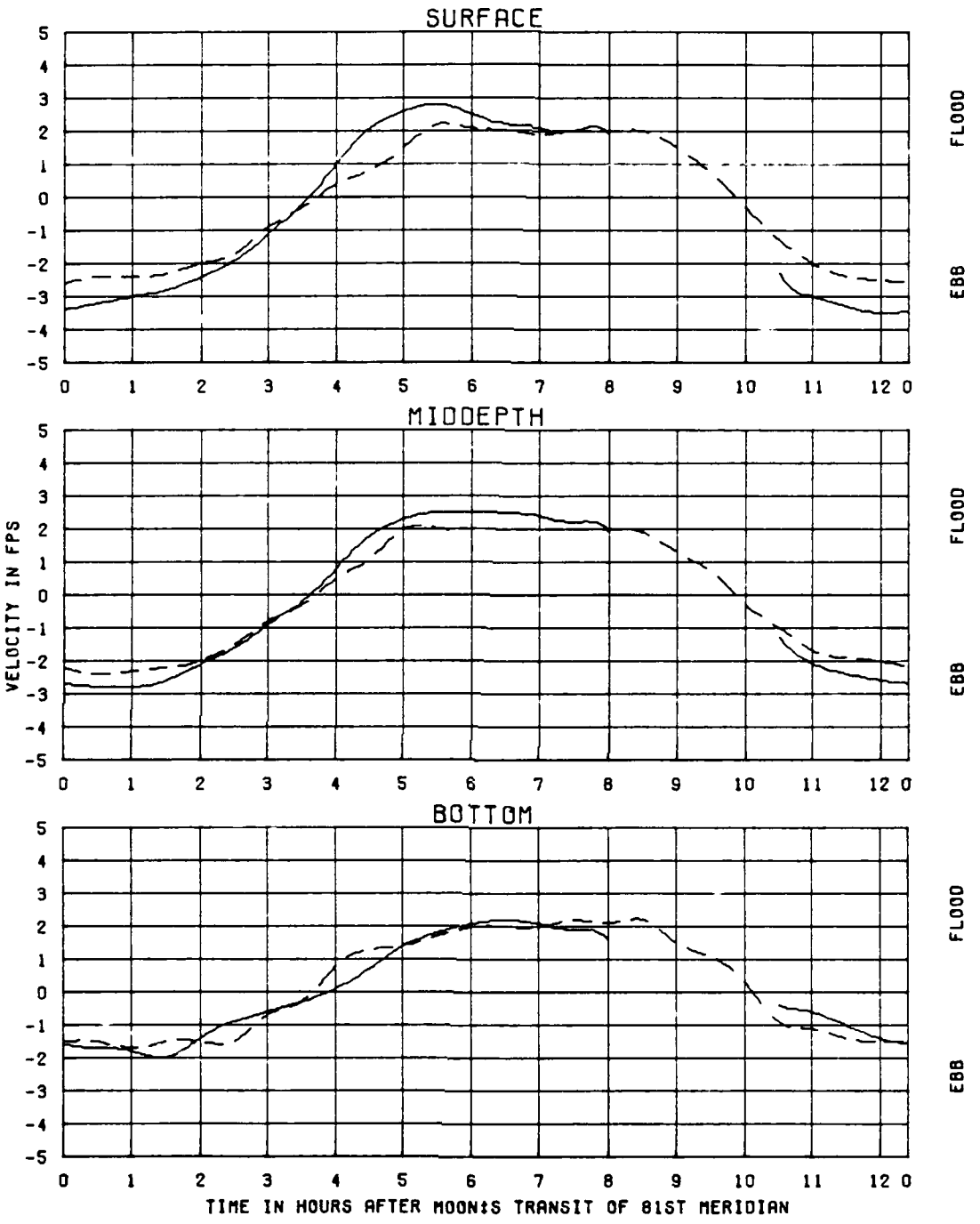

TEST CONDITIONS

TIDE RANGE AT GAGE 1	6.2 FT
OCEAN SALINITY(TOTAL SALT)	32.5 PPT
FRESHWATER INFLOW	1100 CFS

LEGEND
PROTOTYPE ———
MODEL — — —

KINGS BAY MODEL

VERIFICATION OF VELOCITIES FOR 11-12-82 TIDE

STATION 48

PLATE B24

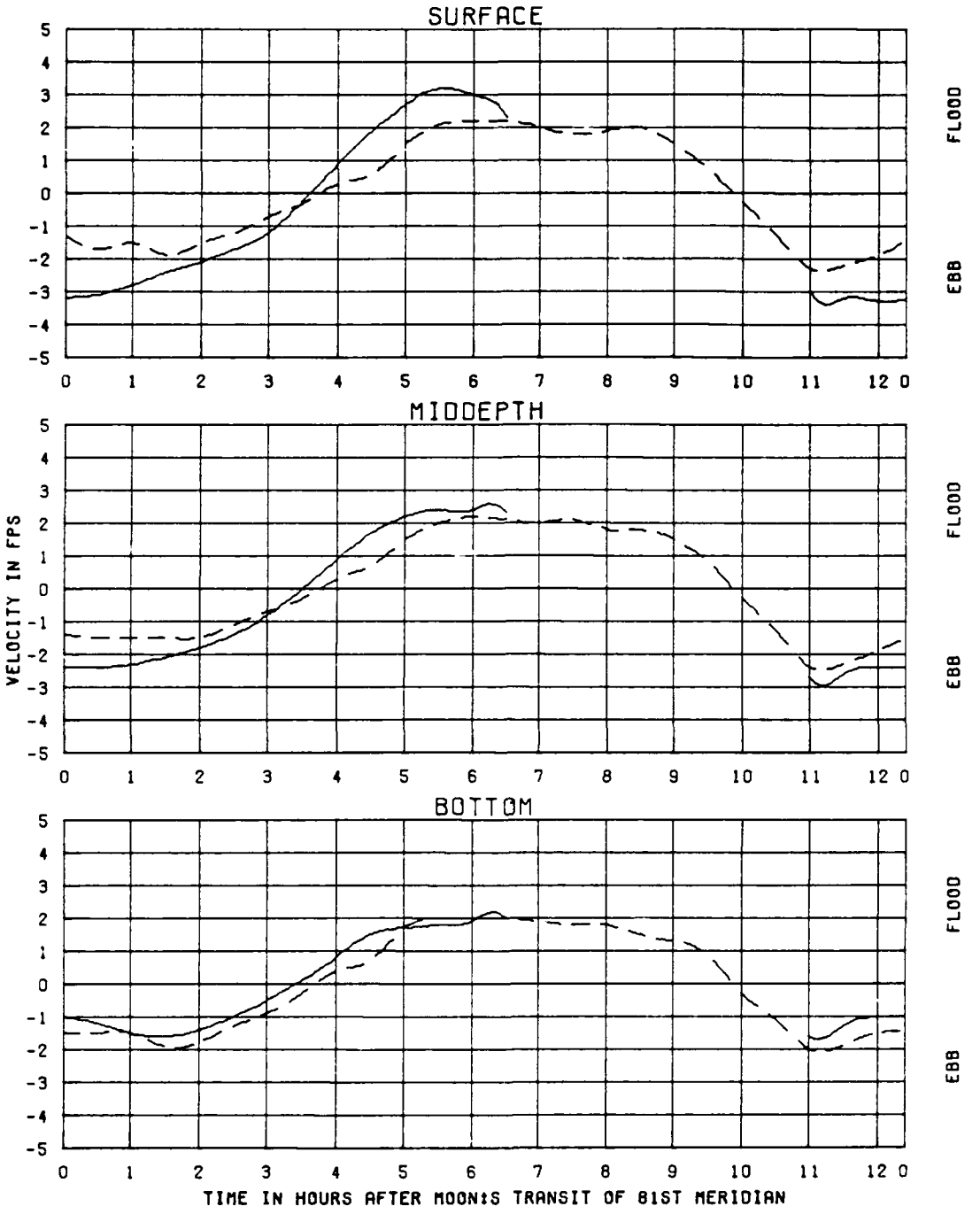

TEST CONDITIONS

TIDE RANGE AT GAGE 1	6.2 FT
OCEAN SALINITY(TOTAL SALT)	32.5 PPT
FRESHWATER INFLOW	1100 CFS

LEGEND
PROTOTYPE ———
MODEL — — —

KINGS BAY MODEL

VERIFICATION OF VELOCITIES FOR 11-12-82 TIDE

STATION 4C

PLATE B25

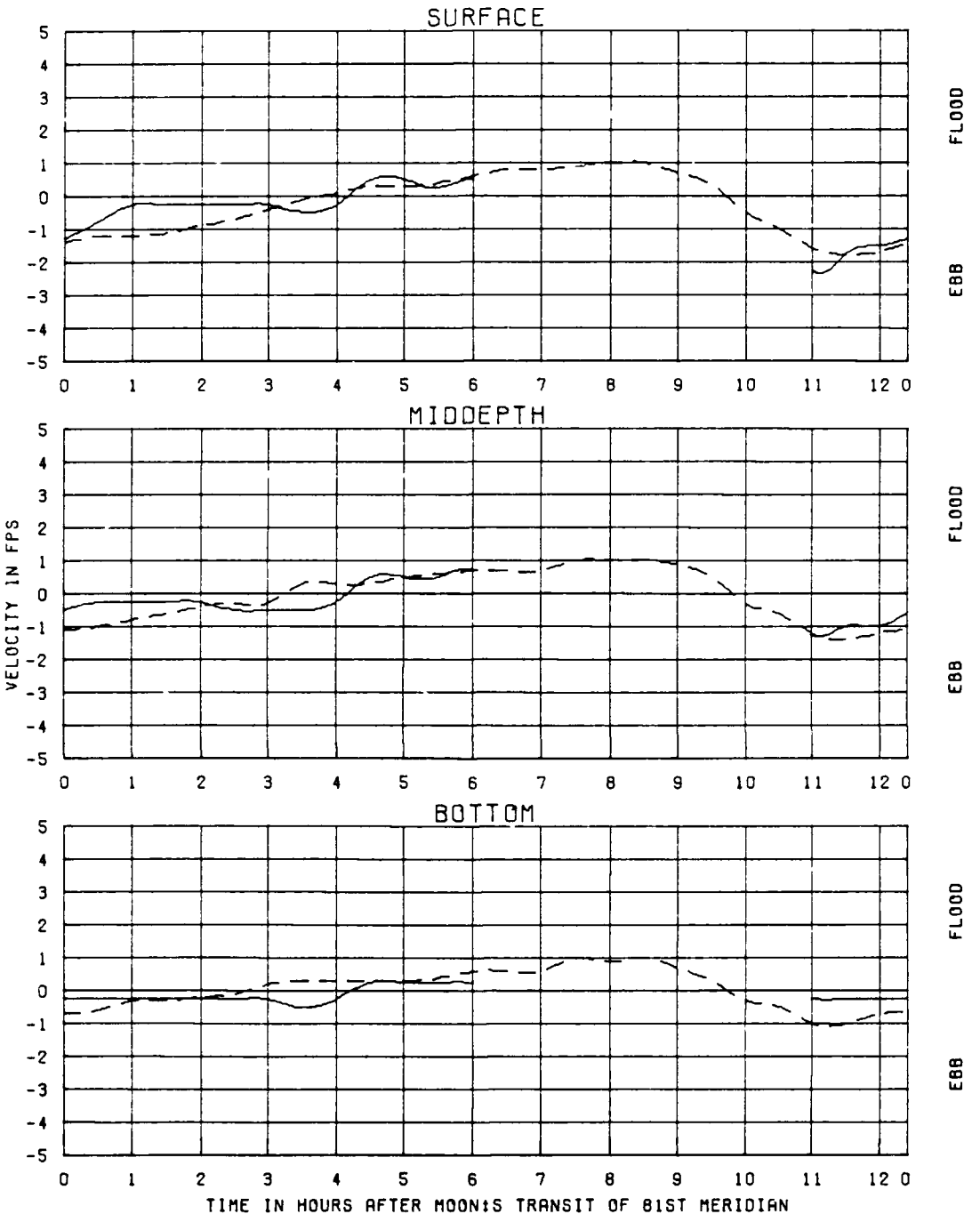

TEST CONDITIONS

TIDE RANGE AT GAGE 1	6.2 FT
OCEAN SALINITY(TOTAL SALT)	32.5 PPT
FRESHWATER INFLOW	1100 CFS

LEGEND
PROTOTYPE ———
MODEL — — —

KINGS BAY MODEL

VERIFICATION OF VELOCITIES FOR 11-12-82 TIDE

STATION
5A

PLATE B26

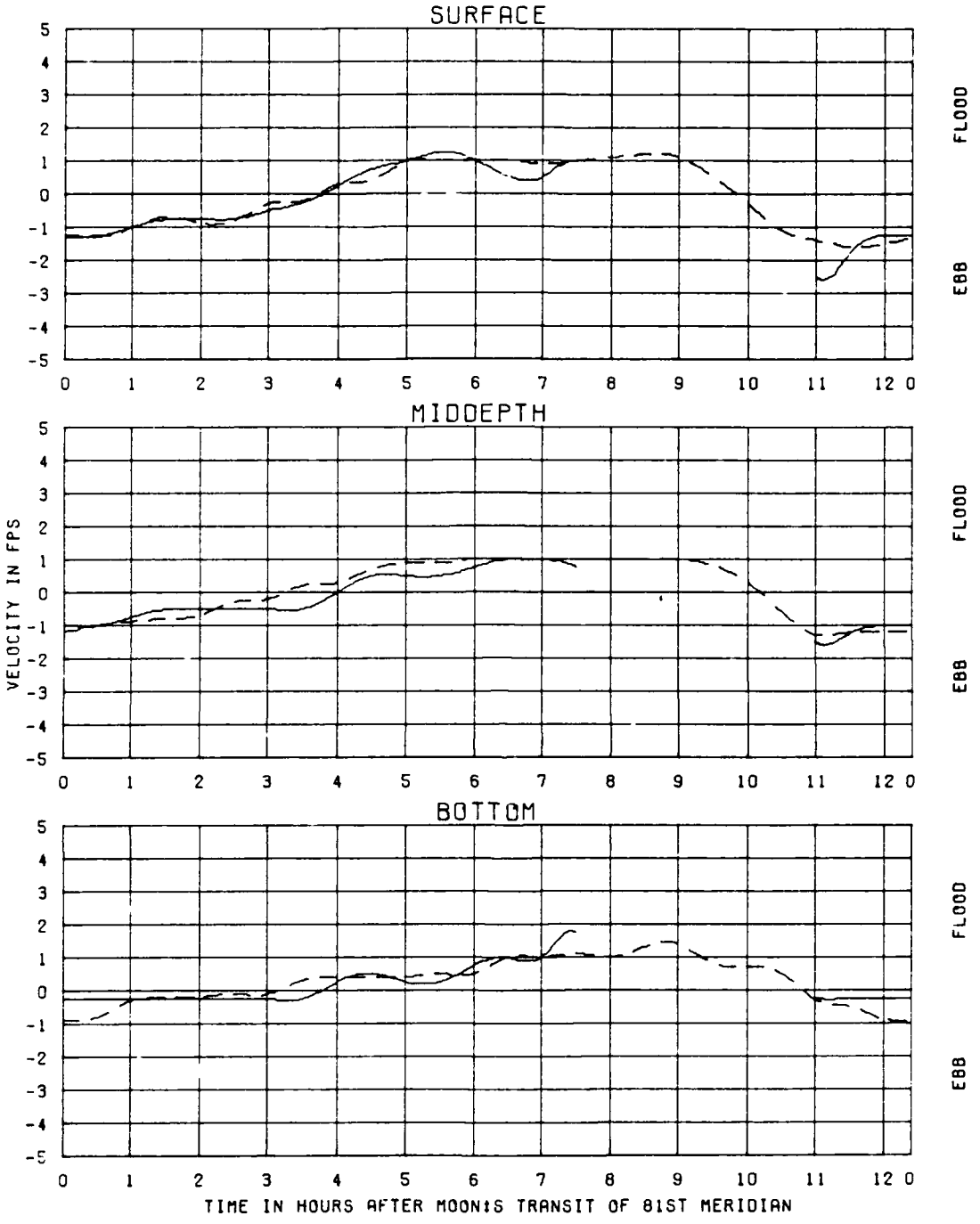

TEST CONDITIONS

TIDE RANGE AT GAGE 1	6.2 FT
OCEAN SALINITY(TOTAL SALT)	32.5 PPT
FRESHWATER INFLOW	1100 CFS

LEGEND
PROTOTYPE ———
MODEL — — —

KINGS BAY MODEL

VERIFICATION OF VELOCITIES FOR 11-12-82 TIDE

STATION
58

PLATE B27

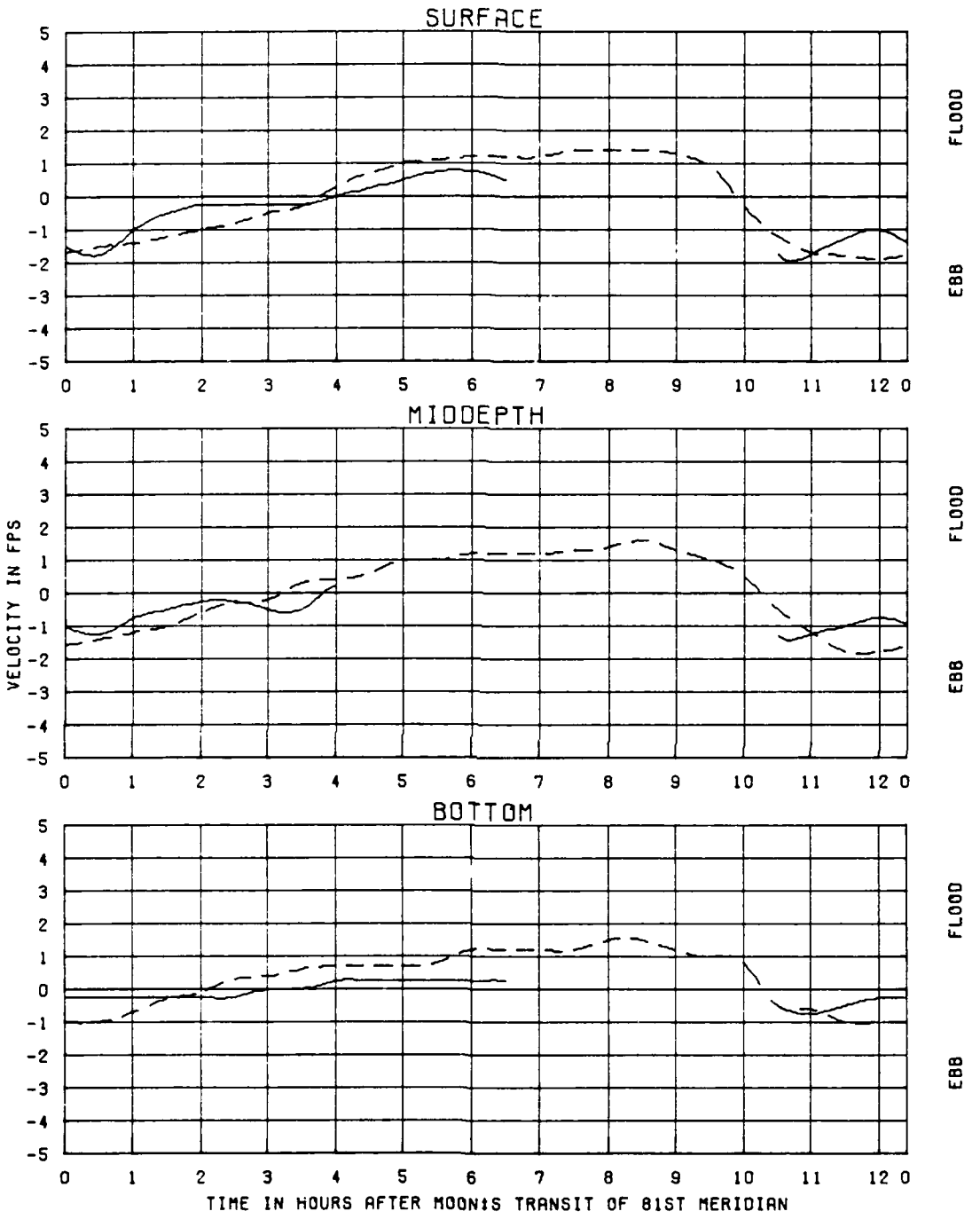

TEST CONDITIONS	
TIDE RANGE AT GAGE 1	6.2 FT
OCEAN SALINITY(TOTAL SALT)	32.5 PPT
FRESHWATER INFLOW	1100 CFS

LEGEND
PROTOTYPE ———
MODEL — — —

KINGS BAY MODEL

VERIFICATION OF VELOCITIES FOR 11-12-82 TIDE

STATION
5C

PLATE B28

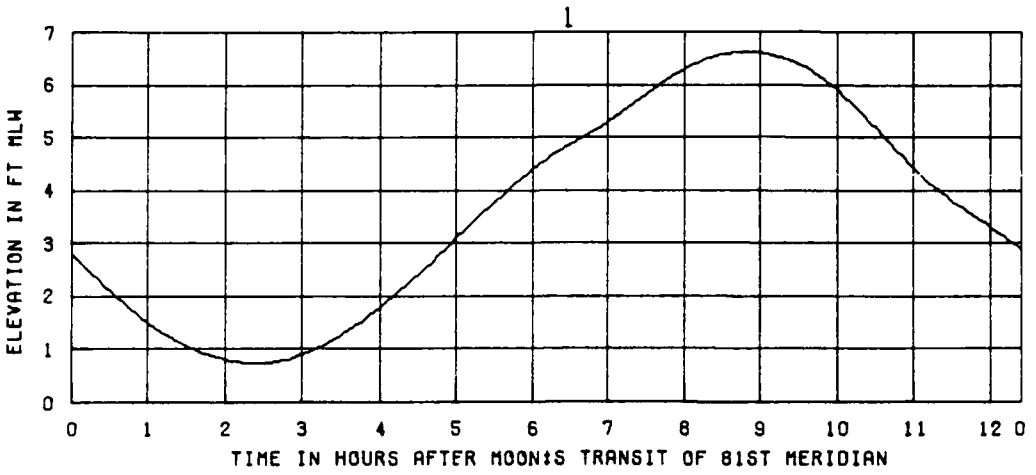

TEST CONDITIONS

TIDE RANGE AT GAGE 1	5.8 FT
OCEAN SALINITY(TOTAL SALT)	32.5 PPT
FRESHWATER INFLOW	1100 CFS

LEGEND

PROTOTYPE ———

MODEL — — —

KINGS BAY MODEL

VERIFICATION OF TIDE HEIGHTS FOR 7/14/82 TIDE

STATION 1

PLATE B29

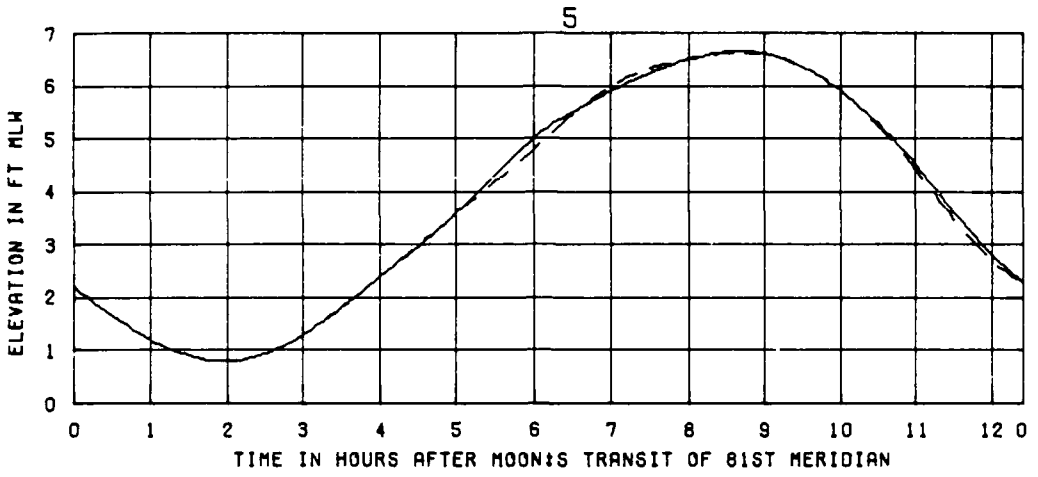

TEST CONDITIONS

TIDE RANGE AT GAGE 1	5.8 FT
OCEAN SALINITY(TOTAL SALT)	32.5 PPT
FRESHWATER INFLOW	1100 CFS

LEGEND
PROTOTYPE ———
MODEL — — —

KINGS BAY MODEL

VERIFICATION OF
TIDE HEIGHTS
FOR 7/14/82 TIDE
STATION
5

PLATE B30

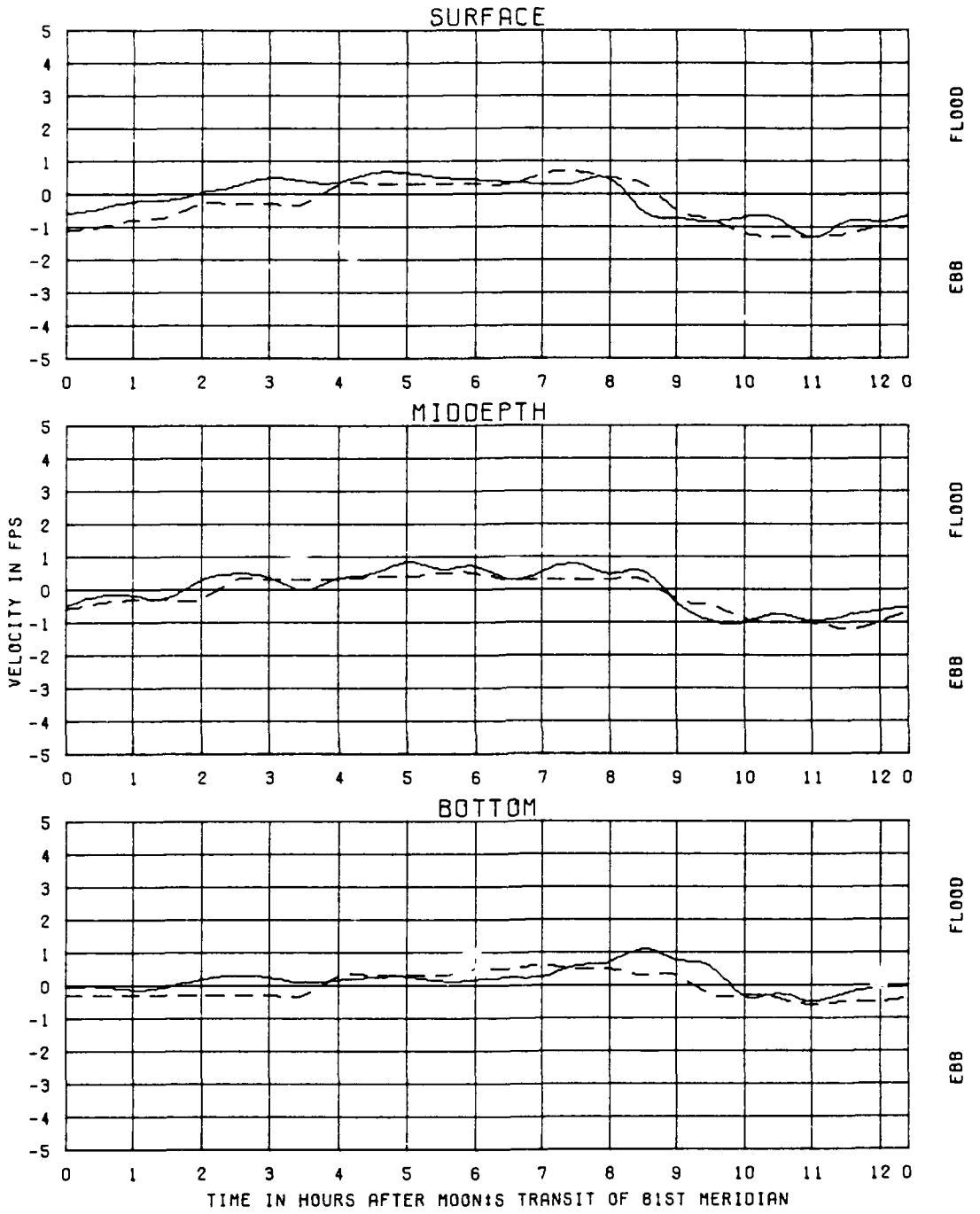

TEST CONDITIONS

TIDE RANGE AT GAGE 1	5.8 FT
OCEAN SALINITY(TOTAL SALT)	32.5 PPT
FRESHWATER INFLOW	1100 CFS

LEGEND

PROTOTYPE ———

MODEL — — —

KINGS BAY MODEL

VERIFICATION OF VELOCITIES FOR 7-14-82 TIDE

STATION 5A

PLATE B31

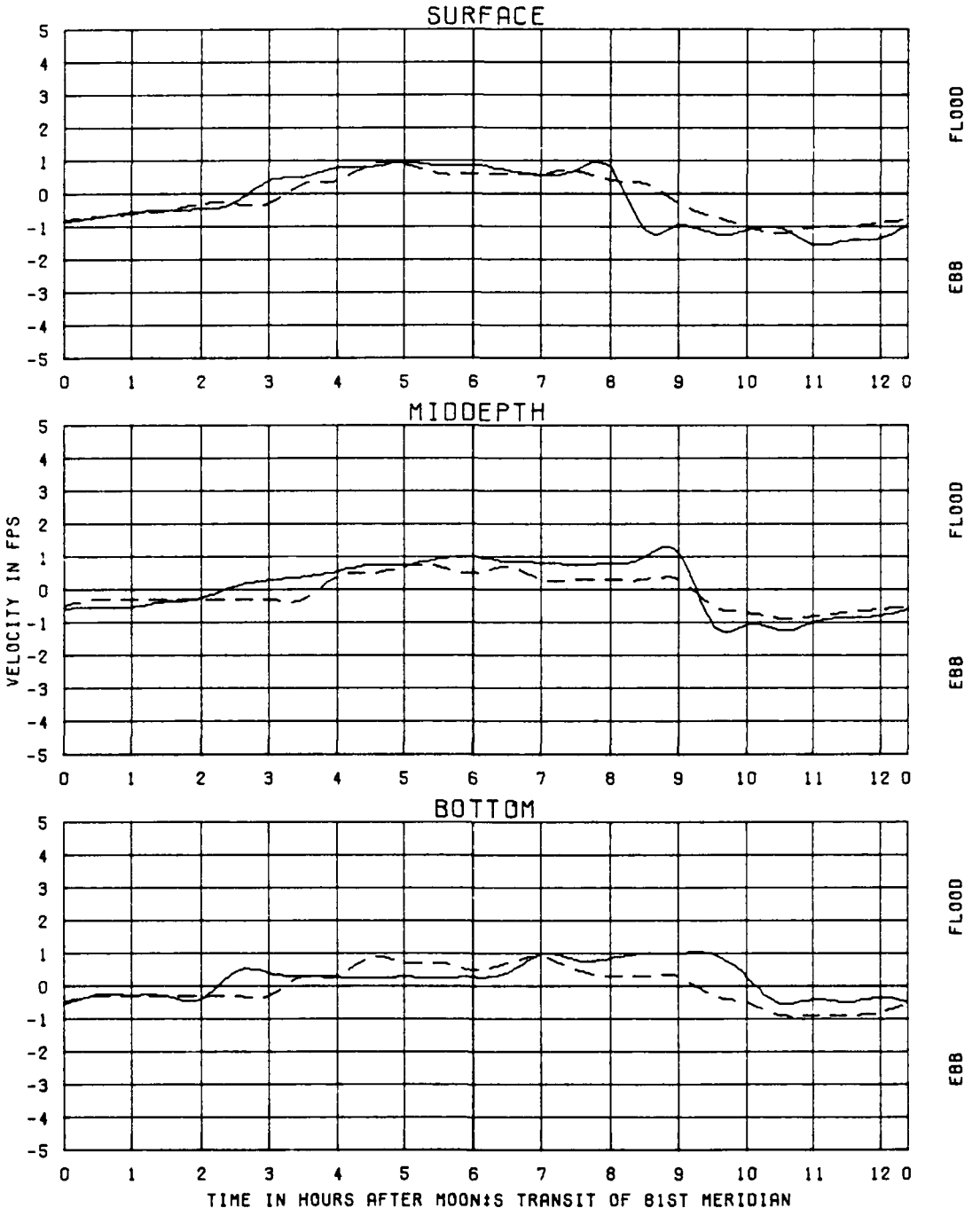

TEST CONDITIONS

TIDE RANGE AT GAGE 1	5.8 FT
OCEAN SALINITY(TOTAL SALT)	32.5 PPT
FRESHWATER INFLOW	1100 CFS

LEGEND
PROTOTYPE ———
MODEL — — —

KINGS BAY MODEL

VERIFICATION OF VELOCITIES FOR 7-14-82 TIDE

STATION
SB

PLATE B32

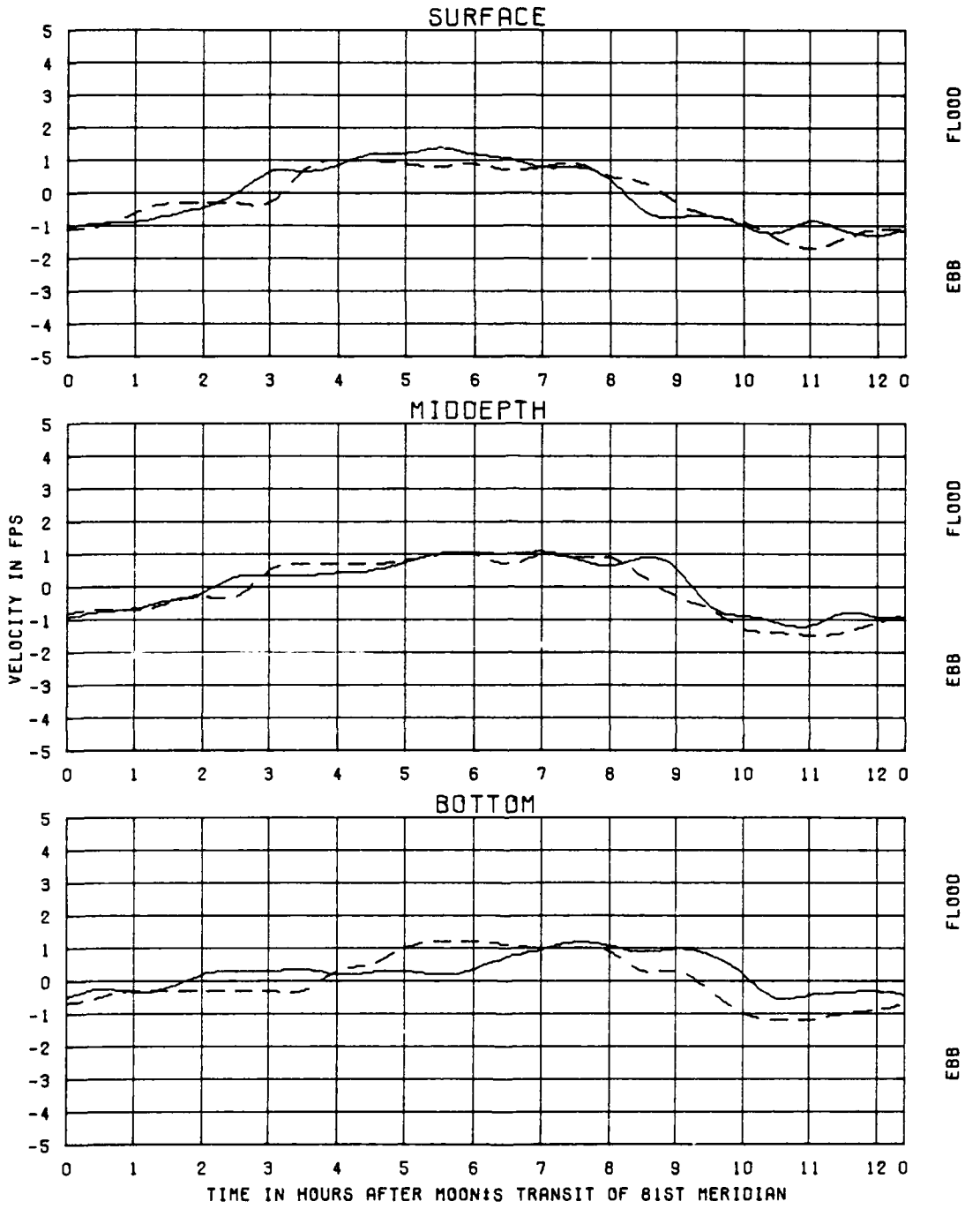

TEST CONDITIONS

TIDE RANGE AT GAGE 1	5.8 FT
OCEAN SALINITY(TOTAL SALT)	32.5 PPT
FRESHWATER INFLOW	1100 CFS

LEGEND
PROTOTYPE ———
MODEL — — —

KINGS BAY MODEL

VERIFICATION OF VELOCITIES FOR 7-14-82 TIDE

STATION
SC

PLATE B33

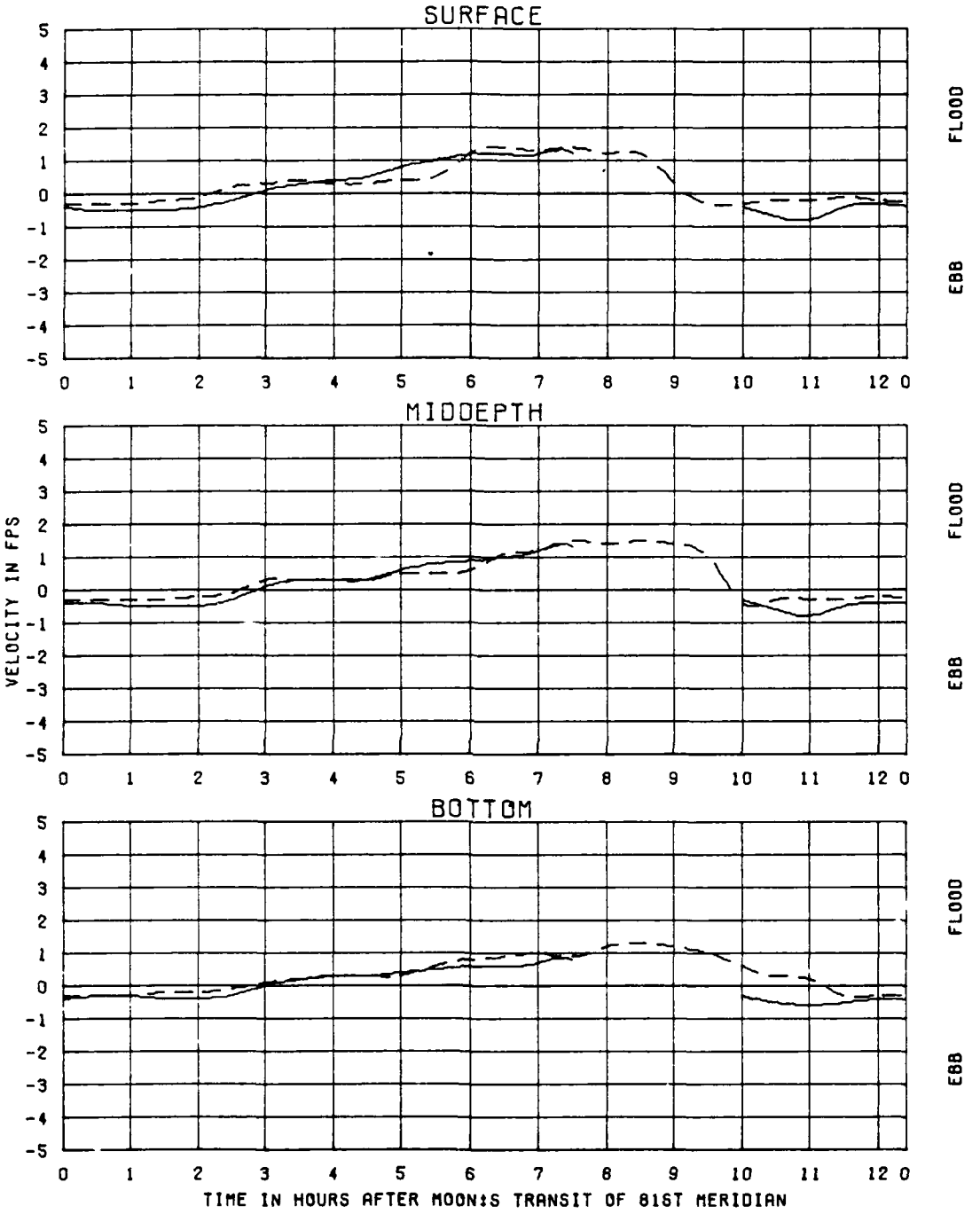

TEST CONDITIONS

TIDE RANGE AT GAGE 1	6.2 FT
OCEAN SALINITY(TOTAL SALT)	32.5 PPT
FRESHWATER INFLOW	1100 CFS

KINGS BAY MODEL

VERIFICATION OF VELOCITIES FOR 11-12-82 TIDE

STATION 6A

LEGEND

PROTOTYPE ———

MODEL — — —

PLATE B34

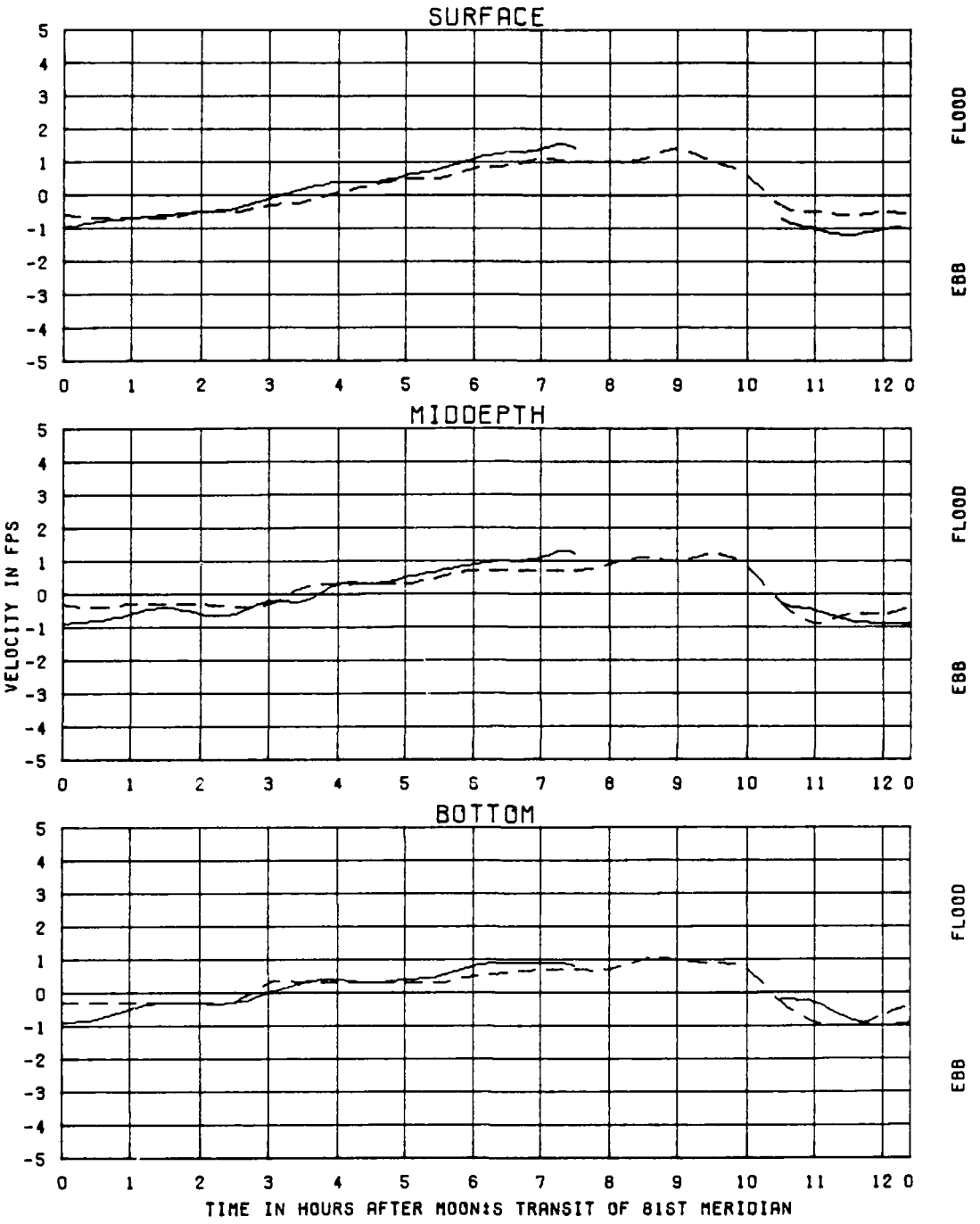

TEST CONDITIONS

TIDE RANGE AT GAGE 1	6.2 FT
OCEAN SALINITY(TOTAL SALT)	32.5 PPT
FRESHWATER INFLOW	1100 CFS

LEGEND
PROTOTYPE ———
MODEL — — —

KINGS BAY MODEL

VERIFICATION OF VELOCITIES FOR 11-12-82 TIDE

STATION
68

PLATE B35

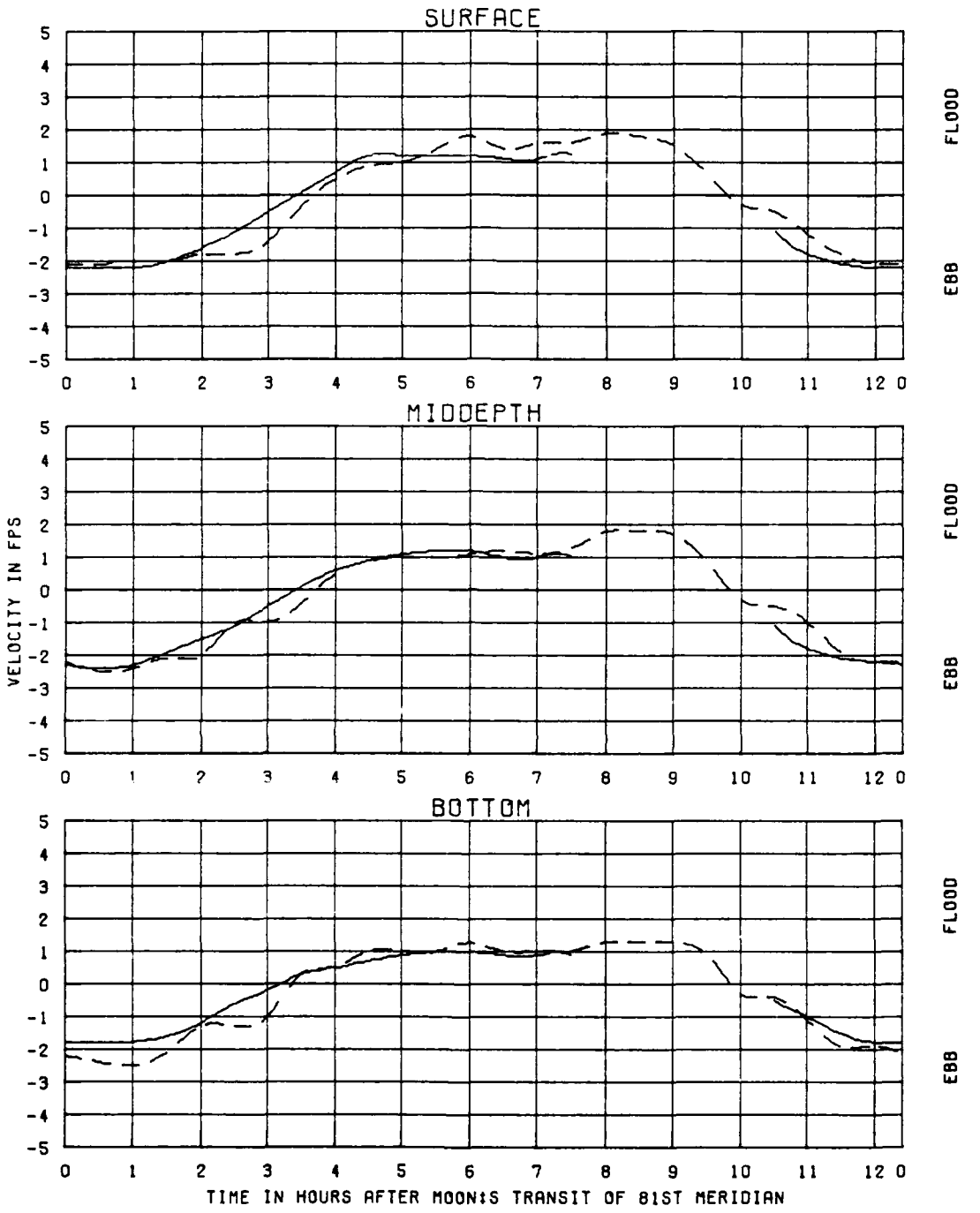

TEST CONDITIONS	
TIDE RANGE AT GAGE 1	6.2 FT
OCEAN SALINITY(TOTAL SALT)	32.5 PPT
FRESHWATER INFLOW	1100 CFS

KINGS BAY MODEL

VERIFICATION OF VELOCITIES FOR 11-12-82 TIDE

STATION 6C

LEGEND
PROTOTYPE ———
MODEL — — —

PLATE B36

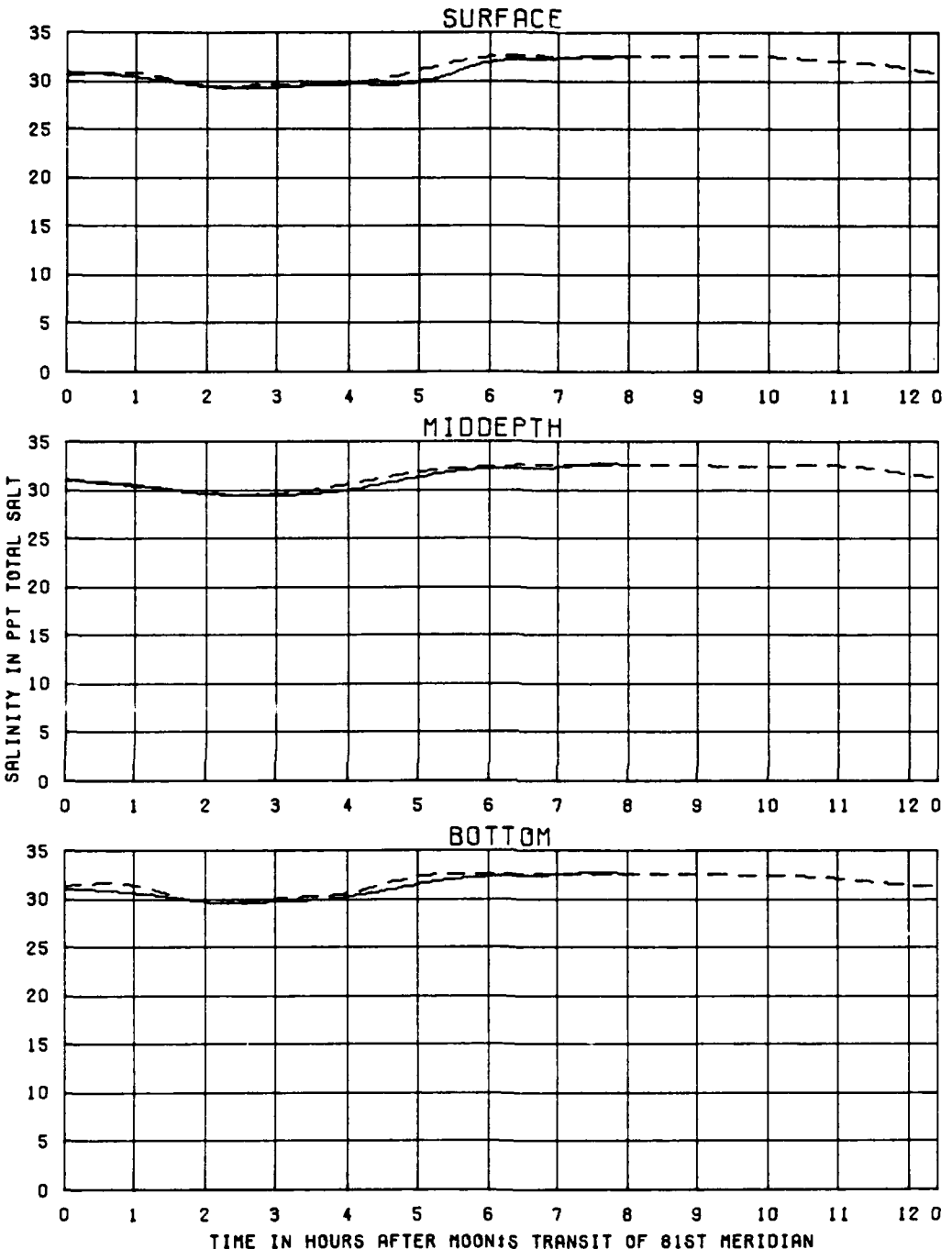

TEST CONDITIONS

TIDE RANGE AT GAGE 1	5.8 FT
OCEAN SALINITY(TOTAL SALT)	32.5 PPT
FRESHWATER INFLOW	1100 CFS

KINGS BAY MODEL

VERIFICATION OF SALINITIES FOR 11-10-82 TIDE

STATION 1A

LEGEND

PROTOTYPE ———

MODEL — — —

PLATE B37

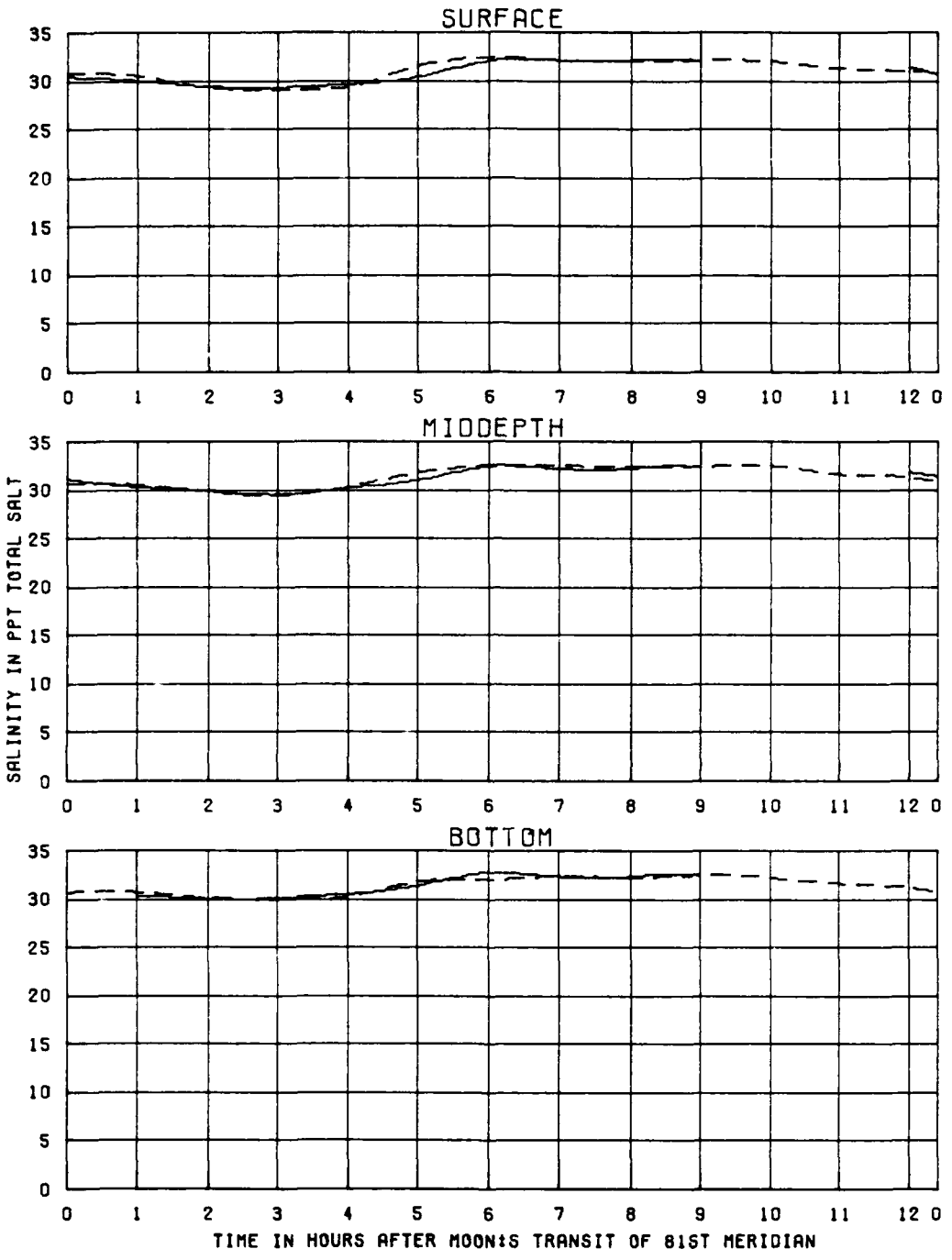

TEST CONDITIONS

TIDE RANGE AT GAGE 1	5.8 FT
OCEAN SALINITY(TOTAL SALT)	32.5 PPT
FRESHWATER INFLOW	1100 CFS

LEGEND
PROTOTYPE ———
MODEL — — —

KINGS BAY MODEL

VERIFICATION OF SALINITIES FOR 11-10-82 TIDE
STATION 1B

PLATE B38

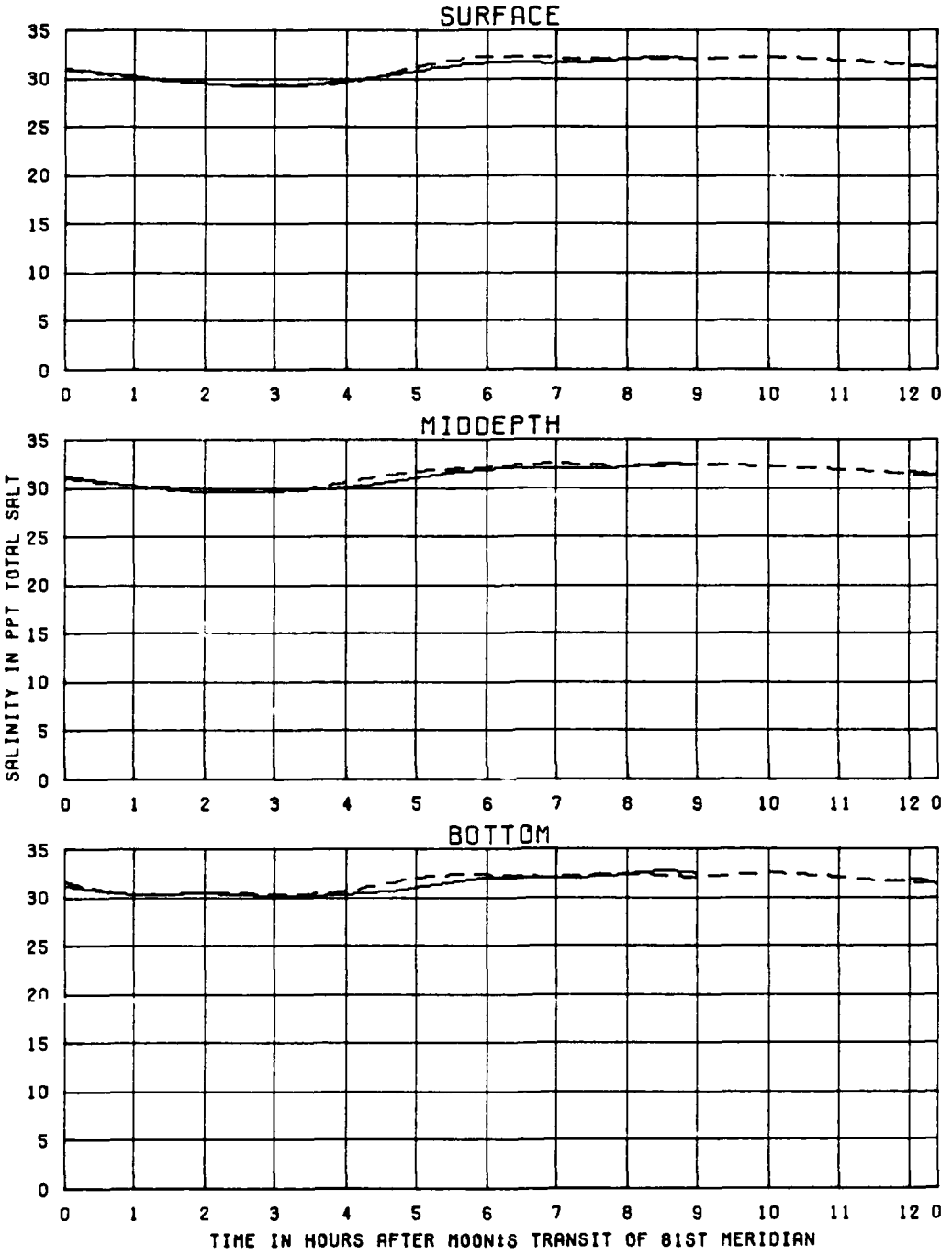

TEST CONDITIONS

TIDE RANGE AT GAGE 1	5.8 FT
OCEAN SALINITY(TOTAL SALT)	32.5 PPT
FRESHWATER INFLOW	1100 CFS

LEGEND
PROTOTYPE ———
MODEL — — —

KINGS BAY MODEL

VERIFICATION OF SALINITIES FOR 11-10-82 TIDE

STATION
1C

PLATE B39

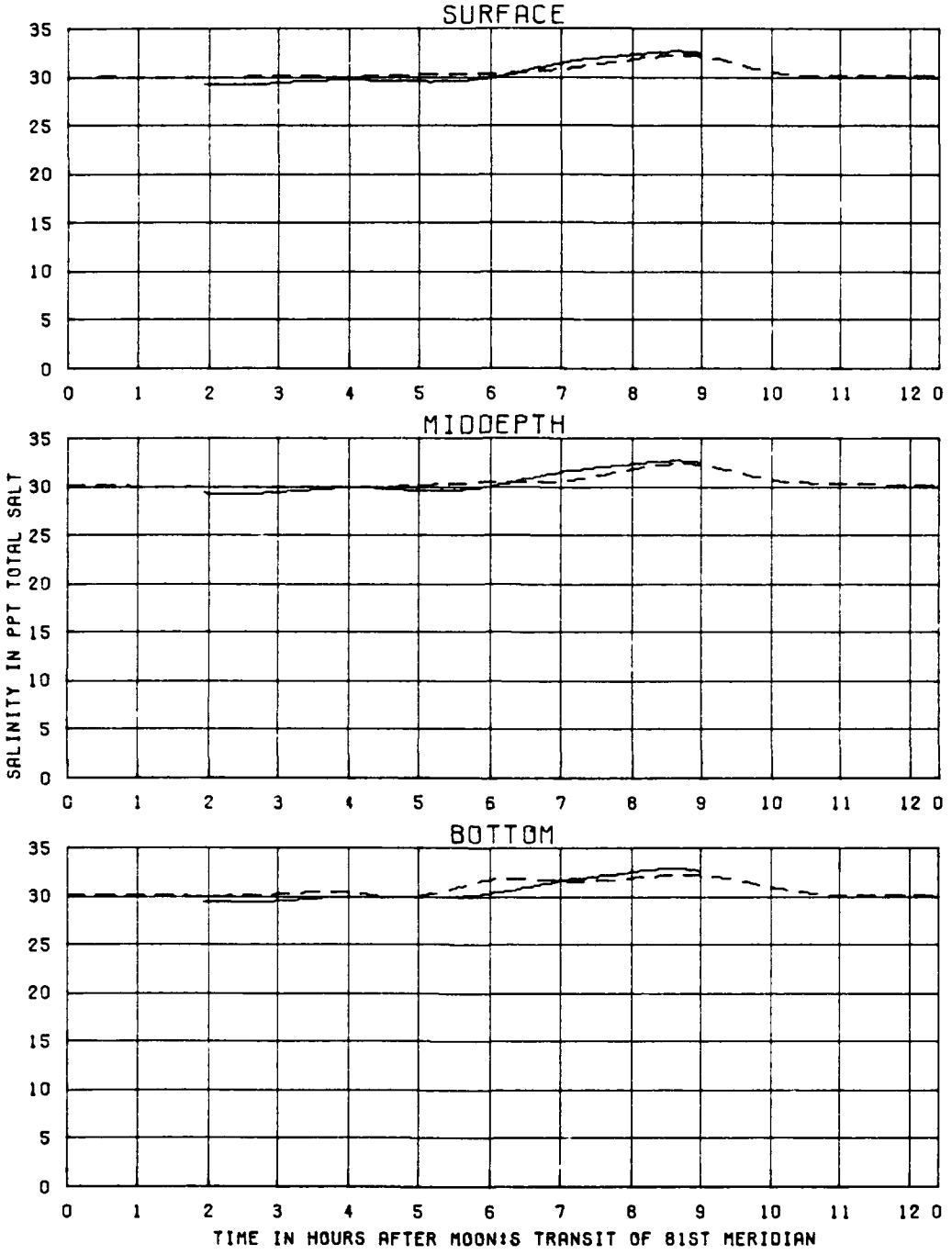

TEST CONDITIONS

TIDE RANGE AT GAGE 1	5.8 FT
OCEAN SALINITY(TOTAL SALT)	32.5 PPT
FRESHWATER INFLOW	1100 CFS

LEGEND
PROTOTYPE ———
MODEL — — —

KINGS BAY MODEL

VERIFICATION OF SALINITIES FOR 11-10-82 TIDE

STATION 2A

PLATE B40

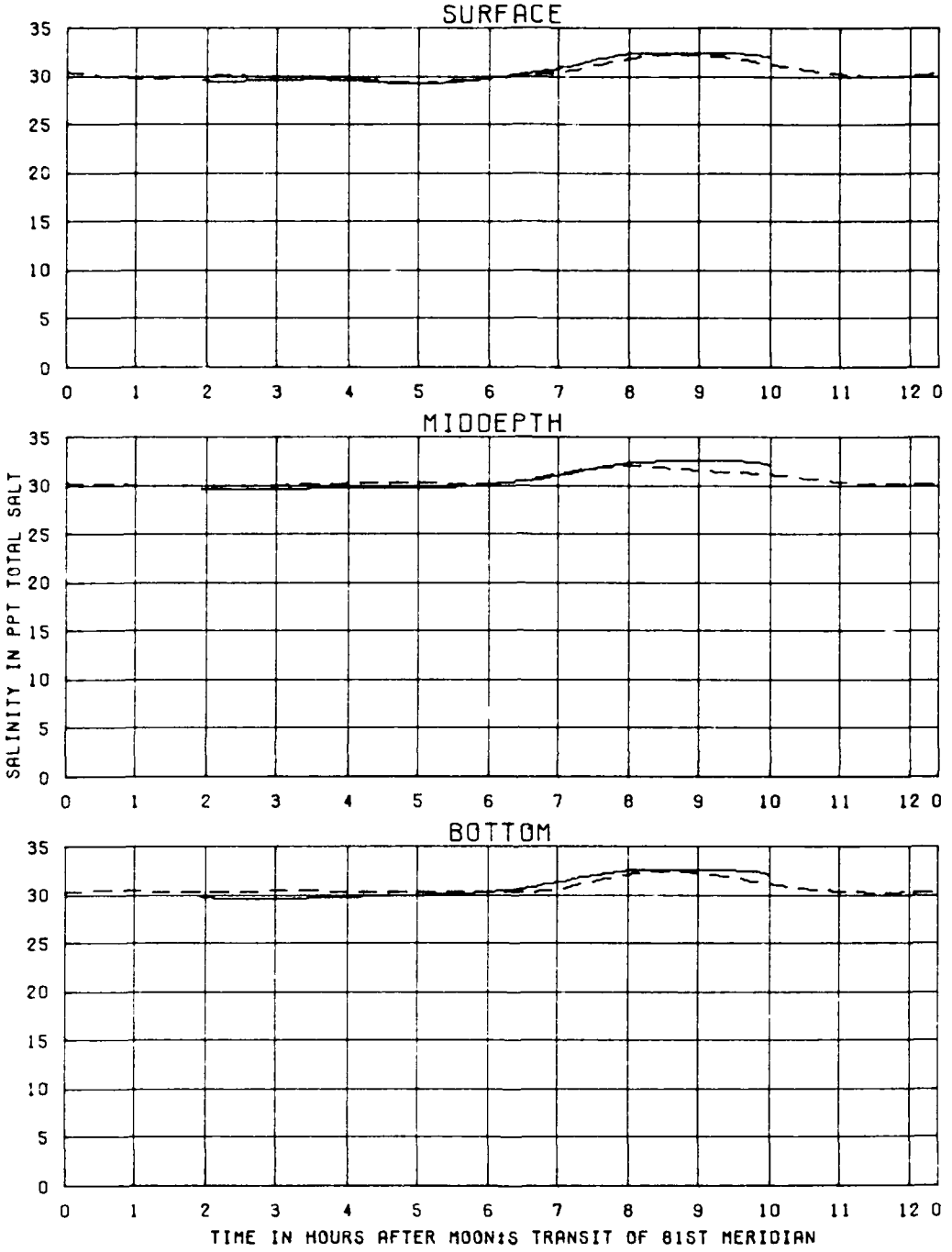

TEST CONDITIONS

TIDE RANGE AT GAGE 1	5.8 FT
OCEAN SALINITY(TOTAL SALT)	32.5 PPT
FRESHWATER INFLOW	1100 CFS

LEGEND
PROTOTYPE ———
MODEL — — —

KINGS BAY MODEL

VERIFICATION OF SALINITIES FOR 11-10-82 TIDE

STATION
28

PLATE B41

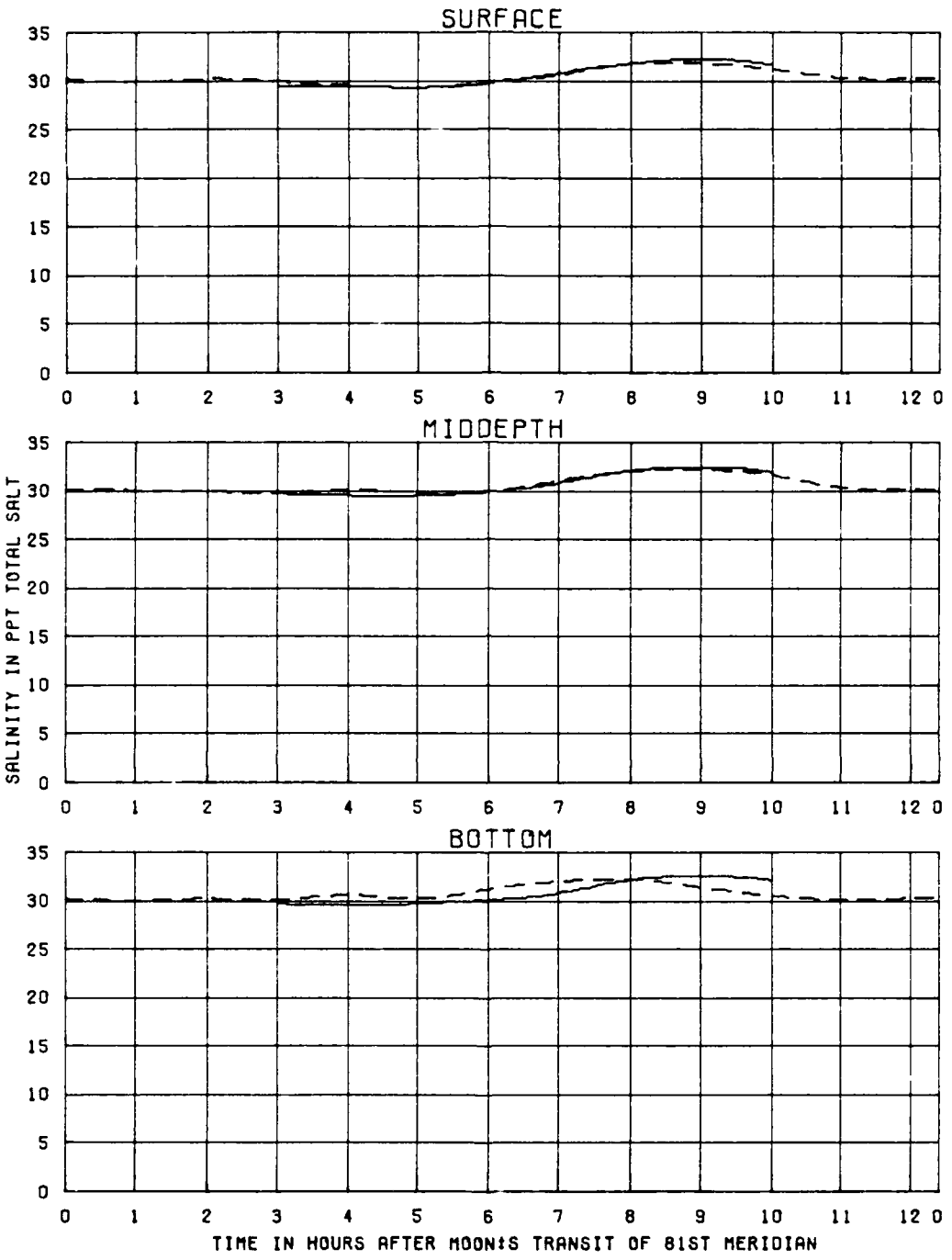

TEST CONDITIONS

TIDE RANGE AT GAGE 1	5.8 FT
OCEAN SALINITY(TOTAL SALT)	32.5 PPT
FRESHWATER INFLOW	1100 CFS

LEGEND
PROTOTYPE ———
MODEL — — —

KINGS BAY MODEL

VERIFICATION OF SALINITIES FOR 11-10-82 TIDE

STATION 2C

PLATE B42

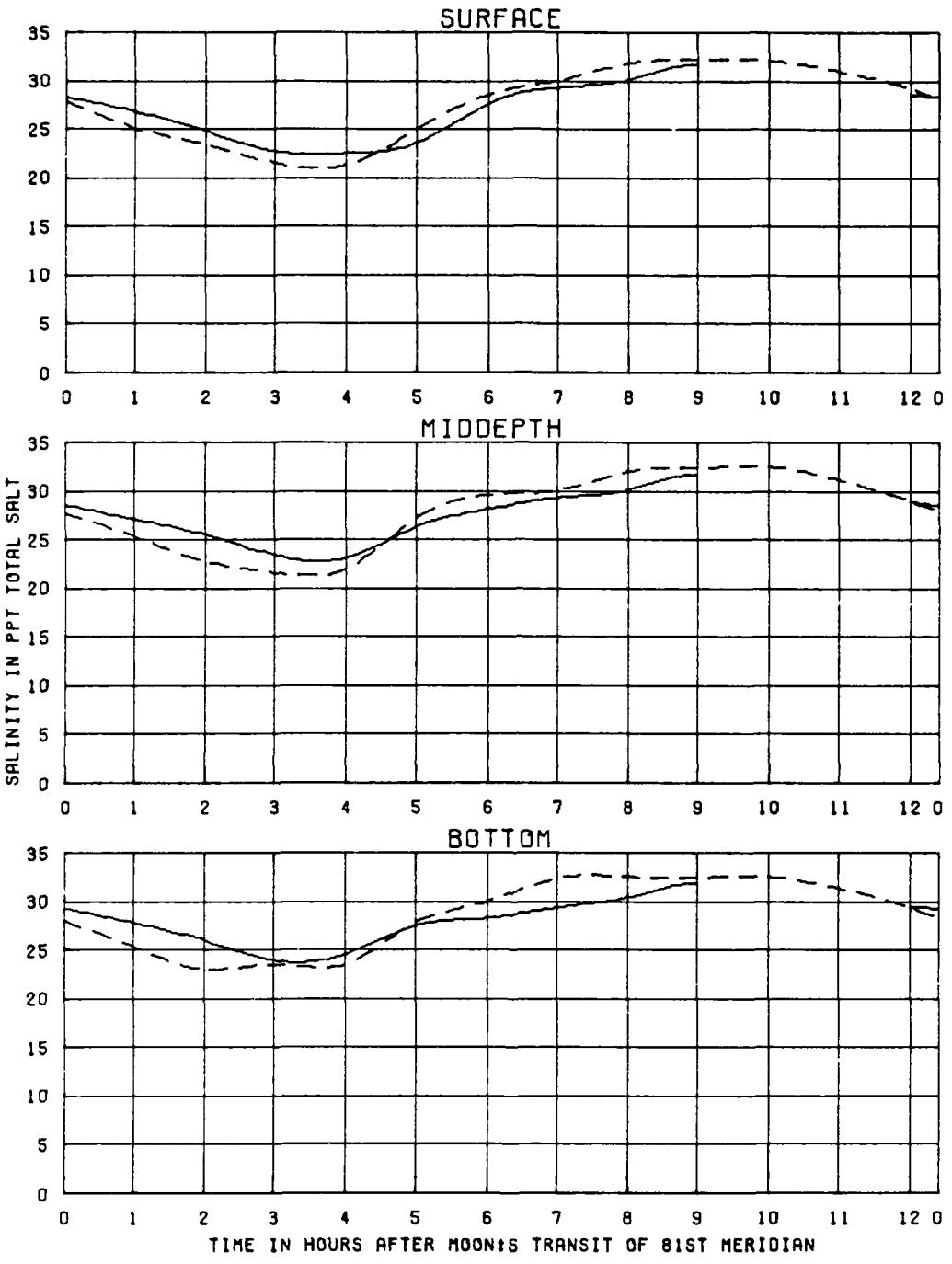

TEST CONDITIONS

TIDE RANGE AT GAGE 1	5.8 FT
OCEAN SALINITY(TOTAL SALT)	32.5 PPT
FRESHWATER INFLOW	1100 CFS

LEGEND
PROTOTYPE ———
MODEL — — —

KINGS BAY MODEL

VERIFICATION OF SALINITIES FOR 11-10-82 TIDE

STATION 3A

PLATE B43

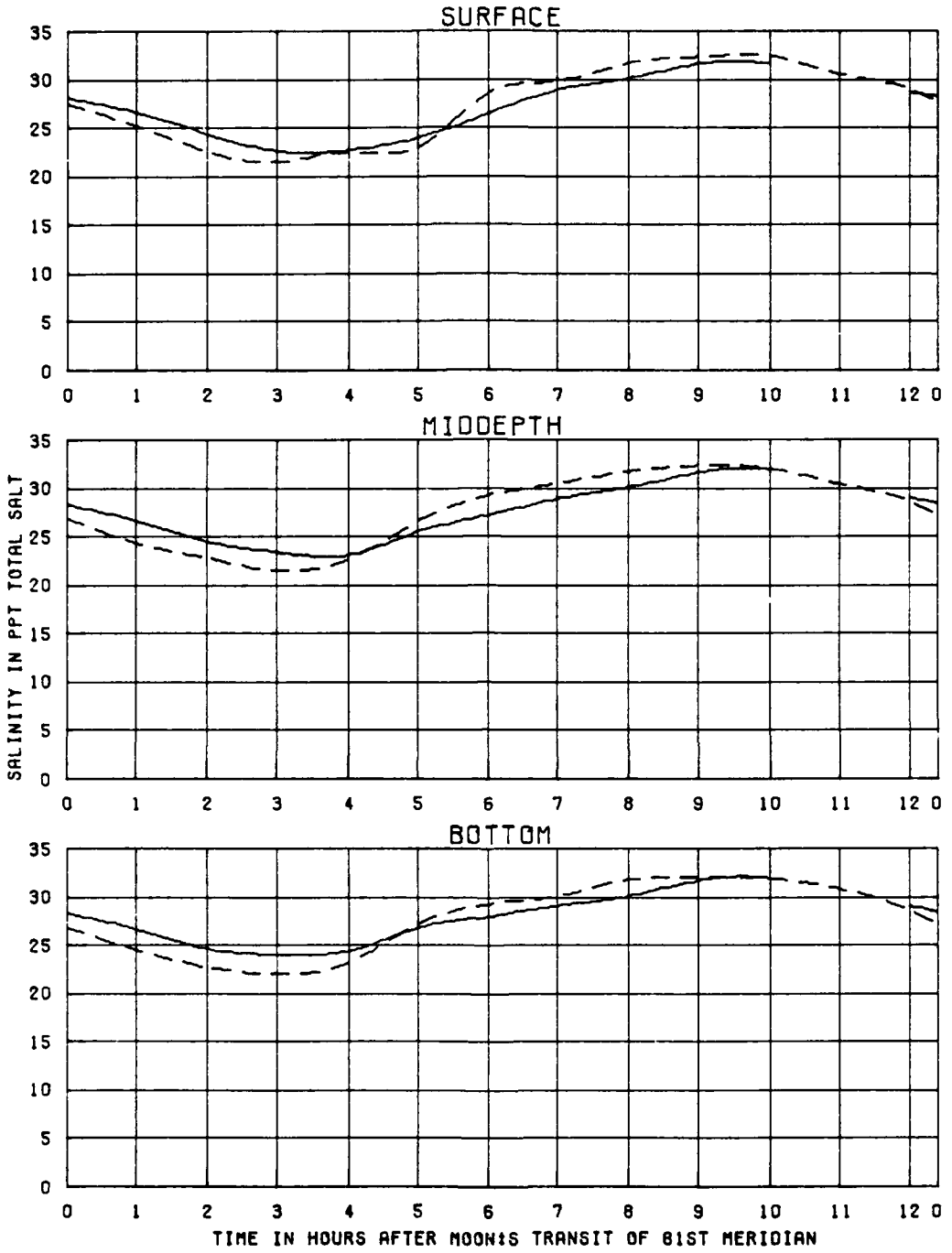

TEST CONDITIONS

TIDE RANGE AT GAGE 1	5.8 FT
OCEAN SALINITY(TOTAL SALT)	32.5 PPT
FRESHWATER INFLOW	1100 CFS

LEGEND
PROTOTYPE ———
MODEL — — —

KINGS BAY MODEL

VERIFICATION OF SALINITIES FOR 11-10-82 TIDE

STATION
3B

PLATE B44

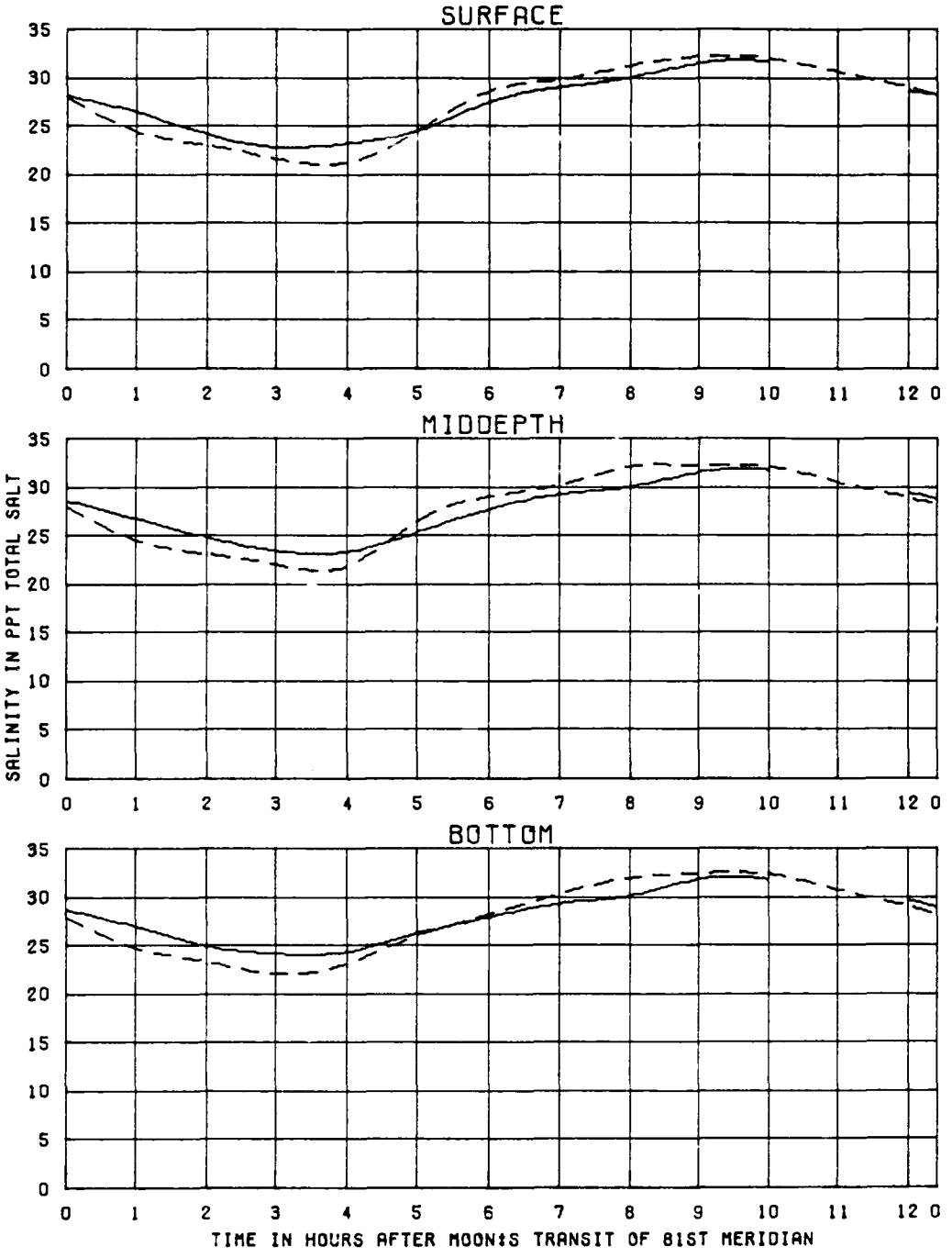

TEST CONDITIONS

TIDE RANGE AT GAGE 1	5.8 FT
OCEAN SALINITY(TOTAL SALT)	32.5 PPT
FRESHWATER INFLOW	1100 CFS

LEGEND
PROTOTYPE ———
MODEL — — —

KINGS BAY MODEL

VERIFICATION Of
SALINITIES
FOR 11-10-82 TIDE
STATION
3C

PLATE B45

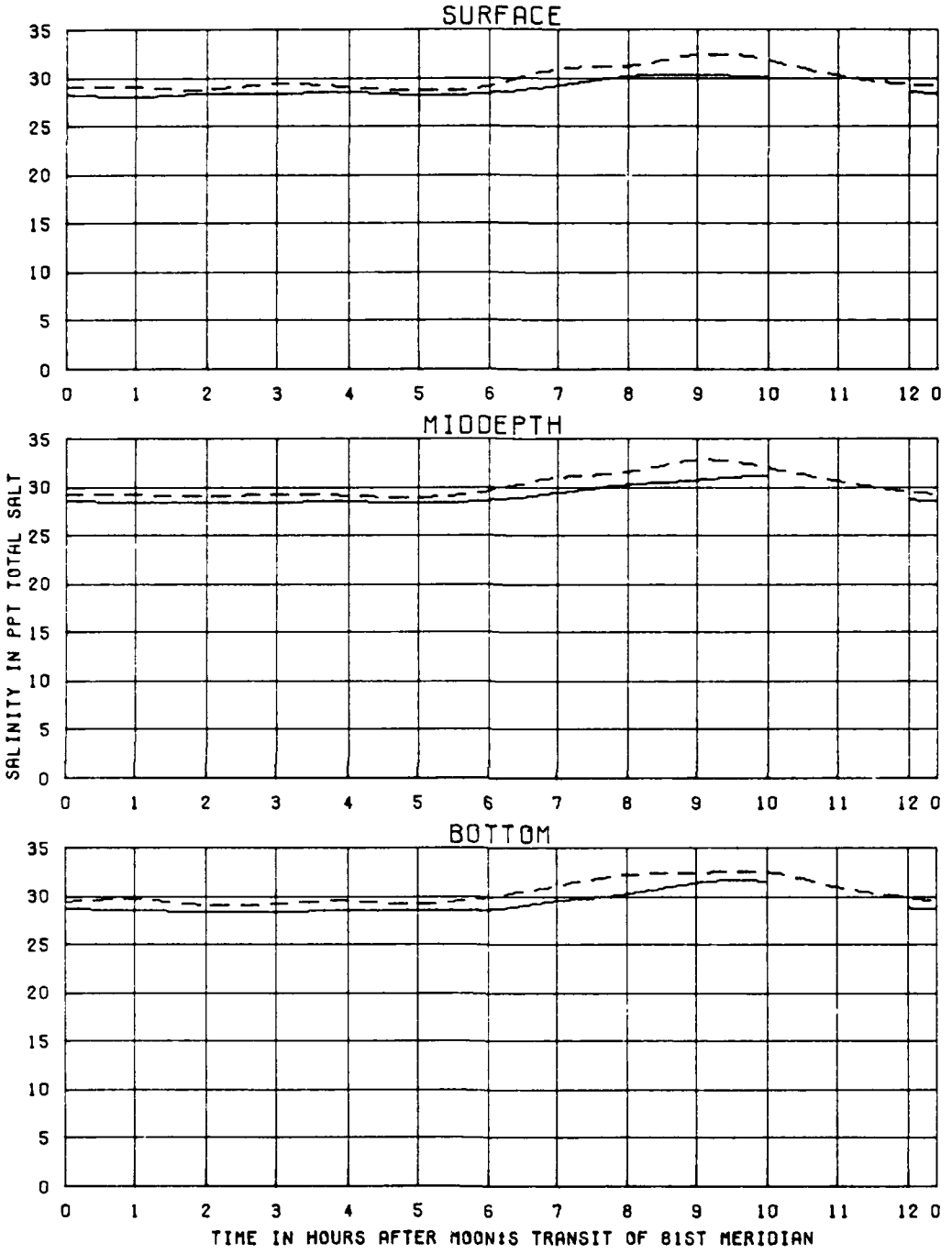

TEST CONDITIONS

TIDE RANGE AT GAGE 1	5.8 FT
OCEAN SALINITY(TOTAL SALT)	32.5 PPT
FRESHWATER INFLOW	1100 CFS

LEGEND
PROTOTYPE ———
MODEL — — —

KINGS BAY MODEL

VERIFICATION OF
SALINITIES
FOR 11-10-82 TIDE
STATION
4A

PLATE B46

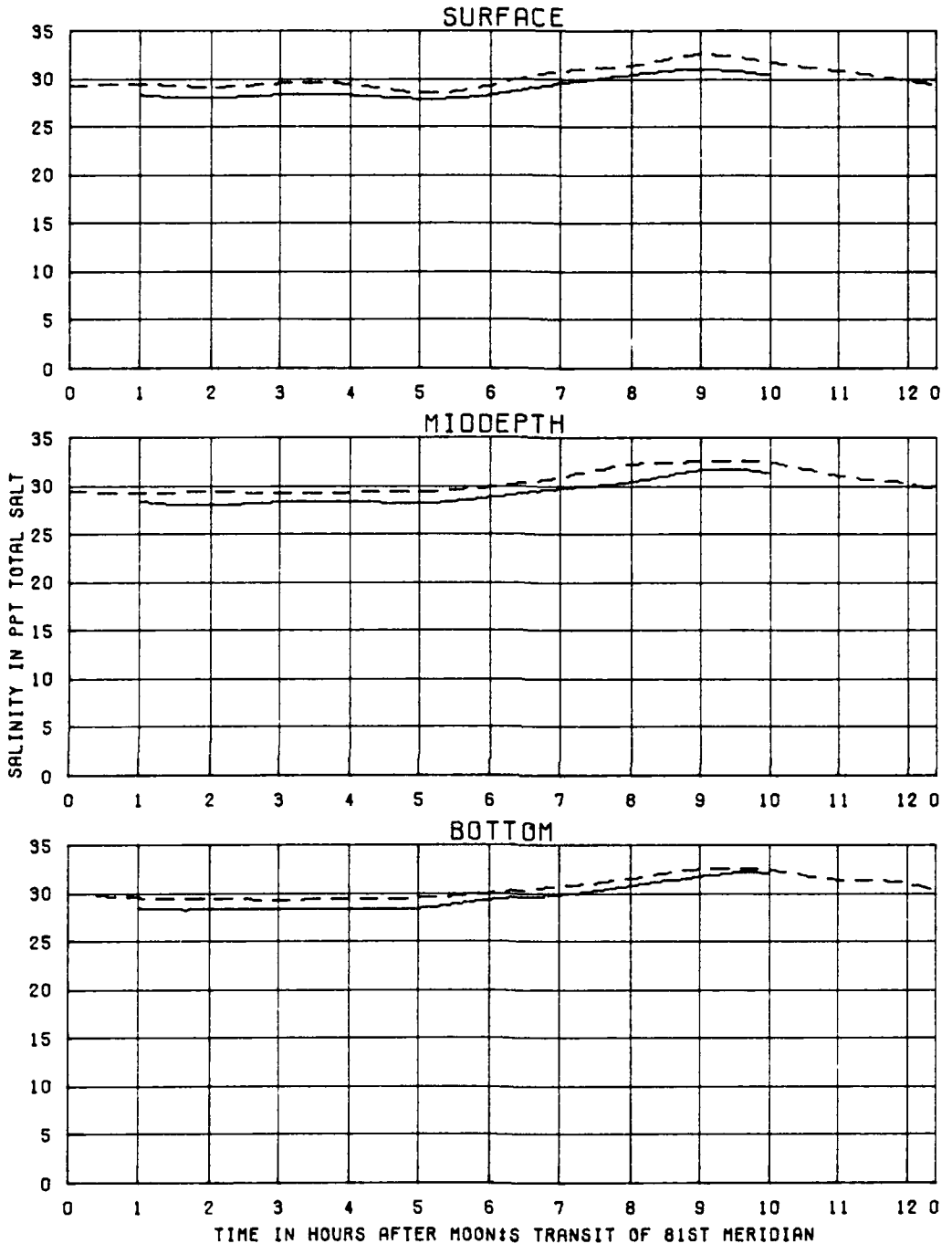

TEST CONDITIONS

TIDE RANGE AT GAGE 1	5.8 FT
OCEAN SALINITY(TOTAL SALT)	32.5 PPT
FRESHWATER INFLOW	1100 CFS

LEGEND
PROTOTYPE ———
MODEL — — —

KINGS BAY MODEL

VERIFICATION OF SALINITIES FOR 11-10-82 TIDE
STATION 48

PLATE B47

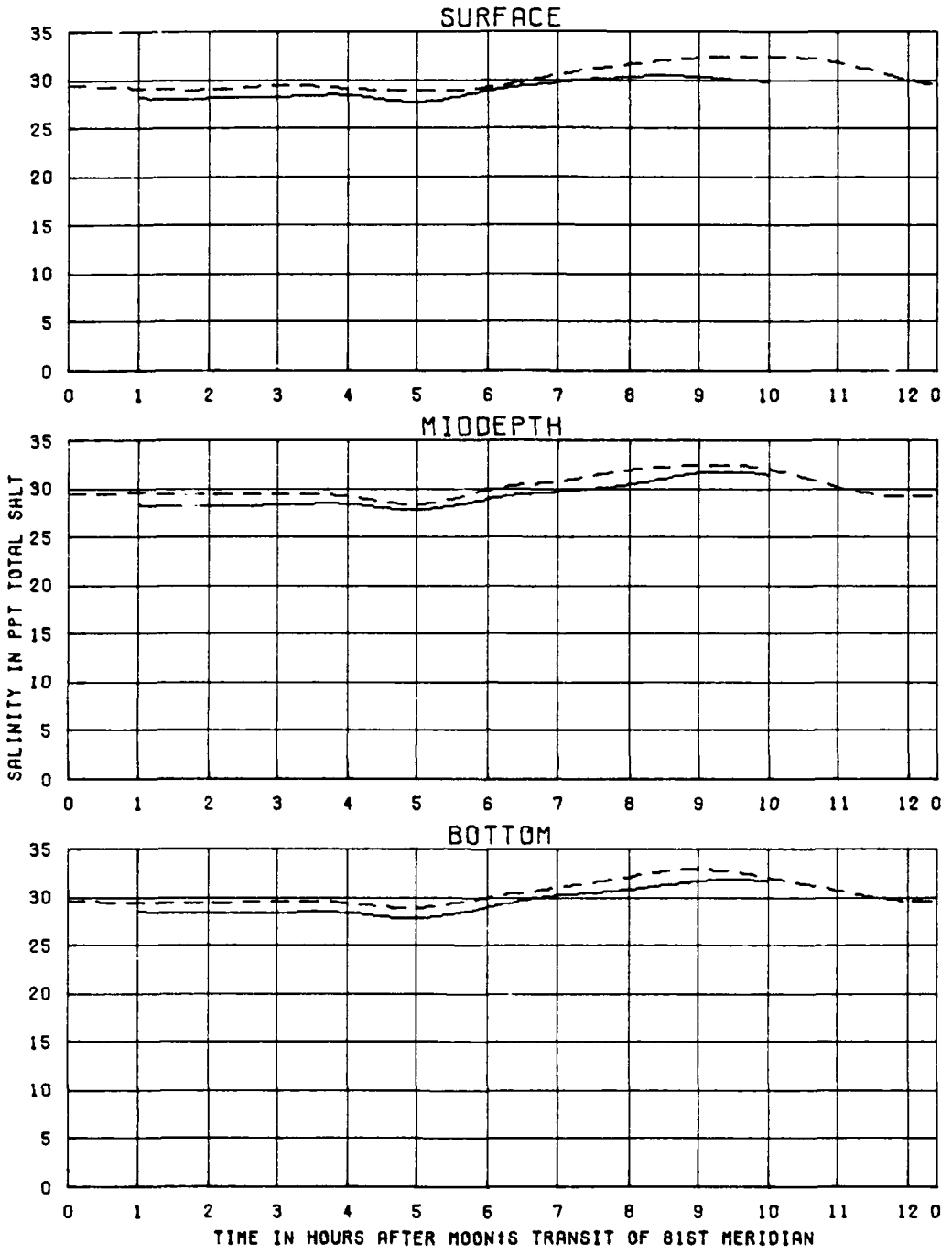

TEST CONDITIONS

TIDE RANGE AT GAGE 1	5.8 FT
OCEAN SALINITY(TOTAL SALT)	32.5 PPT
FRESHWATER INFLOW	1100 CFS

KINGS BAY MODEL

VERIFICATION OF SALINITIES FOR 11-10-82 TIDE

STATION 4C

LEGEND
PROTOTYPE ———
MODEL — — —

PLATE B48

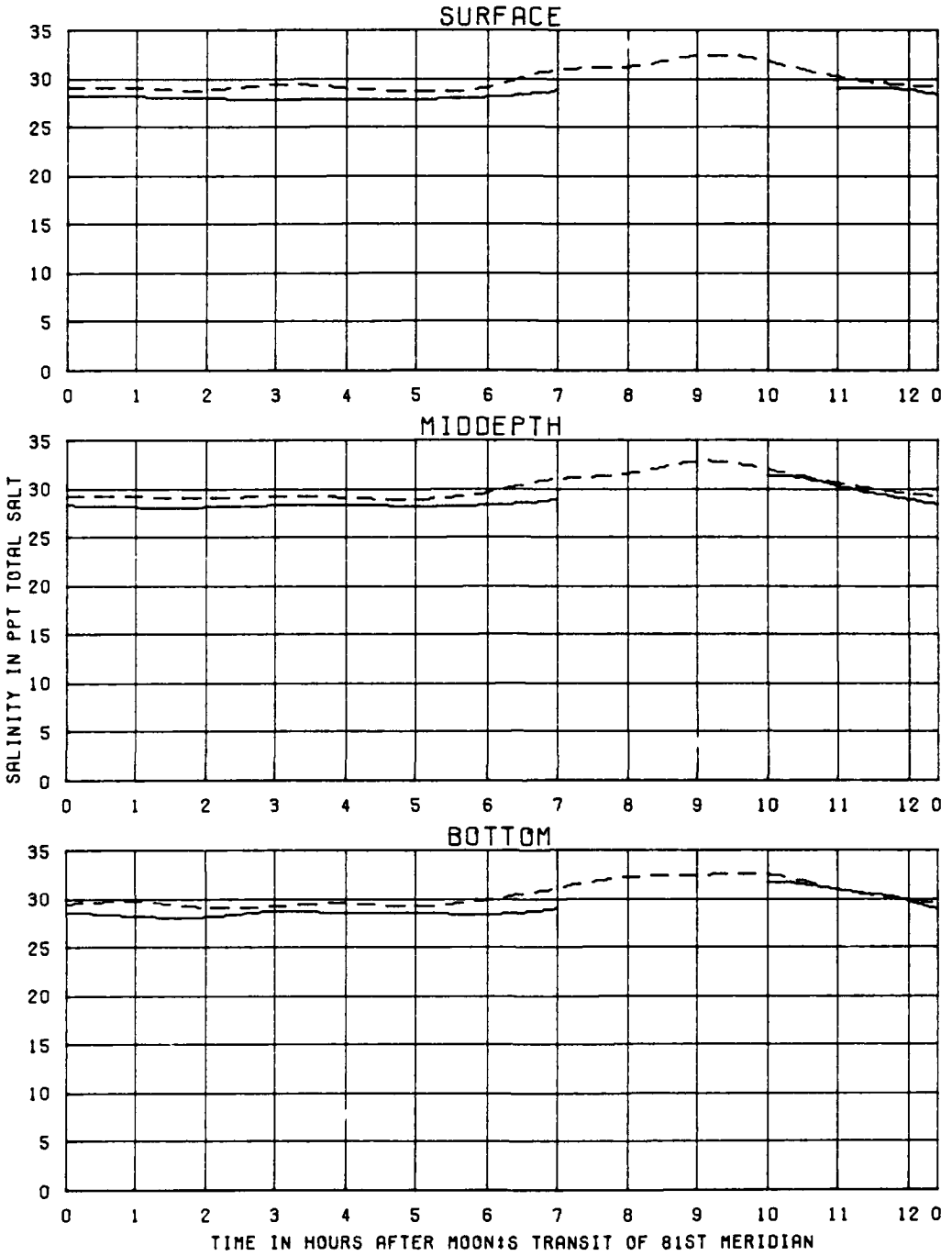

TEST CONDITIONS	
TIDE RANGE AT GAGE 1	6.2 FT
OCEAN SALINITY(TOTAL SALT)	32.5 PPT
FRESHWATER INFLOW	1100 CFS

LEGEND
PROTOTYPE ———
MODEL — — —

KINGS BAY MODEL

VERIFICATION OF SALINITIES FOR 11-12-82 TIDE

STATION
4A

PLATE B49

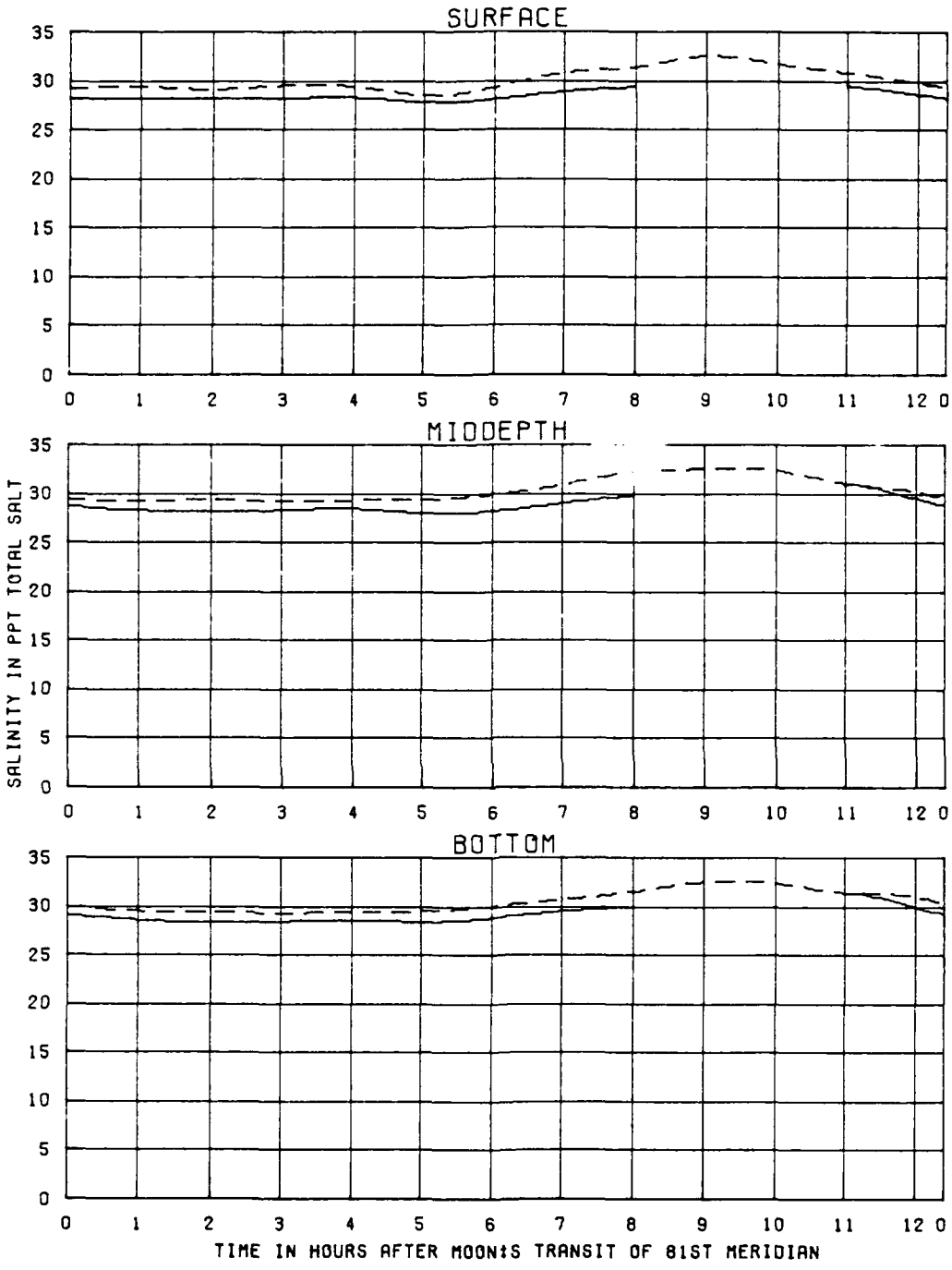

TEST CONDITIONS

TIDE RANGE AT GAGE 1	6.2 FT
OCEAN SALINITY(TOTAL SALT)	32.5 PPT
FRESHWATER INFLOW	1100 CFS

LEGEND
PROTOTYPE ———
MODEL — — —

KINGS BAY MODEL

VERIFICATION OF SALINITIES FOR 11-12-82 TIDE

STATION
48

PLATE B50

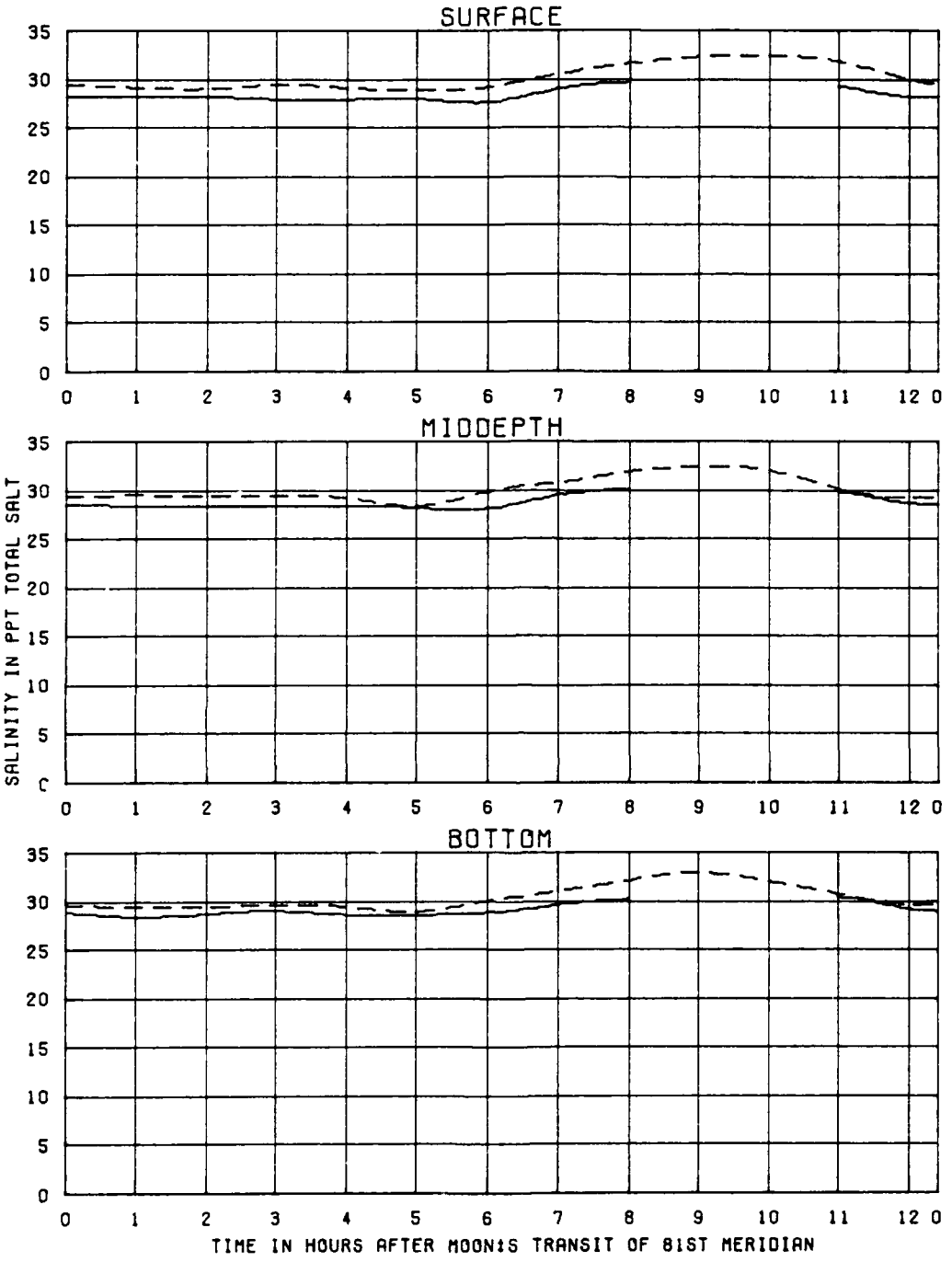

TEST CONDITIONS

TIDE RANGE AT GAGE 1	6.2 FT
OCEAN SALINITY(TOTAL SALT)	32.5 PPT
FRESHWATER INFLOW	1100 CFS

LEGEND
PROTOTYPE ———
MODEL — — —

KINGS BAY MODEL

VERIFICATION OF SALINITIES FOR 11-12-82 TIDE

STATION
4C

PLATE B51

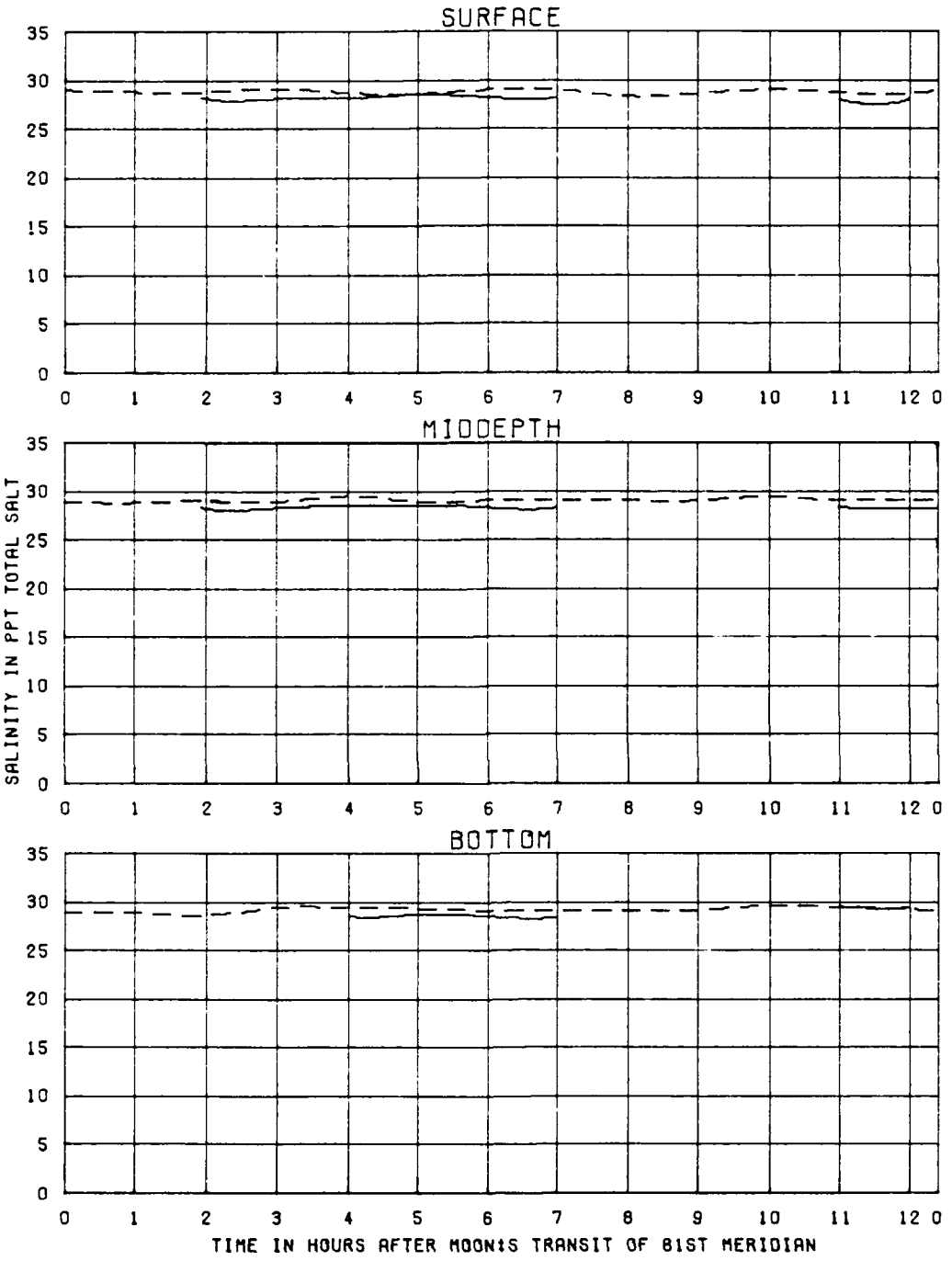

TEST CONDITIONS

TIDE RANGE AT GAGE 1	6.2 FT
OCEAN SALINITY(TOTAL SALT)	32.5 PPT
FRESHWATER INFLOW	1100 CFS

LEGEND
PROTOTYPE ———
MODEL — — —

KINGS BAY MODEL

VERIFICATION OF SALINITIES FOR 11-12-82 TIDE

STATION 5A

PLATE B52

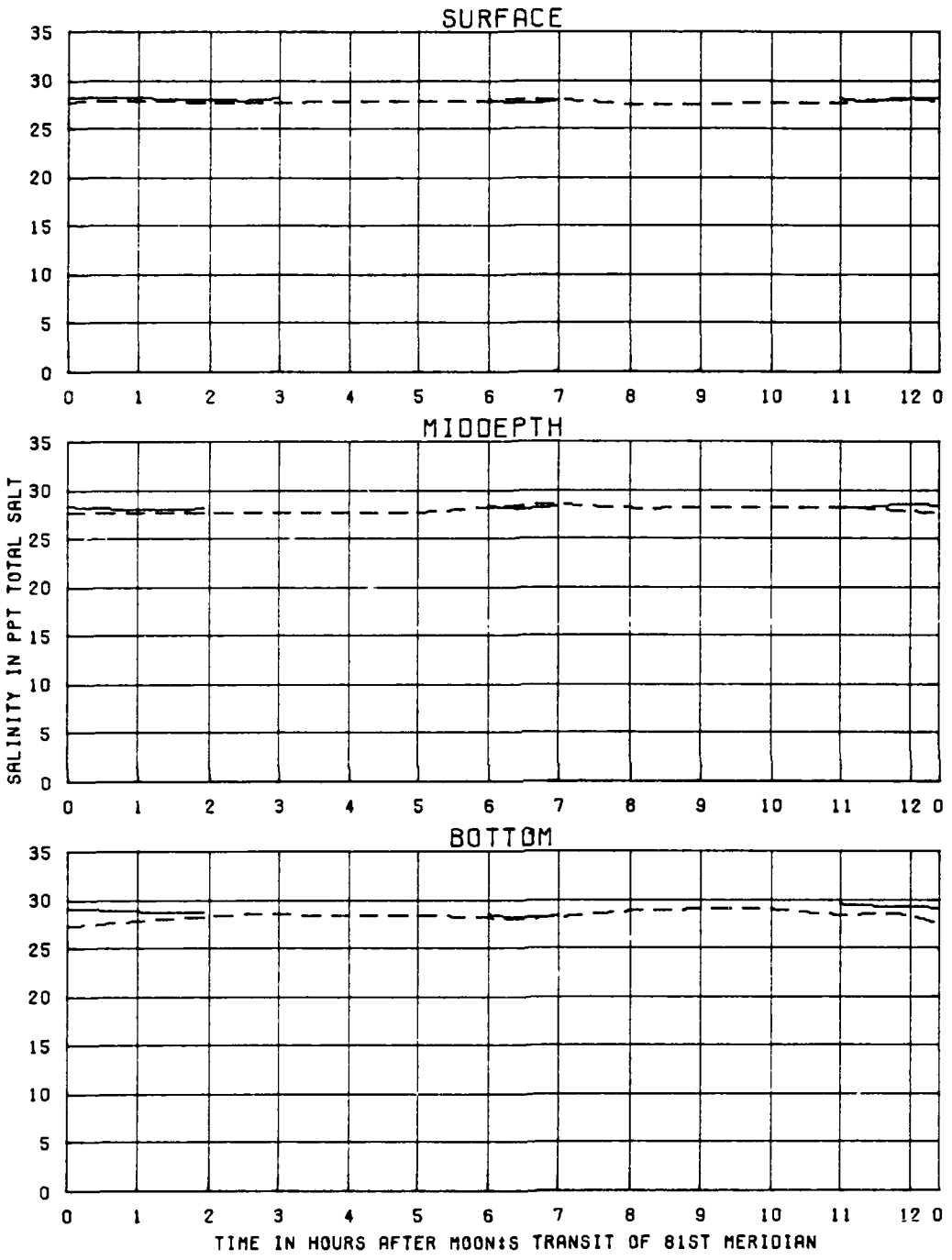

TEST CONDITIONS

TIDE RANGE AT GAGE 1	6.2 FT
OCEAN SALINITY(TOTAL SALT)	32.5 PPT
FRESHWATER INFLOW	1100 CFS

LEGEND

PROTOTYPE ———

MODEL — — —

KINGS BAY MODEL

VERIFICATION OF SALINITIES FOR 11-12-82 TIDE

STATION 58

PLATE B53

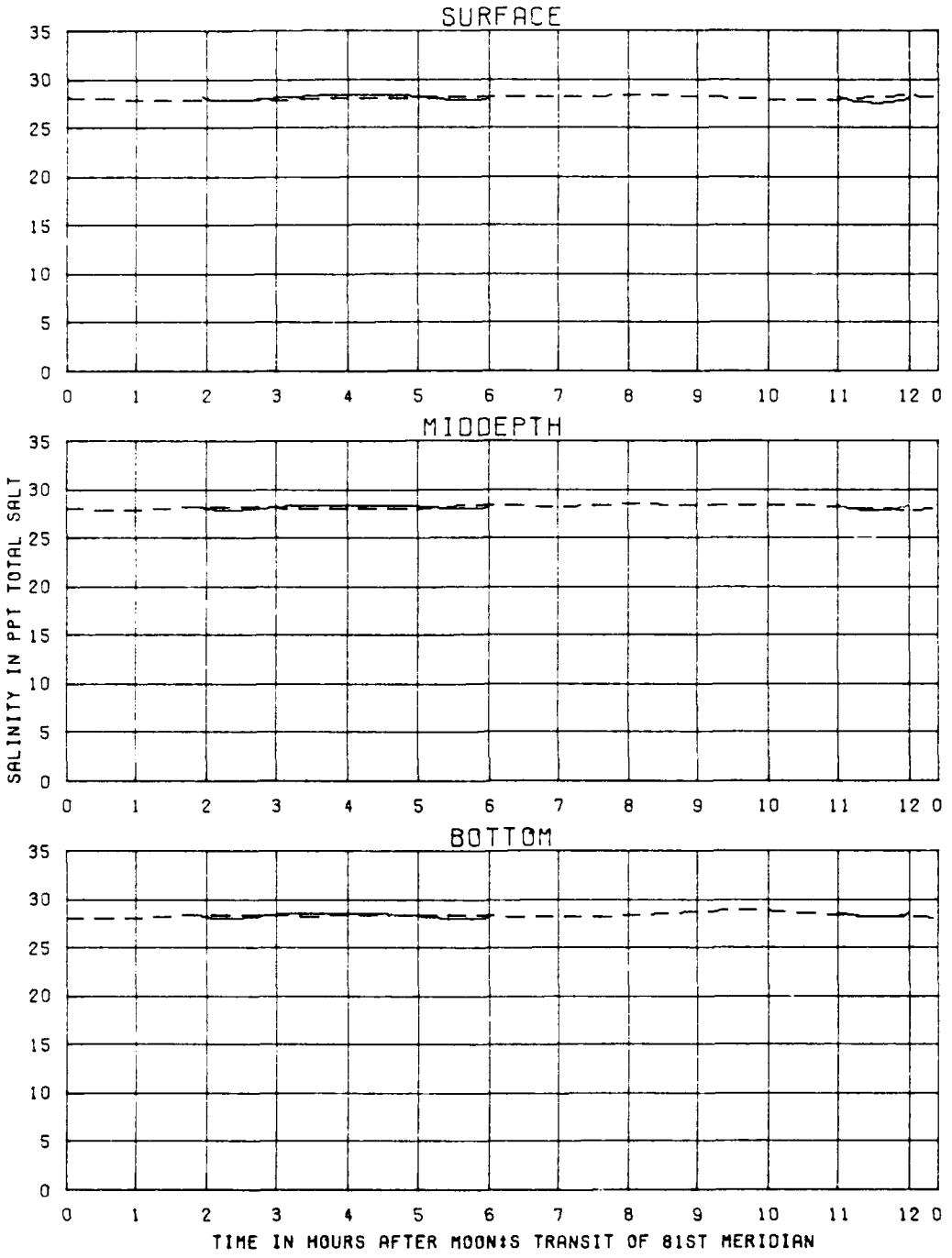

TEST CONDITIONS	
TIDE RANGE AT GAGE 1	6.2 FT
OCEAN SALINITY(TOTAL SALT)	32.5 PPT
FRESHWATER INFLOW	1100 CFS

LEGEND
PROTOTYPE ———
MODEL — — —

KINGS BAY MODEL

VERIFICATION OF SALINITIES FOR 11-12-82 TIDE

STATION
5C

PLATE B54

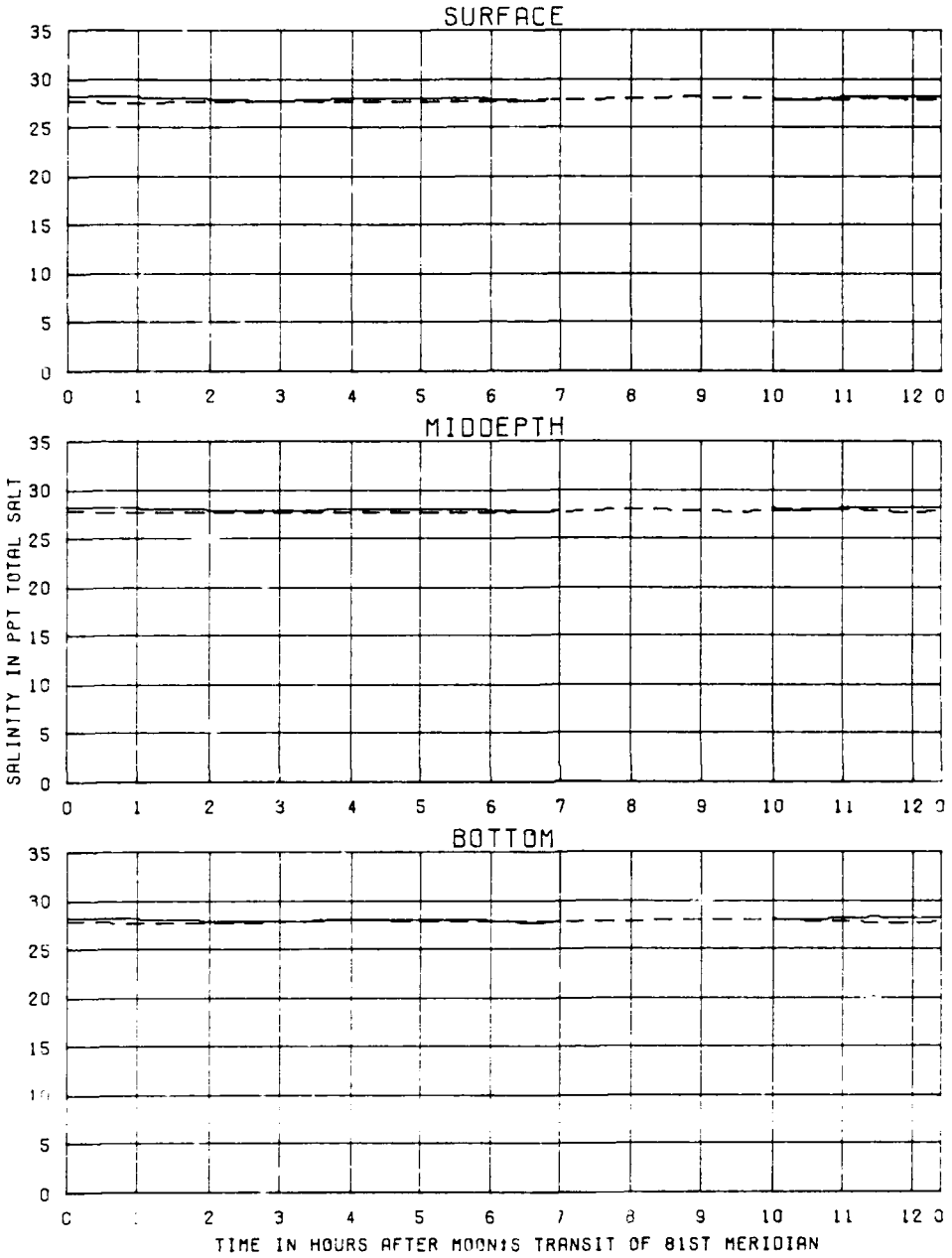

TEST CONDITIONS

TIDE RANGE AT GAGE 1	6.2 FT
OCEAN SALINITY(TOTAL SALT)	32.5 PPT
FRESHWATER INFLOW	1100 CFS

LEGEND

PROTOTYPE ———

MODEL — — —

KINGS BAY MODEL

VERIFICATION OF SALINITIES FOR 11-12-82 TIDE

STATION 6A

PLATE B55

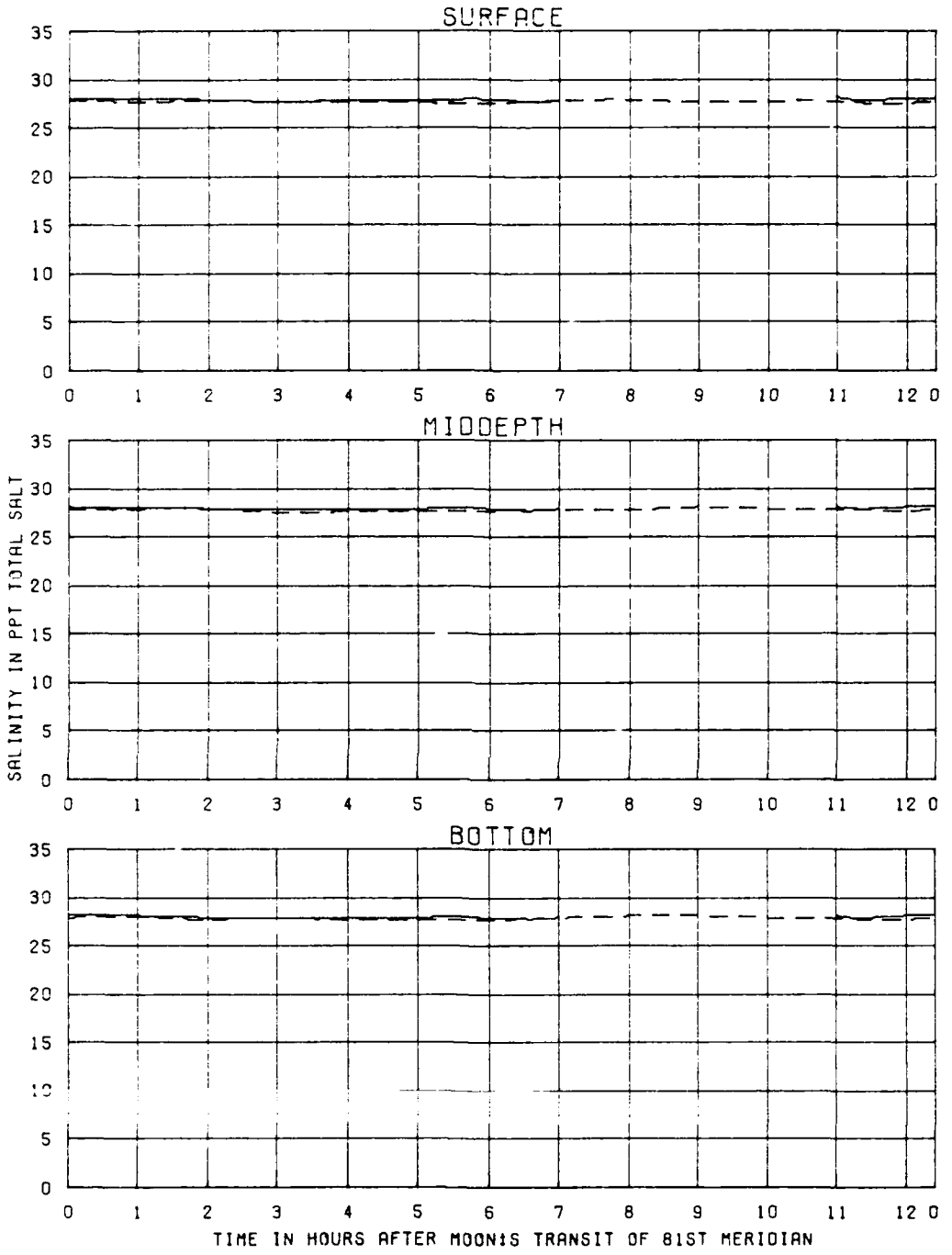

TEST CONDITIONS

TIDE RANGE AT GAGE 1	6.2 FT
OCEAN SALINITY(TOTAL SALT)	32.5 PPT
FRESHWATER INFLOW	1100 CFS

KINGS BAY MODEL

VERIFICATION OF SALINITIES FOR 11-12-82 TIDE

STATION 68

LEGEND
PROTOTYPE ———
MODEL — — —

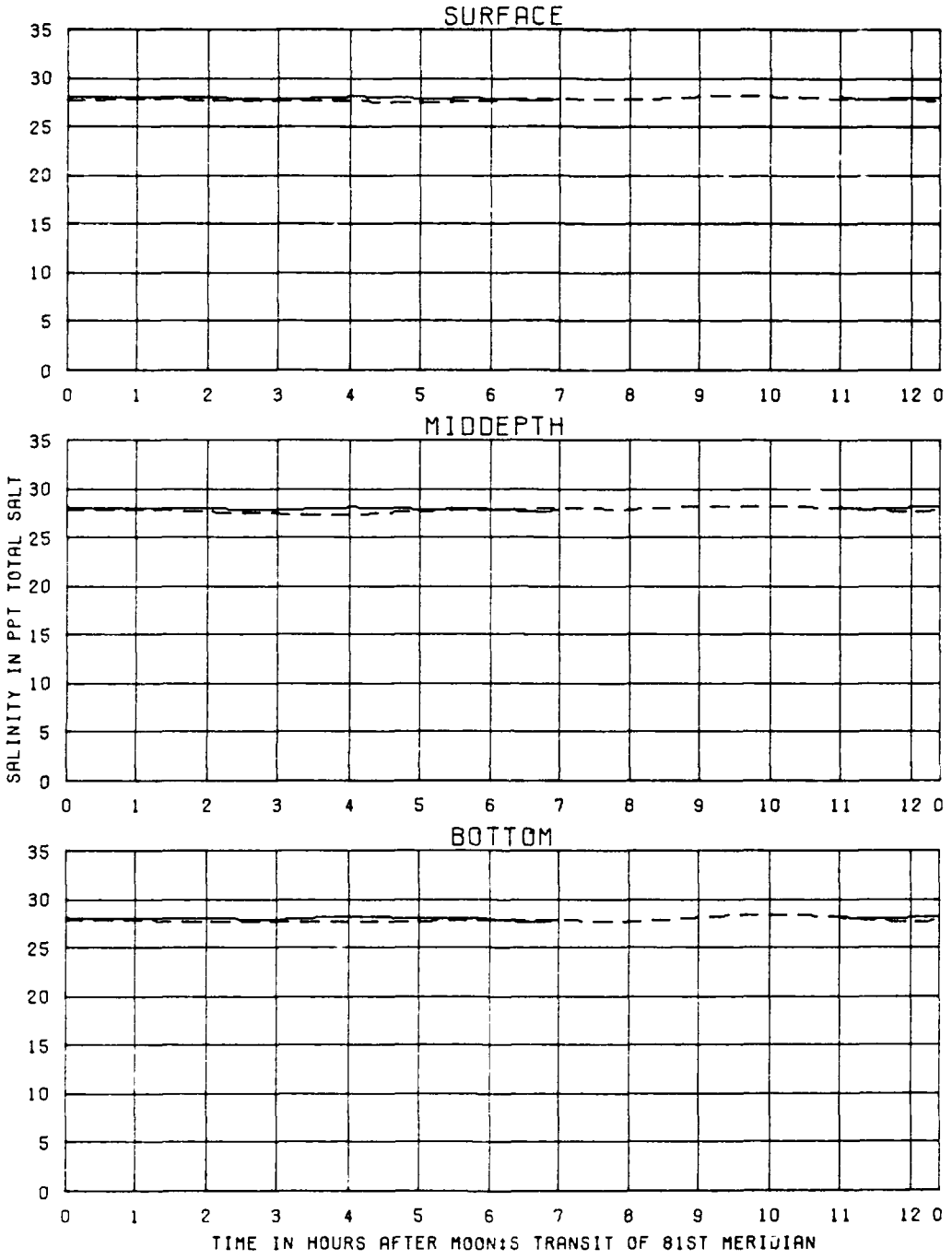

TEST CONDITIONS

TIDE RANGE AT GAGE 1	6.2 FT
OCEAN SALINITY(TOTAL SALT)	32.5 PPT
FRESHWATER INFLOW	1100 CFS

LEGEND
PROTOTYPE ———
MODEL — — —

KINGS BAY MODEL

VERIFICATION OF SALINITIES FOR 11-12-82 TIDE

STATION
6C

APPENDIX C: PHYSICAL MODEL TRANSITIONAL CHANNEL VERIFICATION

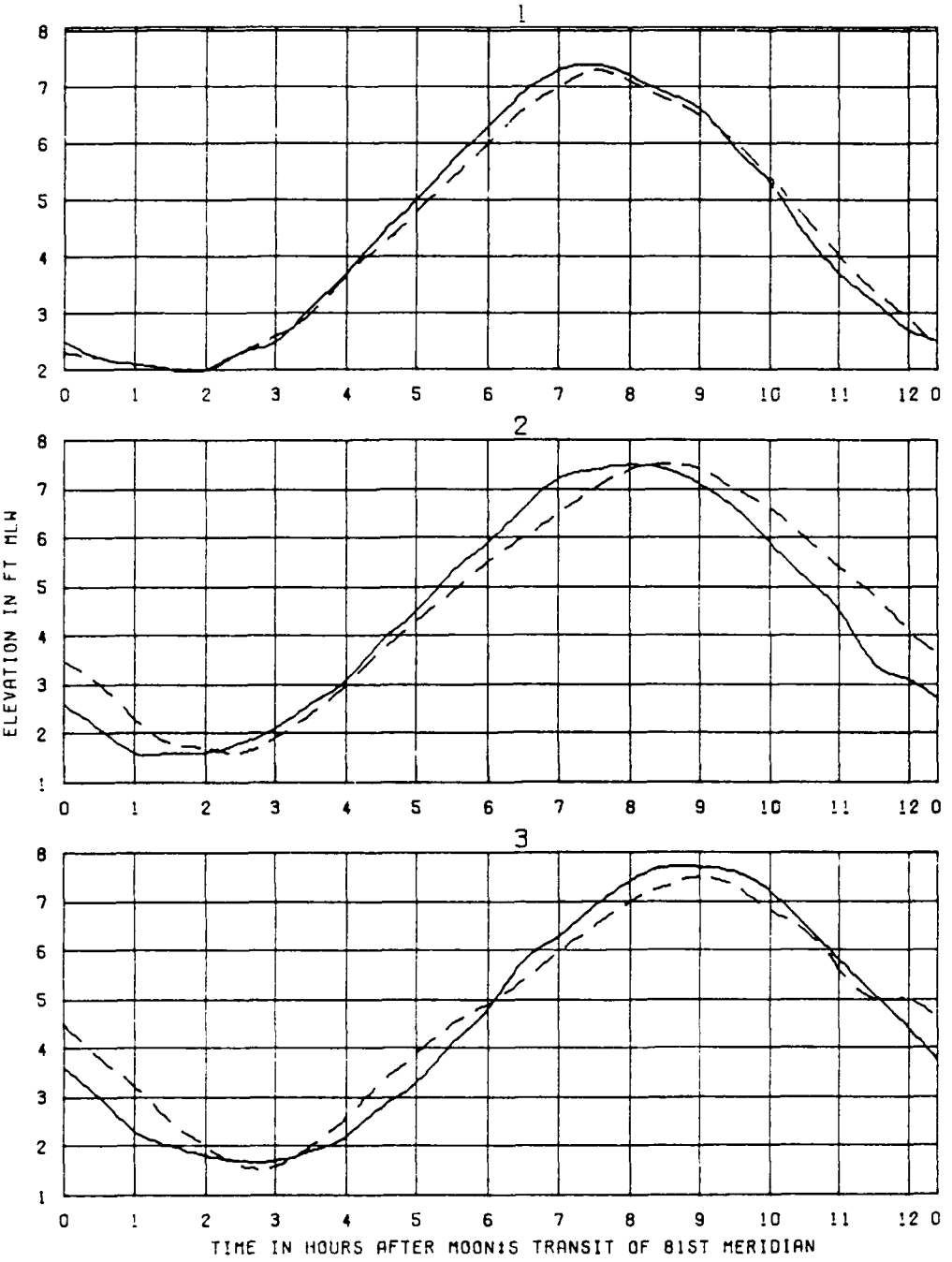

TEST CONDITIONS

TIDAL RANGE AT SOUTH JETTY	5.3 FT
OCEAN SALINITY(TOTAL SALT)	32.5 PPT
FRESHWATER INFLOW	1100 CFS

LEGEND
PROTOTYPE ———
MODEL — — —

KINGS BAY MODEL

VERIFICATION OF TIDAL HEIGHTS FOR JAN 1985 TIDE

STATIONS
1, 2, AND 3

PLATE C1

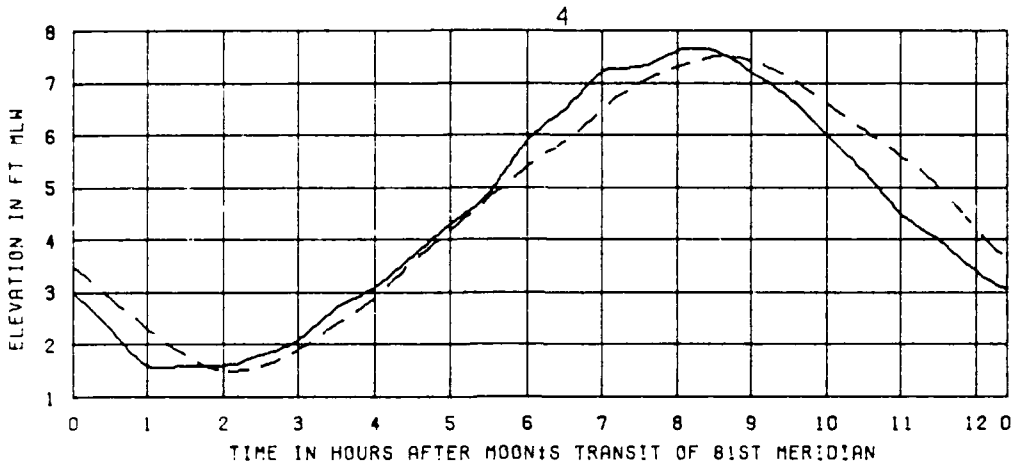

TEST CONDITIONS	
TIDAL RANGE AT SOUTH JETTY	5.3 FT
OCEAN SALINITY(TOTAL SALT)	32.5 PPT
FRESHWATER INFLOW	1100 CFS

LEGEND
PROTOTYPE ——
MODEL — — —

KINGS BAY MODEL

VERIFICATION OF
TIDAL HEIGHTS
FOR JAN 1985 TIDE
STATION
4

PLATE C2

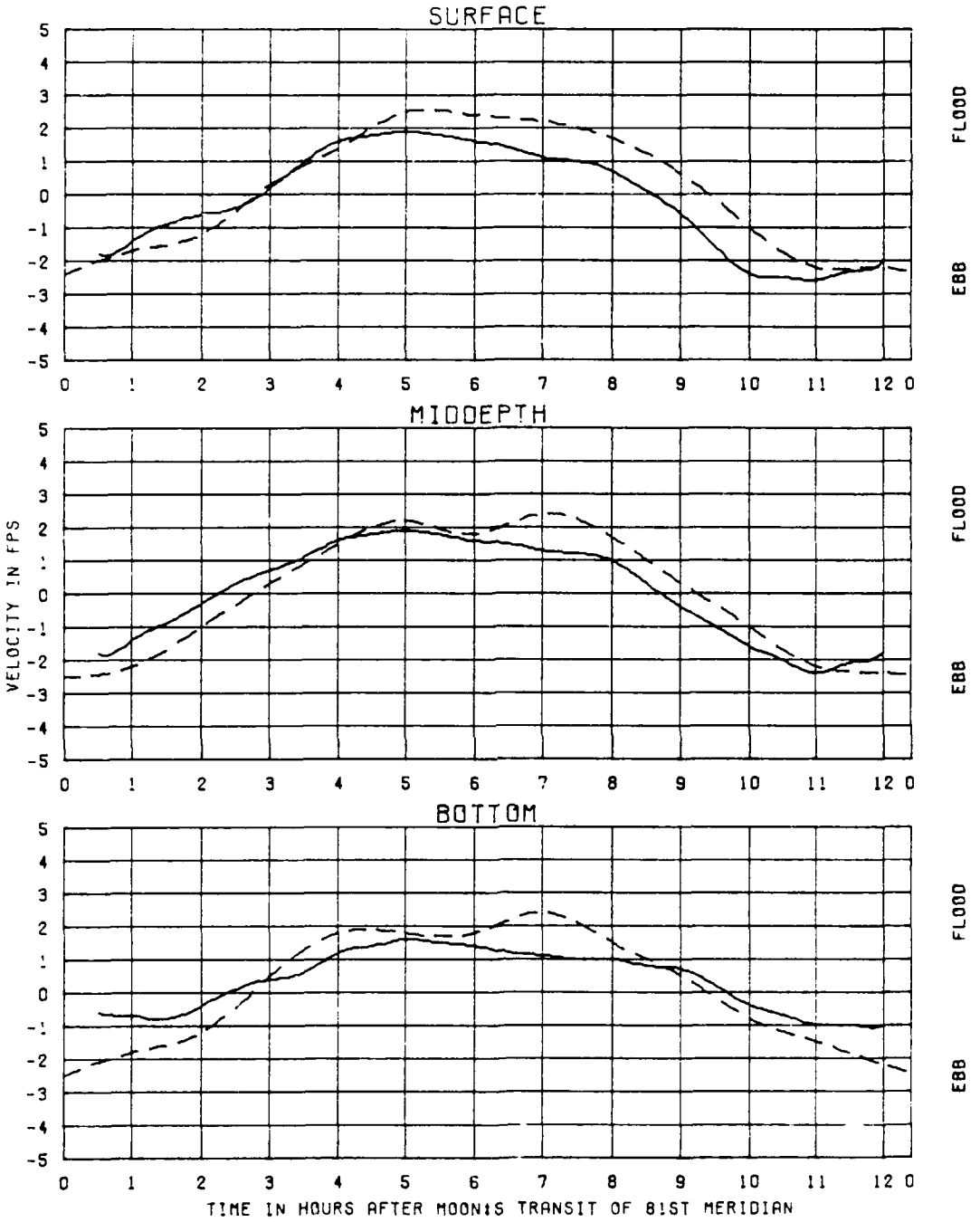

TEST CONDITIONS

TIDAL RANGE AT SOUTH JETTY	5.3 FT
OCEAN SALINITY(TOTAL SALT)	32.5 PPT
FRESHWATER INFLOW	1100 CFS

LEGEND
PROTOTYPE ———
MODEL — — — —

KINGS BAY MODEL

VERIFICATION OF VELOCITIES FOR JAN. 1985 TIDE
STATION 1A

PLATE 3

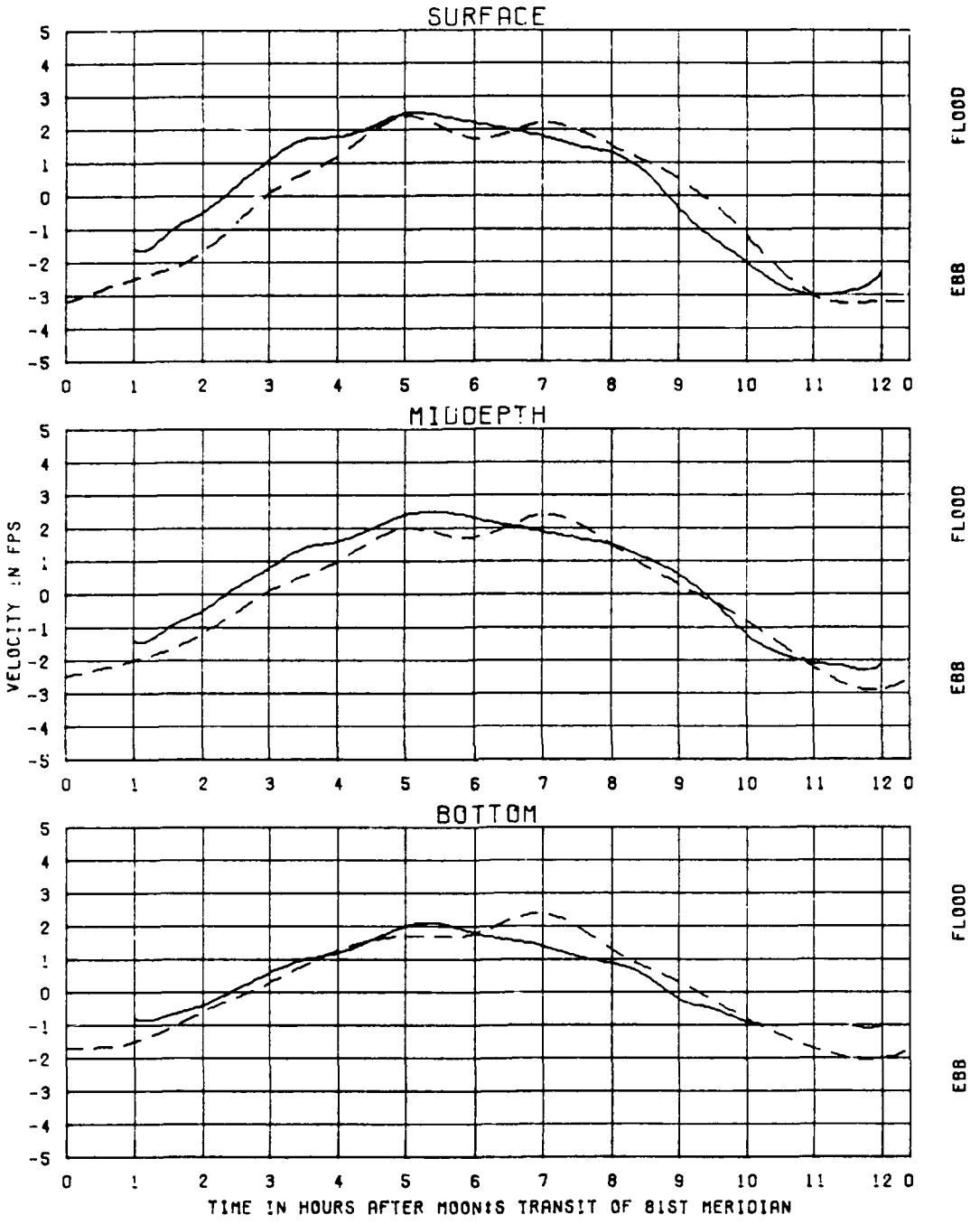

TEST CONDITIONS

TIDAL RANGE AT SOUTH JETTY	5.3 FT
OCEAN SALINITY(TOTAL SALT)	32.5 PPT
FRESHWATER INFLOW	1100 CFS

LEGEND
PROTOTYPE ———
MODEL — — —

KINGS BAY MODEL

VERIFICATION OF VELOCITIES FOR JAN 1985 TIDE
STATION 18

PLATE C4

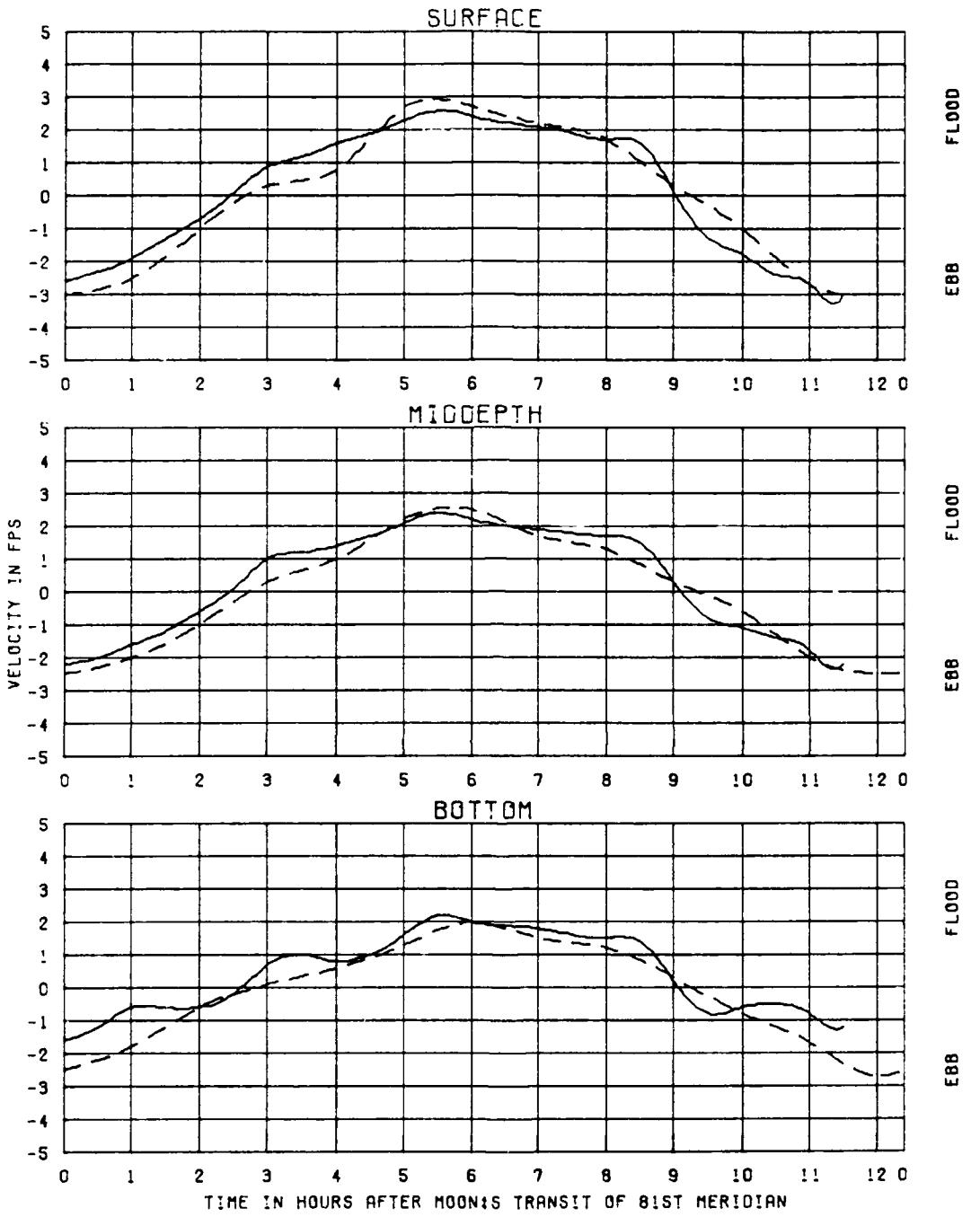

TEST CONDITIONS

TIDAL RANGE AT SOUTH JETTY	5.3 FT
OCEAN SALINITY(TOTAL SALT)	32.5 PPT
FRESHWATER INFLOW	1100 CFS

LEGEND
PROTOTYPE ———
MODEL — — —

KINGS BAY MODEL

VERIFICATION OF
VELOCITIES
FOR JAN 1985 TIDE
STATION
1C

PLATE C5

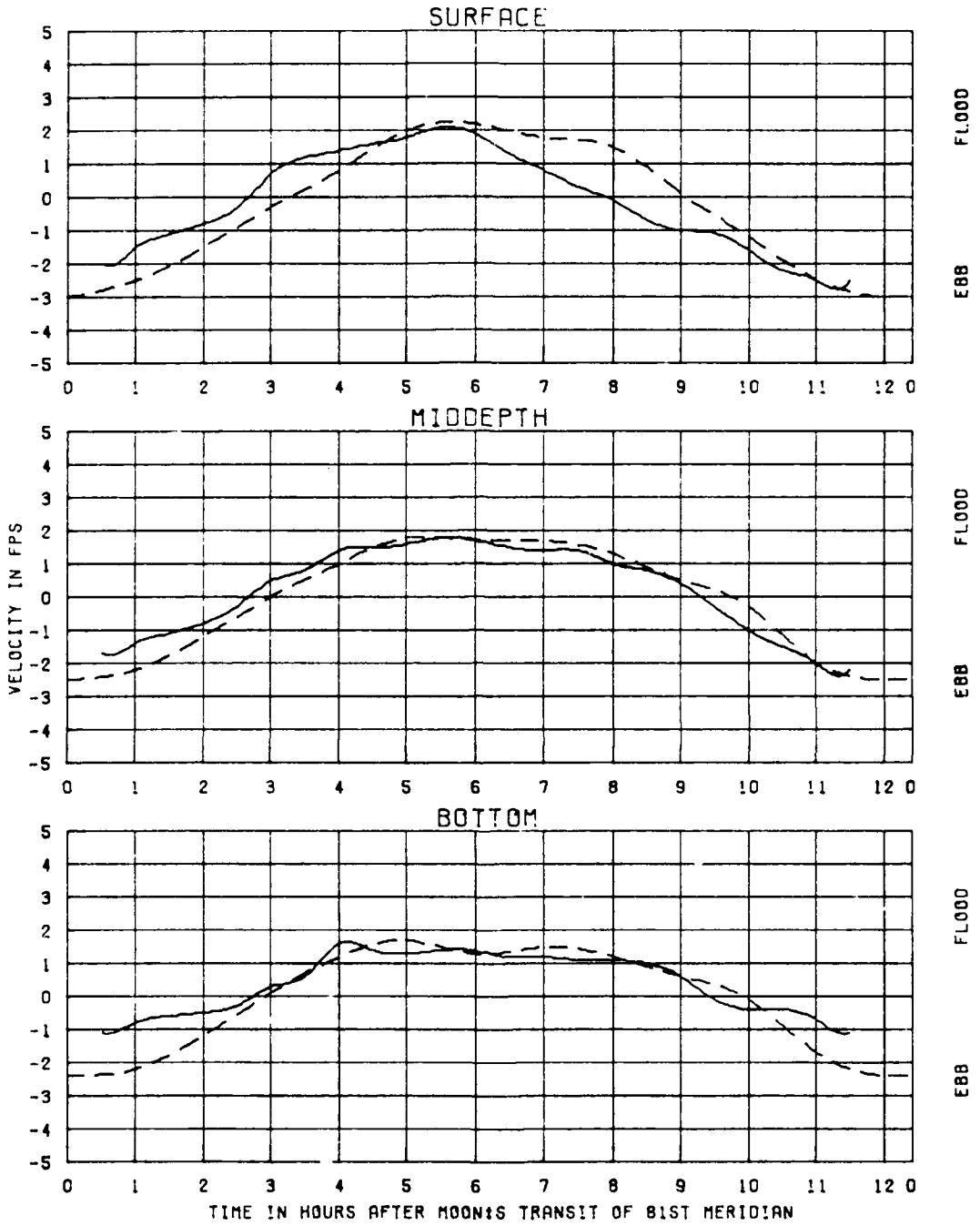

TEST CONDITIONS

TIDAL RANGE AT SOUTH JETTY	5.3 FT
OCEAN SALINITY(TOTAL SALT)	32.5 PPT
FRESHWATER INFLOW	1100 CFS

LEGEND
PROTOTYPE ———
MODEL — — —

KINGS BAY MODEL

VERIFICATION OF VELOCITIES FOR JAN 1985 TIDE

STATION
10

PLATE C6

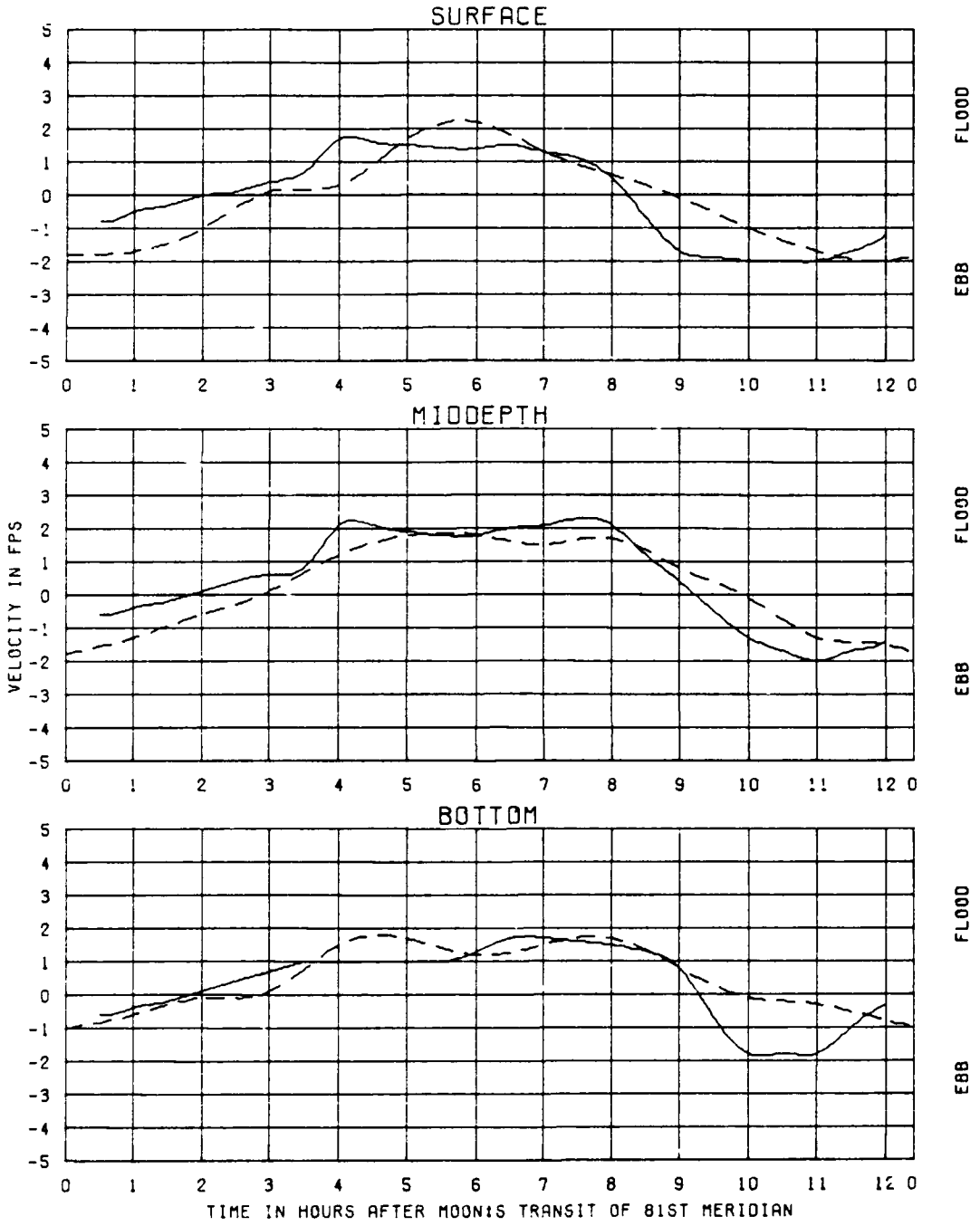

TEST CONDITIONS

TIDAL RANGE AT SOUTH JETTY	5.3 FT
OCEAN SALINITY(TOTAL SALT)	32.5 PPT
FRESHWATER INFLOW	1100 CFS

LEGEND
PROTOTYPE ———
MODEL — — —

KINGS BAY MODEL

VERIFICATION OF VELOCITIES FOR JAN 1985

STATION
2A

PLATE C7

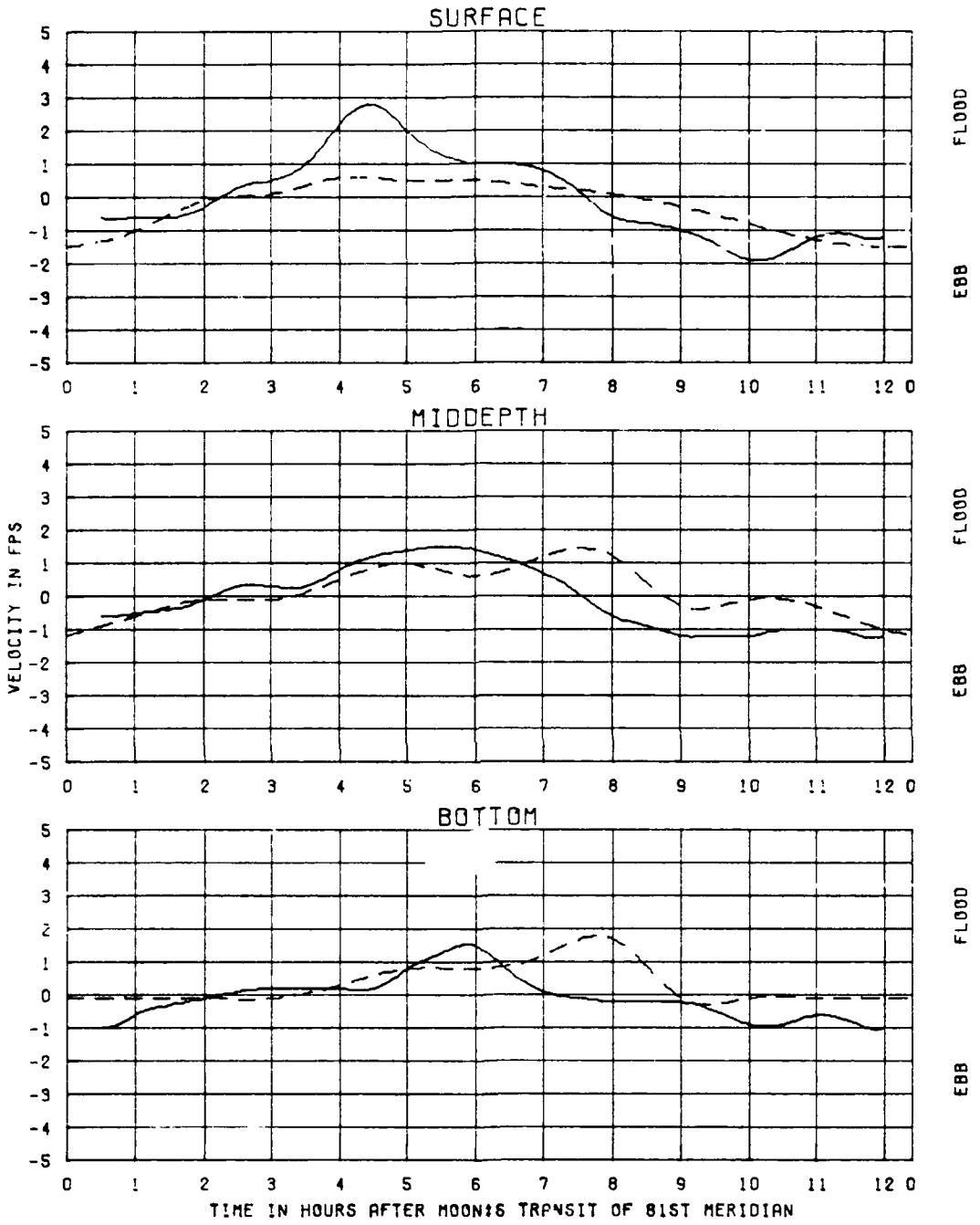

TEST CONDITIONS	
TIDAL RANGE AT SOUTH JETTY	5.3 FT
OCEAN SALINITY(TOTAL SALT)	32.5 PPT
FRESHWATER INFLOW	1100 CFS

LEGEND
PROTOTYPE ———
MODEL — — —

KINGS BAY MODEL

VERIFICATION OF
VELOCITIES
FOR JAN 1985 TIDE
STATION
28

PLATE C8

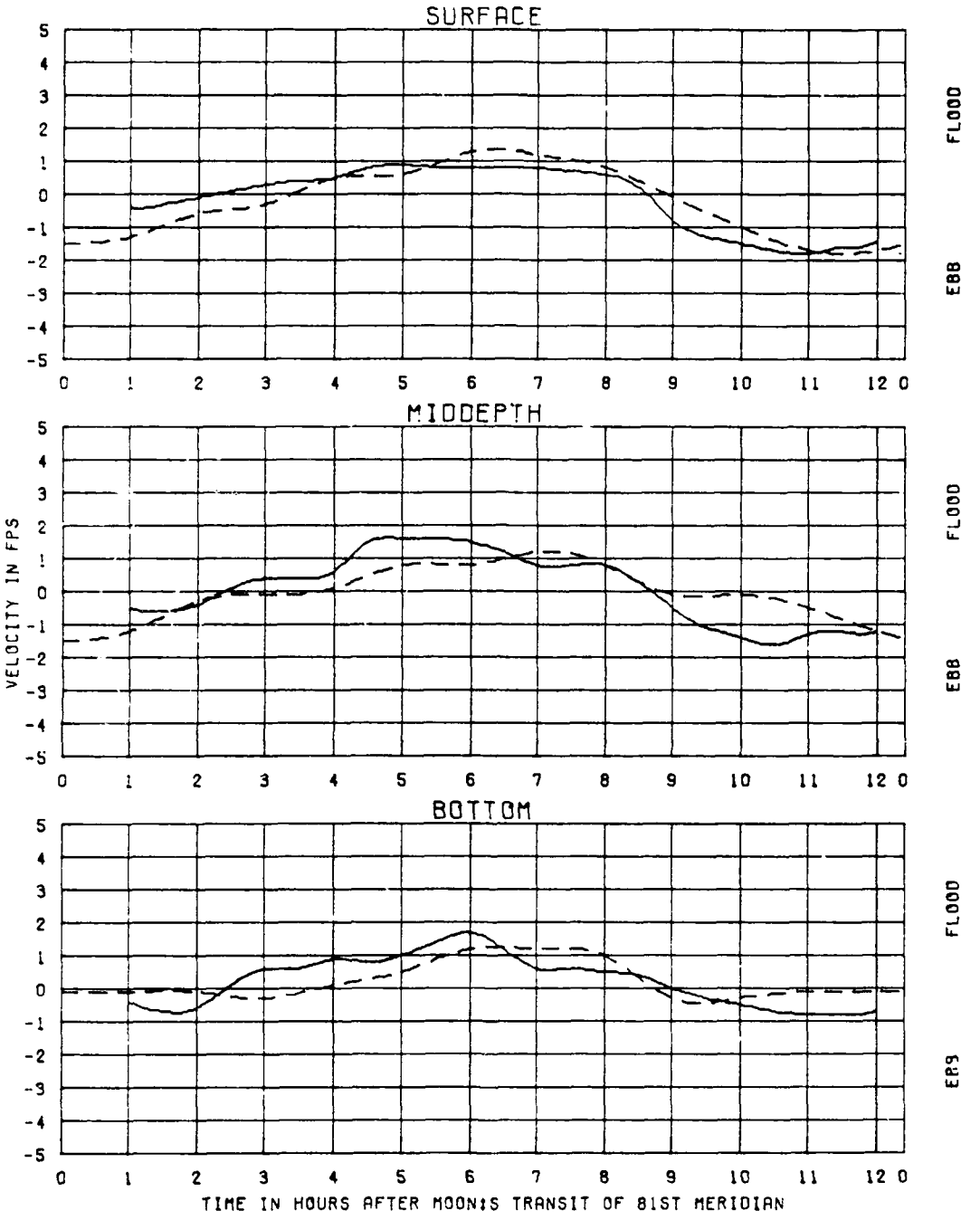

TEST CONDITIONS

TIDAL RANGE AT SOUTH JETTY	5.9 FT
OCEAN SALINITY(TOTAL SALT)	32.5 PPT
FRESHWATER INFLOW	1100 CFS

LEGEND
PROTOTYPE ——
MODEL — — —

KINGS BAY MODEL

VERIFICATION OF VELOCITIES FOR JAN 1985 TIDE

STATION
2C

PLATE C9

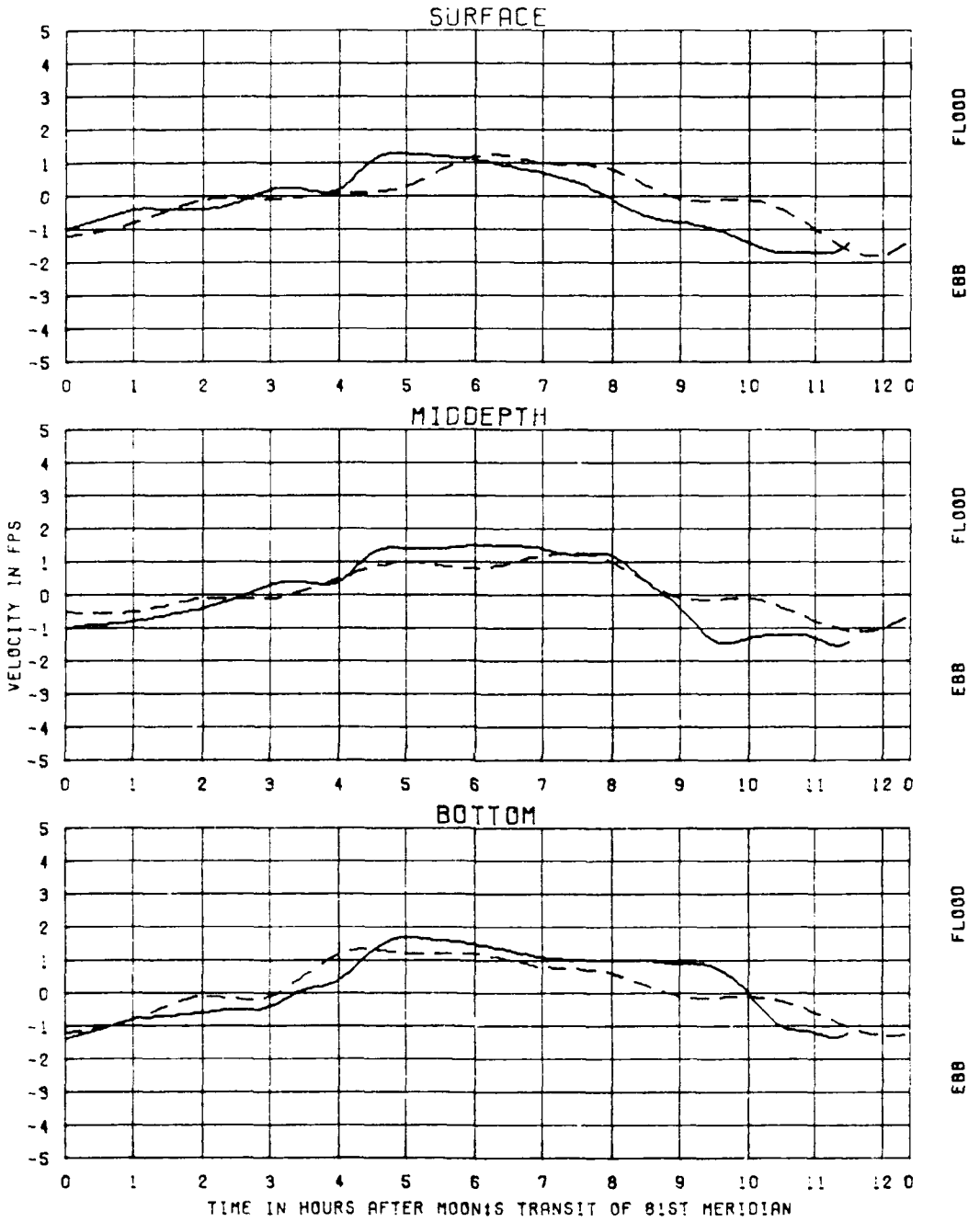

TEST CONDITIONS

TIDAL RANGE AT SOUTH JETTY	5.9 FT
OCEAN SALINITY(TOTAL SALT)	32.5 PPT
FRESHWATER INFLOW	1100 CFS

LEGEND
PROTOTYPE ———
MODEL — — —

KINGS BAY MODEL

VERIFICATION OF VELOCITIES FOR JAN 1985 TIDE

STATION
2D

PLATE C10

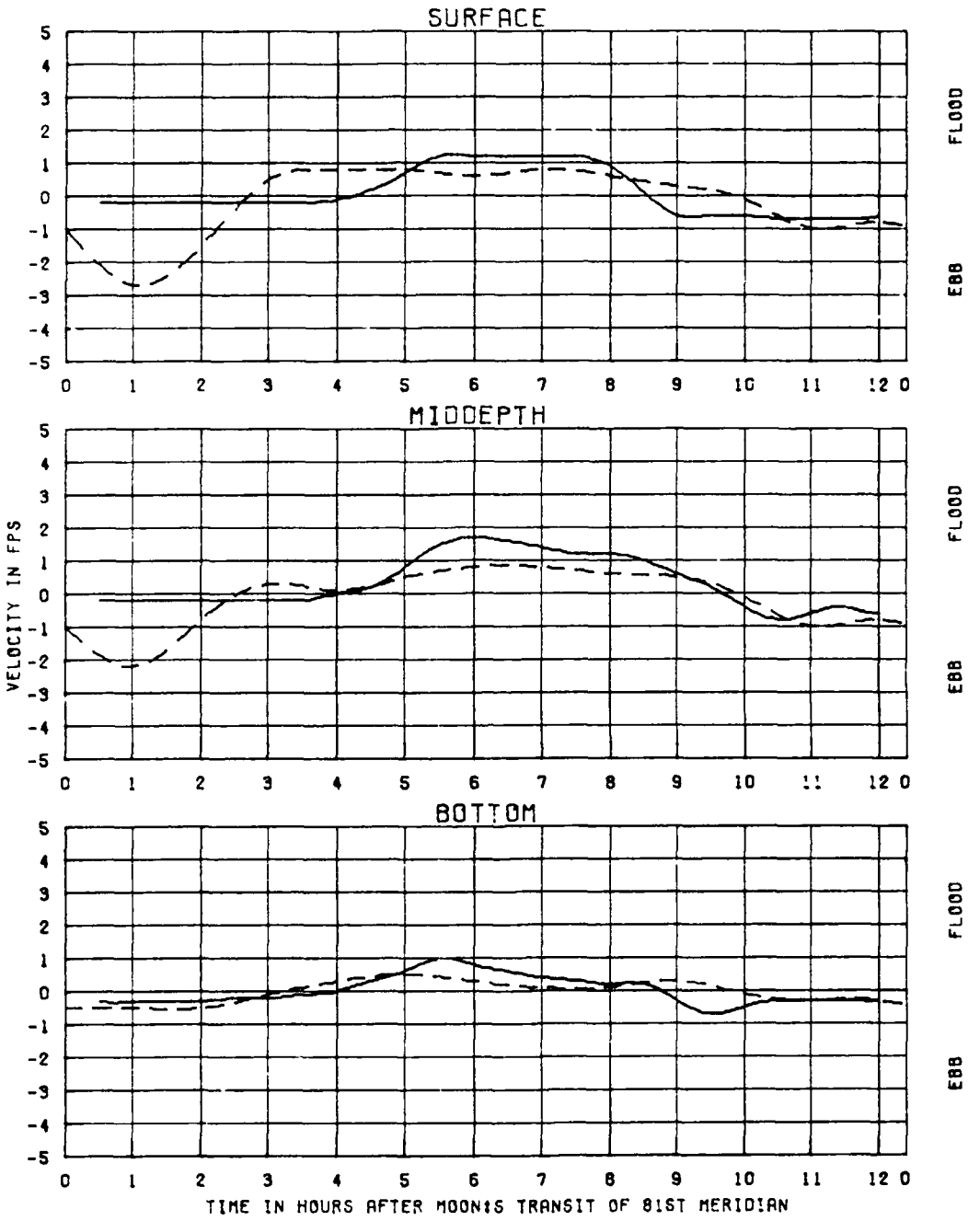

TEST CONDITIONS

TIDAL RANGE AT SOUTH JETTY	5.9 FT
OCEAN SALINITY(TOTAL SALT)	32.5 PPT
FRESHWATER INFLOW	1100 CFS

LEGEND
PROTOTYPE ———
MODEL — — —

KINGS BAY MODEL

VERIFICATION OF VELOCITIES FOR JAN 1985 TIDE

STATION
3A

PLATE C11

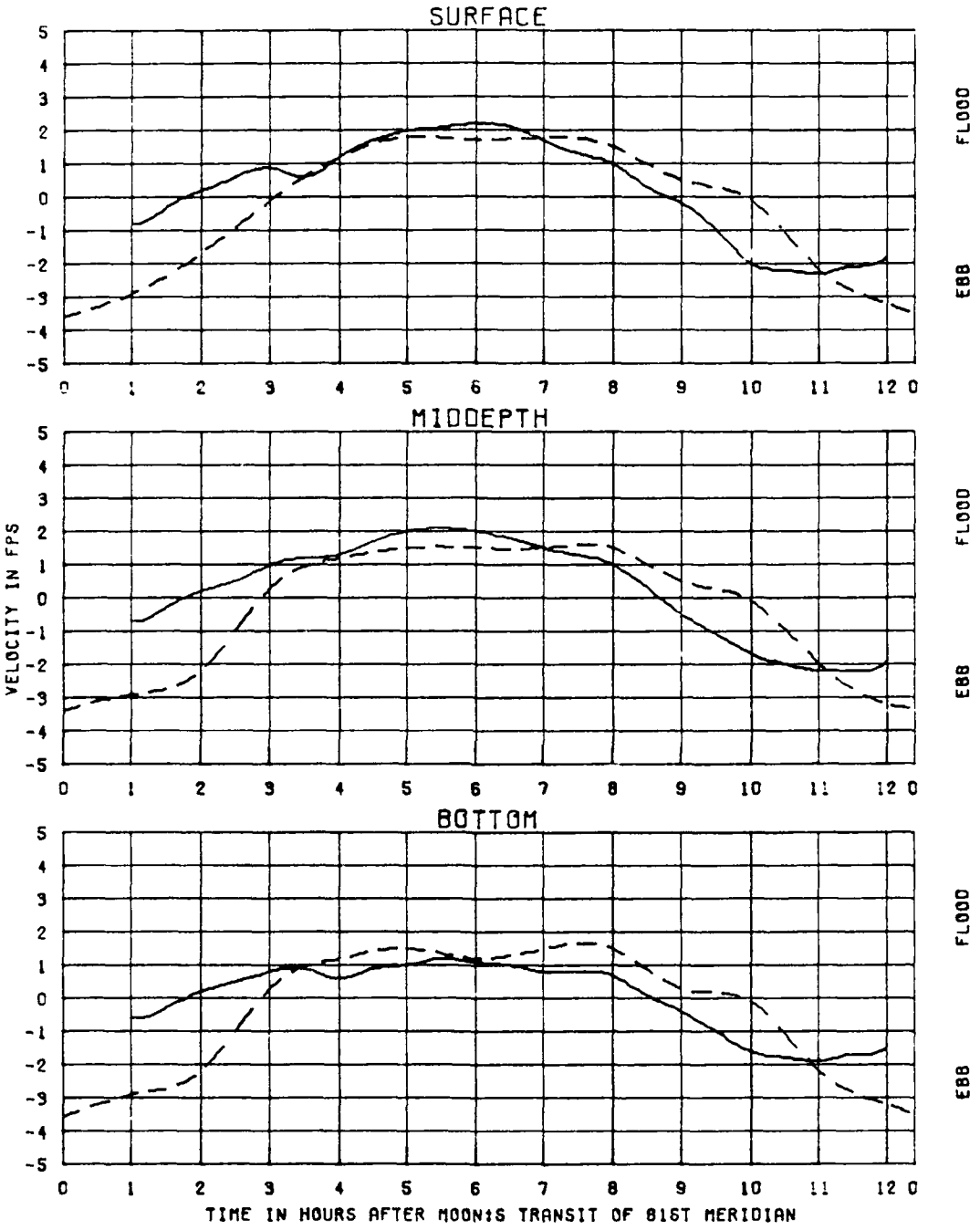

TEST CONDITIONS

TIDAL RANGE AT SOUTH JETTY	5.9 FT
OCEAN SALINITY(TOTAL SALT)	32.5 PPT
FRESHWATER INFLOW	1100 CFS

LEGEND

PROTOTYPE ———

MODEL — — —

KINGS BAY MODEL

VERIFICATION OF VELOCITIES FOR JAN 1985 TIDE

STATION 99

PLATE C12

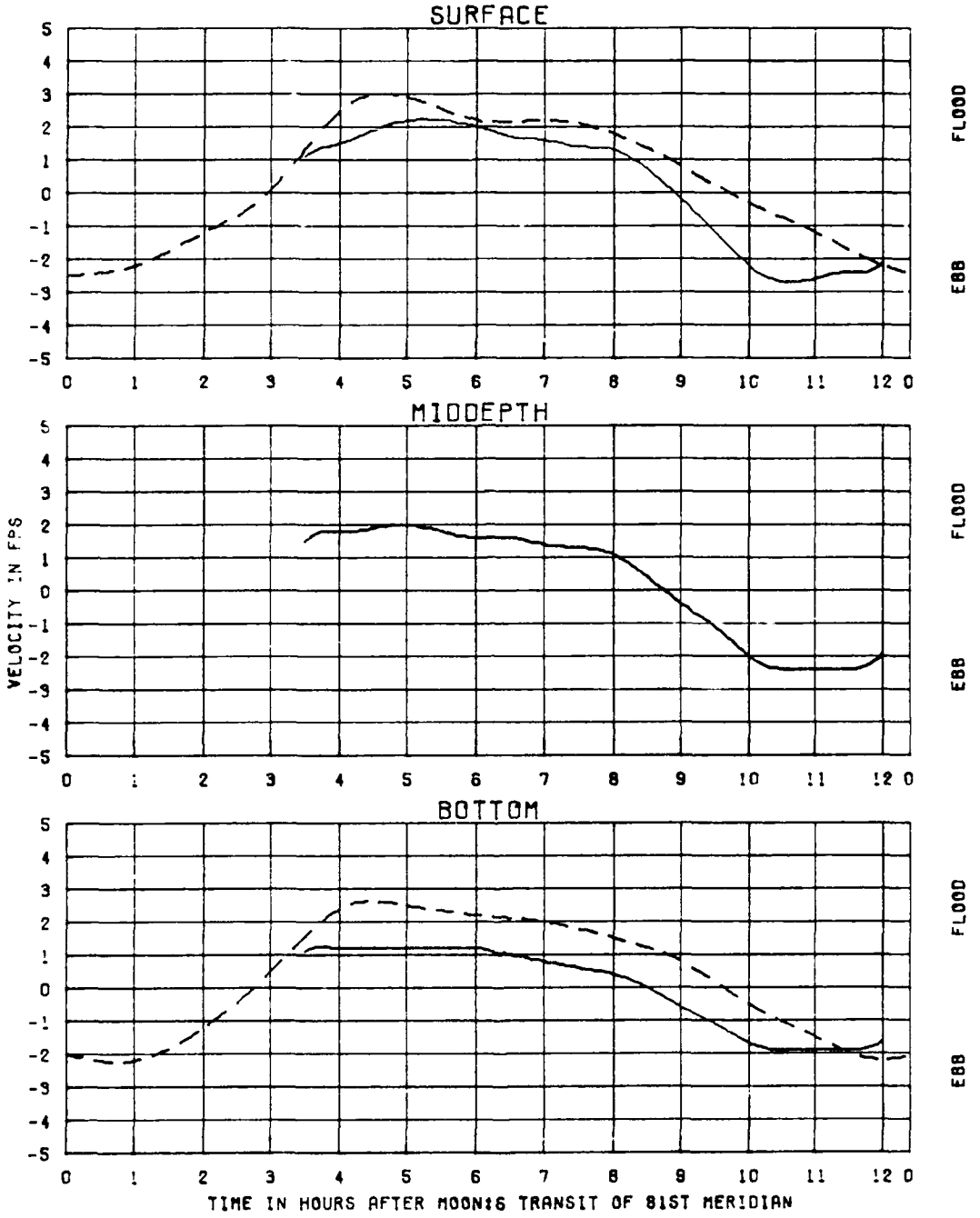

TEST CONDITIONS

TIDAL RANGE AT SOUTH JETTY	5.3 FT
OCEAN SALINITY(TOTAL SALT)	32.5 PPT
FRESHWATER INFLOW	1100 CFS

LEGEND
PROTOTYPE ———
MODEL — — —

KINGS BAY MODEL

VERIFICATION OF VELOCITIES FOR JAN 1985 TIDE

STATION
3C

PLATE C13

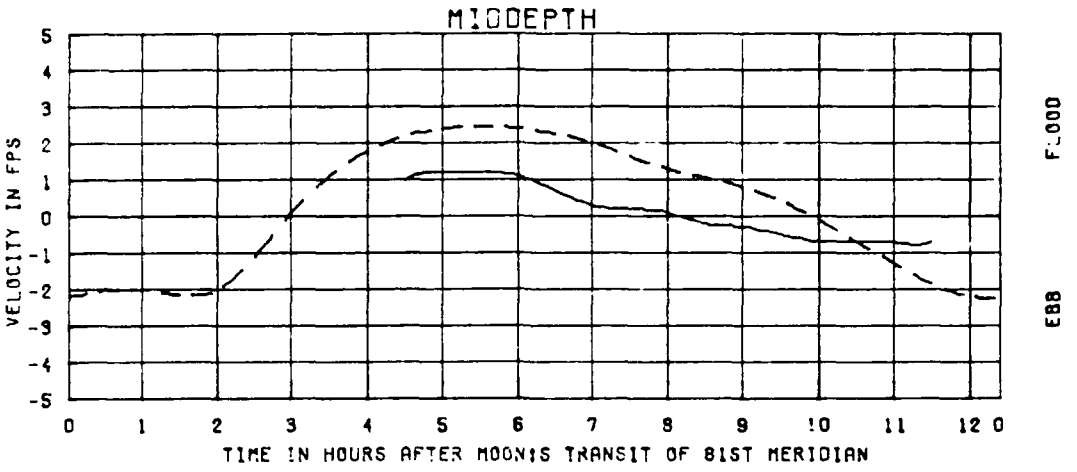

TEST CONDITIONS

TIDAL RANGE AT SOUTH JETTY	5.9 FT
OCEAN SALINITY(TOTAL SALT)	32.5 PPT
FRESHWATER INFLOW	1100 CFS

LEGEND
PROTOTYPE ———
MODEL — — —

KINGS BAY MODEL

VERIFICATION OF
VELOCITIES
FOR JAN 1985 TIDE
STATION
3D

PLATE C14

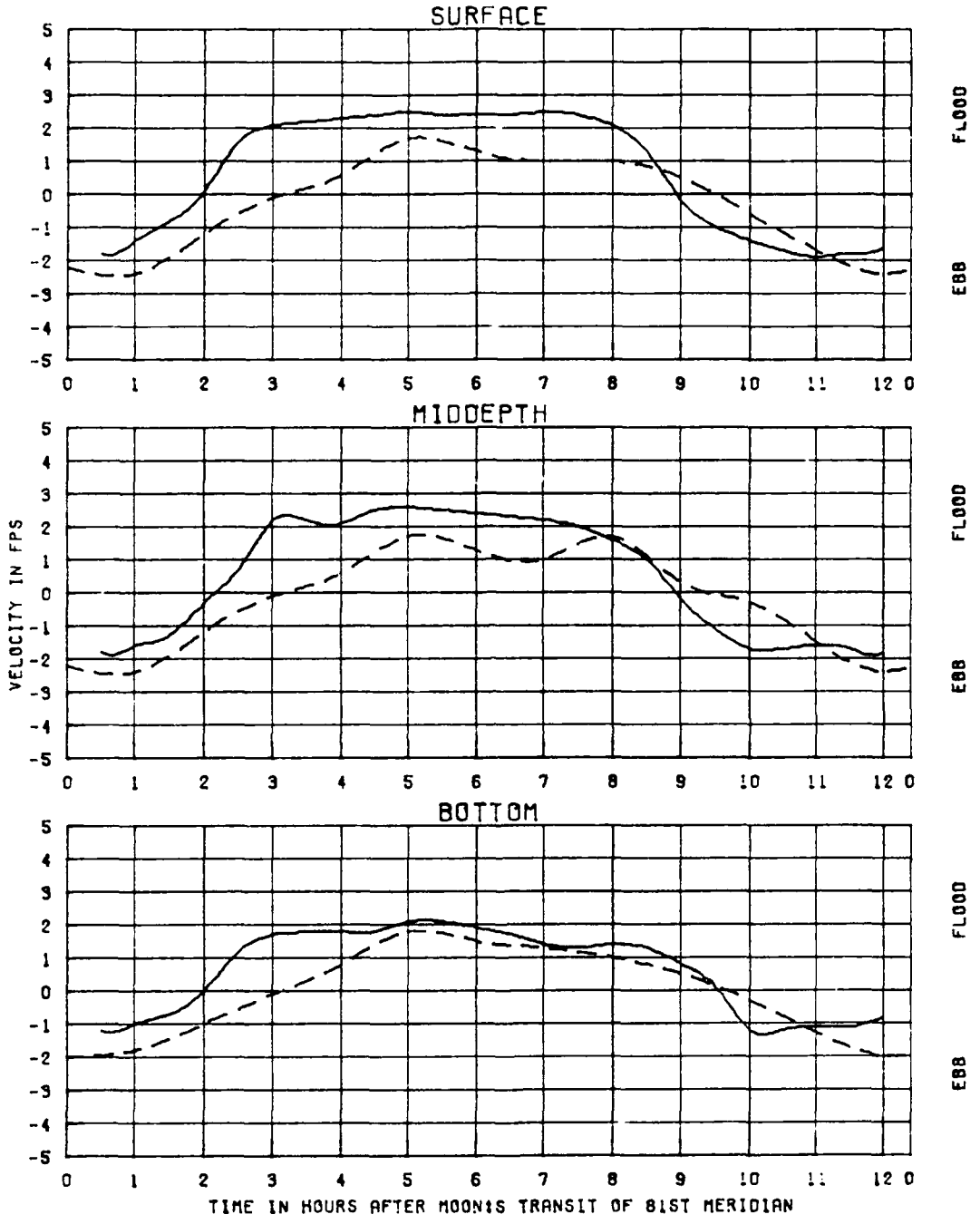

TEST CONDITIONS

TIDAL RANGE AT SOUTH JETTY	5.9 FT
OCEAN SALINITY(TOTAL SALT)	32.5 PPT
FRESHWATER INFLOW	1100 CFS

KINGS BAY MODEL

VERIFICATION OF VELOCITIES FOR JAN 1985 TIDE

STATION 4A

LEGEND
PROTOTYPE ———
MODEL — — —

PLATE C15

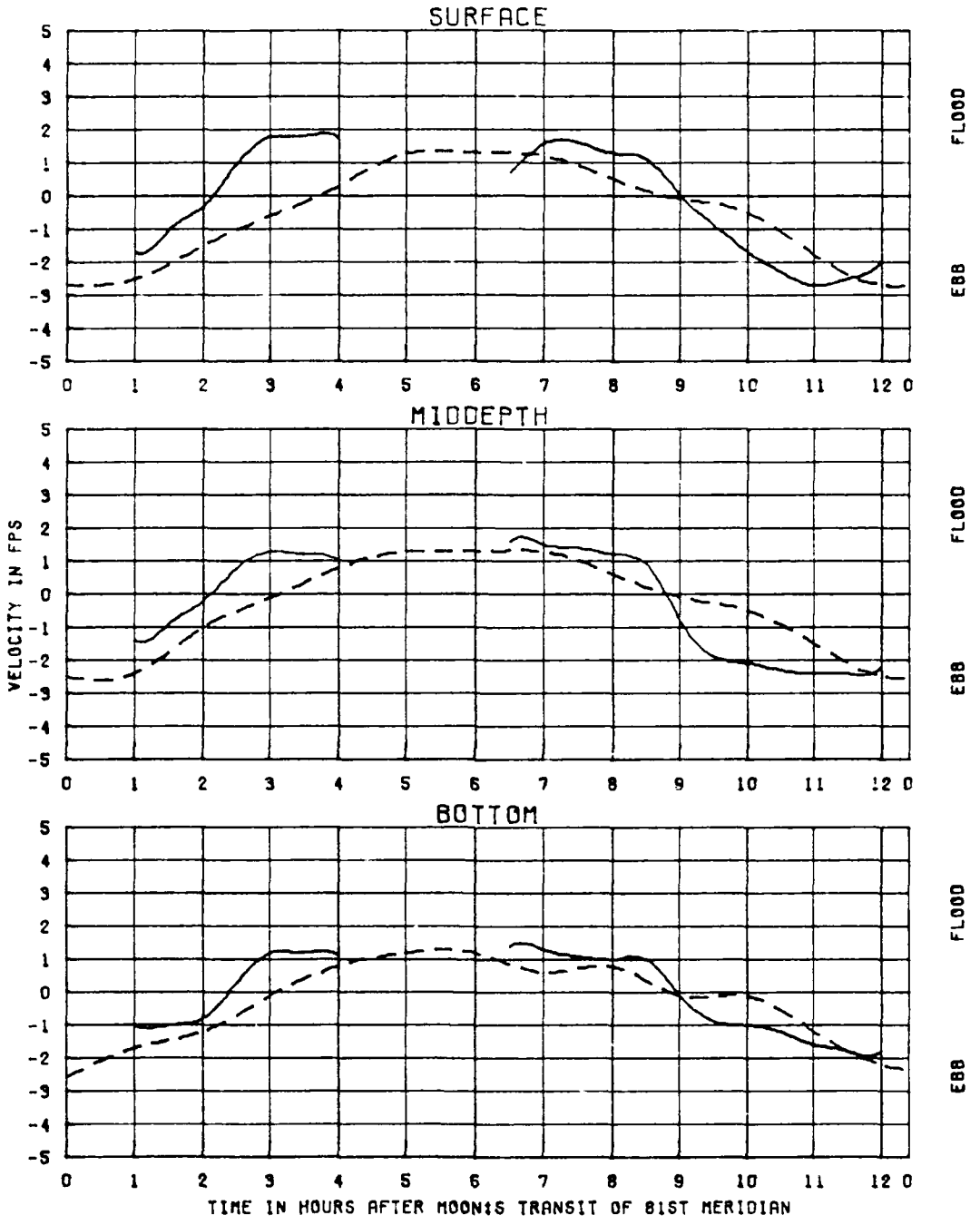

TEST CONDITIONS

TIDAL RANGE AT SOUTH JETTY	5.3 FT
OCEAN SALINITY(TOTAL SALT)	32.5 PPT
FRESHWATER INFLOW	1100 CFS

LEGEND
PROTOTYPE ———
MODEL — — —

KINGS BAY MODEL

VERIFICATION OF VELOCITIES FOR JAN 1985 TIDE

STATION 4B

PLATE C16

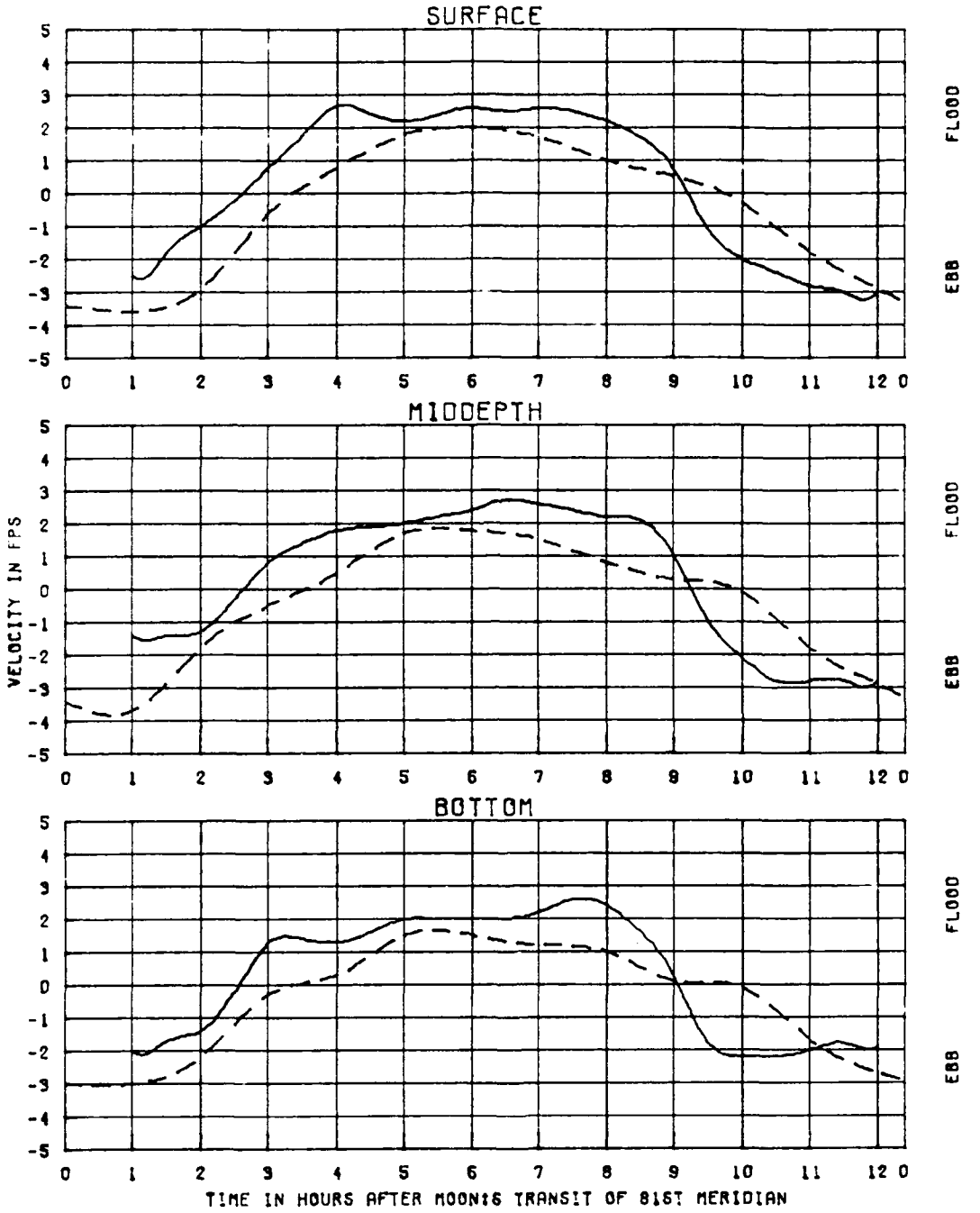

TEST CONDITIONS

TIDAL RANGE AT SOUTH JETTY	5.3 FT
OCEAN SALINITY(TOTAL SALT)	32.5 PPT
FRESHWATER INFLOW	1100 CFS

LEGEND
PROTOTYPE ———
MODEL — — —

KINGS BAY MODEL

VERIFICATION OF VELOCITIES FOR JAN 1985 TIDE

STATION
4C

PLATE C17

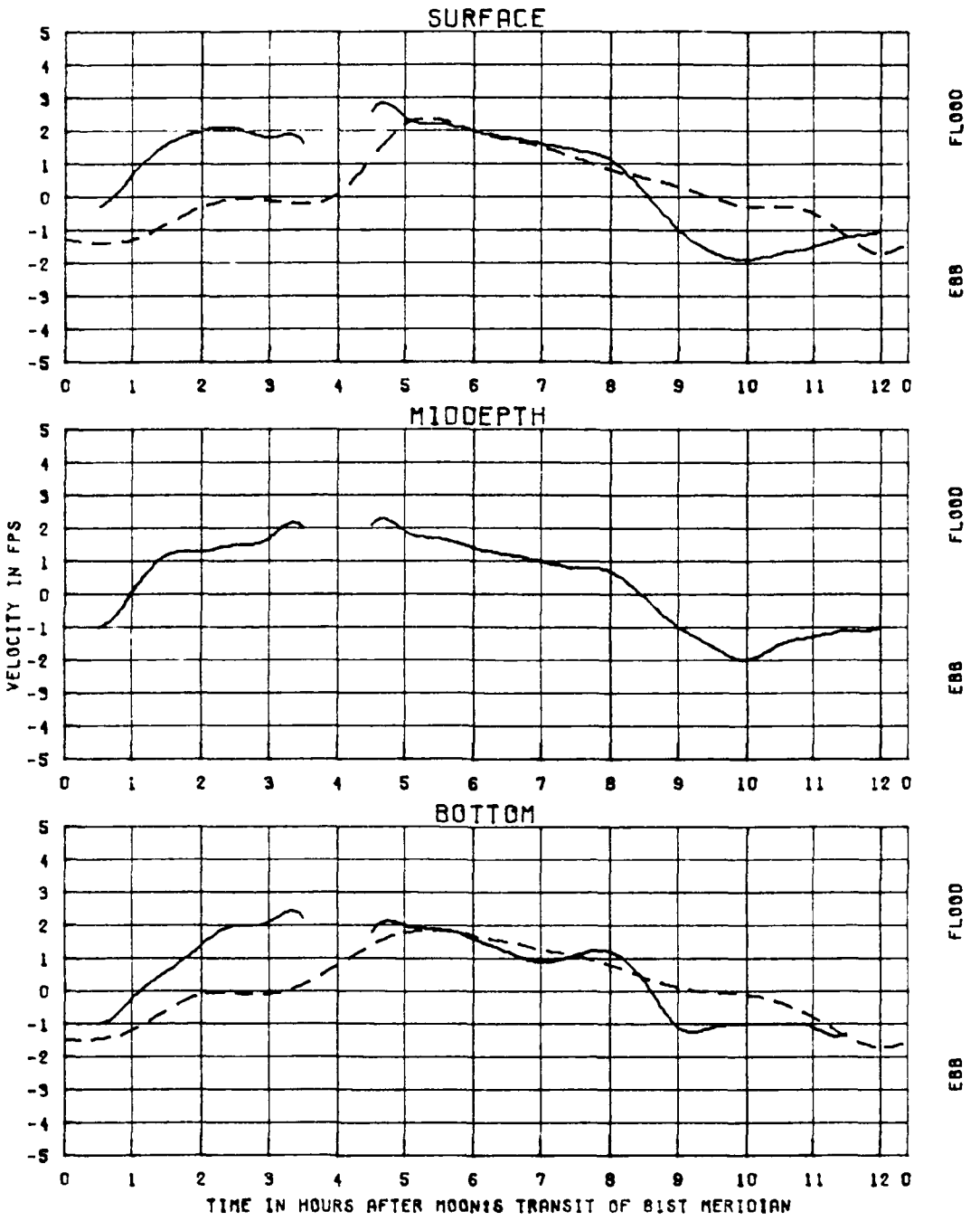

TEST CONDITIONS

TIDAL RANGE AT SOUTH JETTY	5.3 FT
OCEAN SALINITY(TOTAL SALT)	32.5 PPT
FRESHWATER INFLOW	1100 CFS

LEGEND
PROTOTYPE ———
MODEL — — —

KINGS BAY MODEL

VERIFICATION OF VELOCITIES FOR JAN 1985 TIDE

STATION 40

PLATE C18

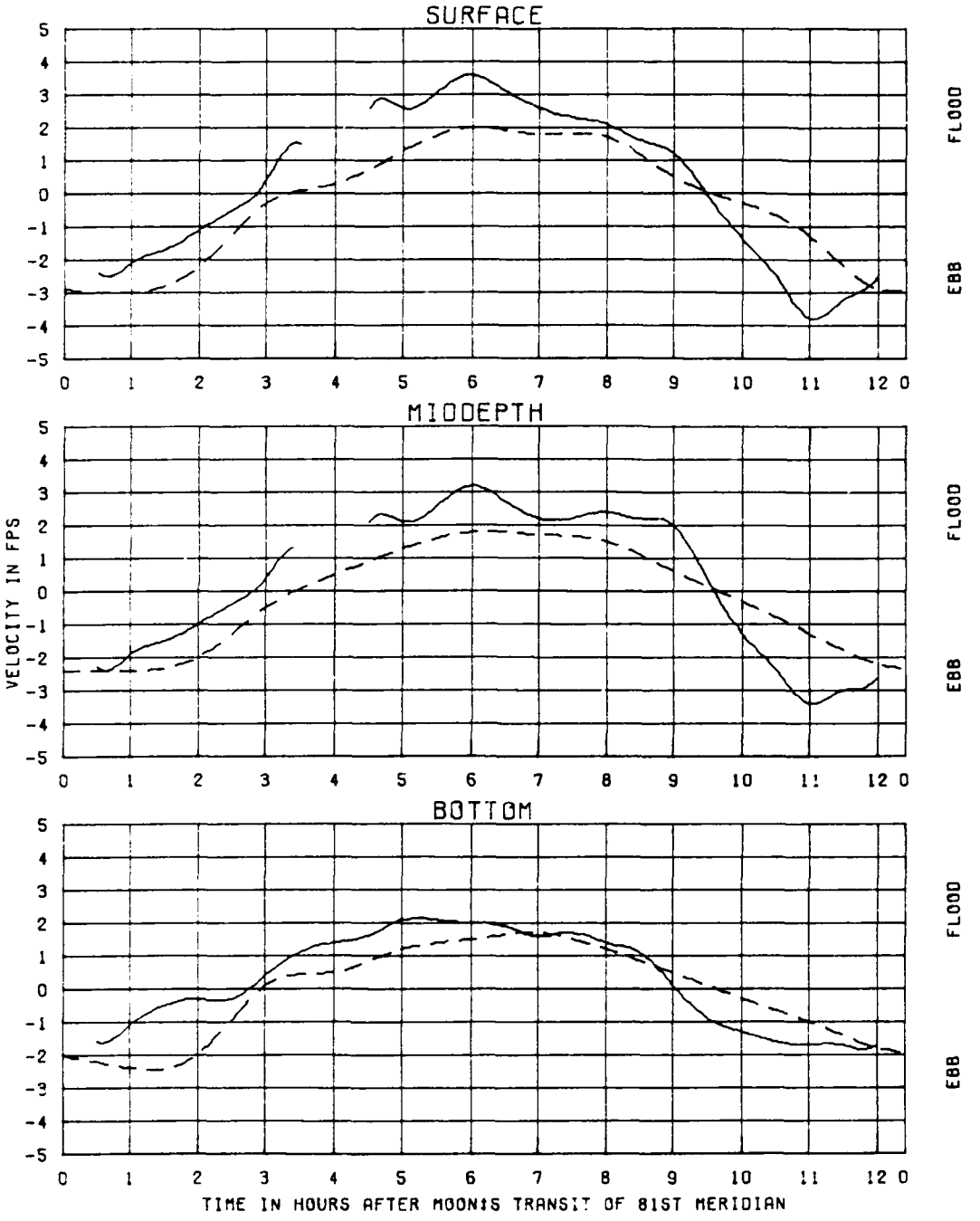

TEST CONDITIONS

TIDAL RANGE AT SOUTH JETTY	5.3 FT
OCEAN SALINITY(TOTAL SALT)	32.5 PPT
FRESHWATER INFLOW	1100 CFS

LEGEND
PROTOTYPE ———
MODEL — — —

KINGS BAY MODEL

VERIFICATION OF VELOCITIES FOR JAN 1985

STATION
5A

PLATE C19

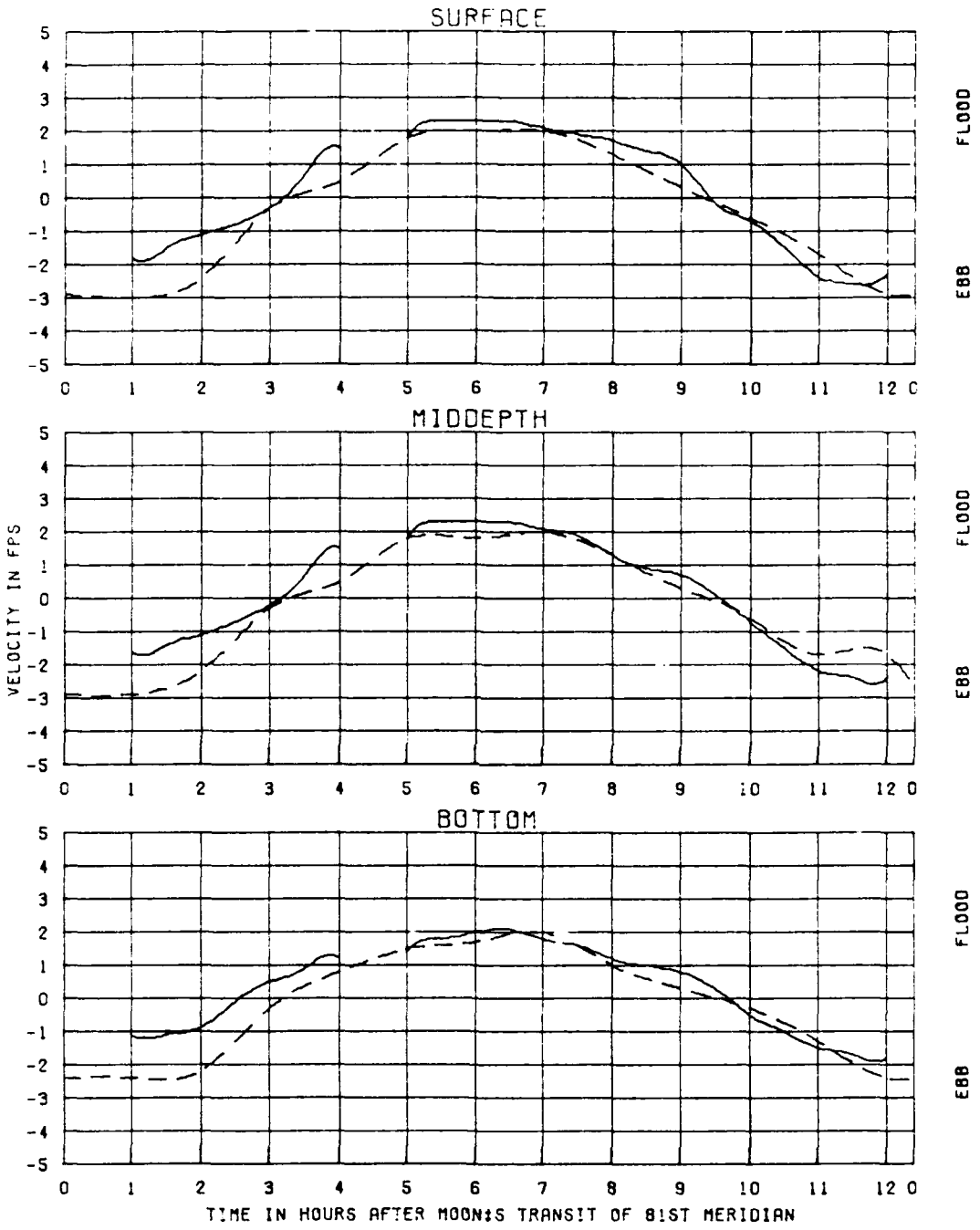

TEST CONDITIONS

TIDAL RANGE AT SOUTH JETTY	5.3 FT
OCEAN SALINITY(TOTAL SALT)	32.5 PPT
FRESHWATER INFLOW	1100 CFS

LEGEND
PROTOTYPE ———
MODEL — — —

KINGS BAY MODEL

VERIFICATION OF VELOCITIES FOR JAN 1985 TIDE

STATION
58

PLATE C20

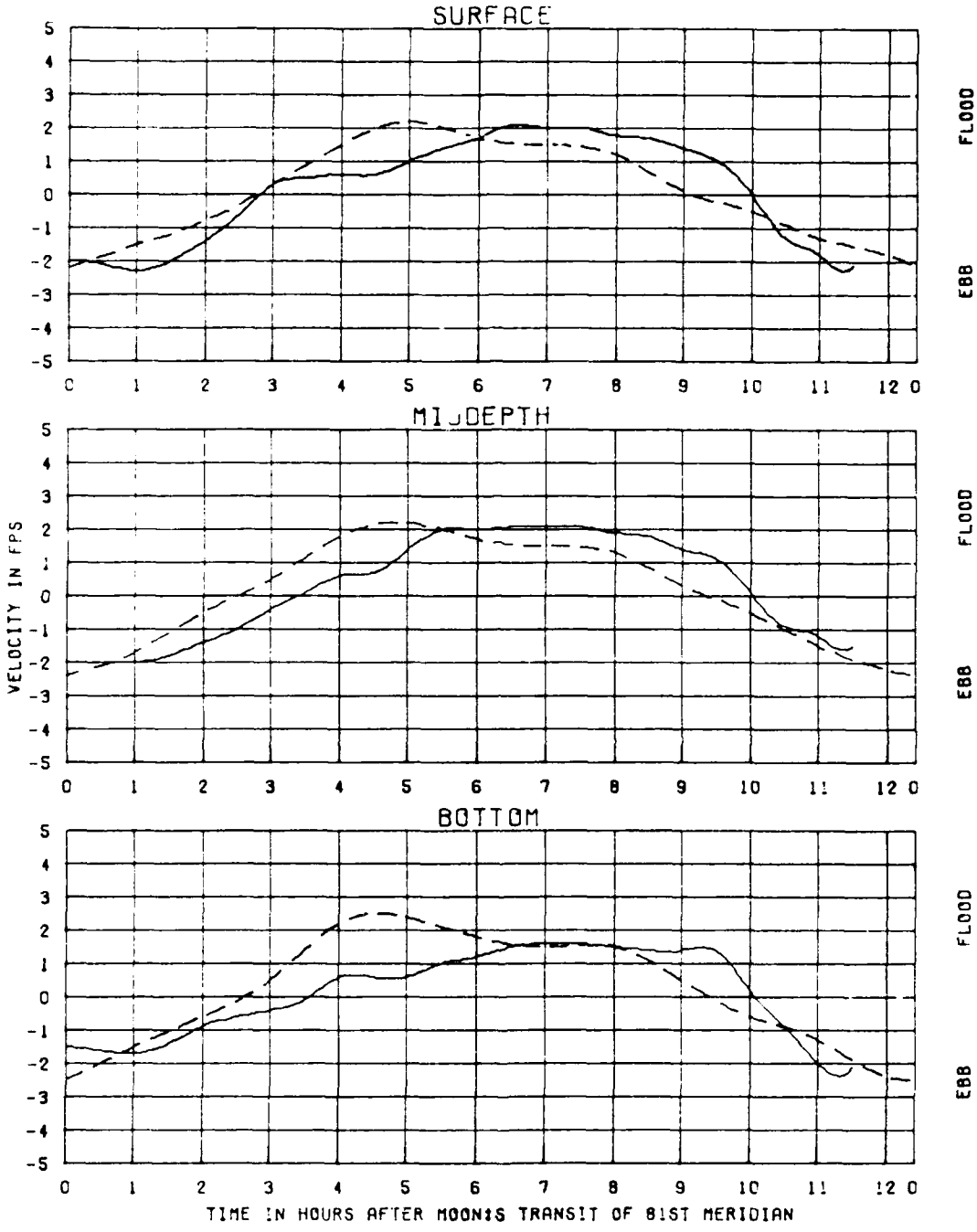

TEST CONDITIONS

TIDAL RANGE AT SOUTH JETTY	5.3 FT
OCEAN SALINITY(TOTAL SALT)	32.5 PPT
FRESHWATER INFLOW	1100 CFS

LEGEND
PROTOTYPE ———
MODEL — — —

KINGS BAY MODEL

VERIFICATION OF VELOCITIES FOR JAN 1985 TIDE

STATION
SC

PLATE C21

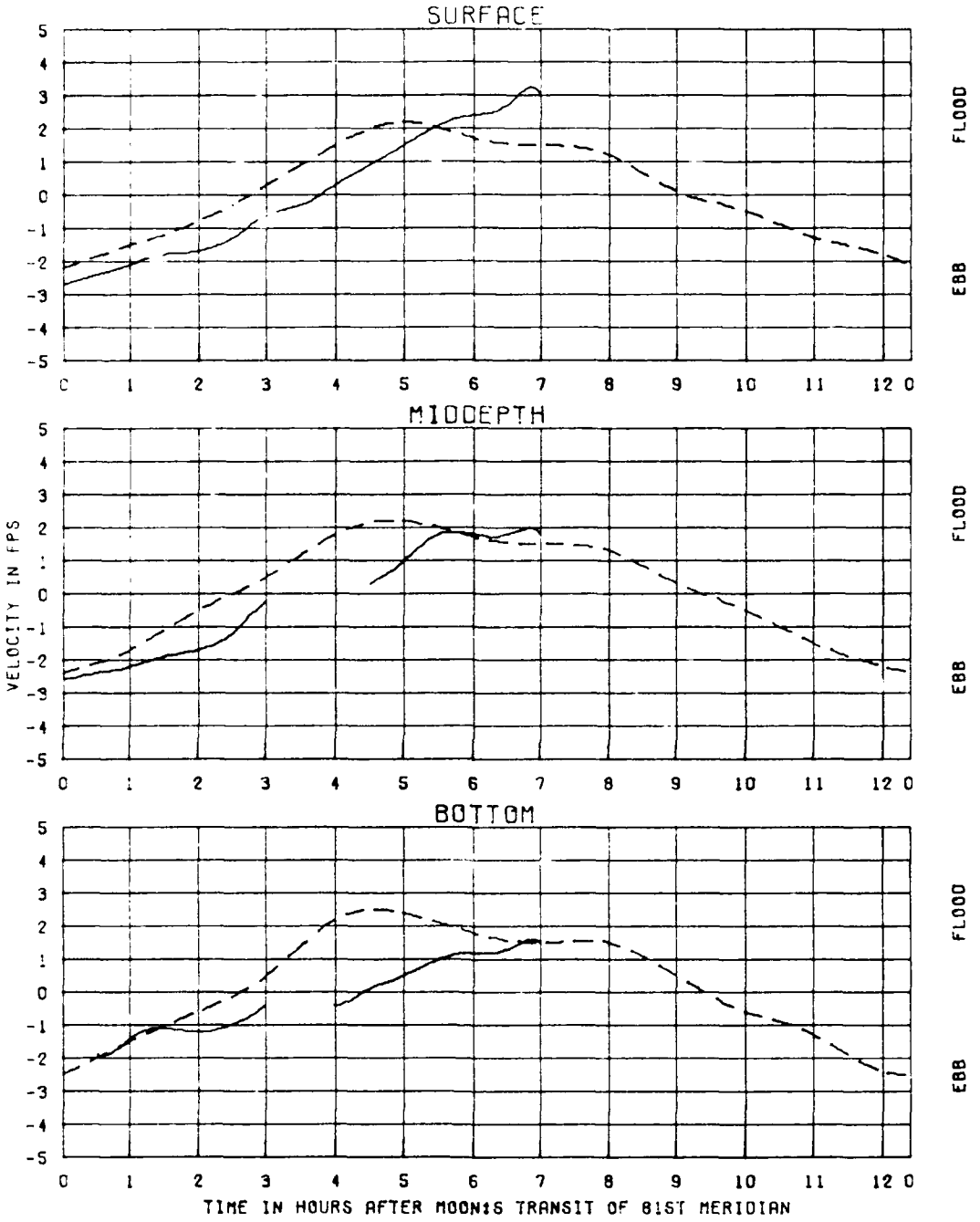

TEST CONDITIONS

TIDAL RANGE AT SOUTH JETTY	5.3 FT
OCEAN SALINITY(TOTAL SALT)	32.5 PPT
FRESHWATER INFLOW	1100 CFS

LEGEND
PROTOTYPE ———
MODEL — — —

KINGS BAY MODEL

VERIFICATION OF VELOCITIES FOR JAN 1985 TIDE

STATION
SD

PLATE C22

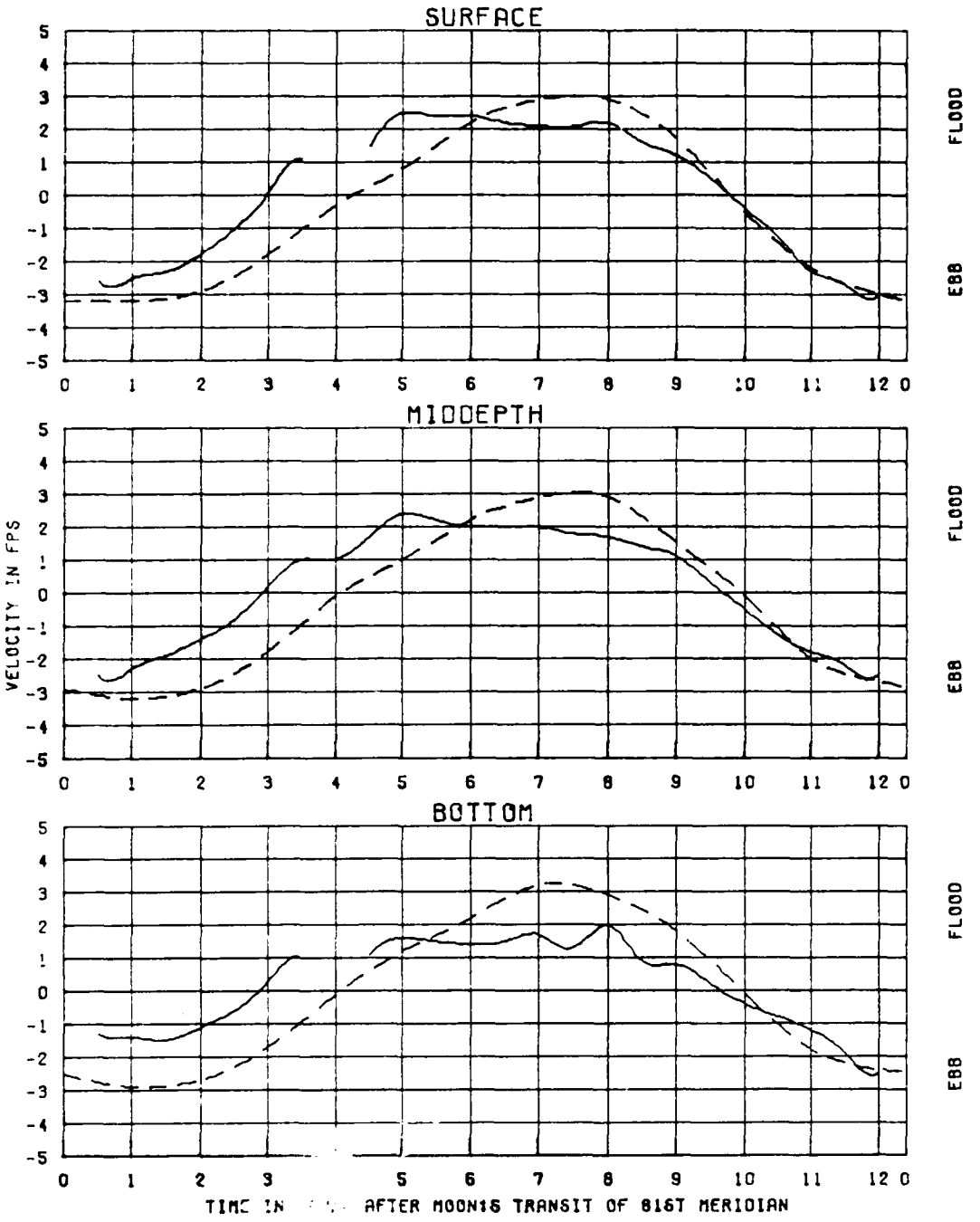

TEST CONDITIONS

TIDAL RANGE AT SOU [illegible]	5.3 FT
OCEAN SALINITY(TOTAL SALT)	32.5 PPT
FRESHWATER INFLOW	1100 CFS

LEGEND
PROTOTYPE ———
MODEL — — —

KINGS BAY MODEL

VERIFICATION OF
VELOCITIES
FOR JAN 1985 TIDE
STATION
6A

PLATE C23

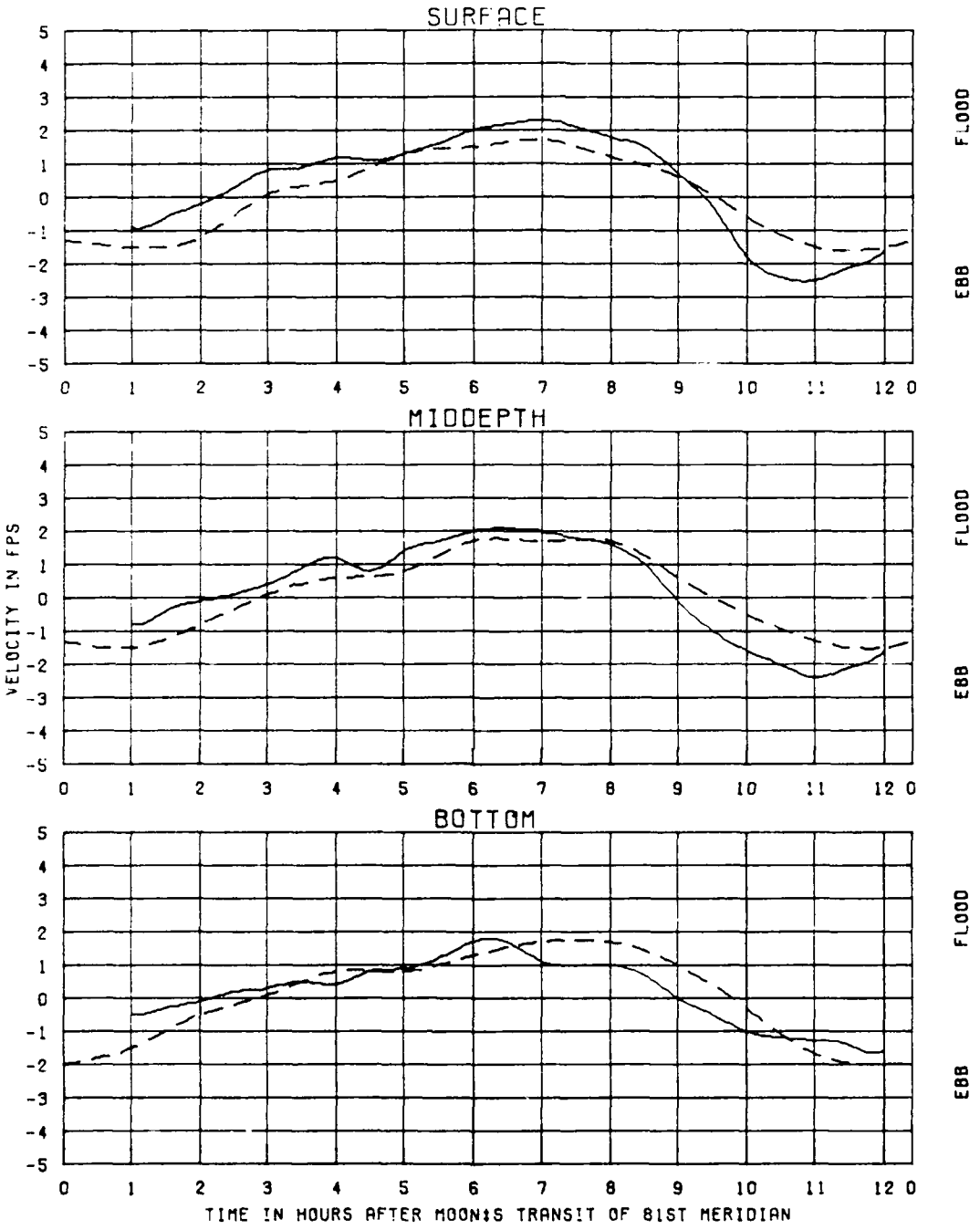

TEST CONDITIONS

TIDAL RANGE AT SOUTH JETTY	5.3 FT
OCEAN SALINITY(TOTAL SALT)	32.5 PPT
FRESHWATER INFLOW	1100 CFS

LEGEND
PROTOTYPE ———
MODEL — — —

KINGS BAY MODEL

VERIFICATION OF VELOCITIES FOR JAN 1985 TIDE

STATION
6B

PLATE C24

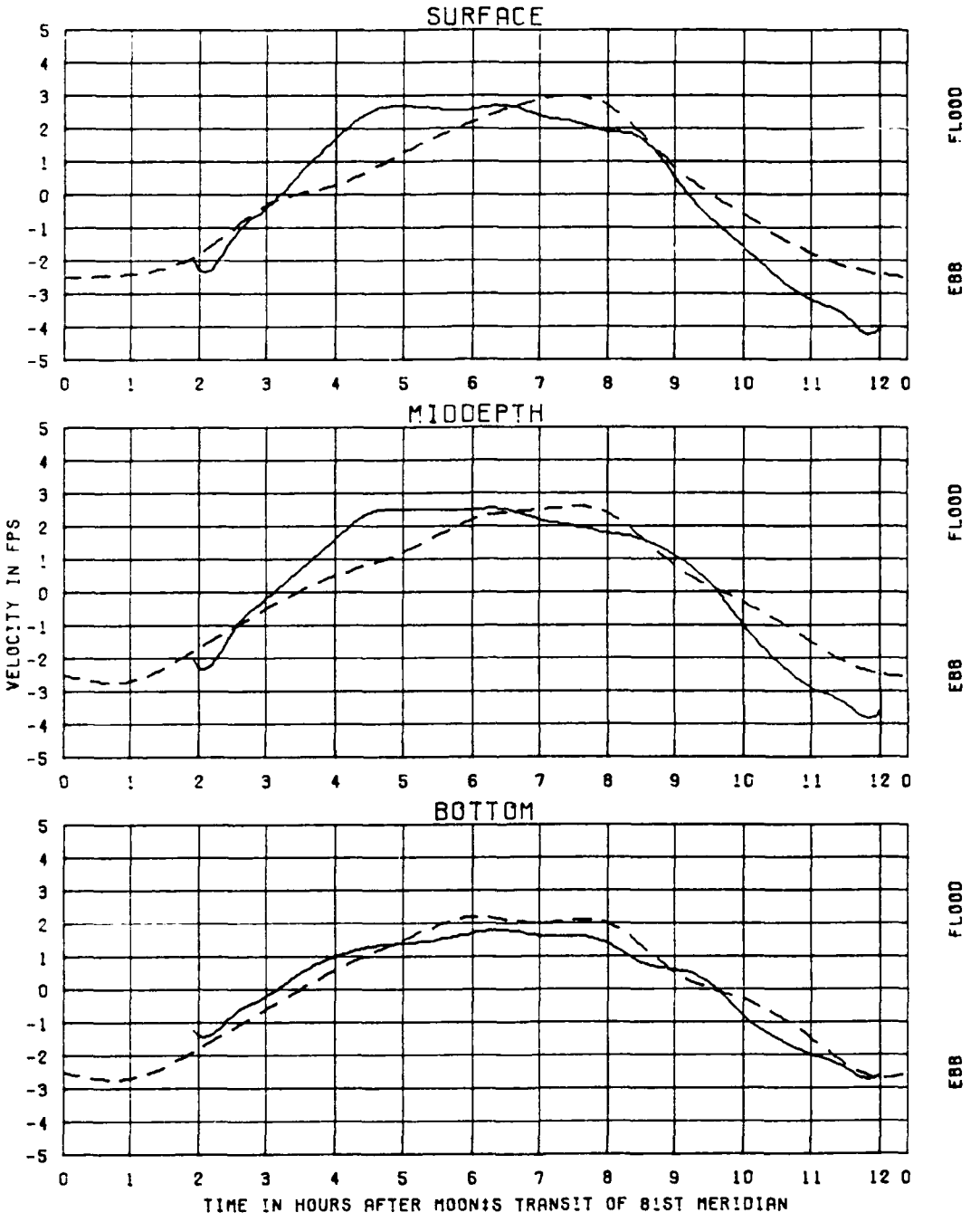

TEST CONDITIONS

TIDAL RANGE AT SOUTH JETTY	5.3 FT
OCEAN SALINITY(TOTAL SALT)	32.5 PPT
FRESHWATER INFLOW	1100 CFS

LEGEND
PROTOTYPE ———
MODEL — — —

KINGS BAY MODEL

VERIFICATION OF
VELOCITIES
FOR JAN 1985 TIDE
STATION
6C

PLATE C25

APPENDIX D: NUMERICAL MODEL PRE-TRIDENT MESH 1 VERIFICATION

NOTE: The term "field station" on plots in this appendix refers to stations in the physical model.

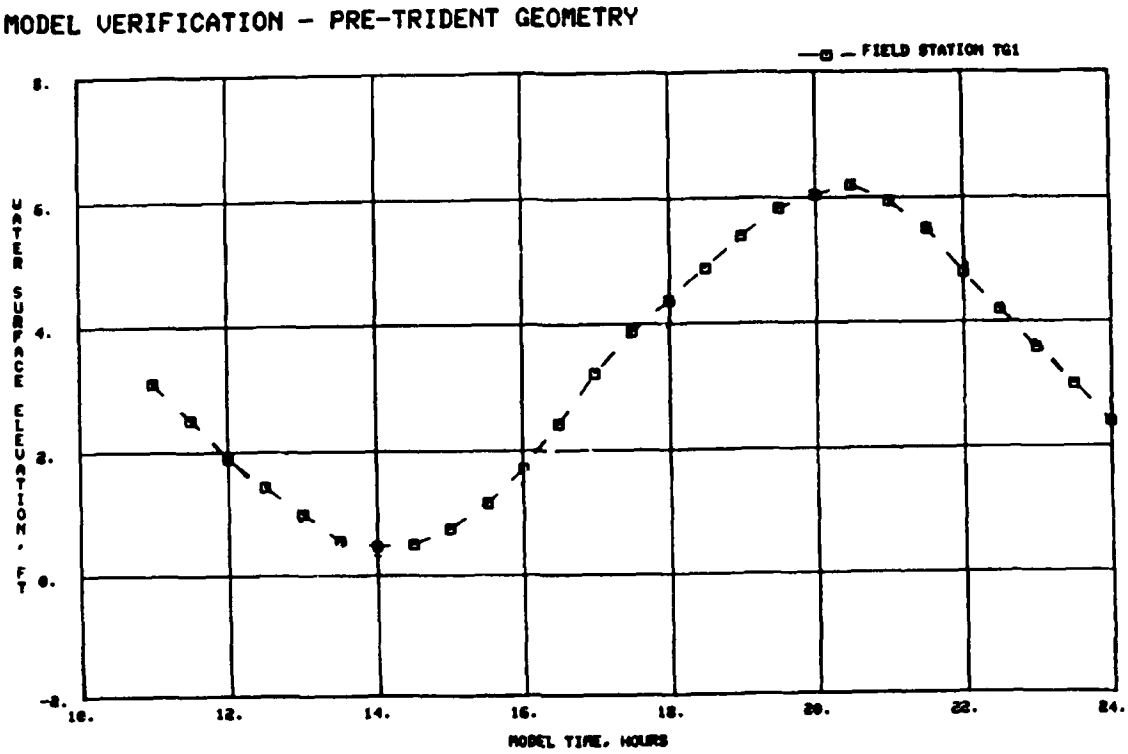

a. Physical model, ocean

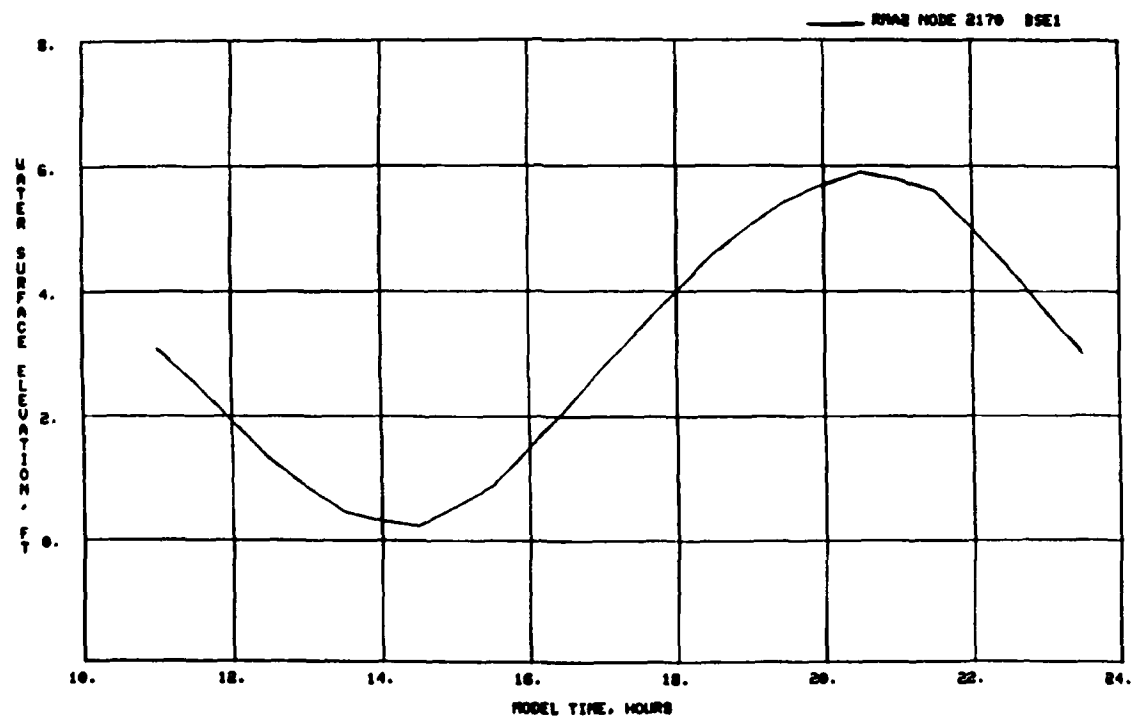

b. Numerical model, St. Marys Inlet

Plate D1. Tidal boundary forcing conditions

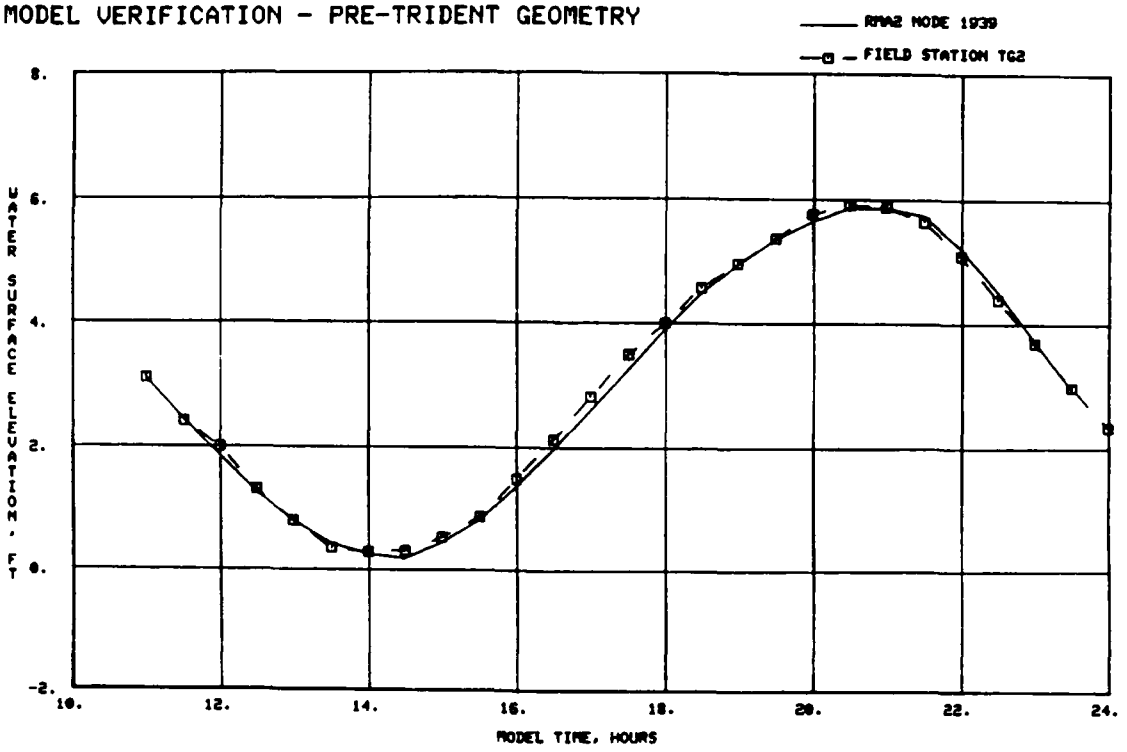

a. St. Marys Inlet

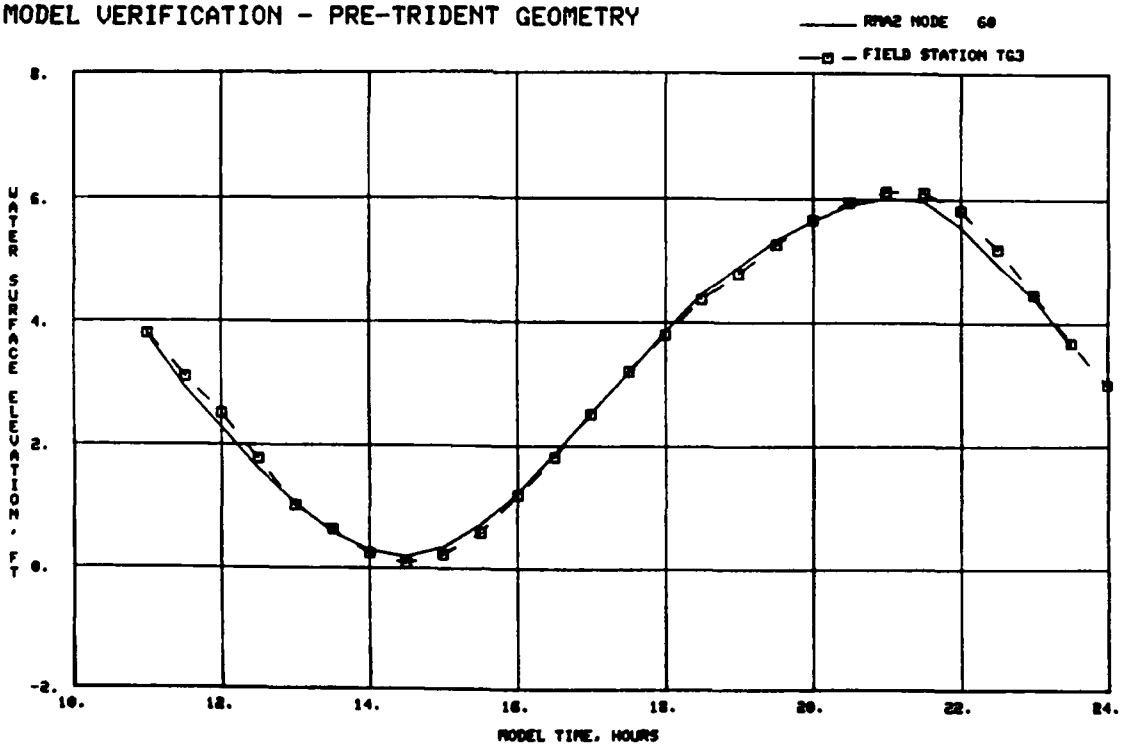

b. Amelia River

Plate D2. Water-surface elevations, physical and numerical model, for St. Marys Inlet and Amelia River

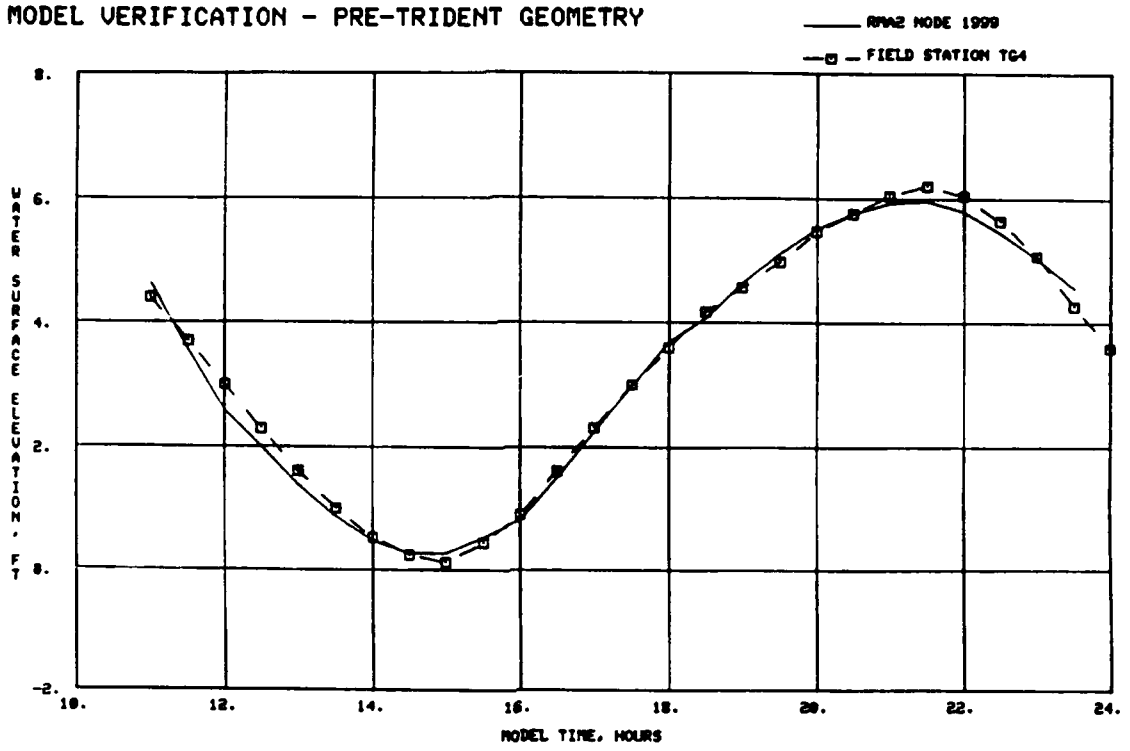

a. Jolly River

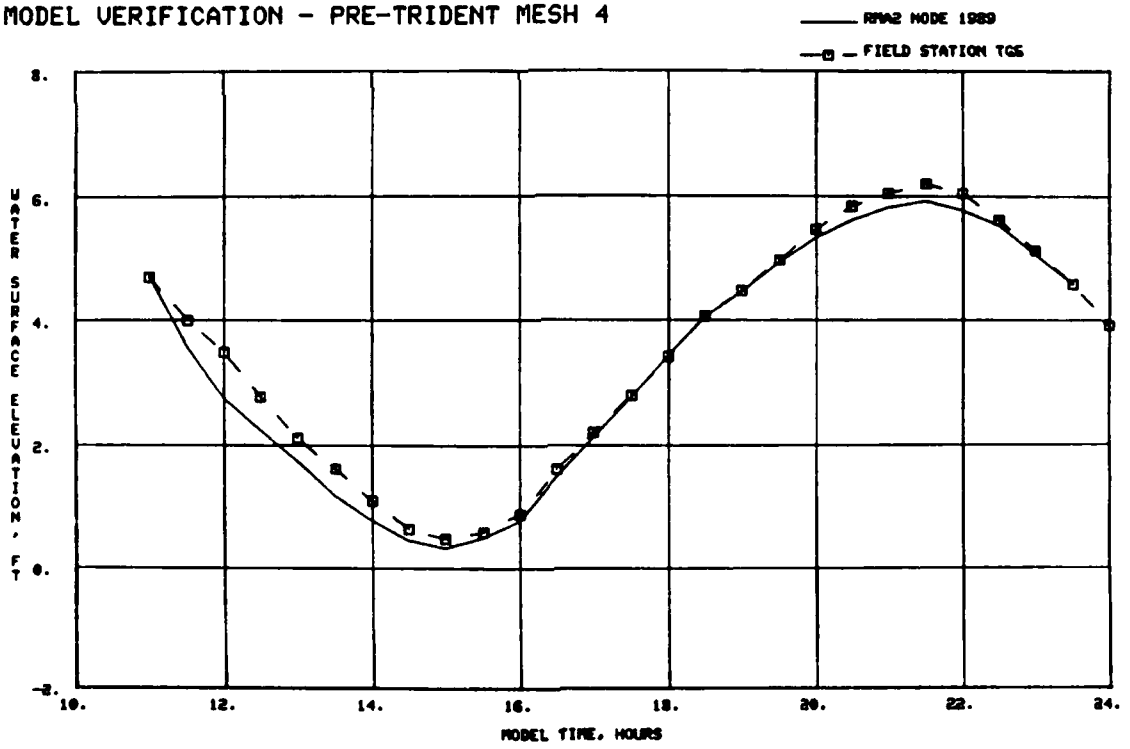

b. St. Marys River

Plate D3. Water-surface elevations, physical and numerical model, for Jolly River and St. Marys River

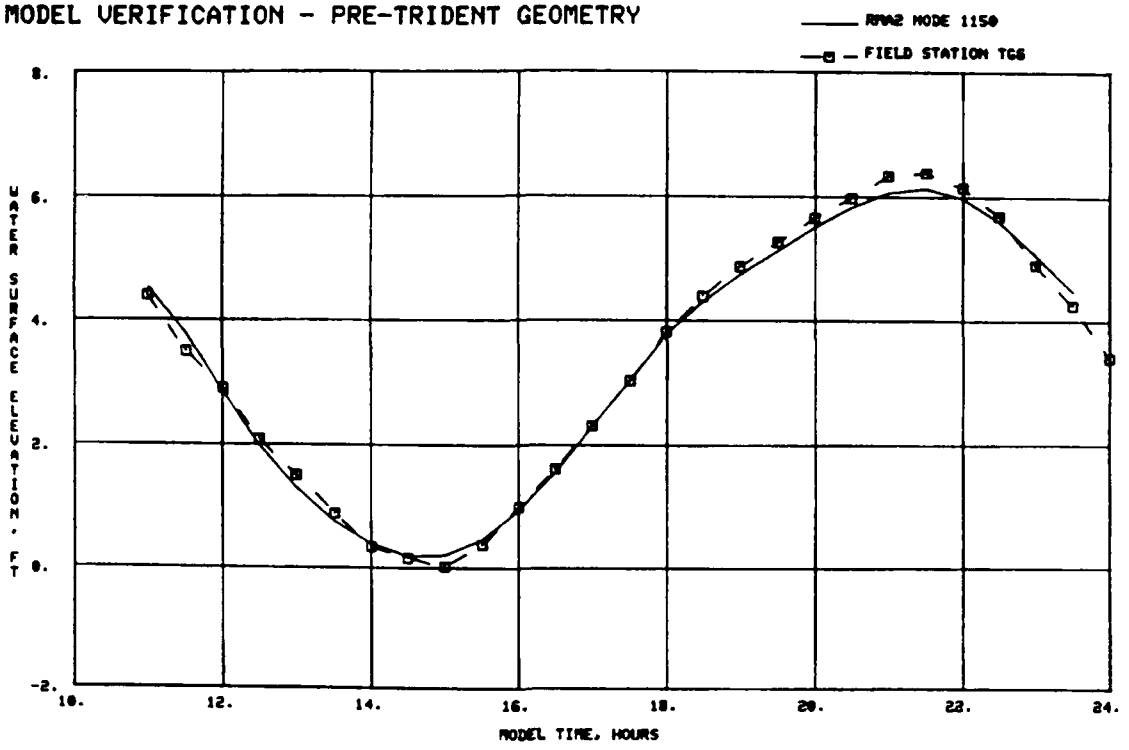

a. Lower Kings Bay

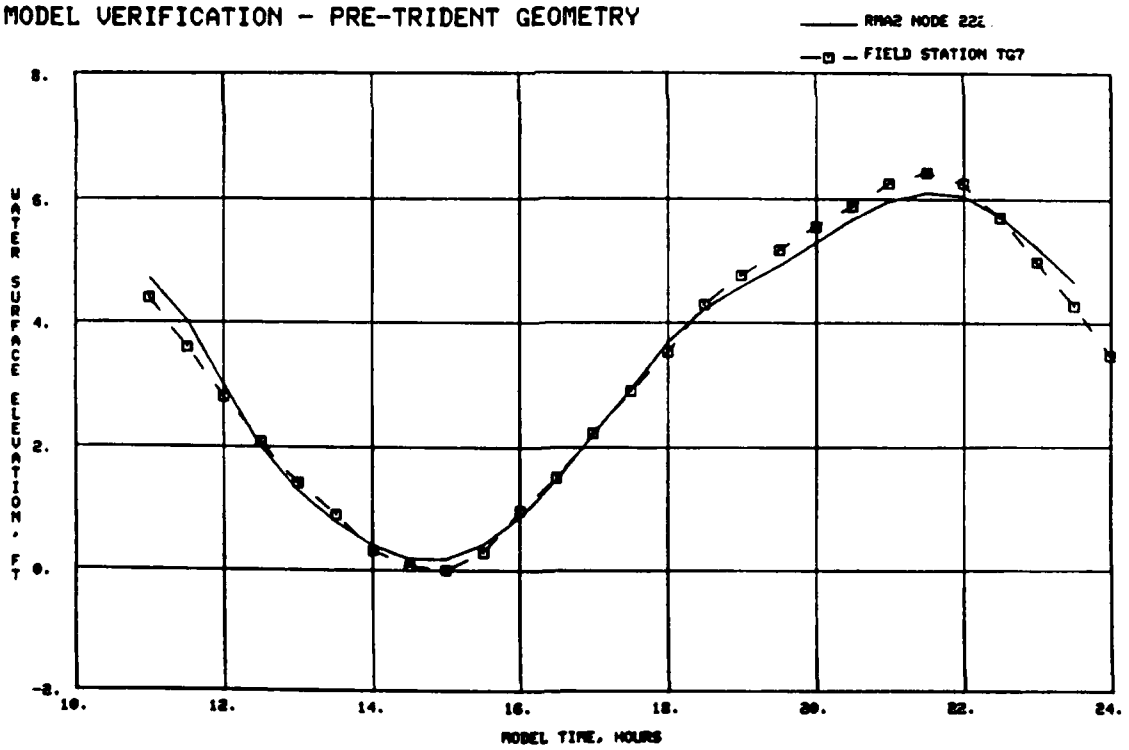

b. Marianna Creek

Plate D4. Water-surface elevations, physical and numerical model, for lower Kings Bay and Marianna Creek

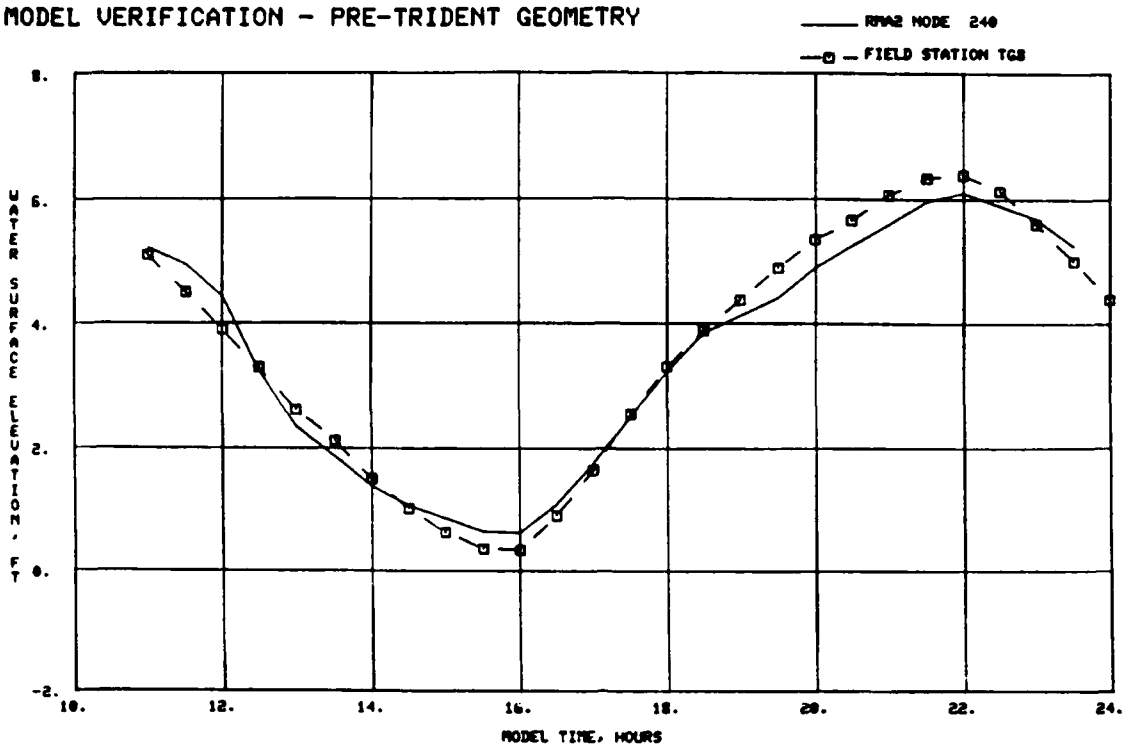

a. Crooked River

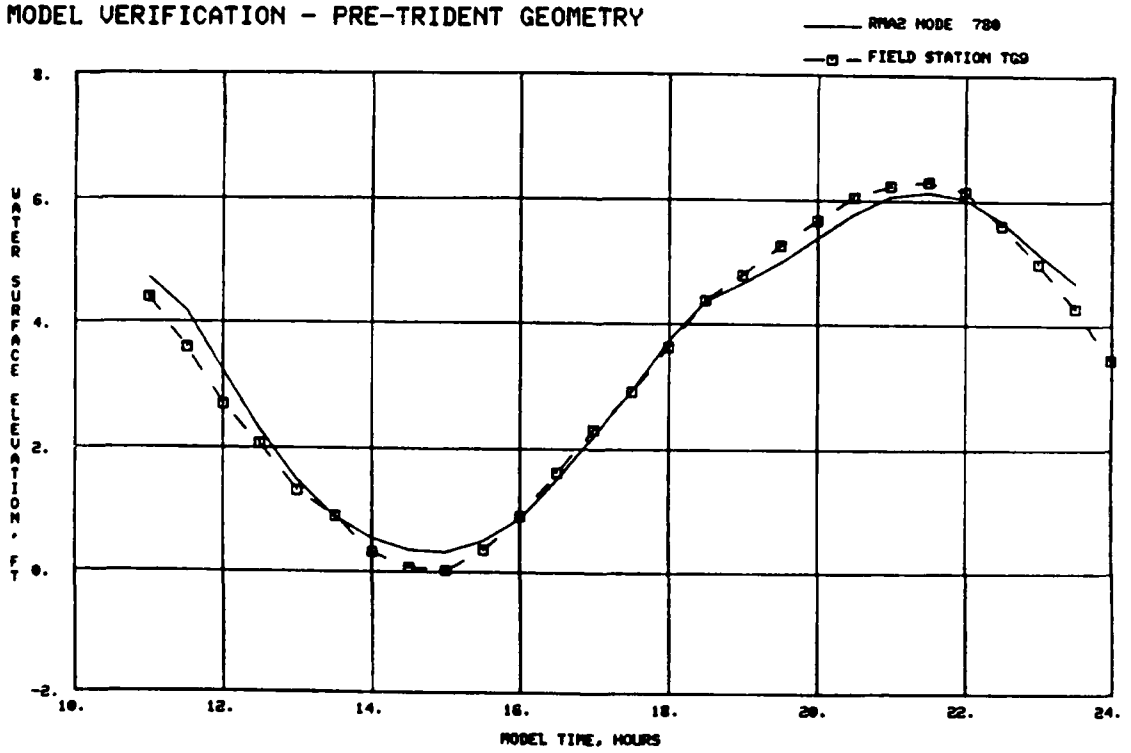

b. Northern Cumberland Sound

Plate D5. Water-surface elevations, physical and numerical model, for Crooked River and northern Cumberland Sound

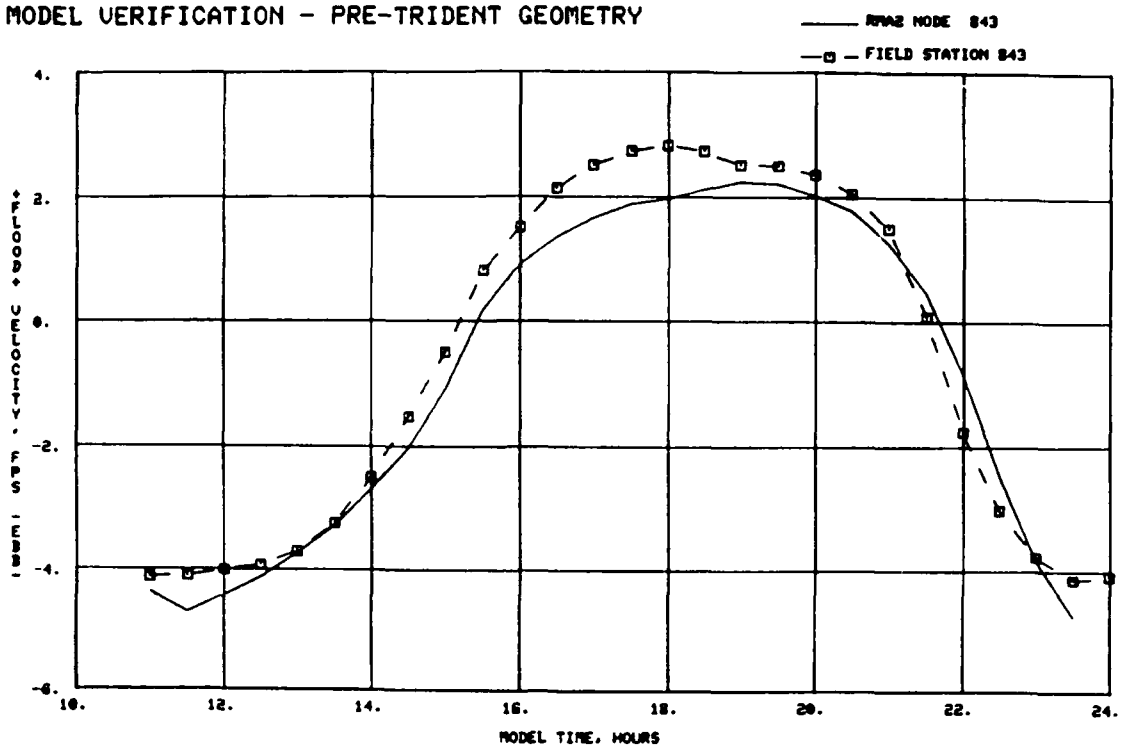

a. Station 843

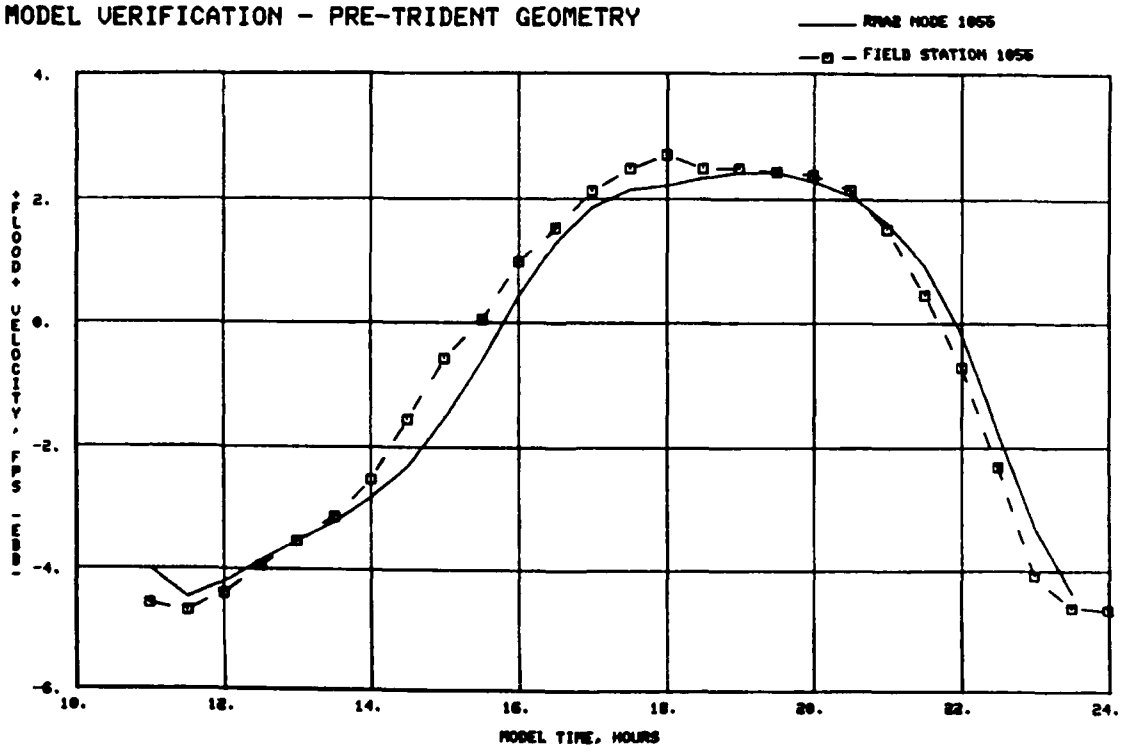

b. Station 1055

Plate D6. Physical and numerical model velocities for stations 843 and 1055

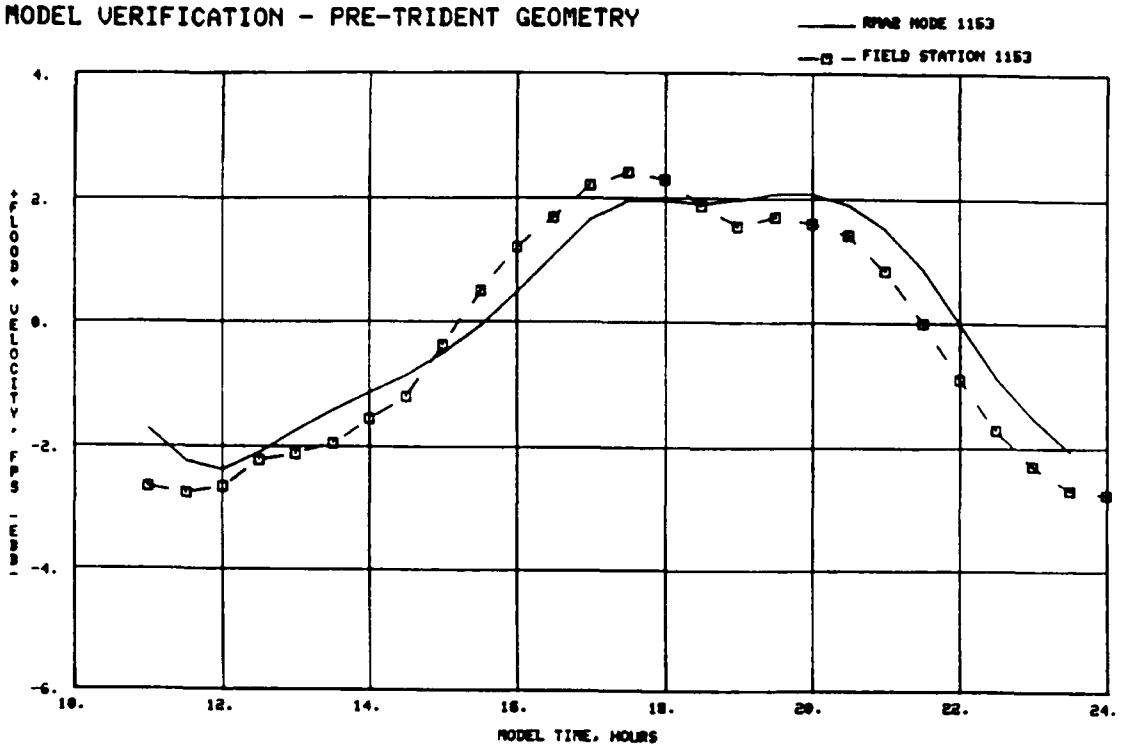

a. Station 1153

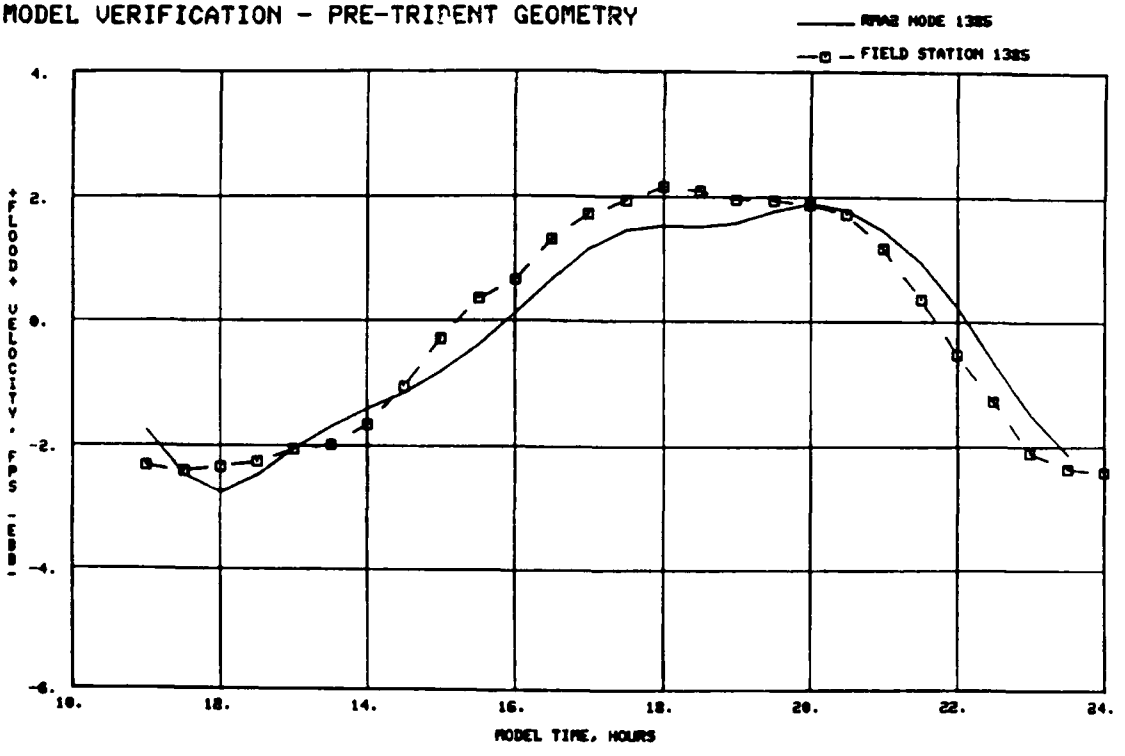

b. Station 1385

Plate D7. Physical and numerical model velocities for stations 1153 and 1385

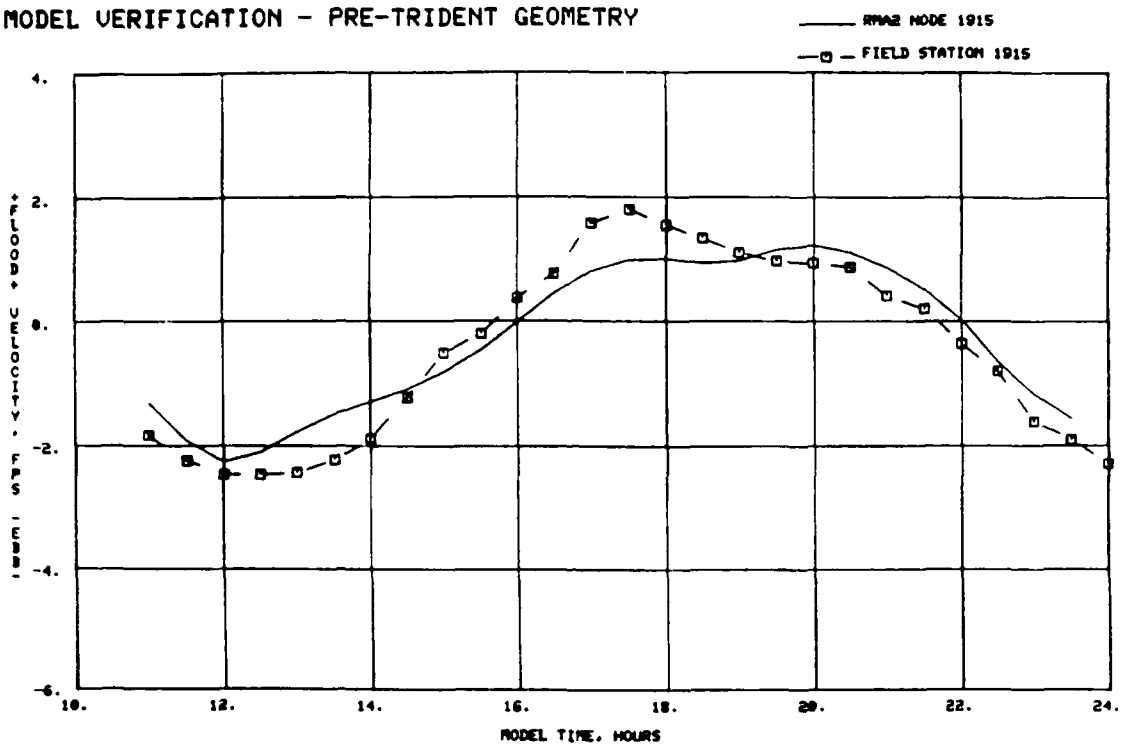

a. Station 1915

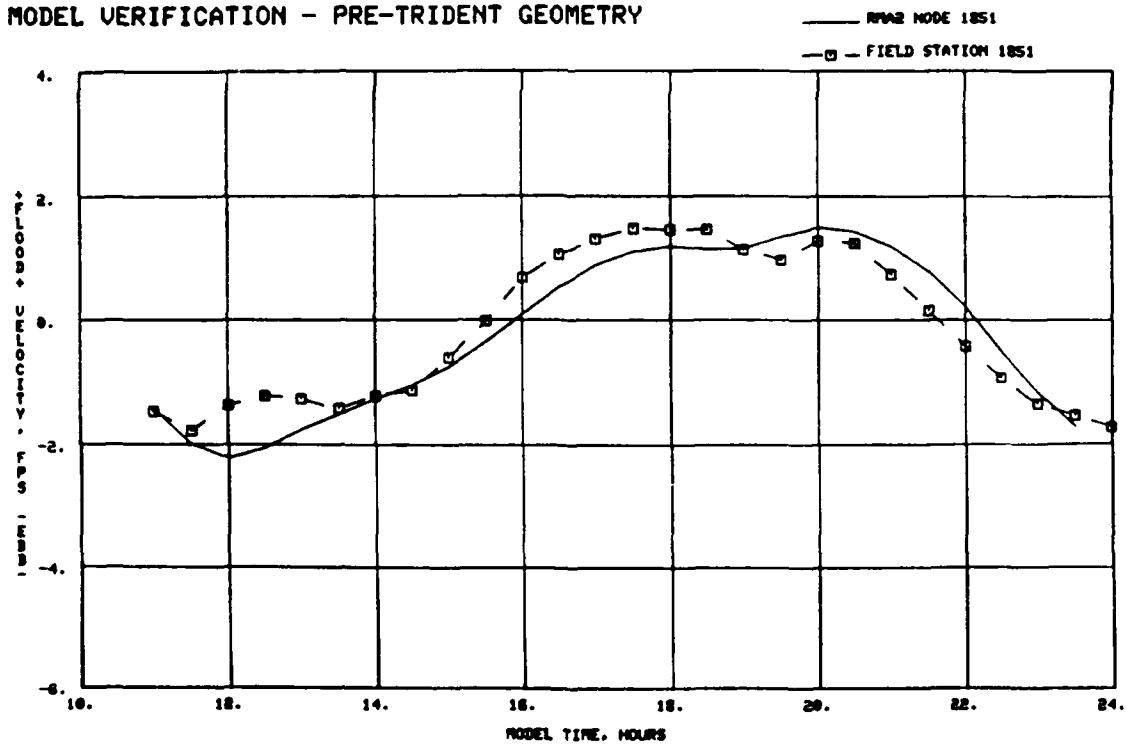

b. Station 1851

Plate D8. Physical and numerical model velocities for stations 1915 and 1851

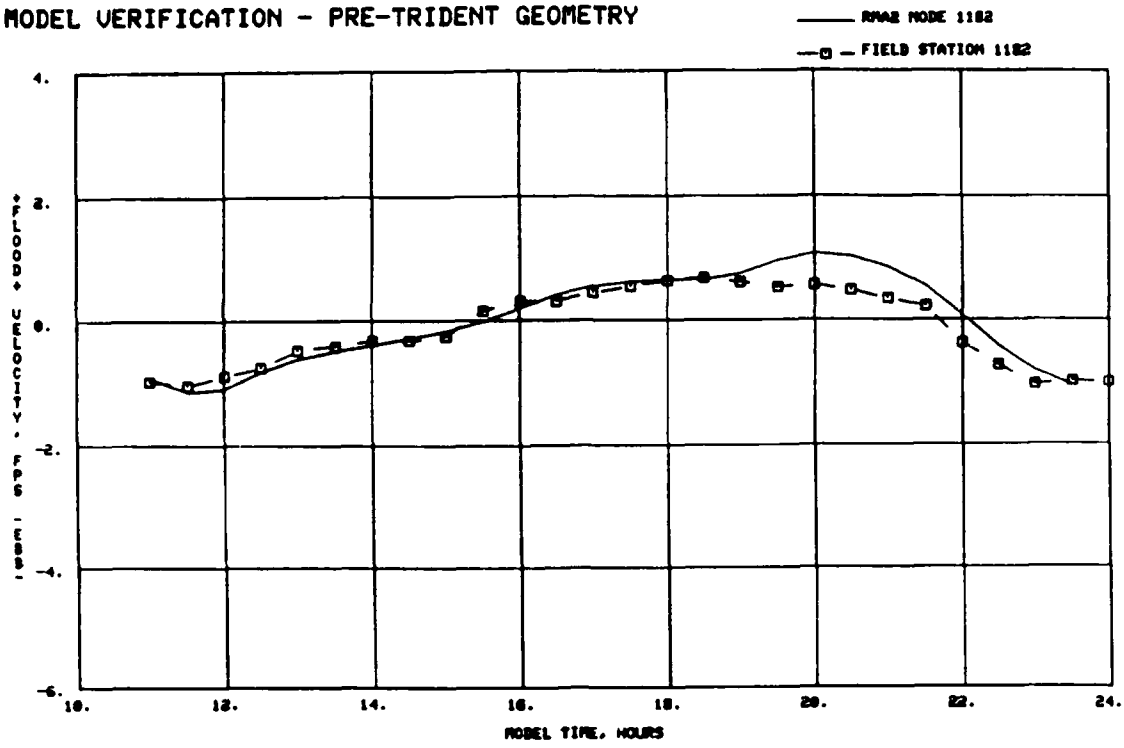

a. Station 1182

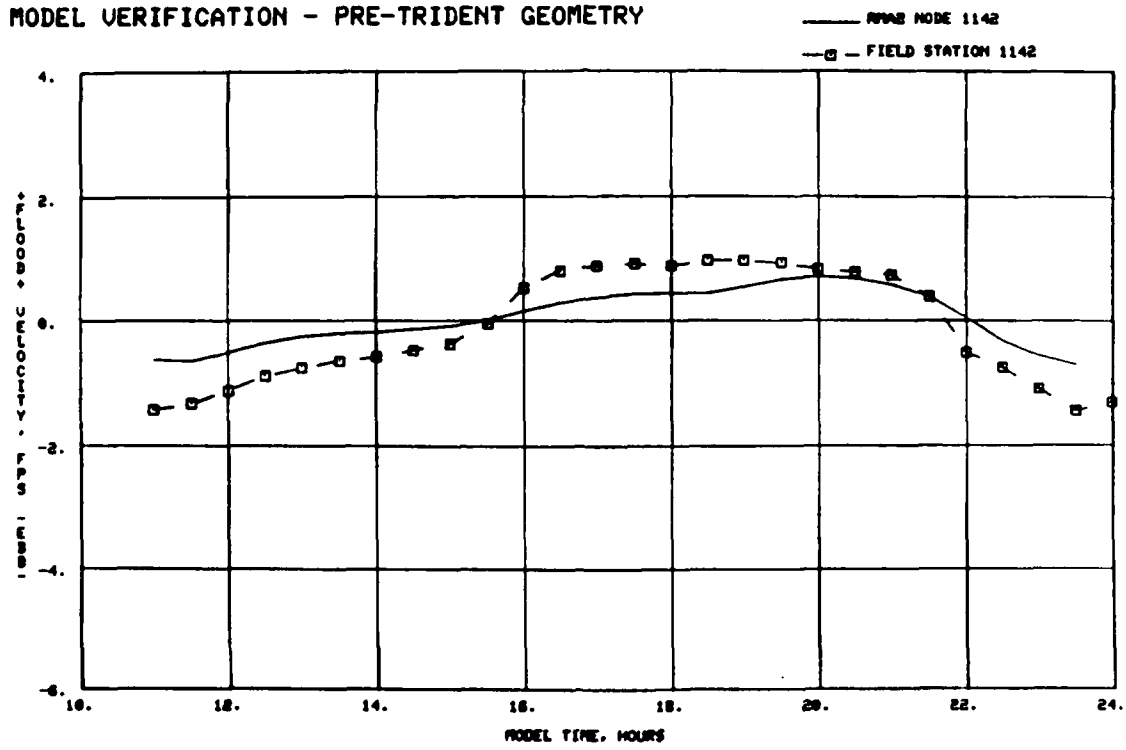

b. Station 1142

Plate D9. Physical and numerical model velocities for stations 1182 and 1142

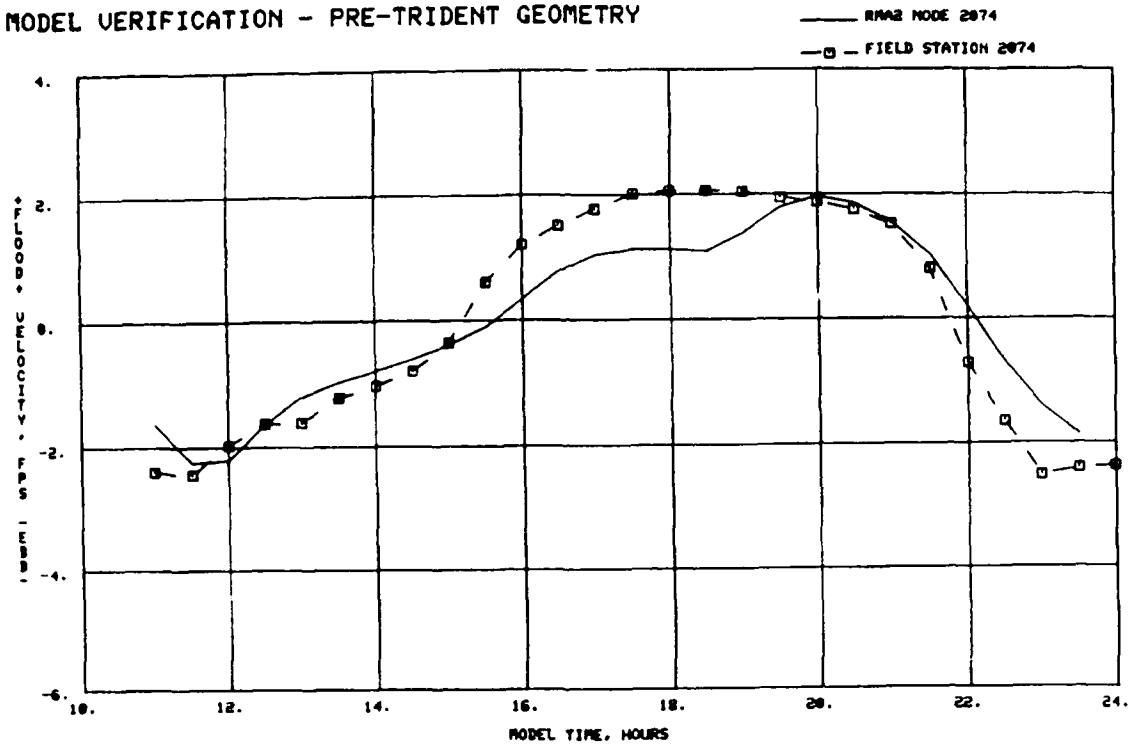

a. Station 2074

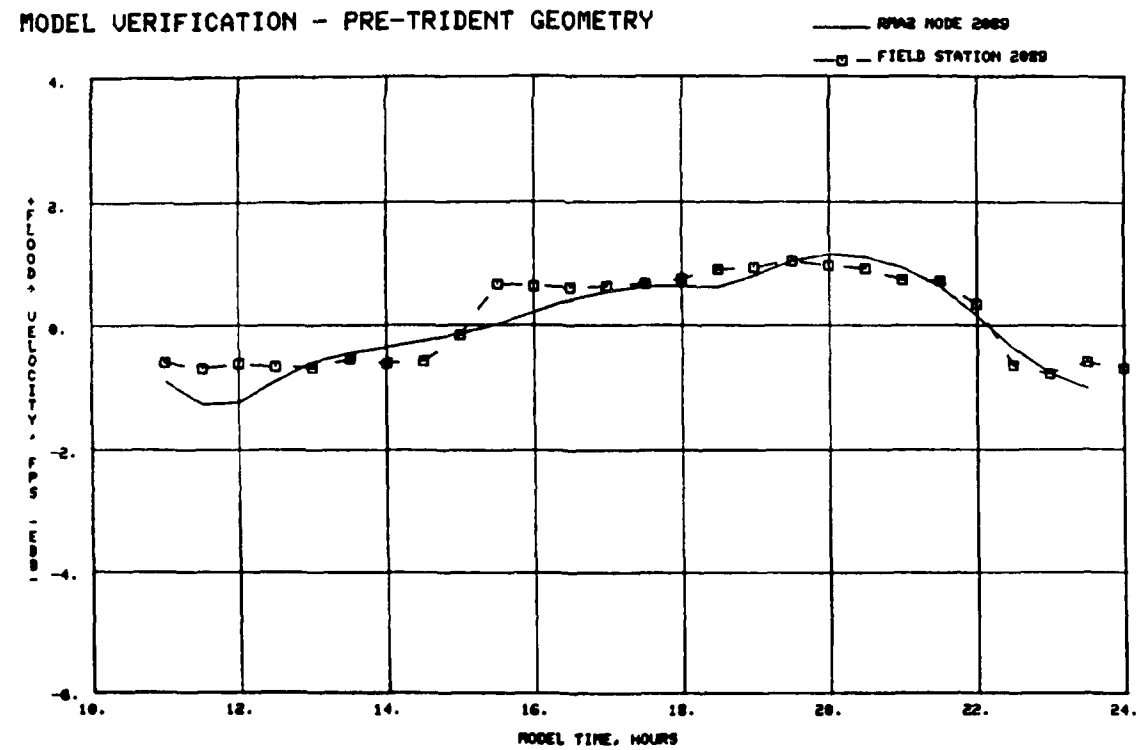

b. Station 2089

Plate D10. Physical and numerical model velocities for stations 2074 and 2089

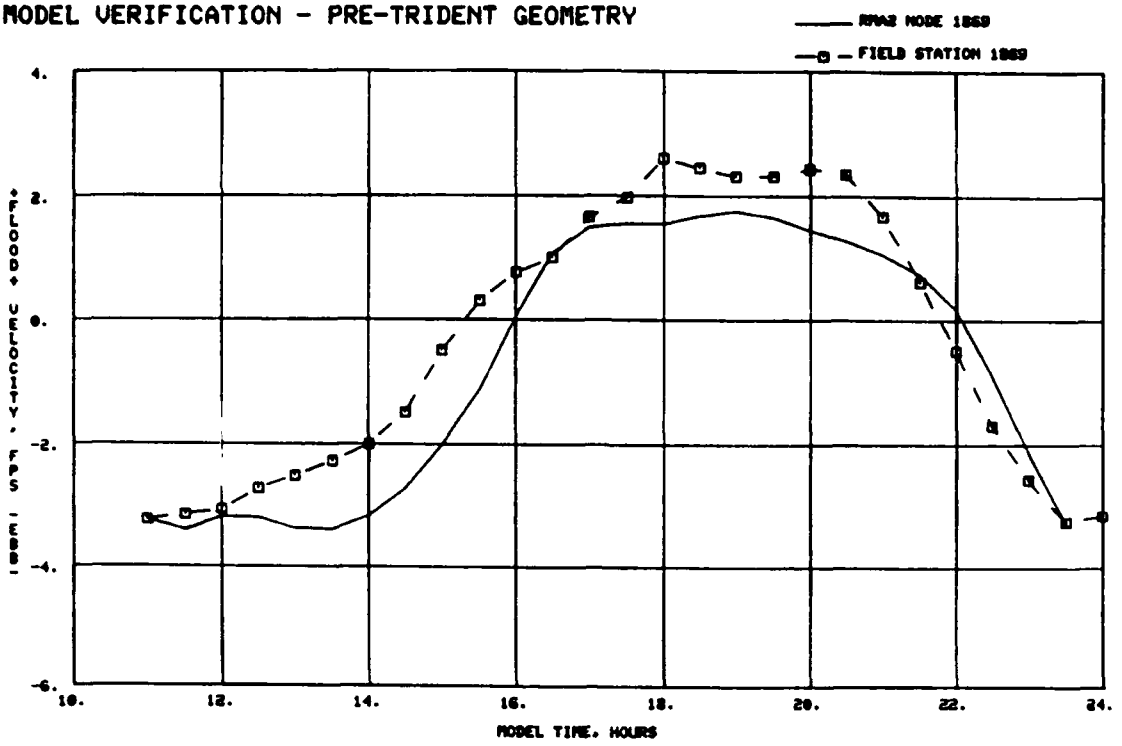

a. Station 1865

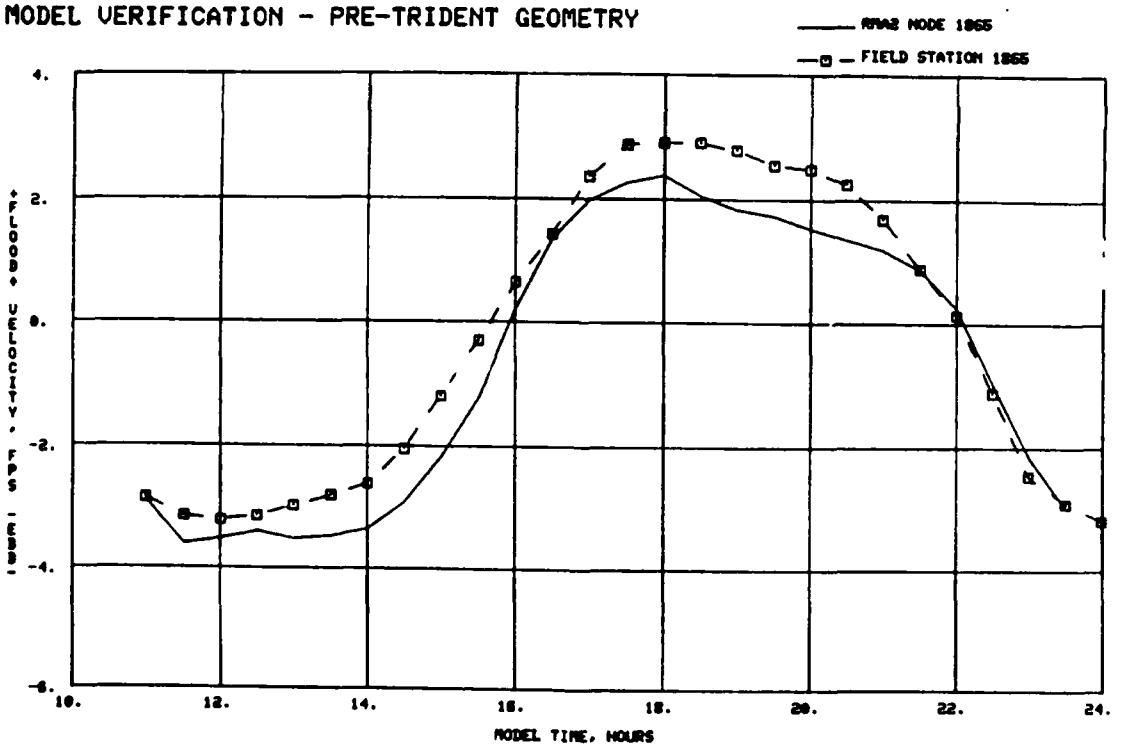

b. Station 1869

Plate D11. Physical and numerical model velocities for stations 1865 and 1869

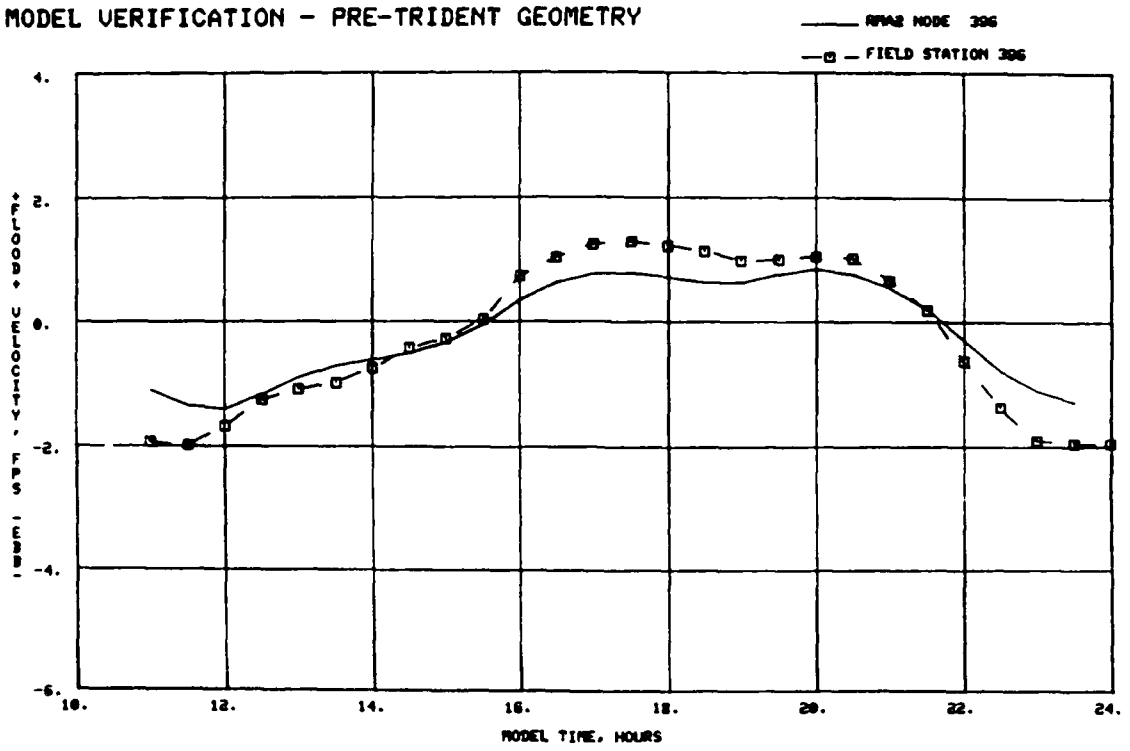

a. Station 396

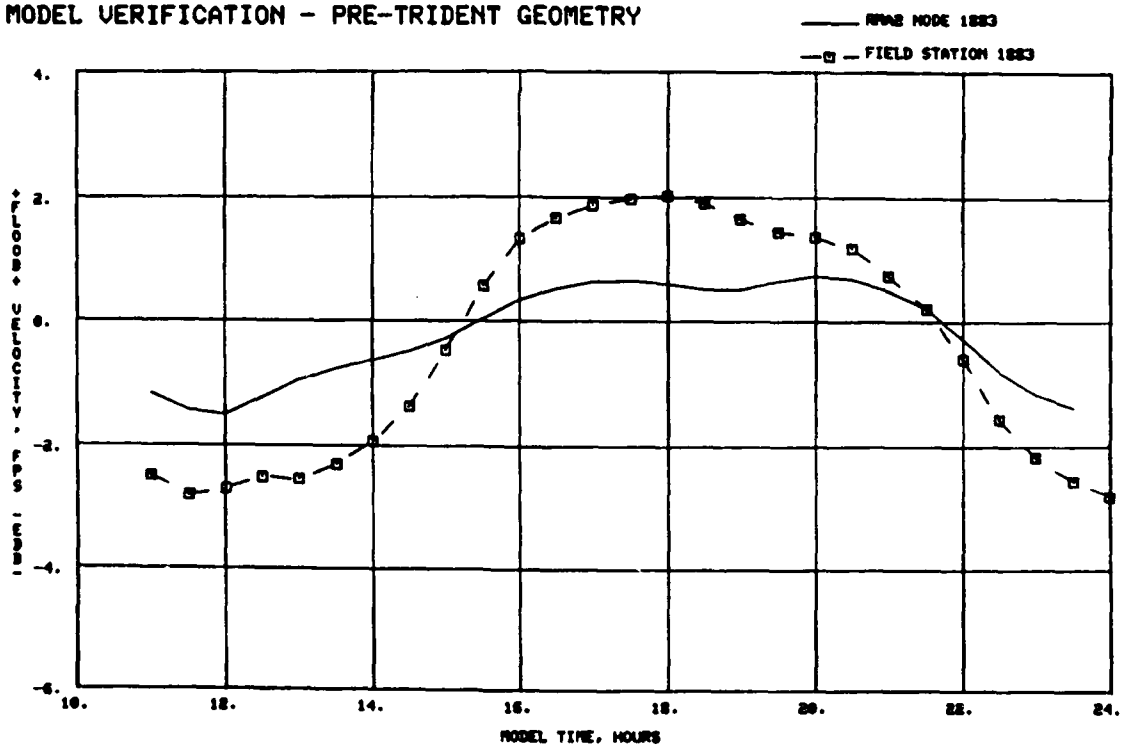

b. Station 1883

Plate D12. Physical and numerical model velocities for stations 396 and 1883

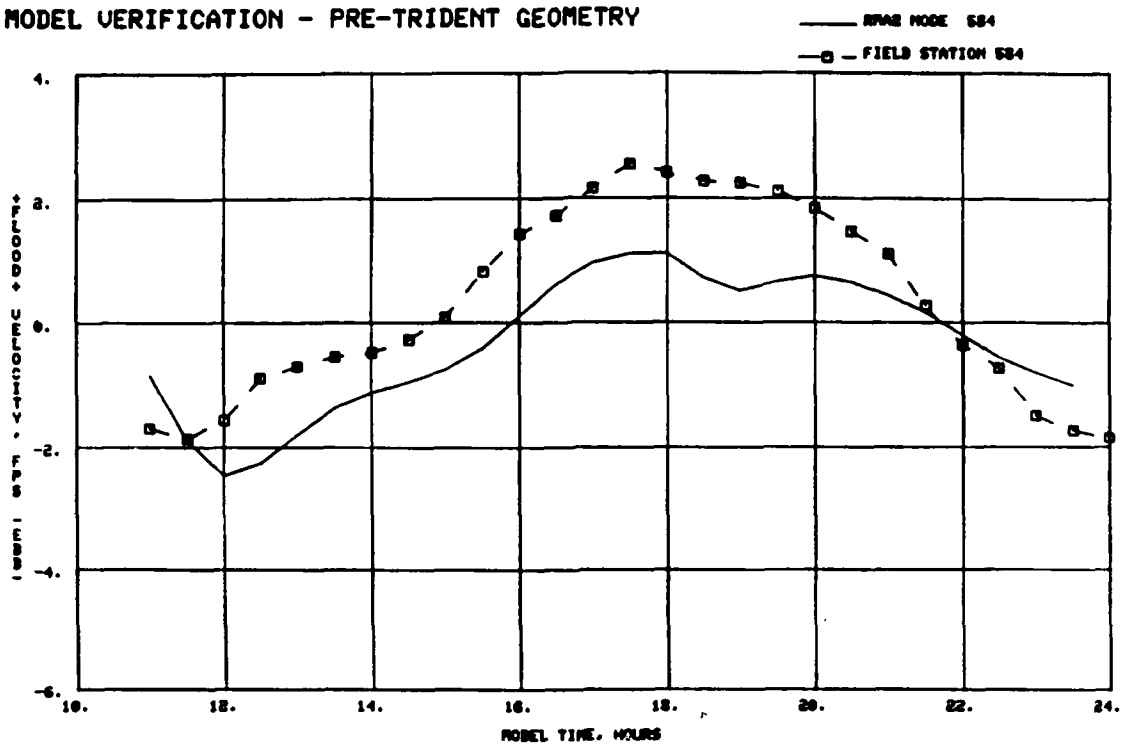

a. Station 584

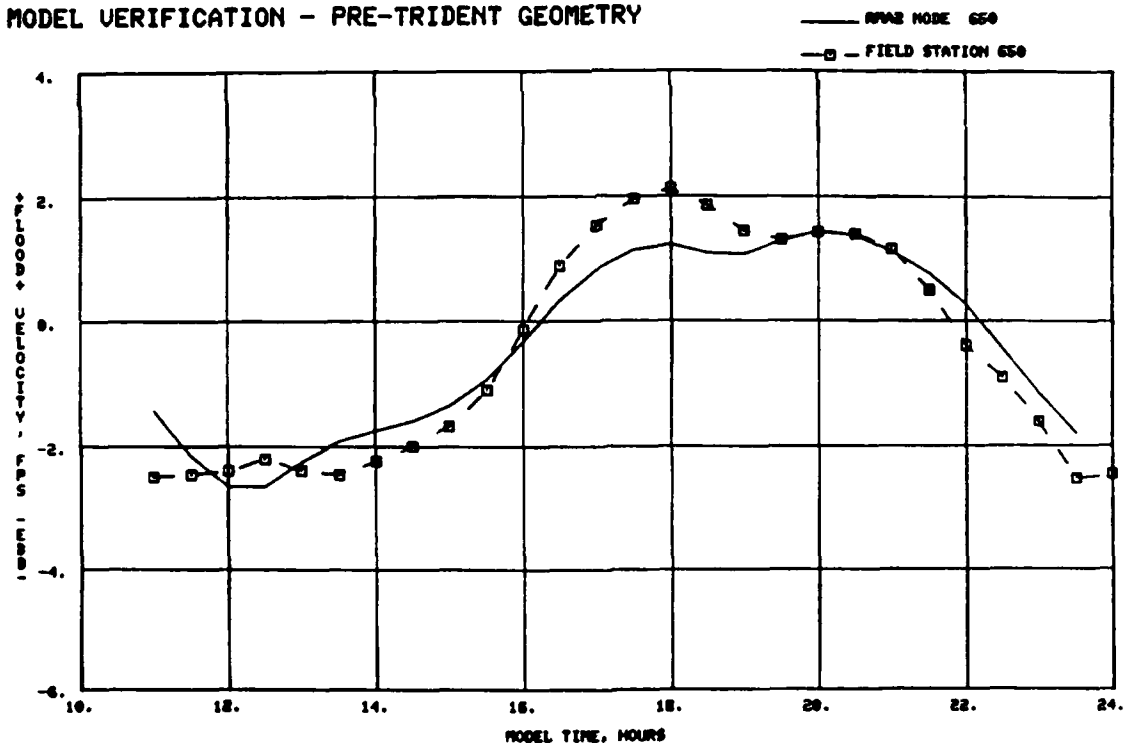

b. Station 650

Plate D13. Physical and numerical model velocities for stations 584 and 650

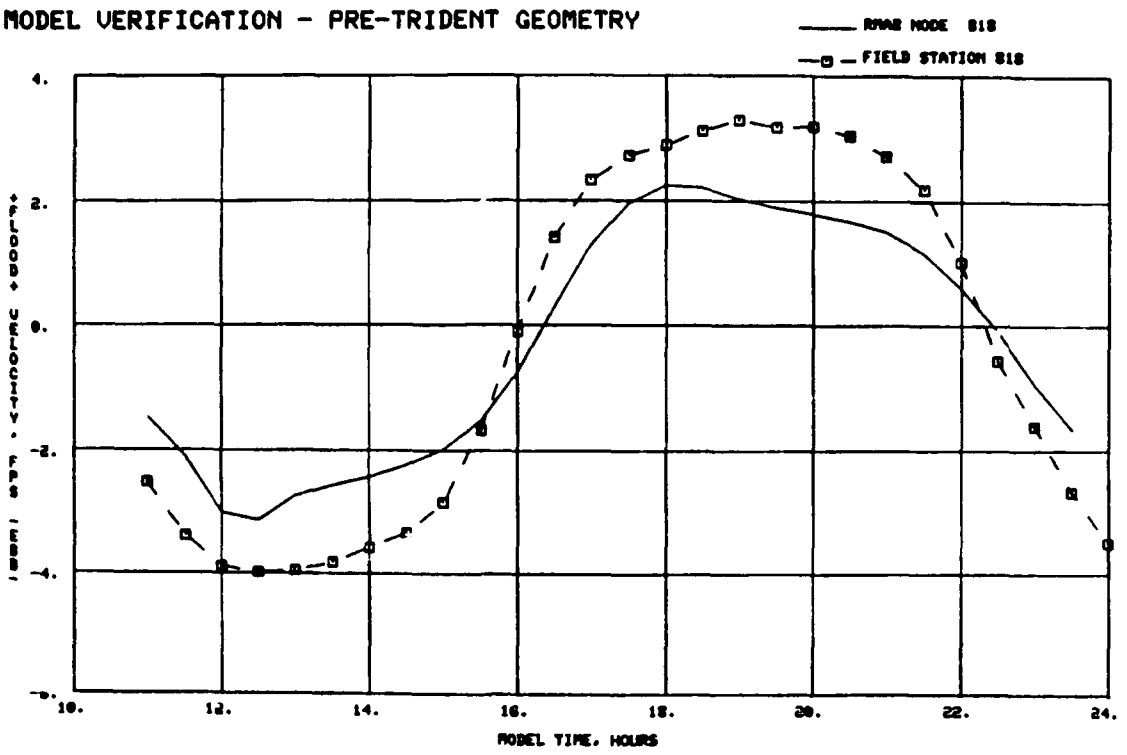

a. Station 818

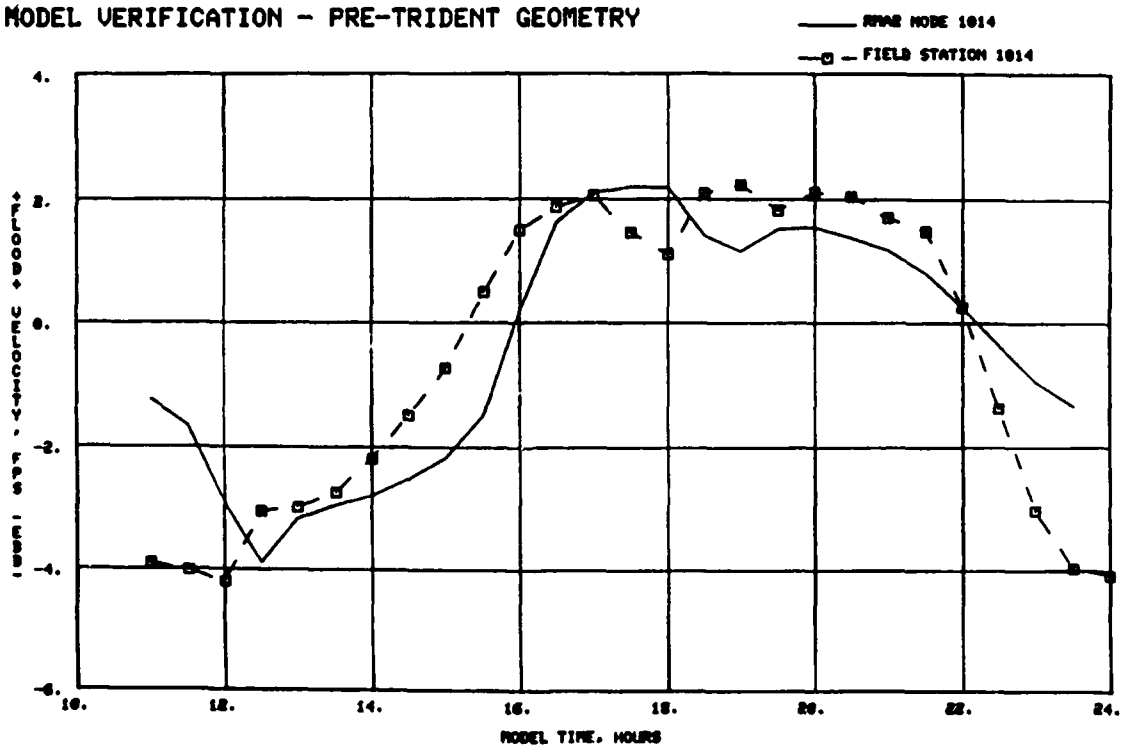

b. Station 1014

Plate D14. Physical and numerical model velocities for stations 818 and 1014

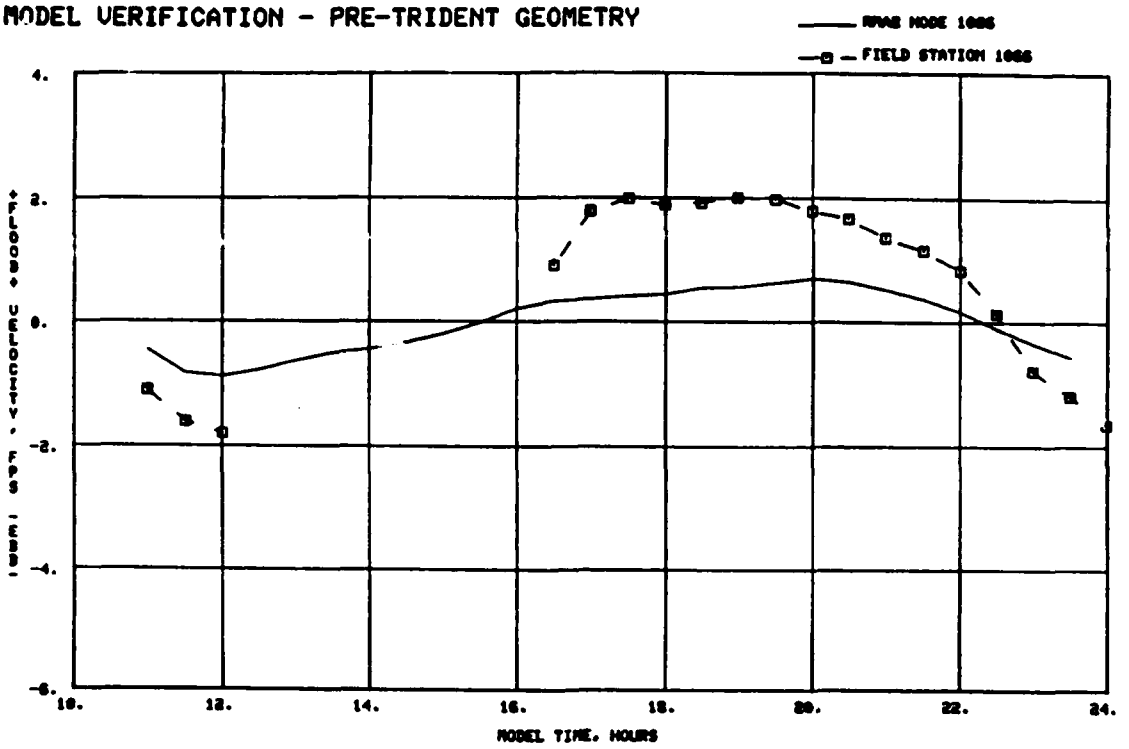

a. Station 1066 (physical model water depths were too shallow for measurements between hours 12.5 and 16.0)

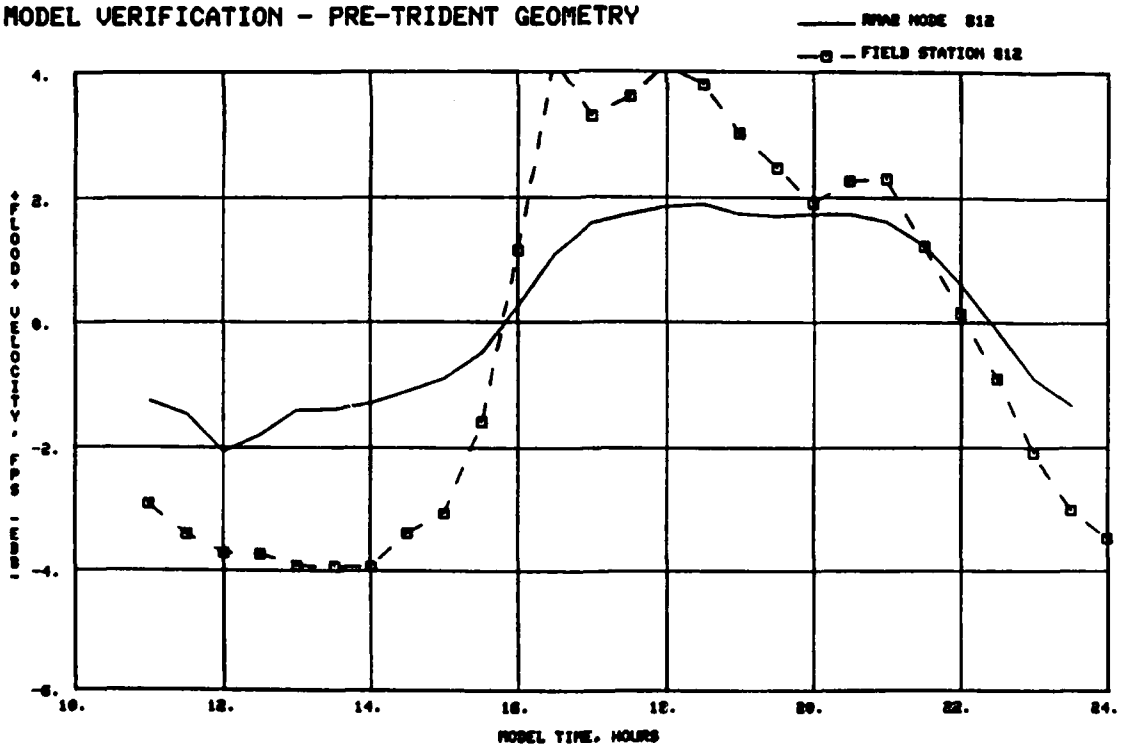

b. Station 812

Plate D15. Physical and numerical model velocities for stations 1066 and 812

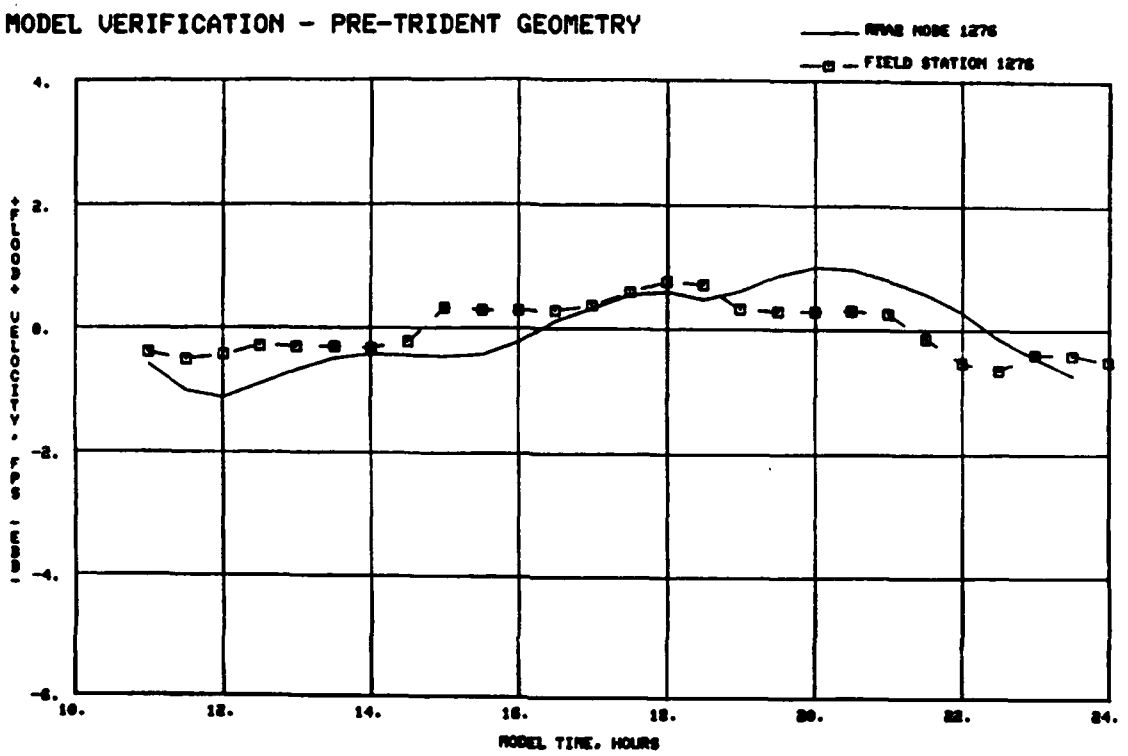

Plate D16. Physical and numerical model velocities for station 1276

APPENDIX E: NUMERICAL MODEL TRANSITIONAL CHANNEL VERIFICATION

NOTE: The term "field station" on plots in this appendix refers to stations in the physical model.

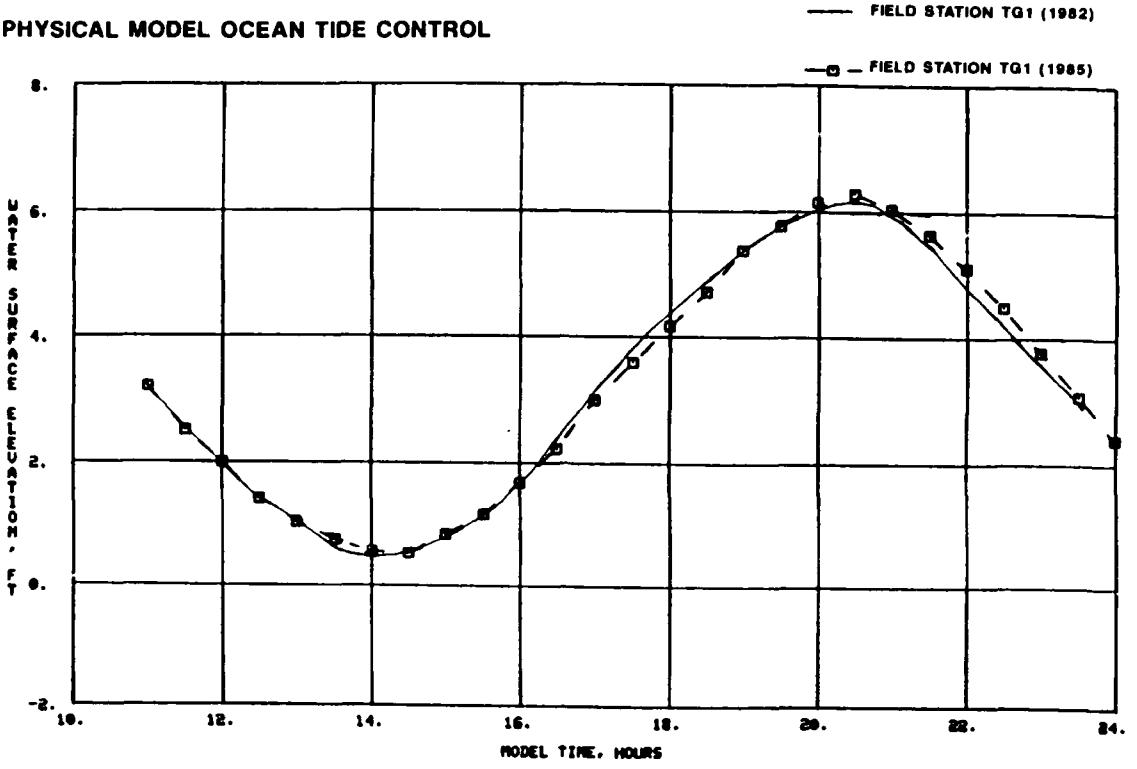

a. Physical model, ocean

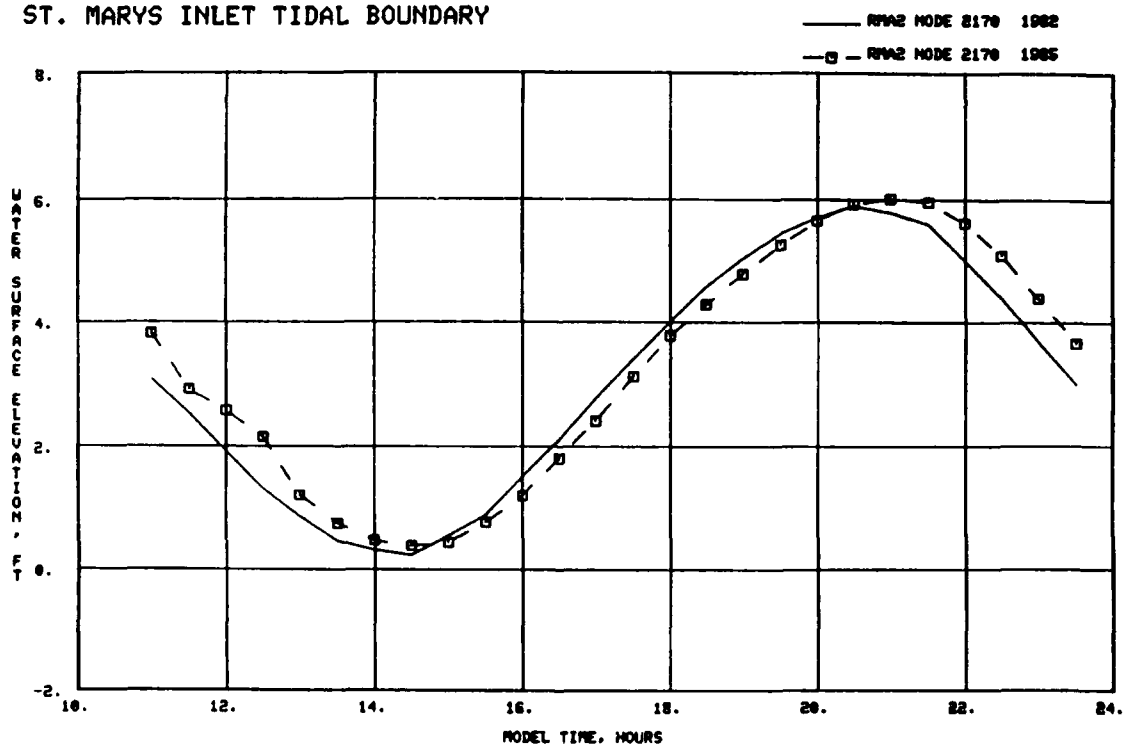

b. Numerical model, St. Marys Inlet

Plate E1. Tidal boundary forcing conditions, Pre-Trident and transitional channel

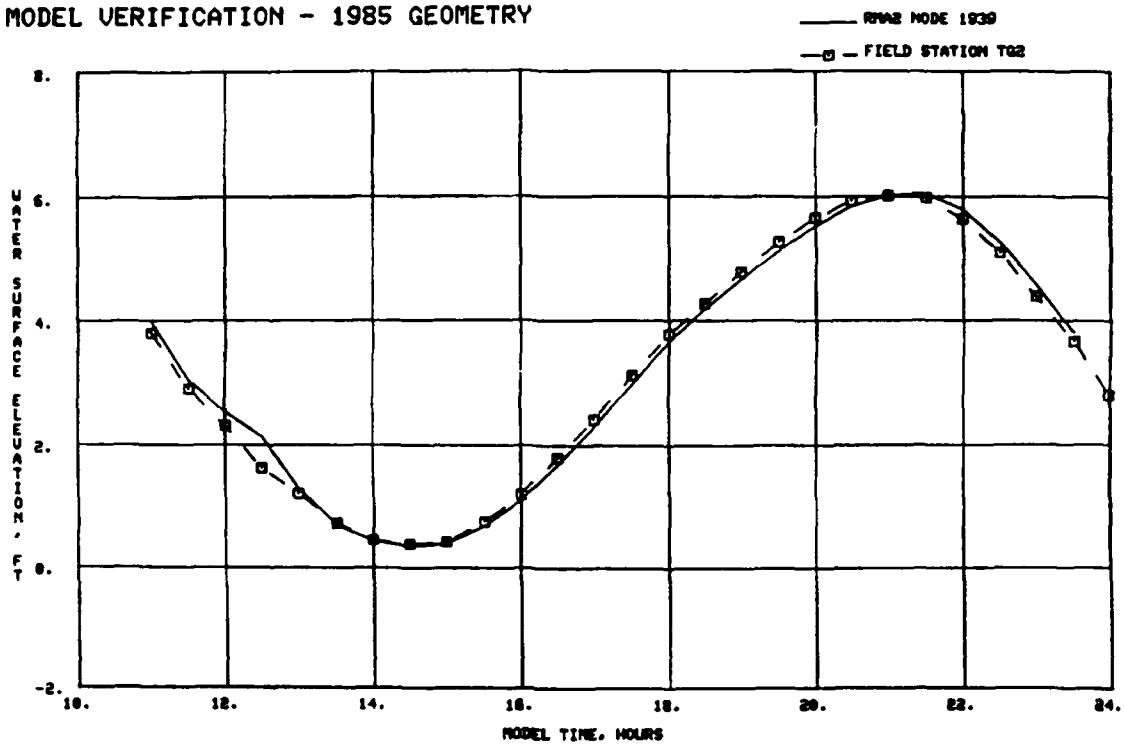

a. St. Marys Inlet

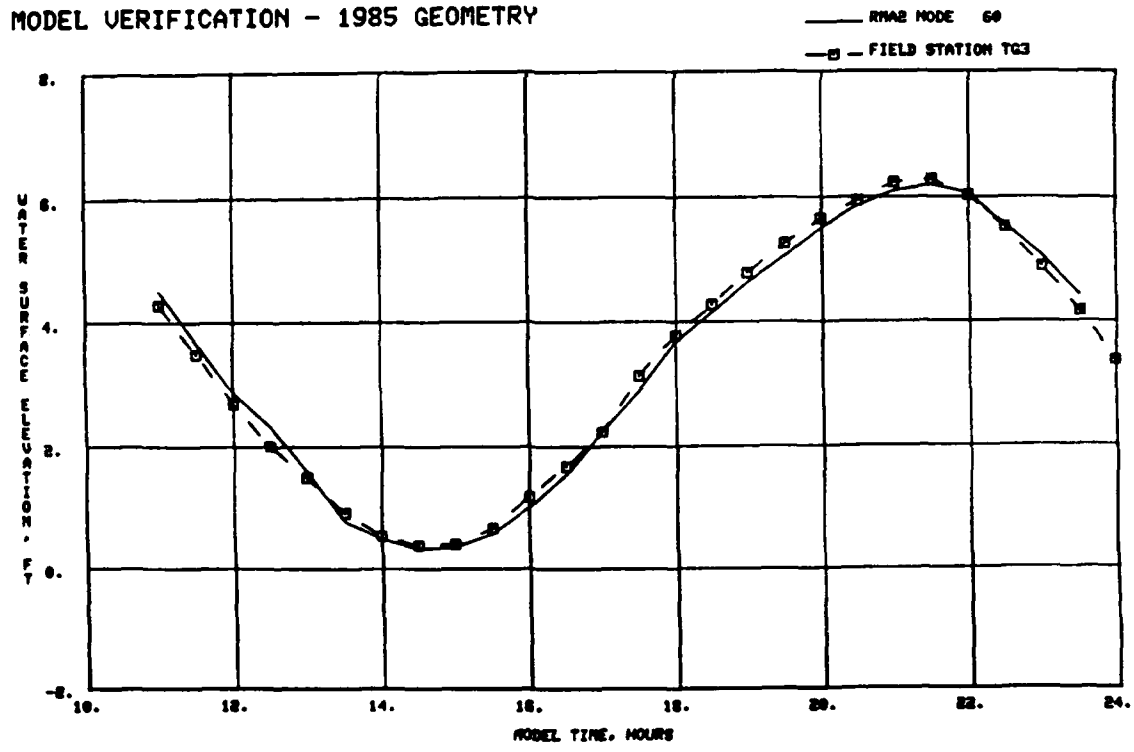

b. Amelia River

Plate E2. Water-surface elevations, physical and numerical model, for St. Marys Inlet and Amelia River

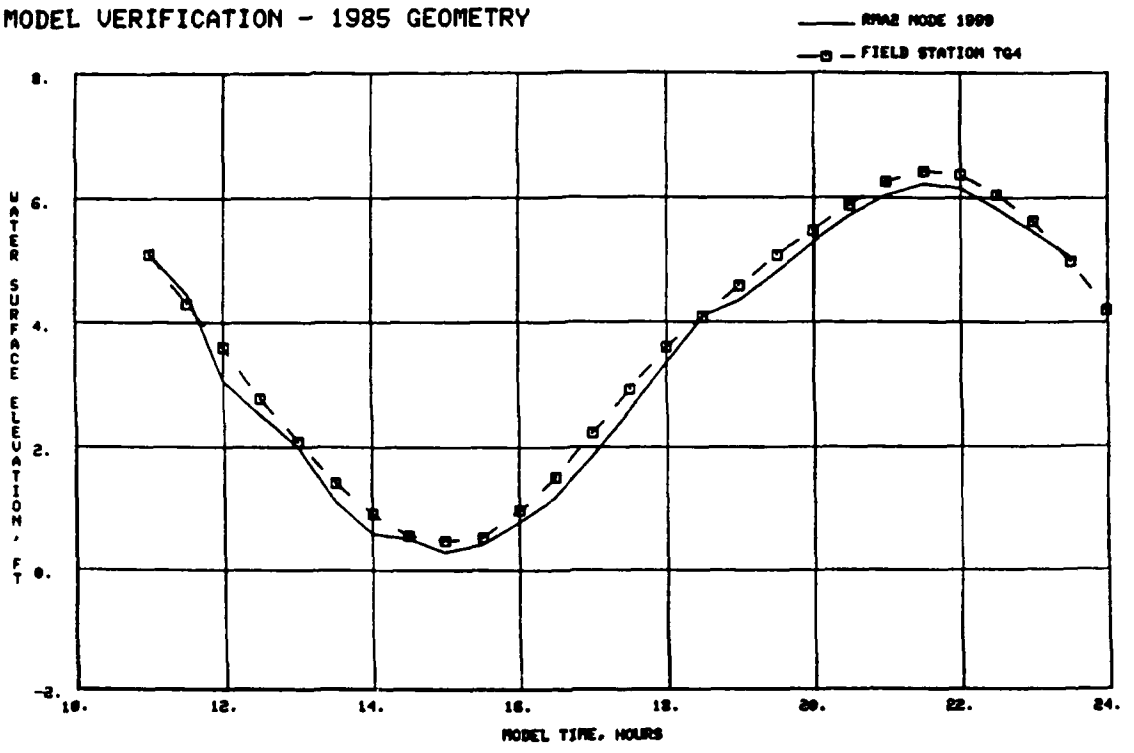

a. Jolly River

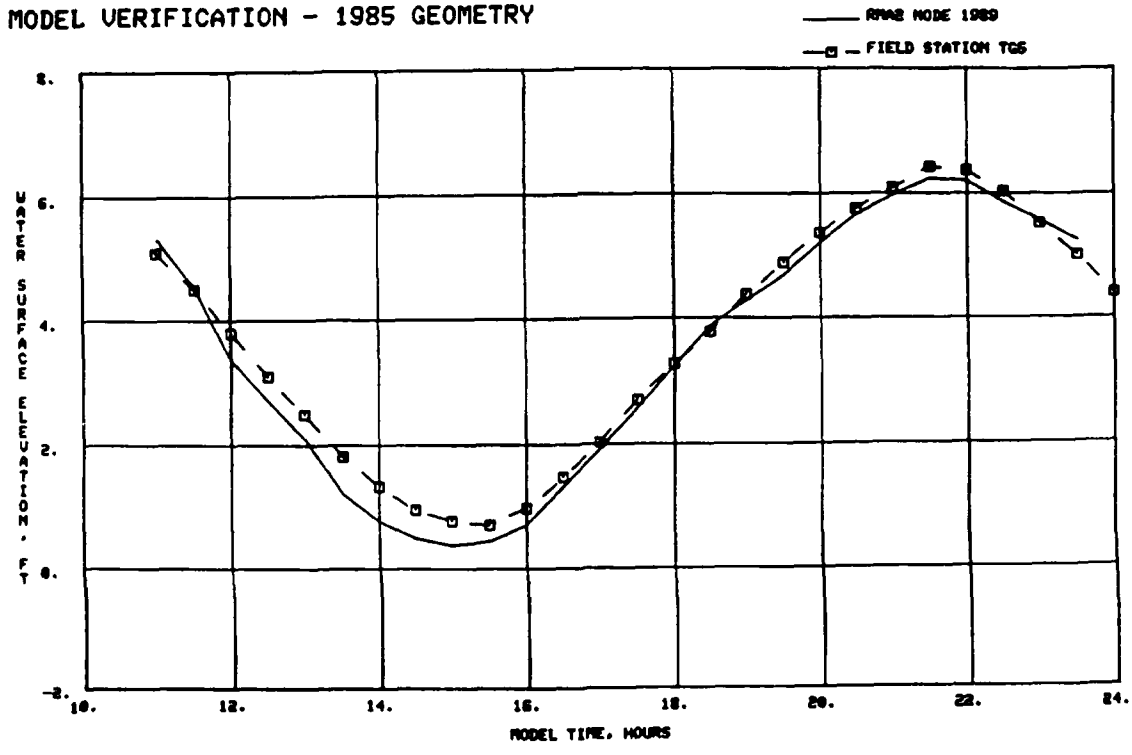

b. St. Marys River

Plate E3. Water-surface elevations, physical and numerical model, for Jolly River and St. Marys River

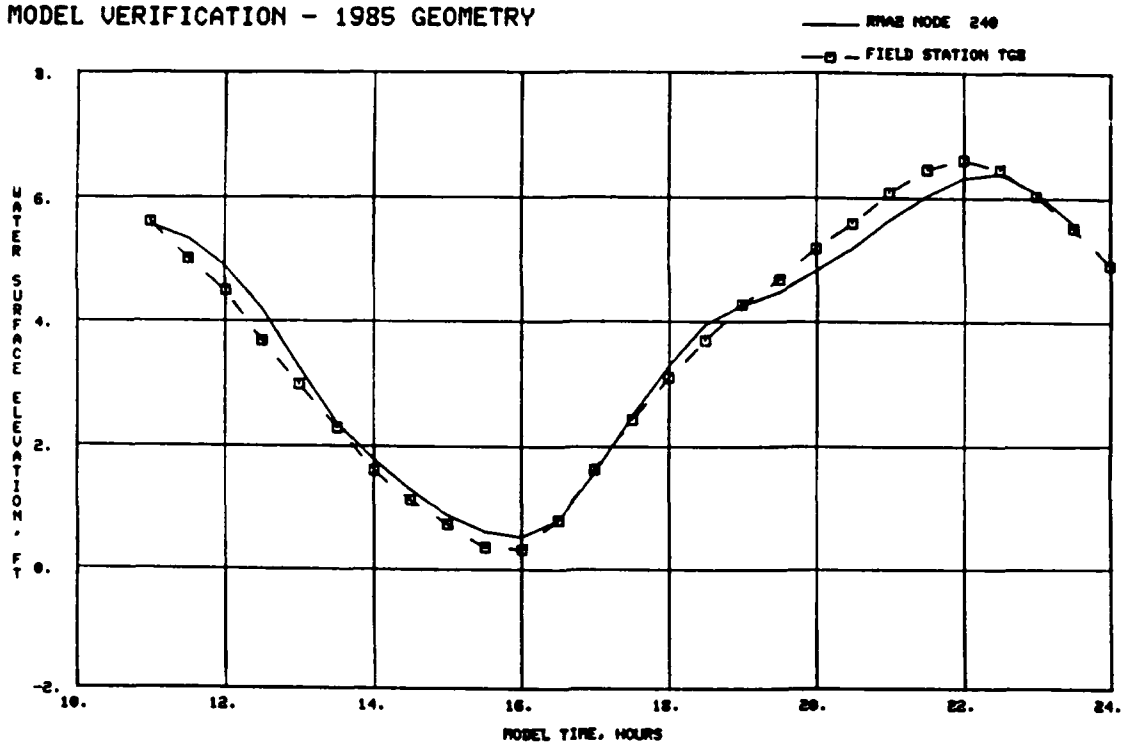

a. Crooked River

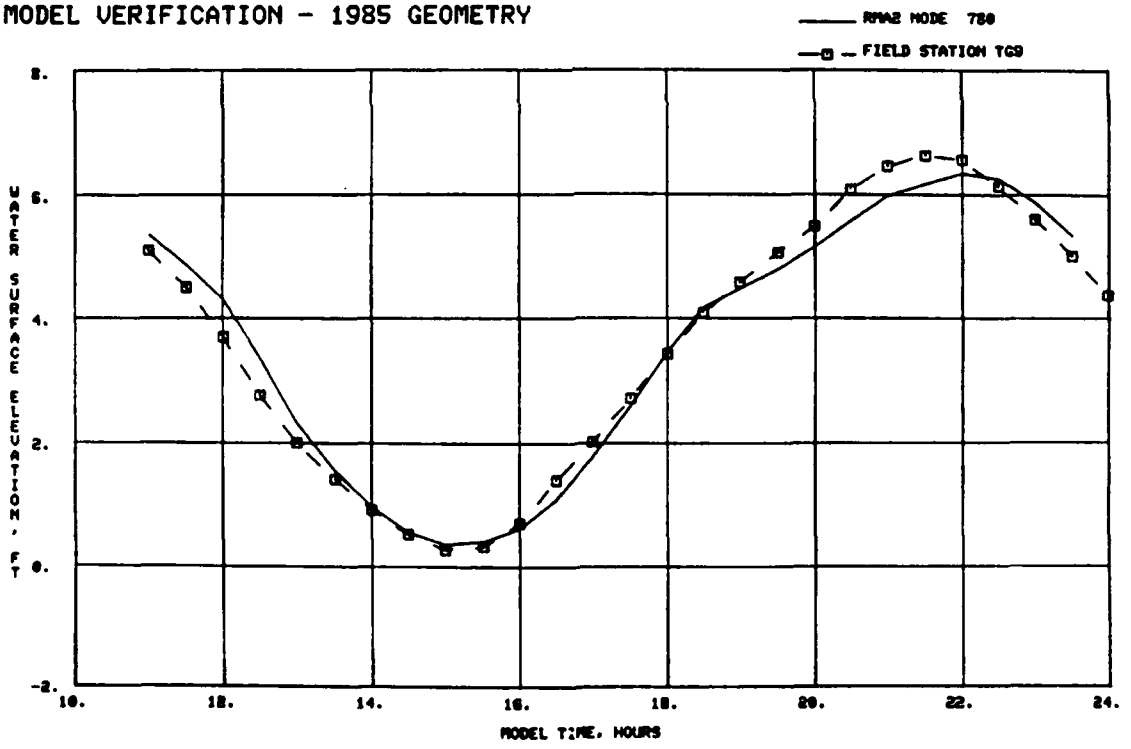

b. Northern Cumberland Sound

Plate E5. Water-surface elevations, physical and numerical model, for Crooked River and northern Cumberland Sound

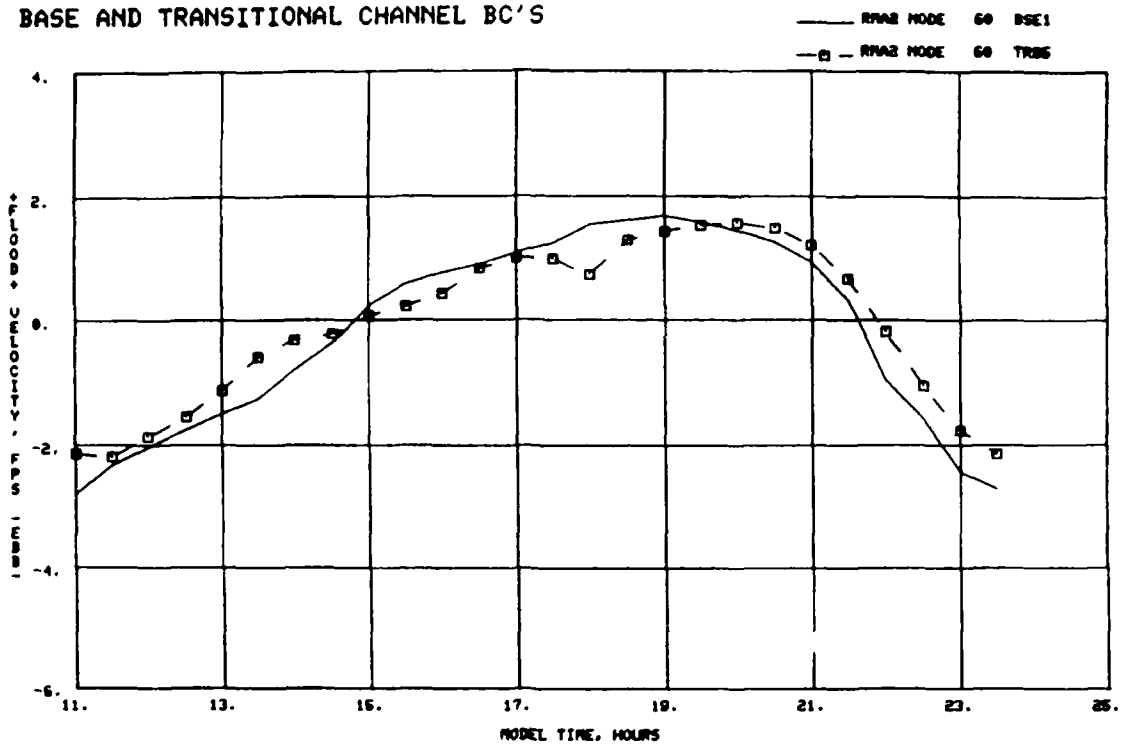

a. Node 60

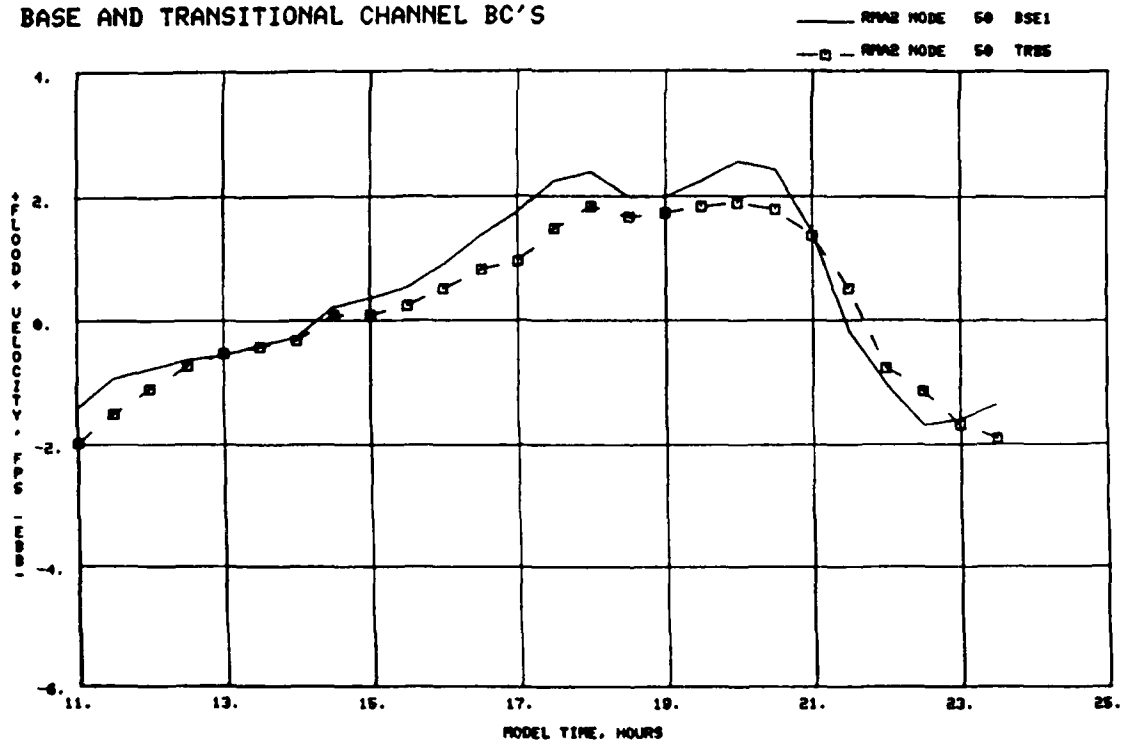

b. Node 50

Plate E6. Velocity boundary forcing conditions for nodes 60 and 50

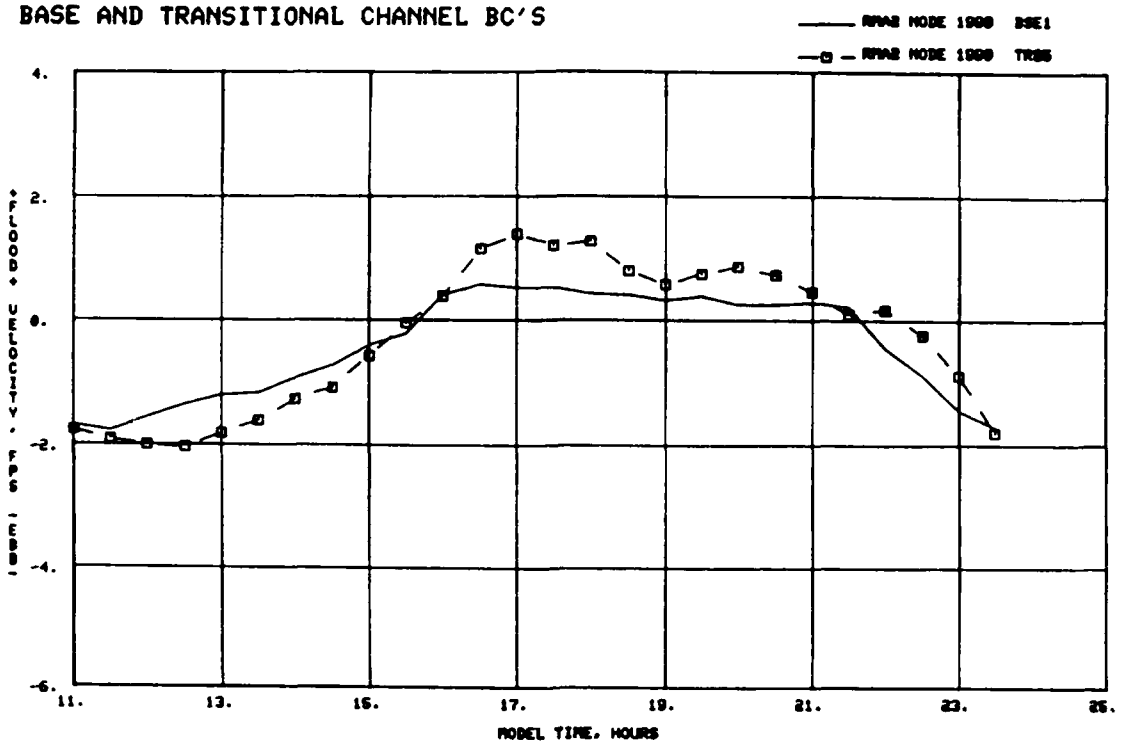

a. Node 1999

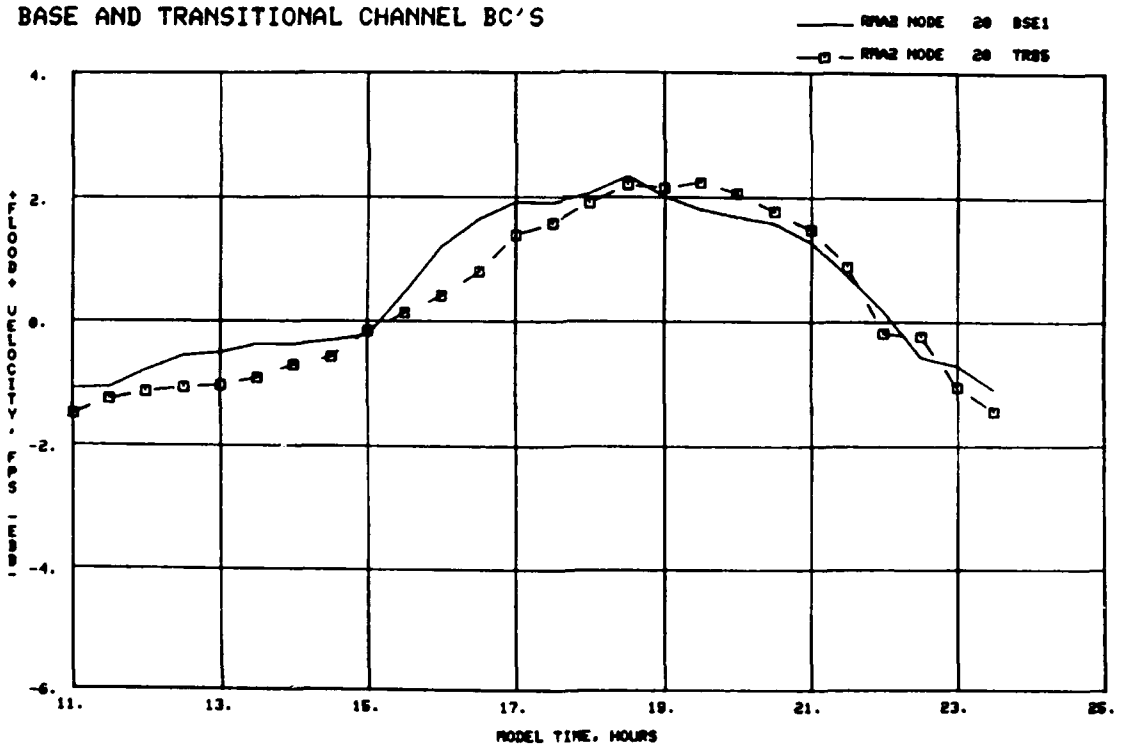

b. Node 20

Plate E7. Velocity boundary forcing conditions for nodes 1999 and 20

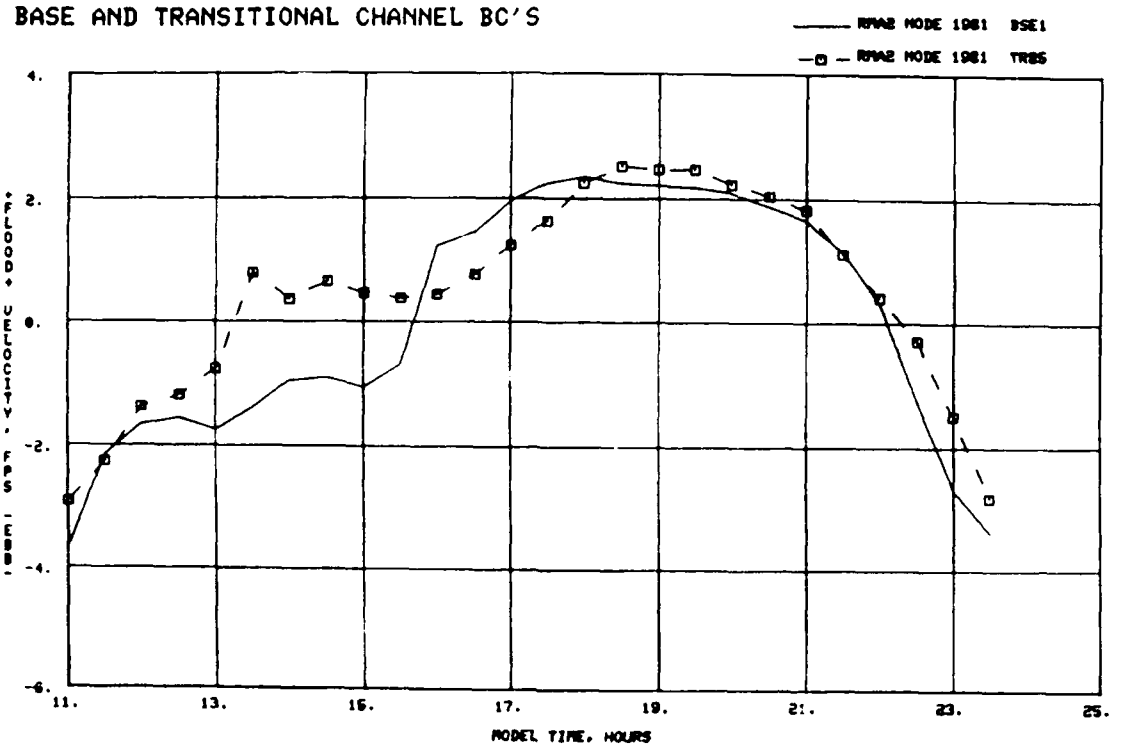

a. Node 1981

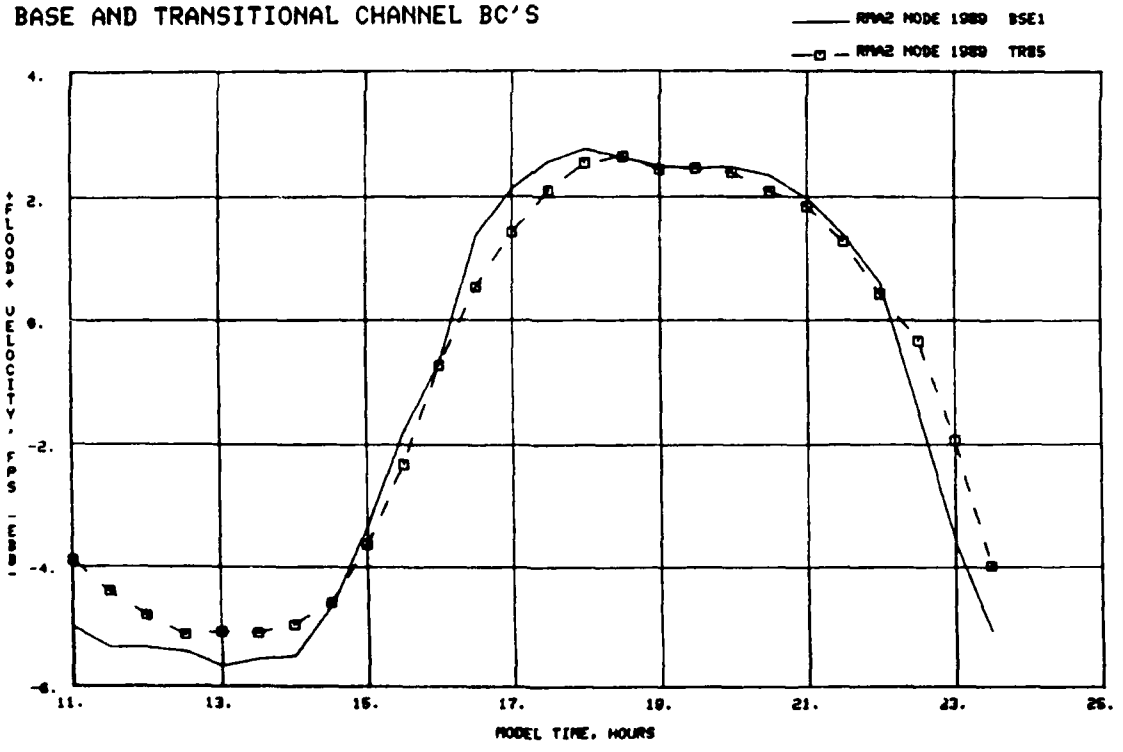

b. Node 1989

Plate E8. Velocity boundary forcing conditions for nodes 1981 and 1989

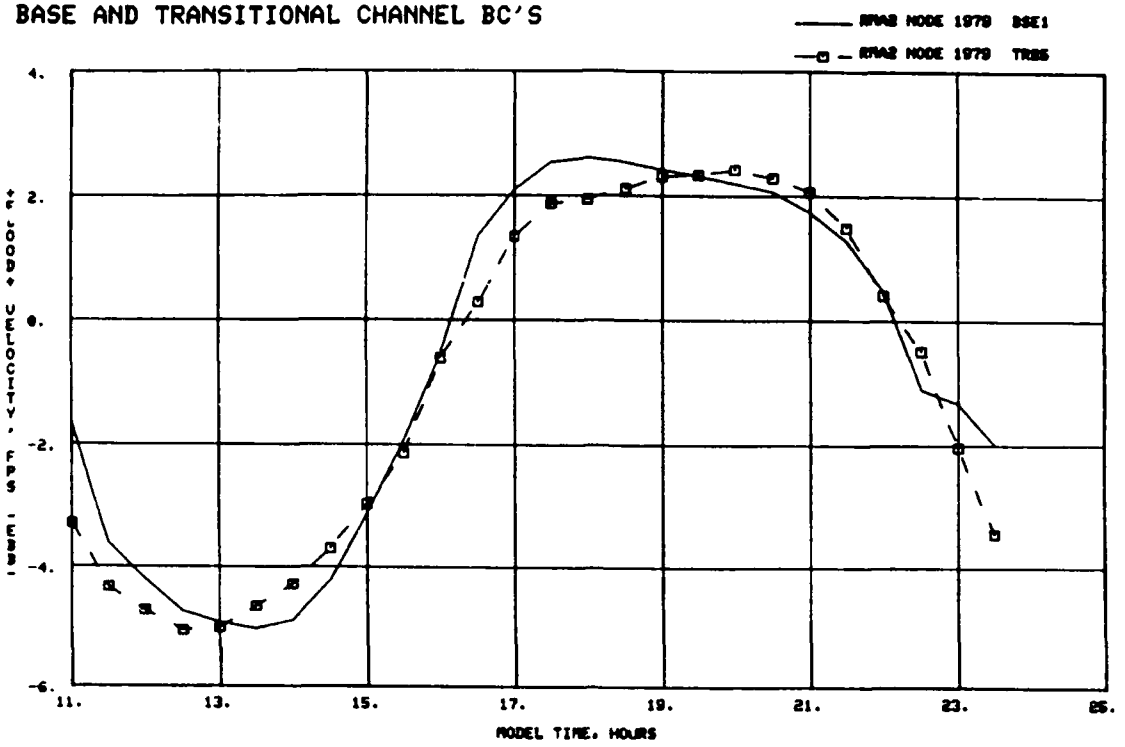

a. Node 1979

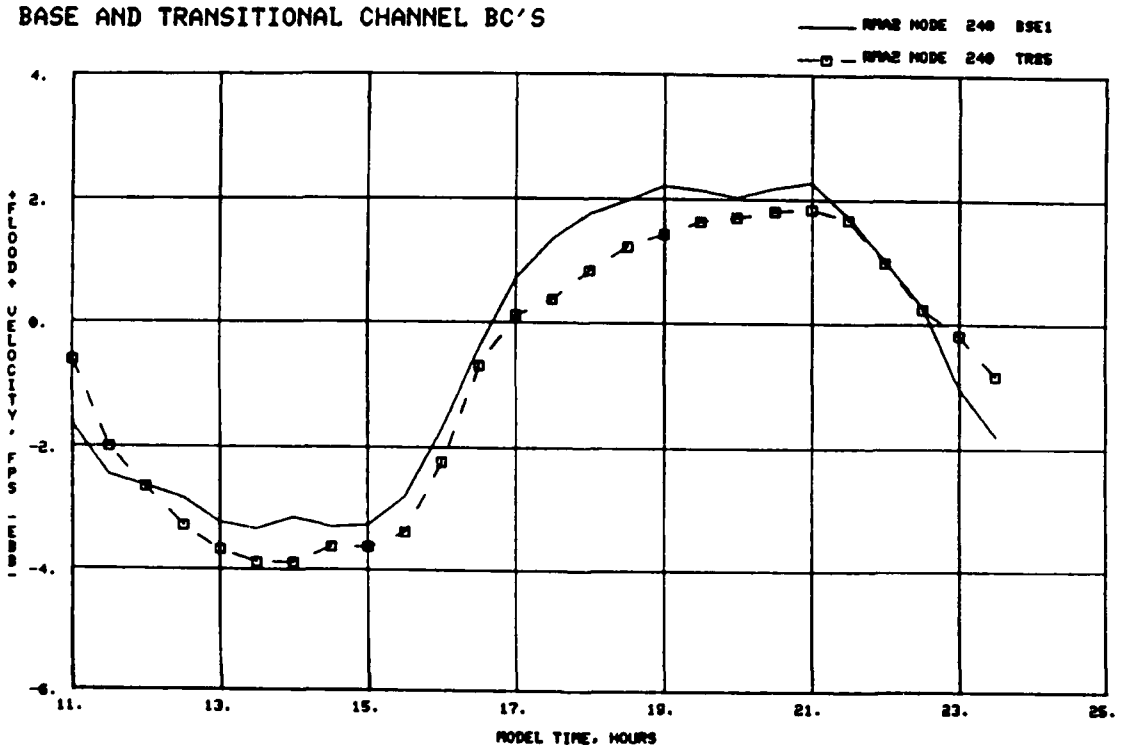

b. Node 240

Plate E9. Velocity boundary forcing conditions for nodes 1979 and 240

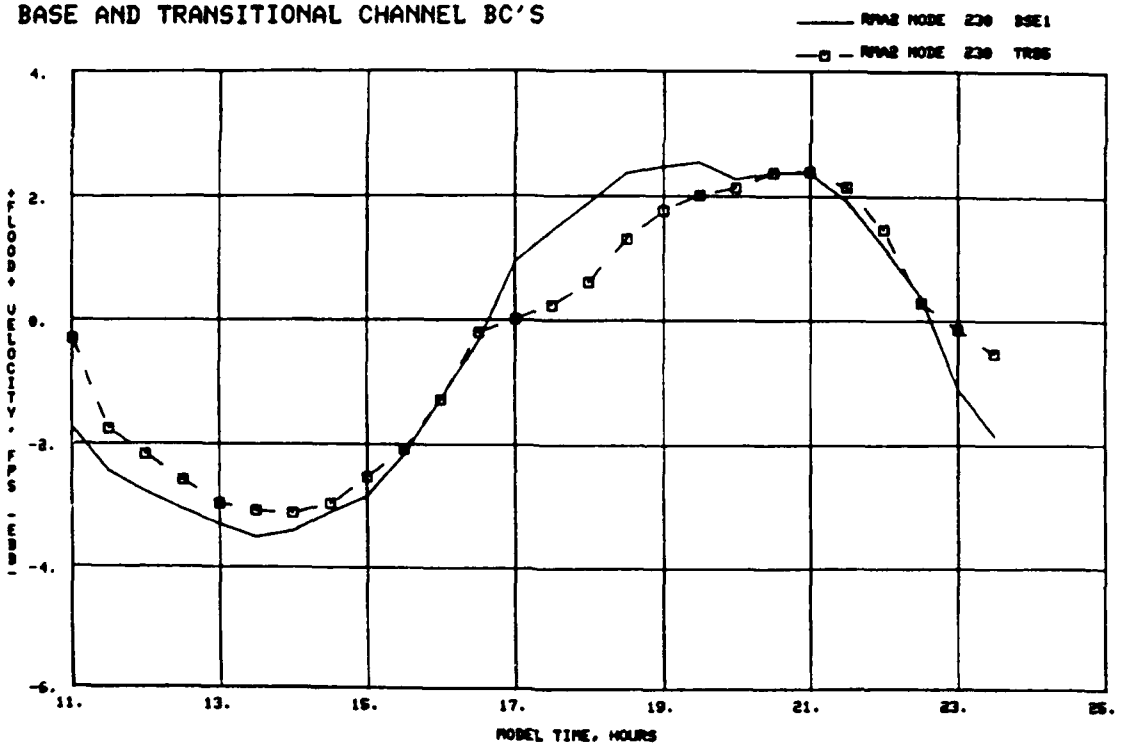

a. Node 230

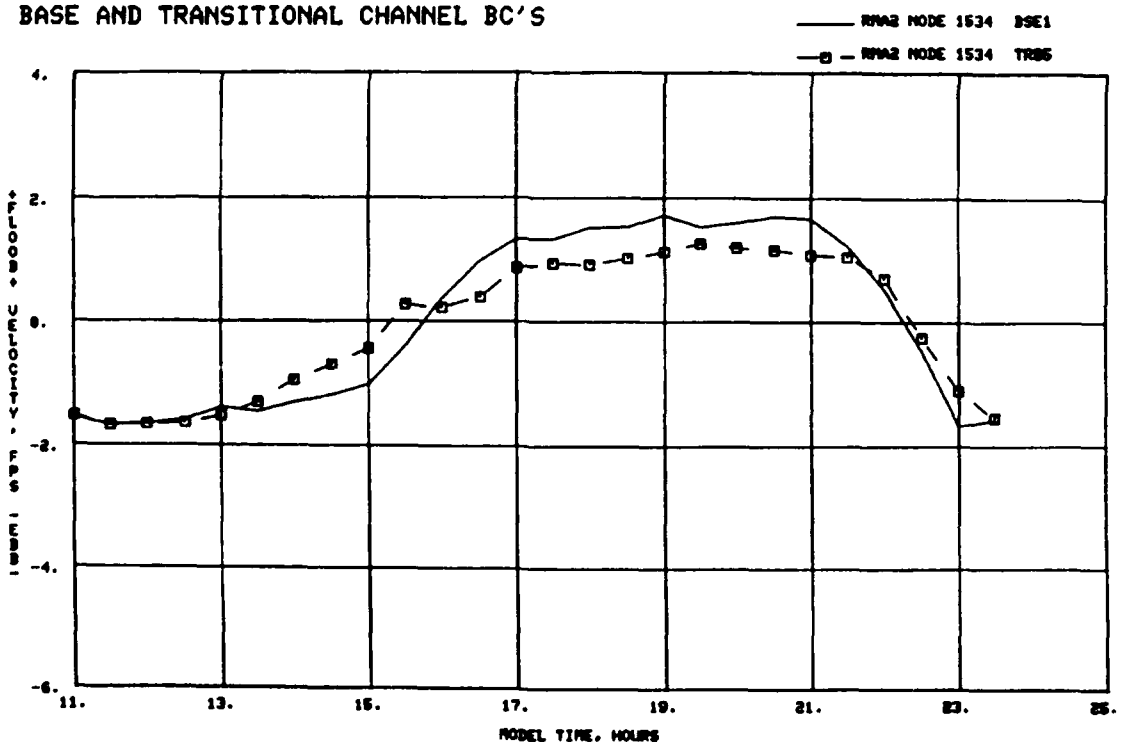

b. Node 1534

Plate E10. Velocity boundary forcing conditions for nodes 230 and 1534

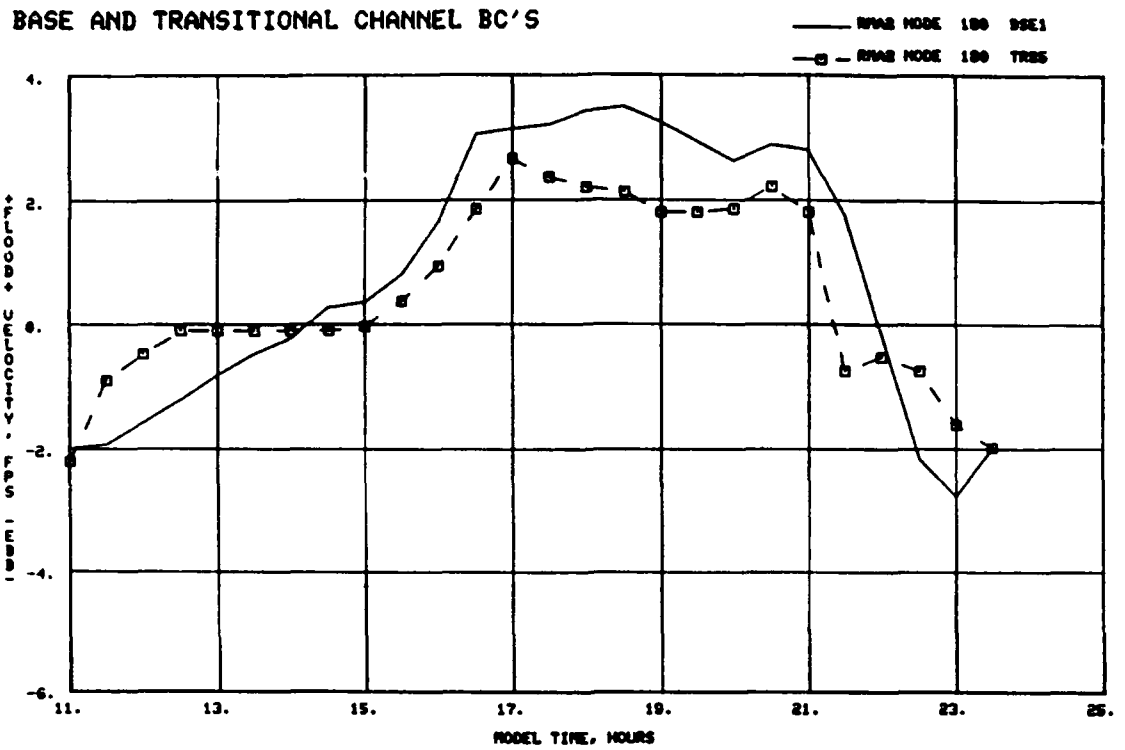

a. Node 180

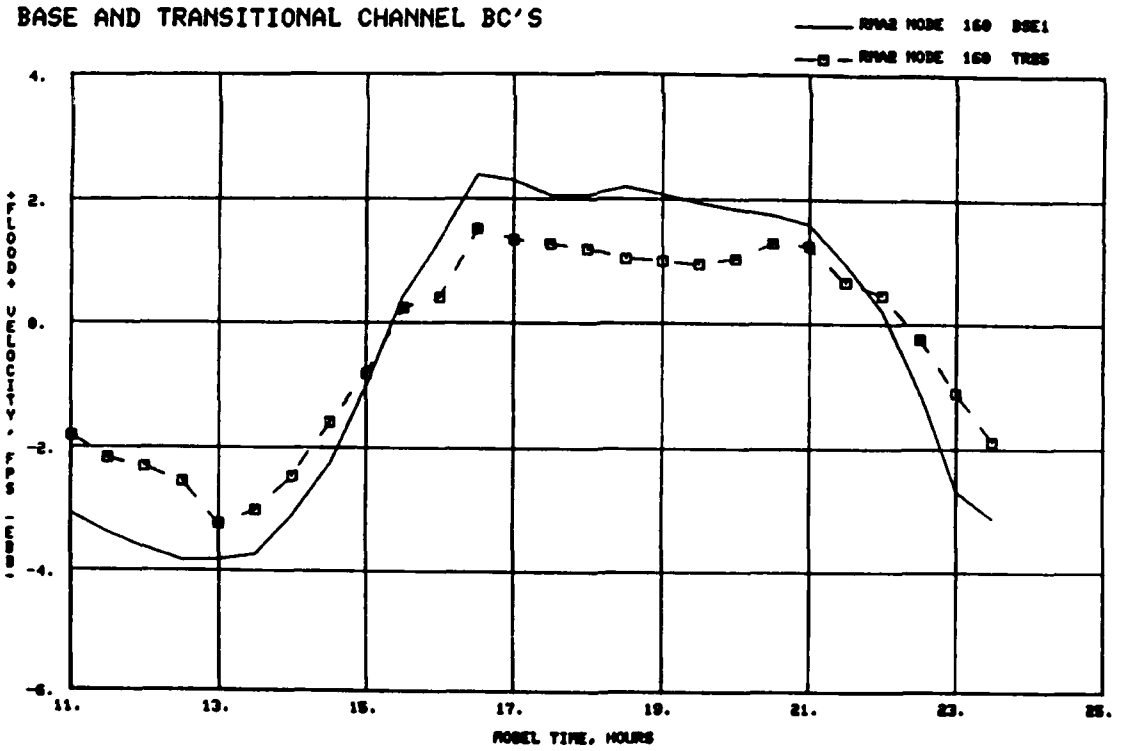

b. Node 160

Plate E11. Velocity boundary forcing conditions for nodes 180 and 160

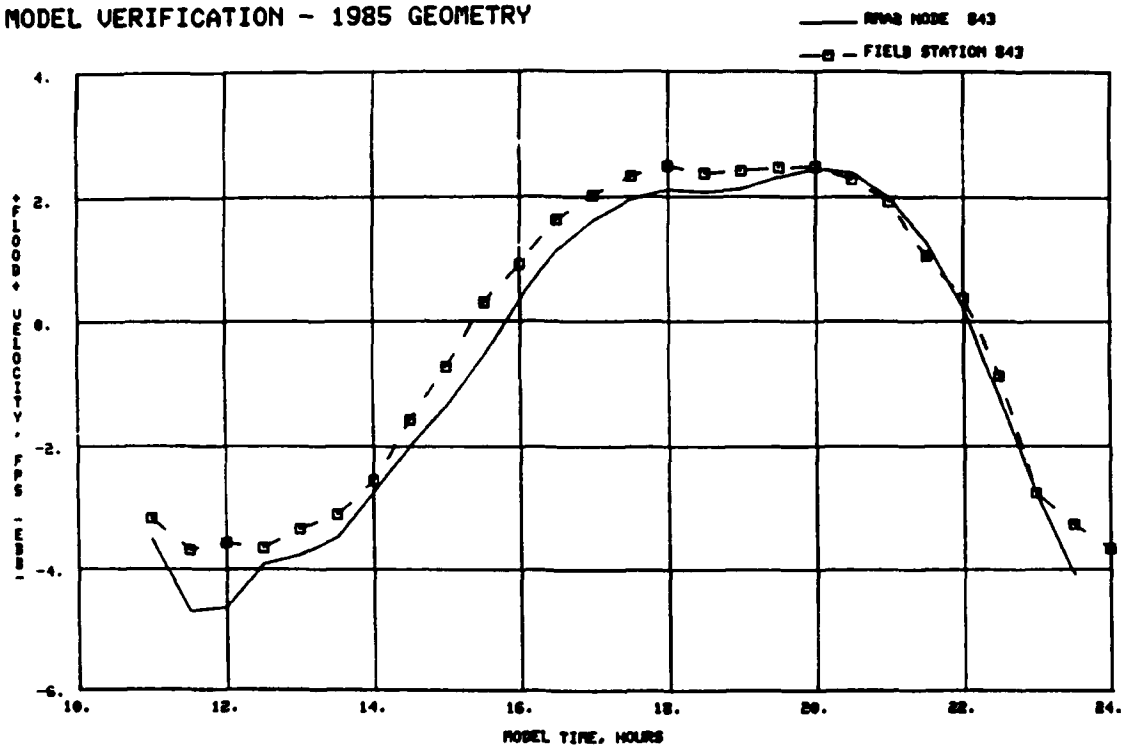

a. Station 843

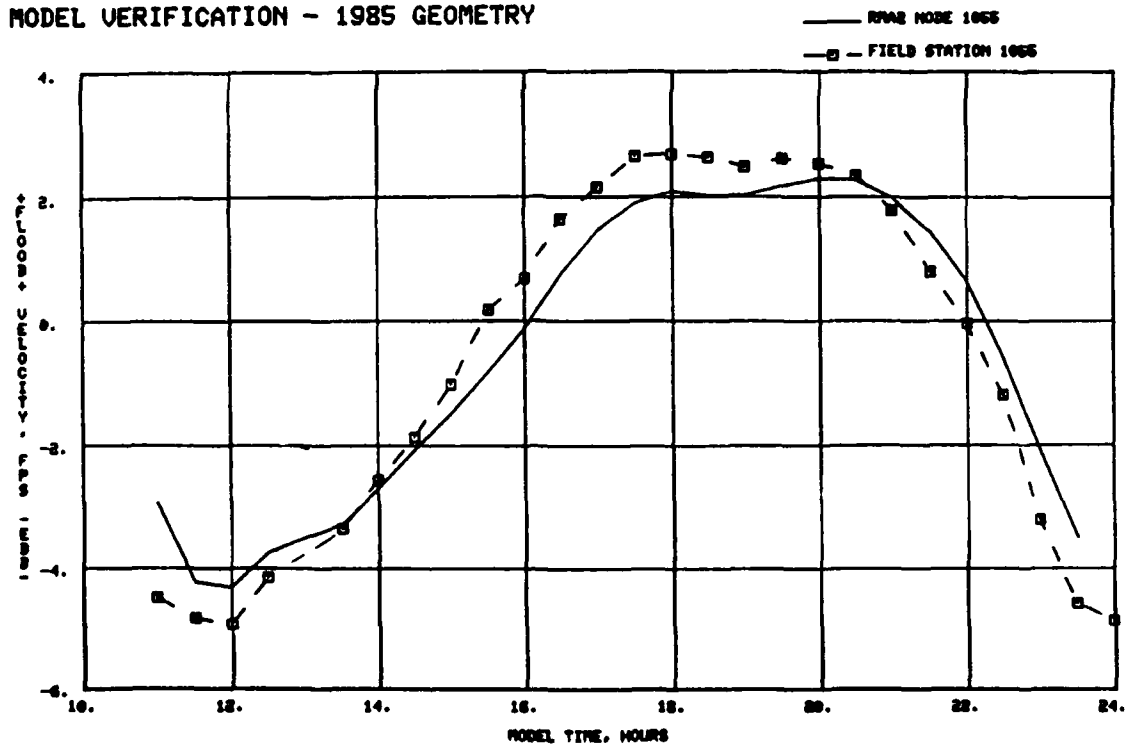

b. Station 1055

Plate E12. Physical and numerical model velocities for stations 843 and 1055

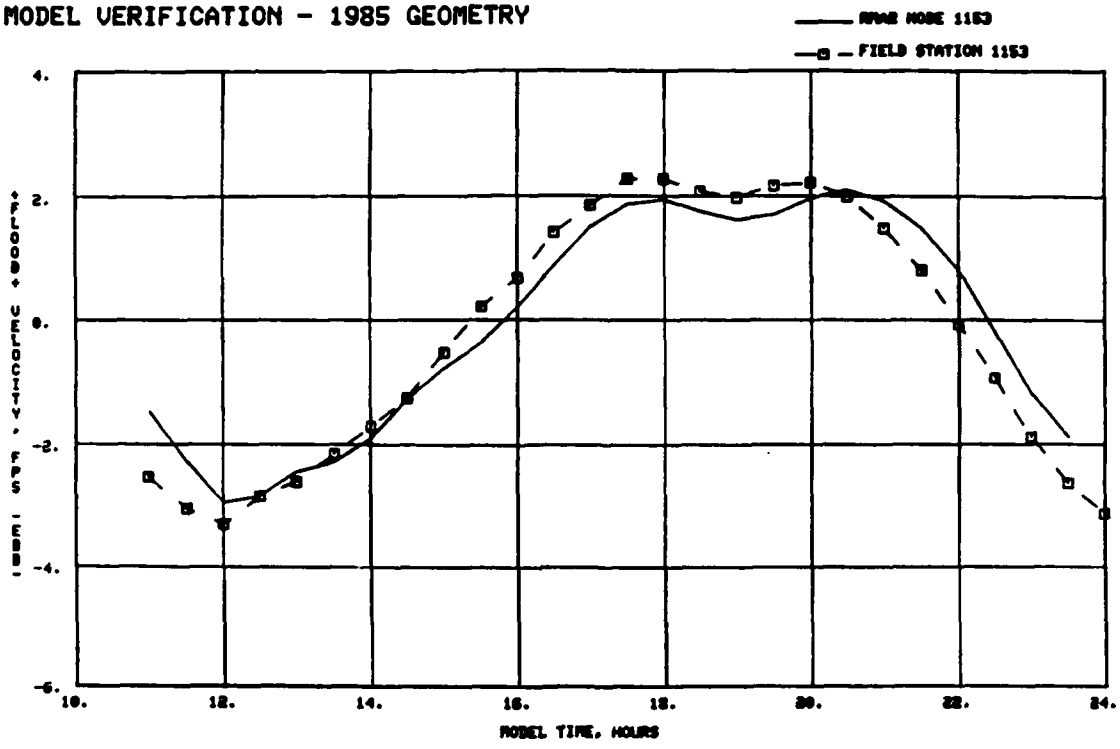

a. Station 1153

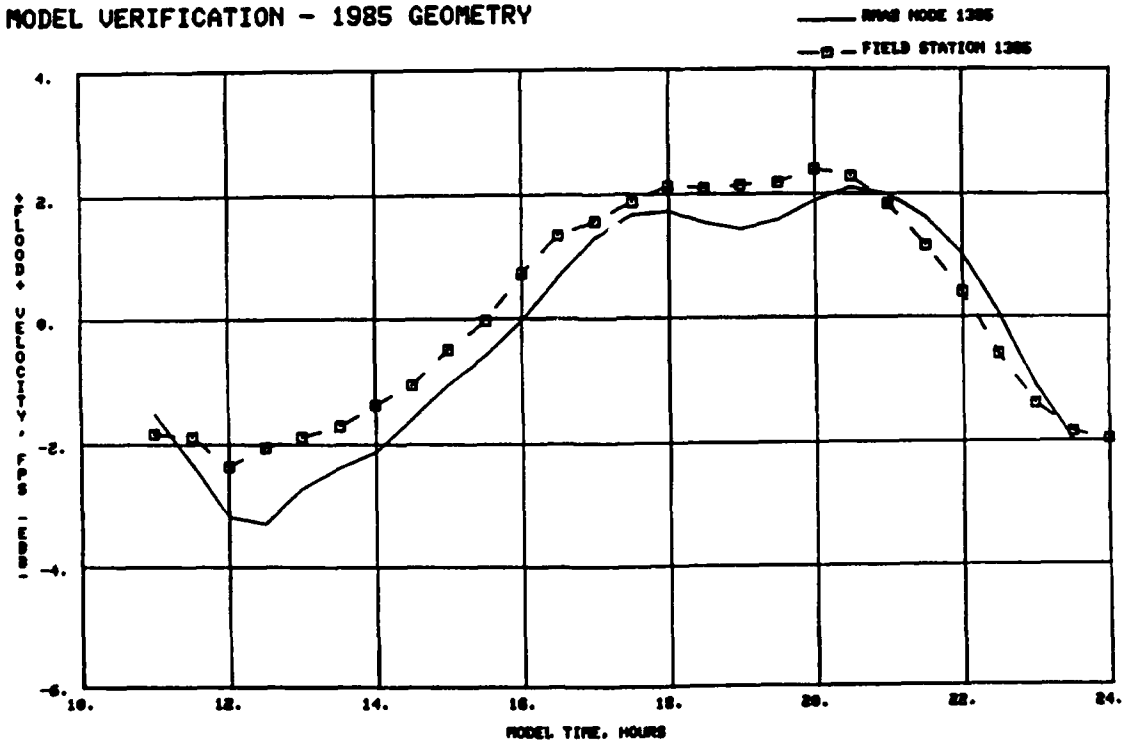

b. Station 1385

Plate E13. Physical and numerical model velocities for stations 1153 and 1385

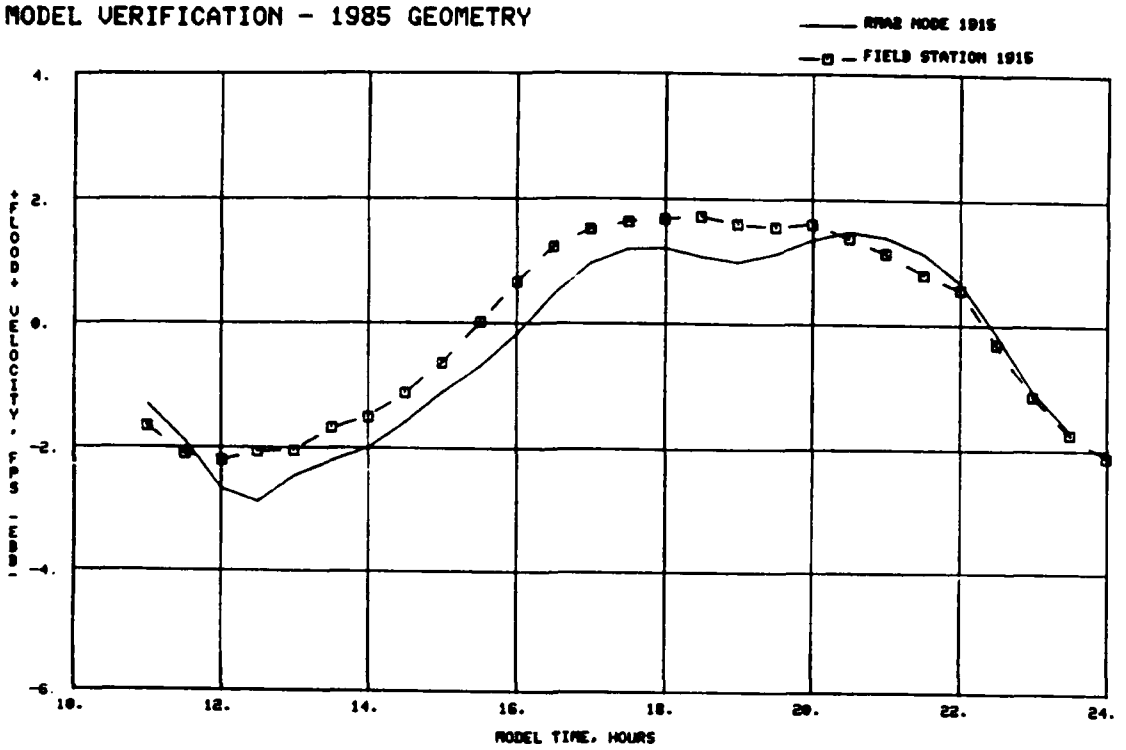

a. Station 1915

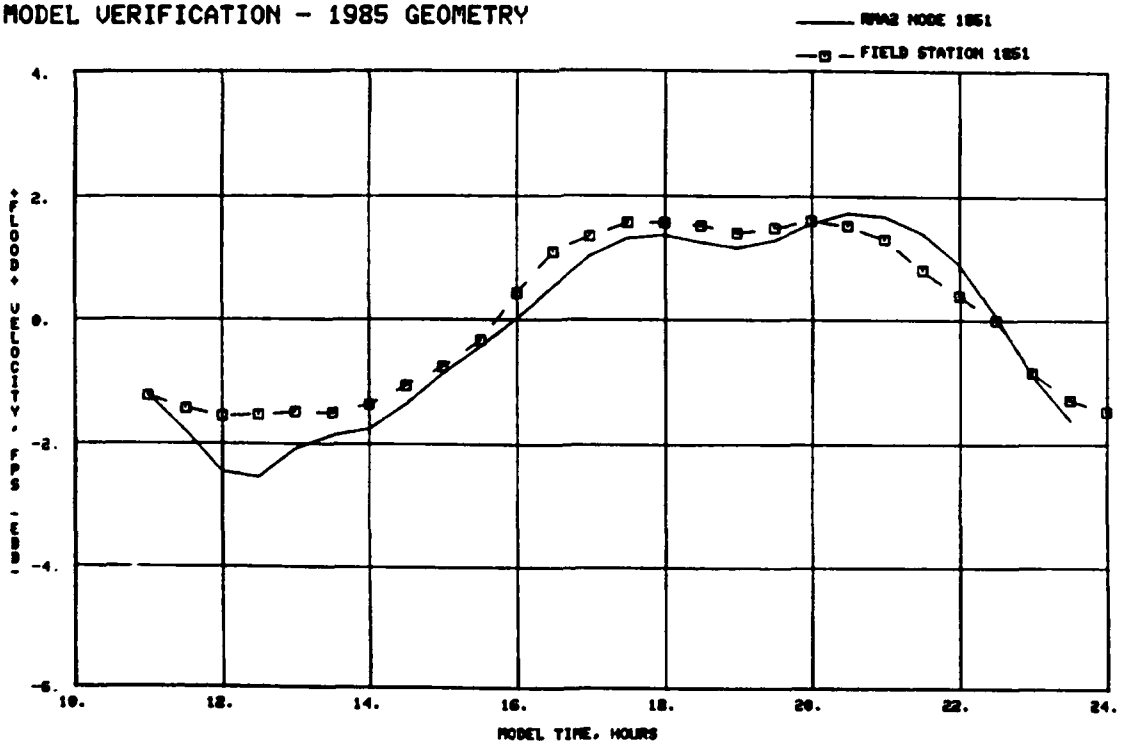

b. Station 1851

Plate E14. Physical and numerical model velocities for stations 1915 and 1851

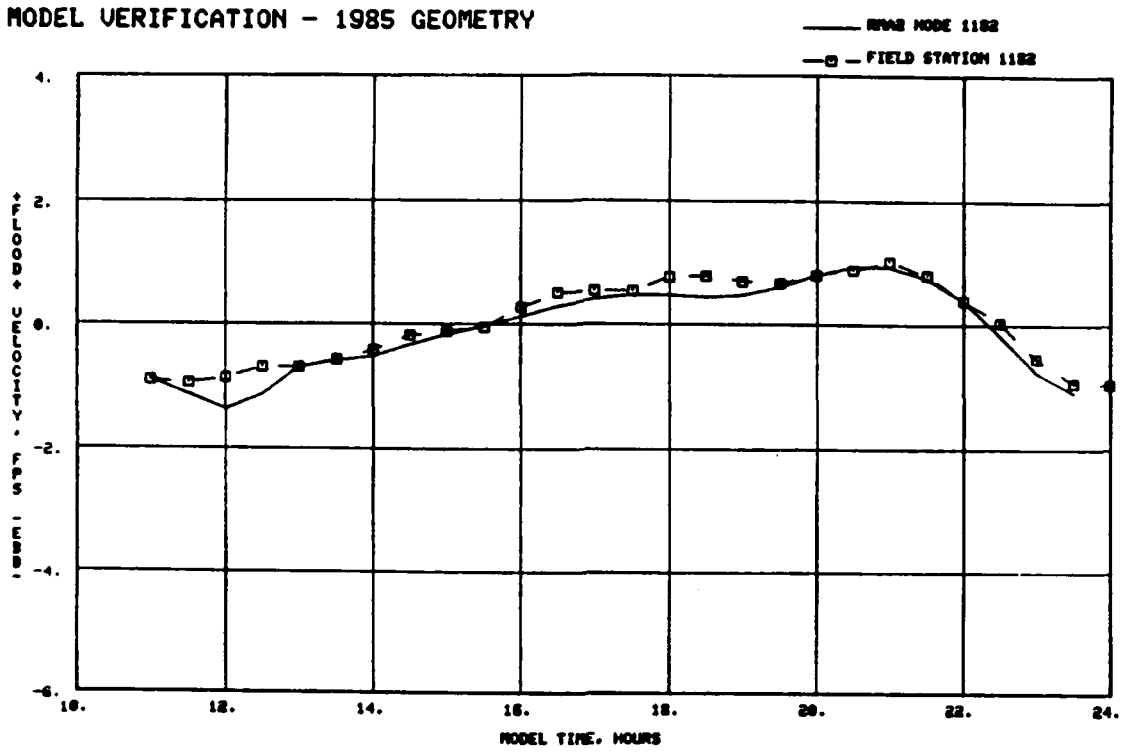

a. Station 1182

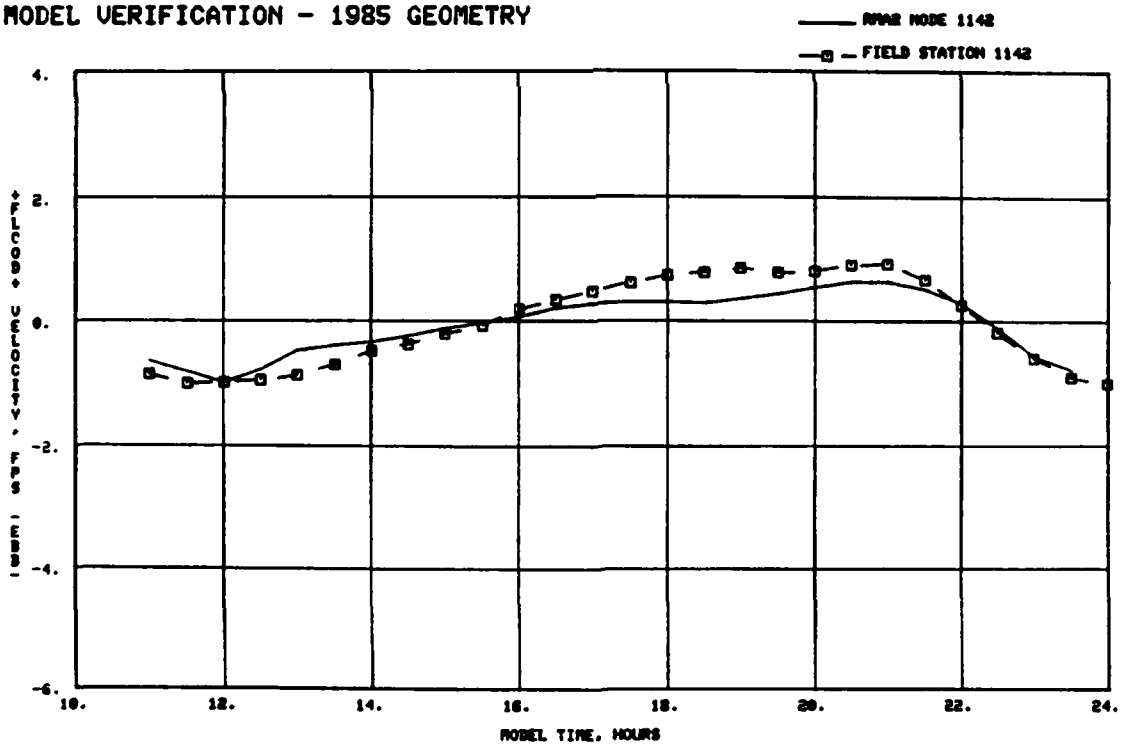

b. Station 1142

Plate E15. Physical and numerical model velocities for stations 1182 and 1142

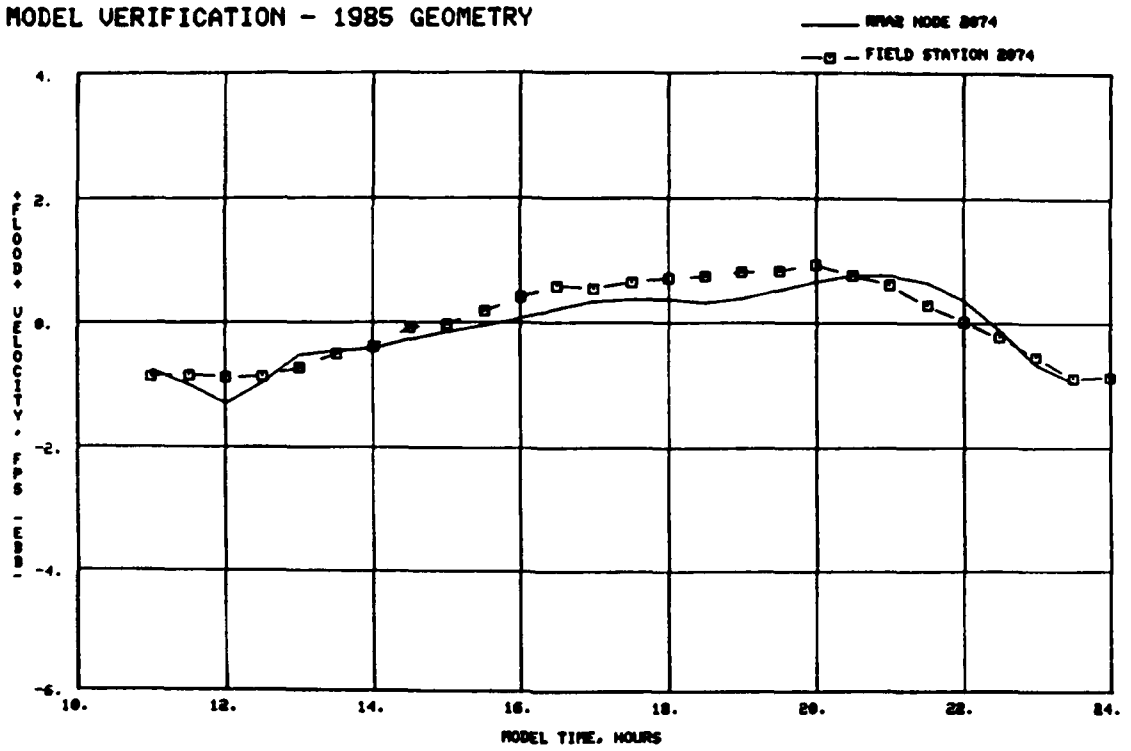

a. Station 2074

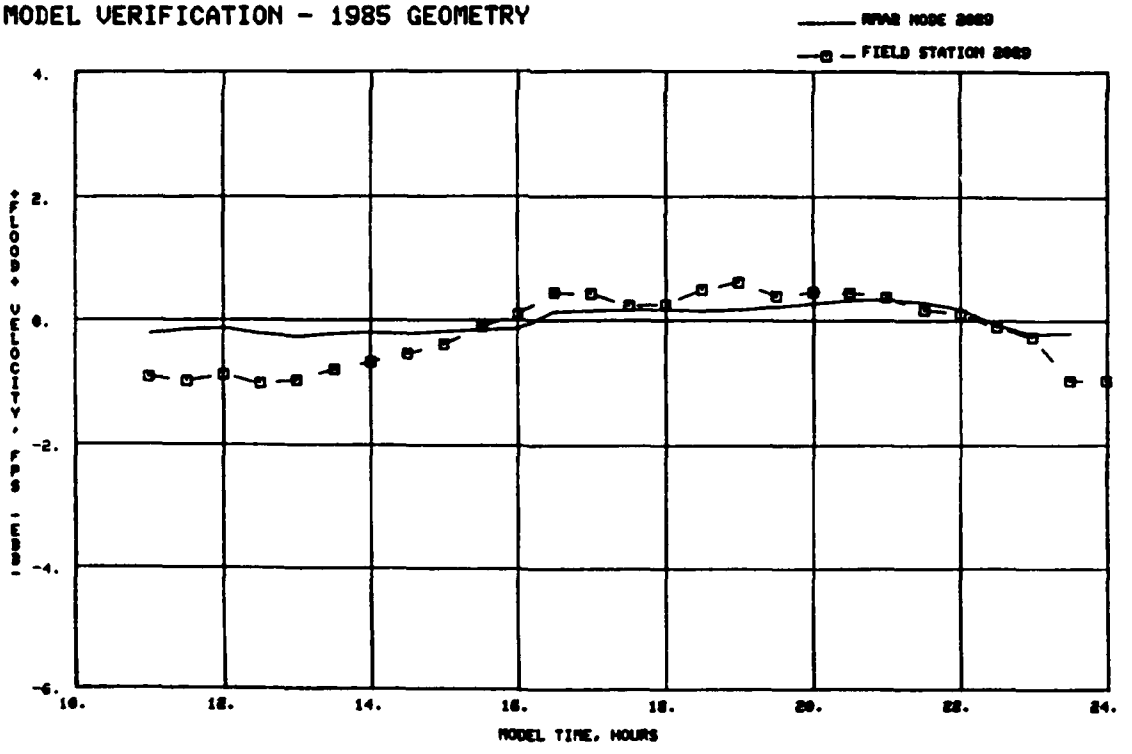

b. Station 2089

Plate E16. Physical and numerical model velocities for stations 2074 and 2089

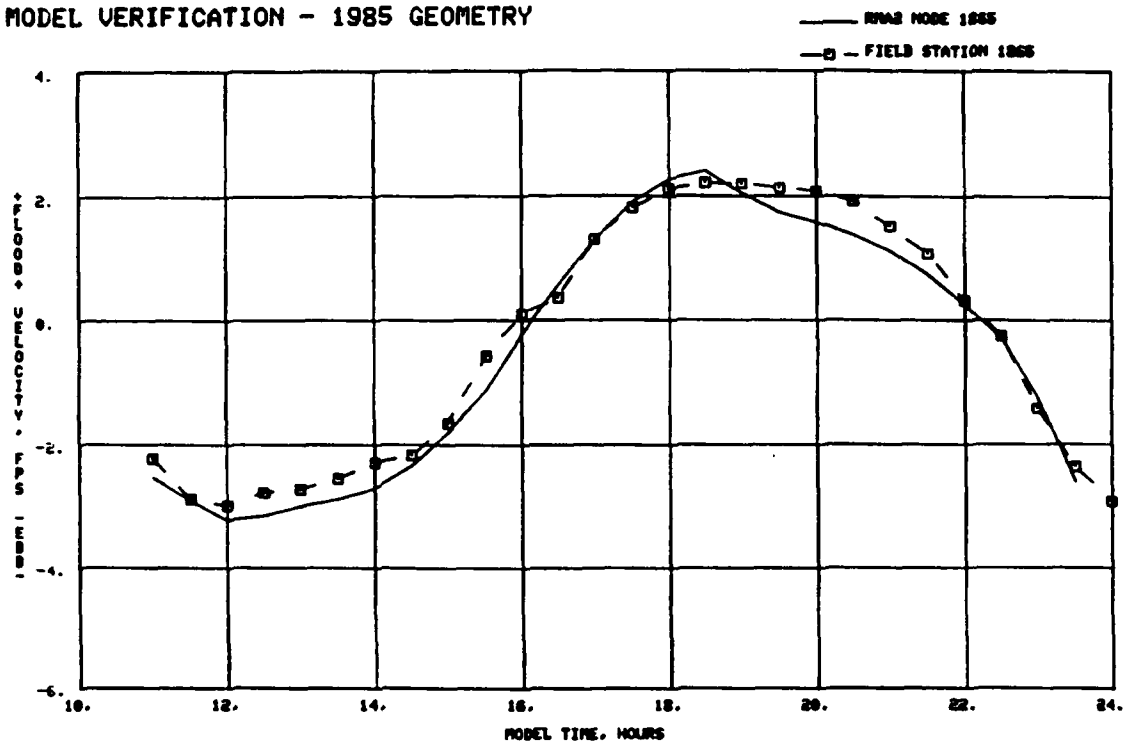

a. Station 1865

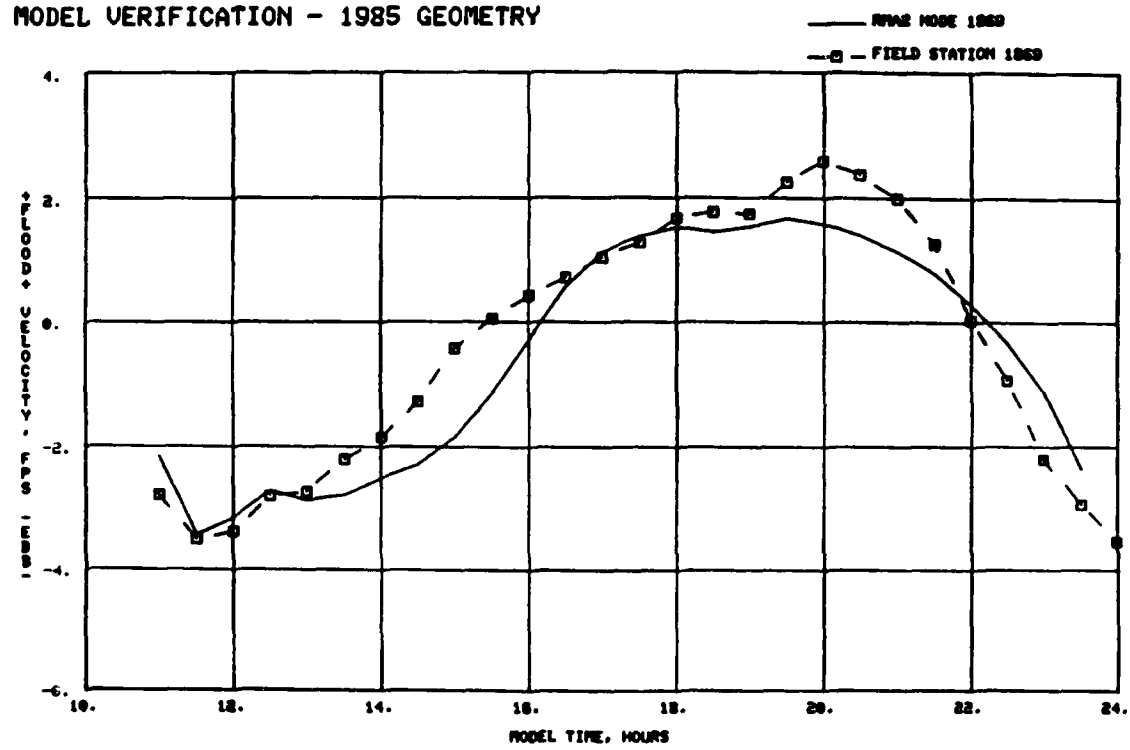

b. Station 1869

Plate E17. Physical and numerical model velocities for stations 1865 and 1869

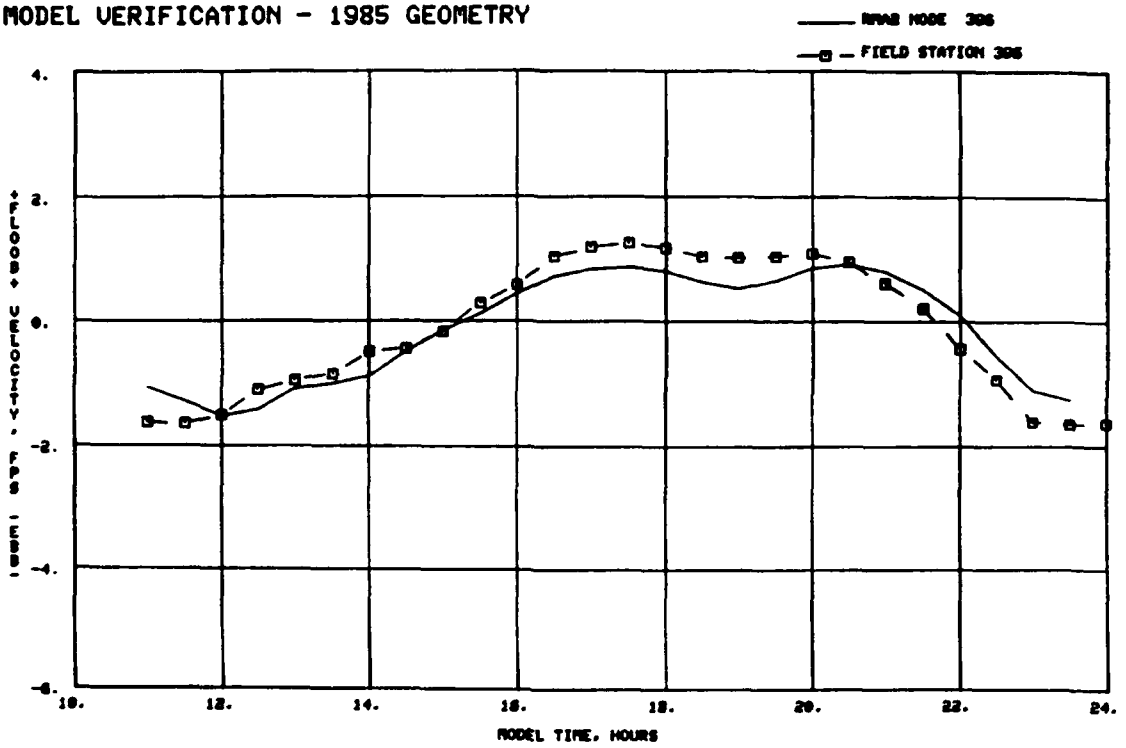

a. Station 396

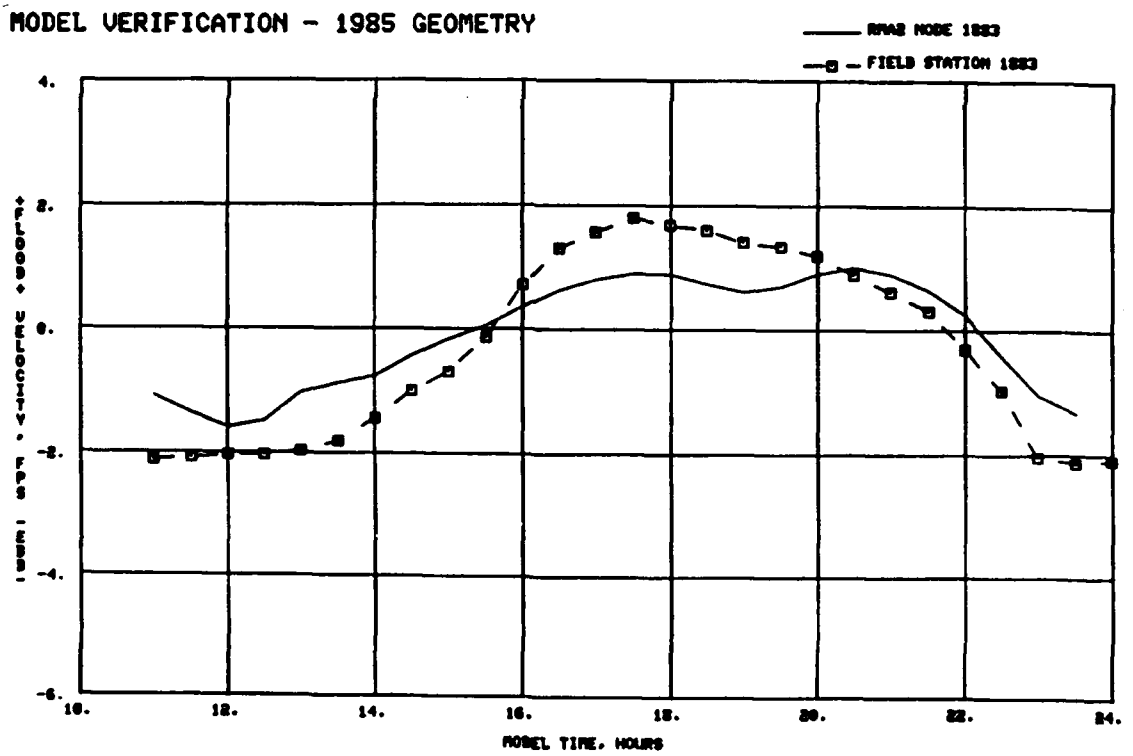

b. Station 1883

Plate E18. Physical and numerical model velocities for Stations 396 and 1883

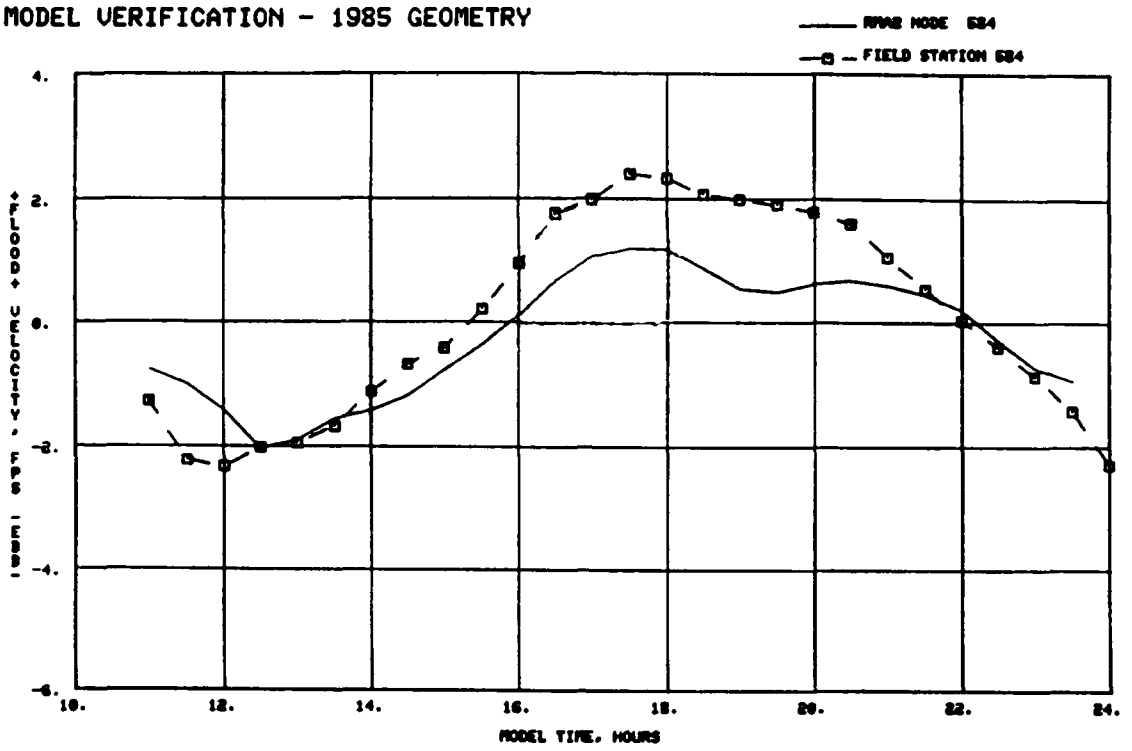

a. Station 584

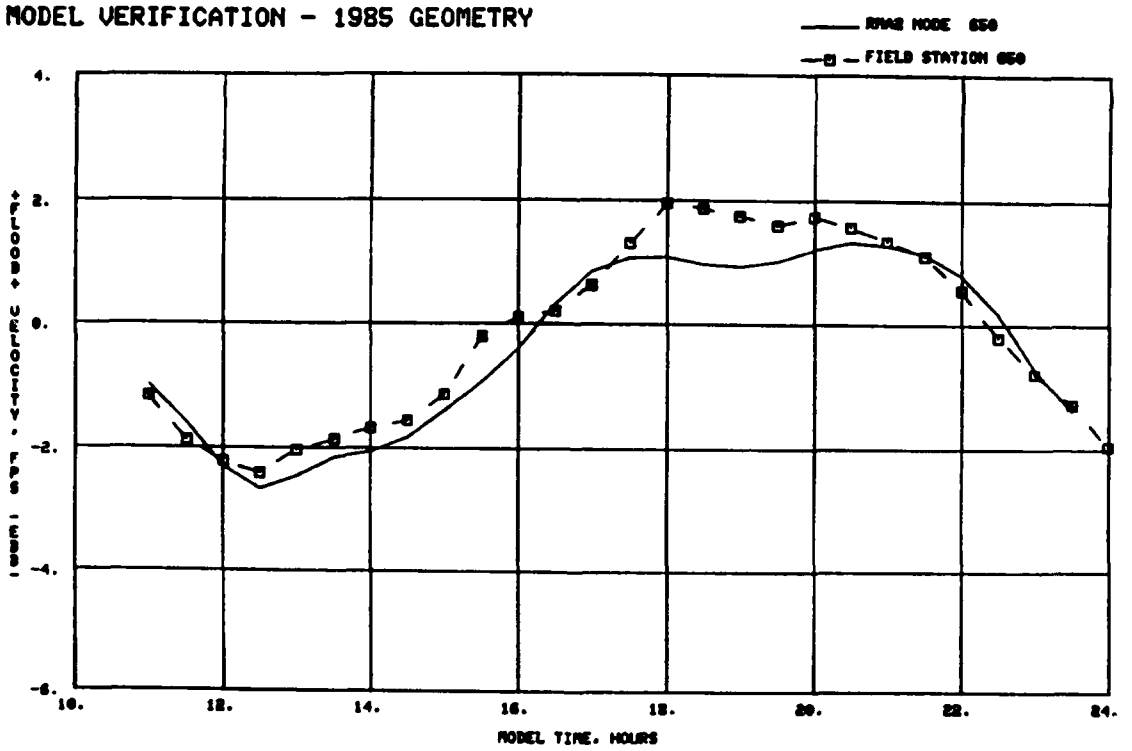

b. Station 650

Plate E19. Physical and numerical model velocities for stations 584 and 650

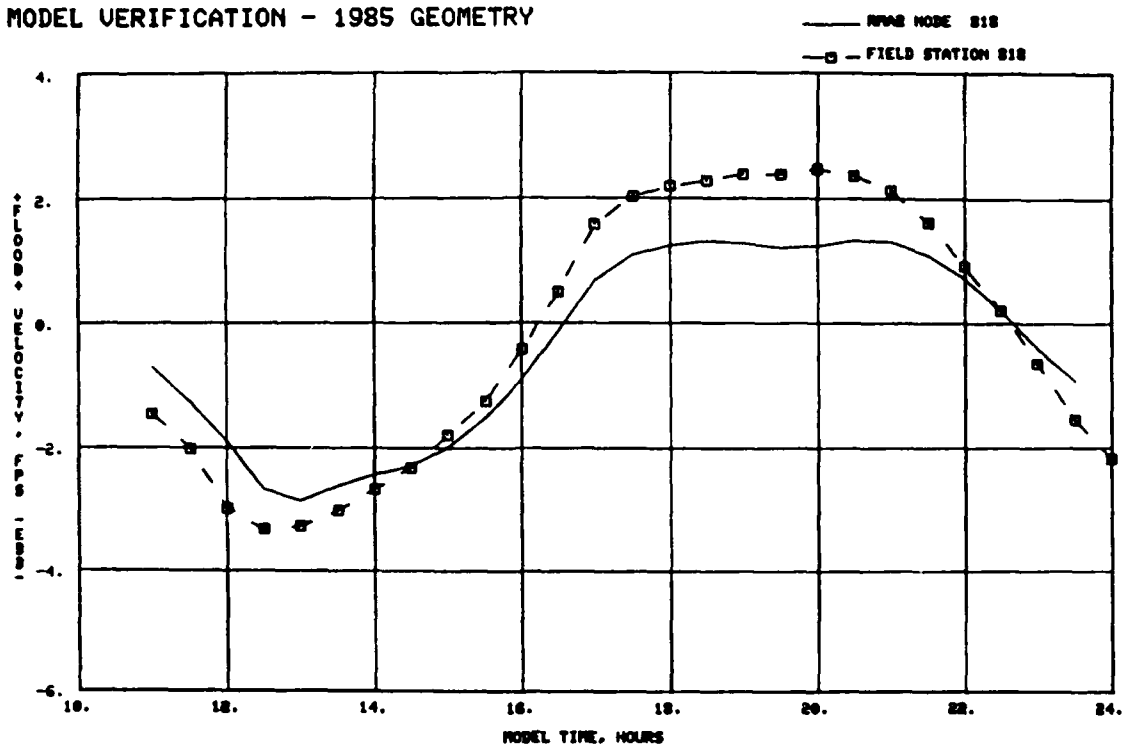

a. Station 818

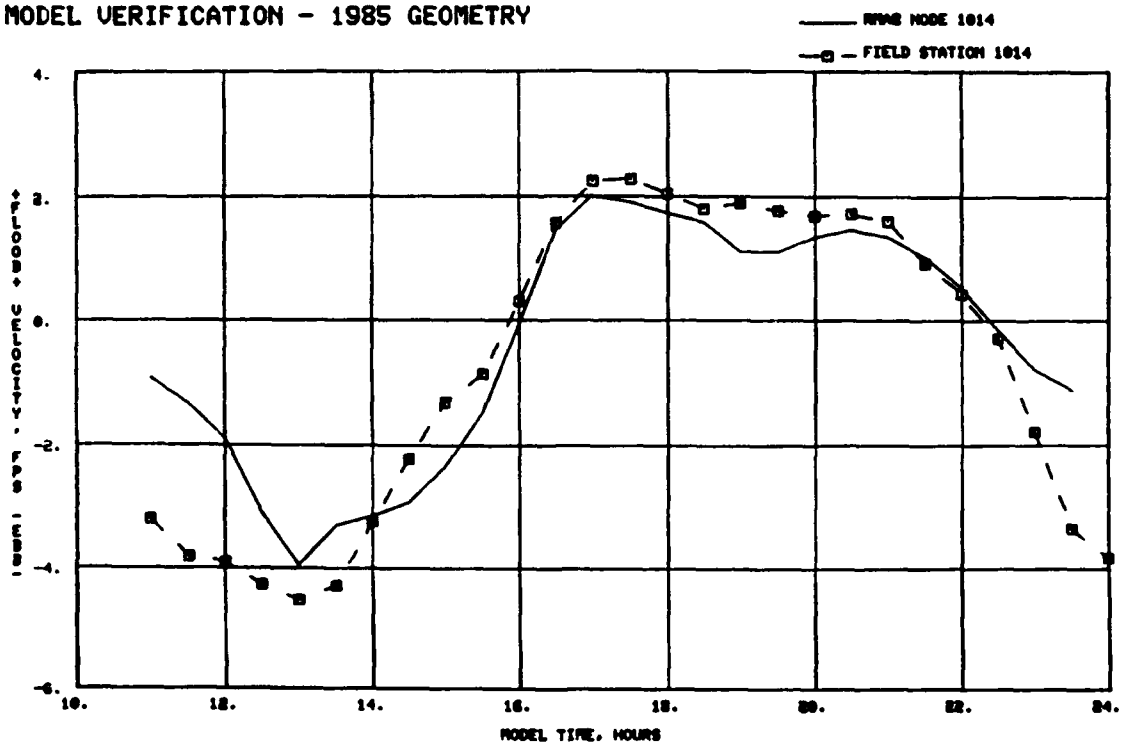

b. Station 1014

Plate E20. Physical and numerical model velocities for stations 818 and 1014

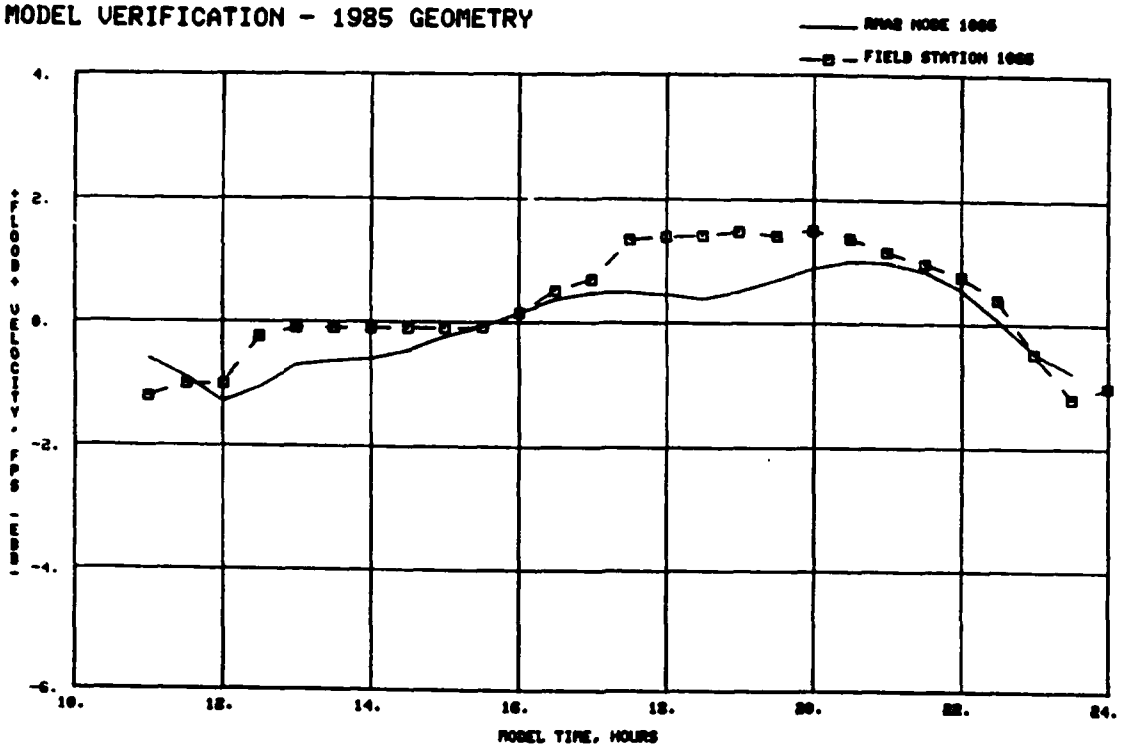

a. Station 1066

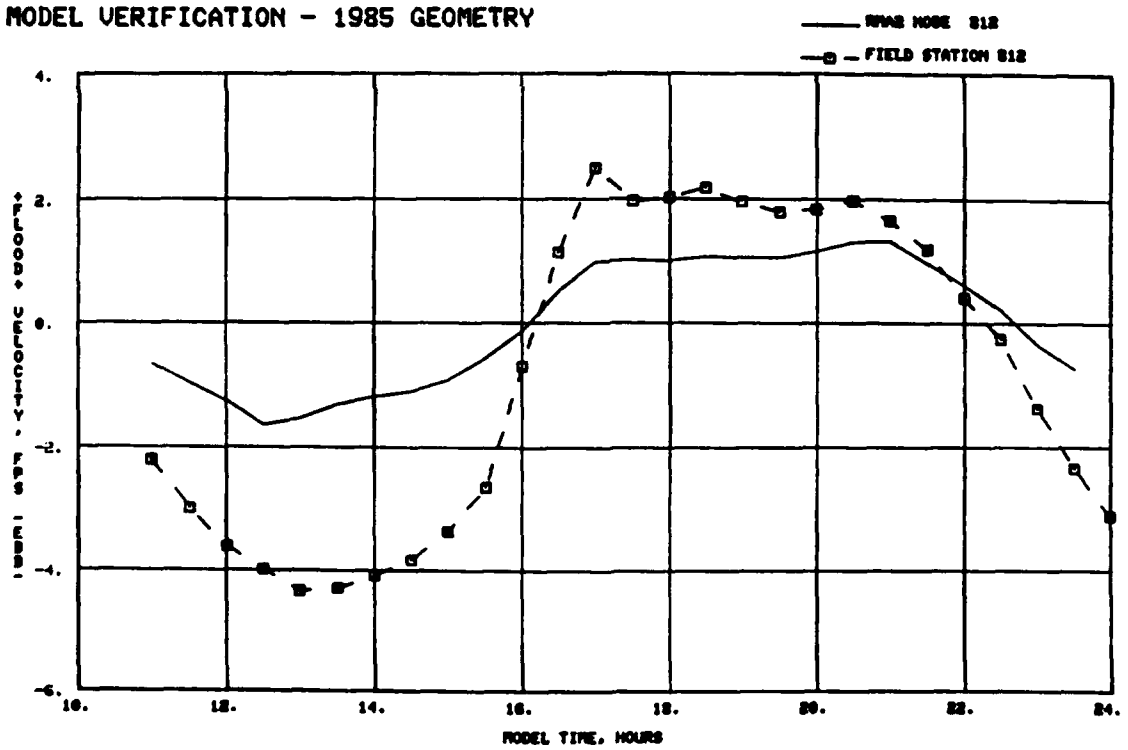

b. Station 812

Plate E21. Physical and numerical model velocities for stations 1066 and 812

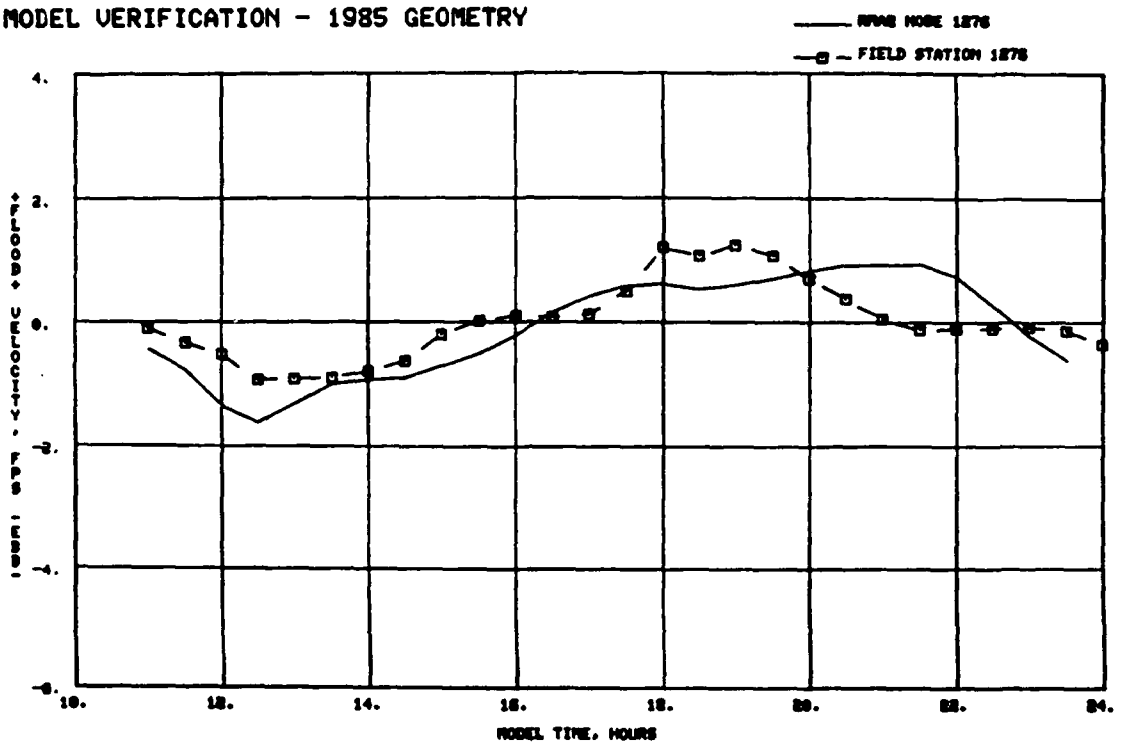

Plate E22. Physical and numerical model velocities for station 1276

APPENDIX F: NUMERICAL MODEL PRE-TRIDENT MESH 4 VERIFICATION

NOTE: The term "field station" on plots in this appendix refers to stations in the physical model.

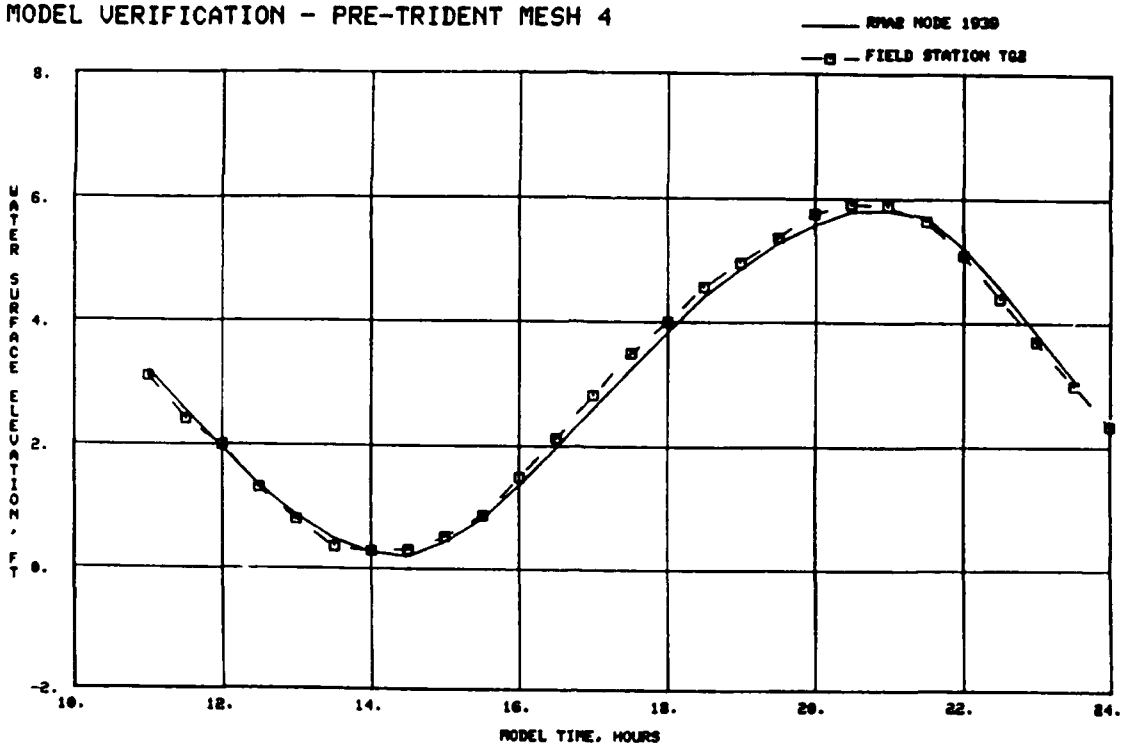

a. St. Marys Inlet

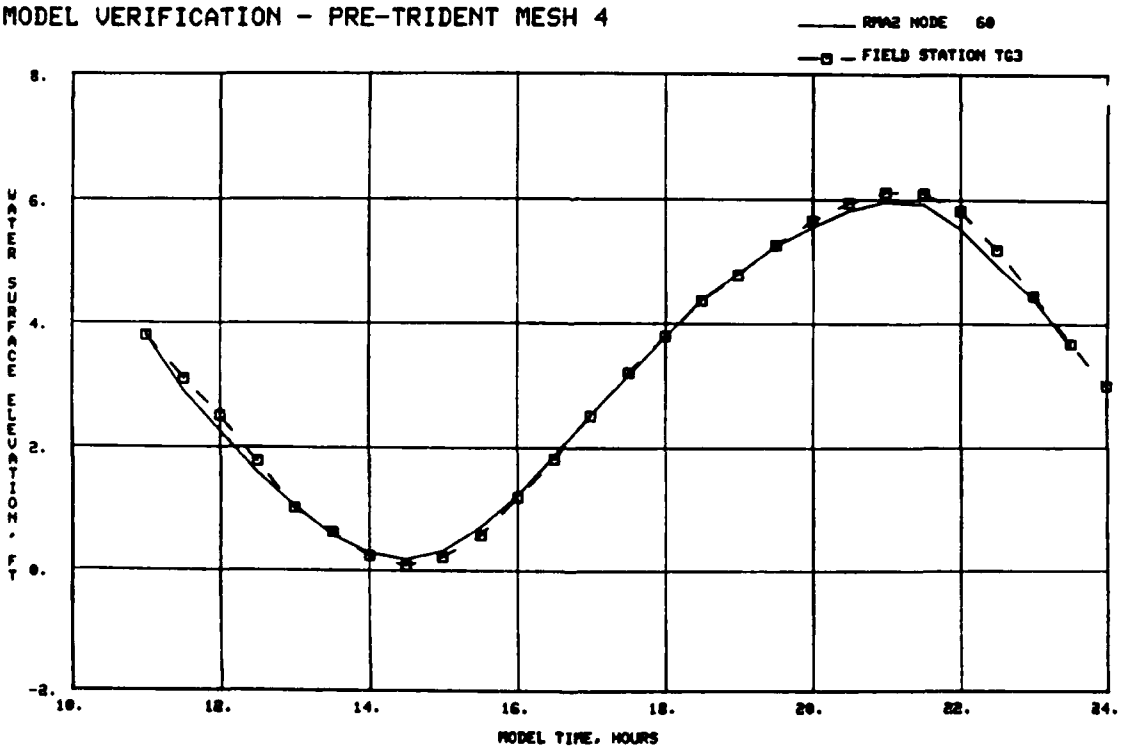

b. Amelia River

Plate F1. Water-surface elevations, physical and numerical model, for St. Marys Inlet and Amelia River

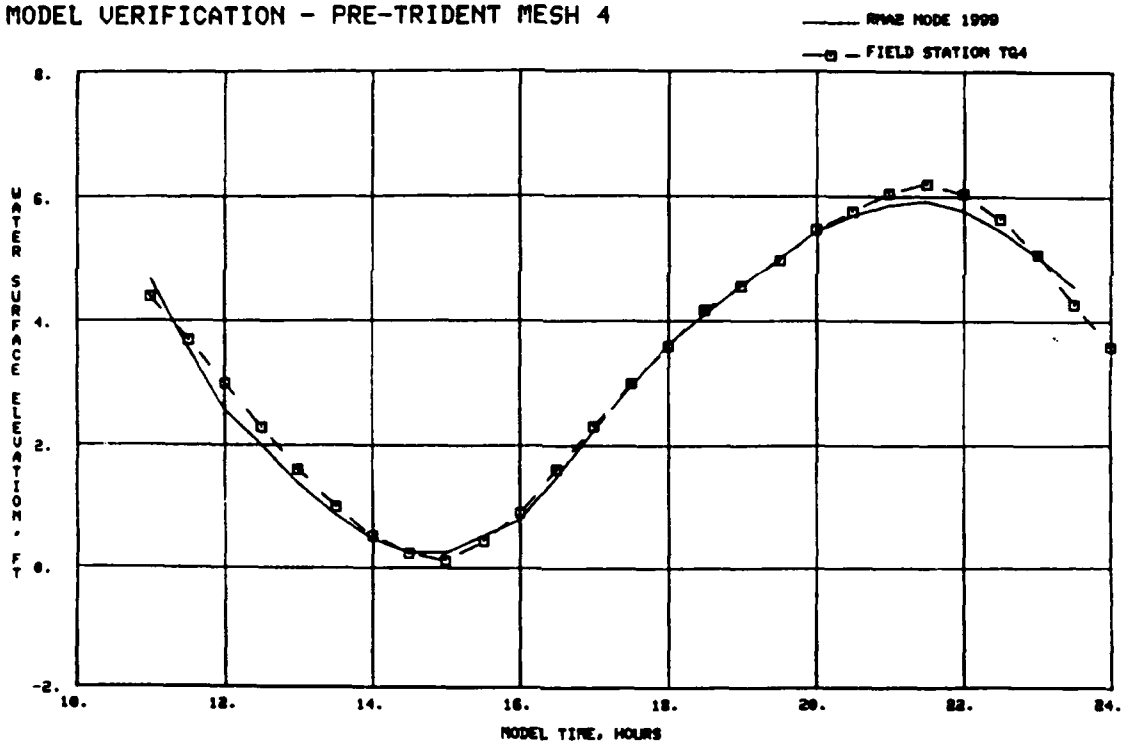

a. Jolly River

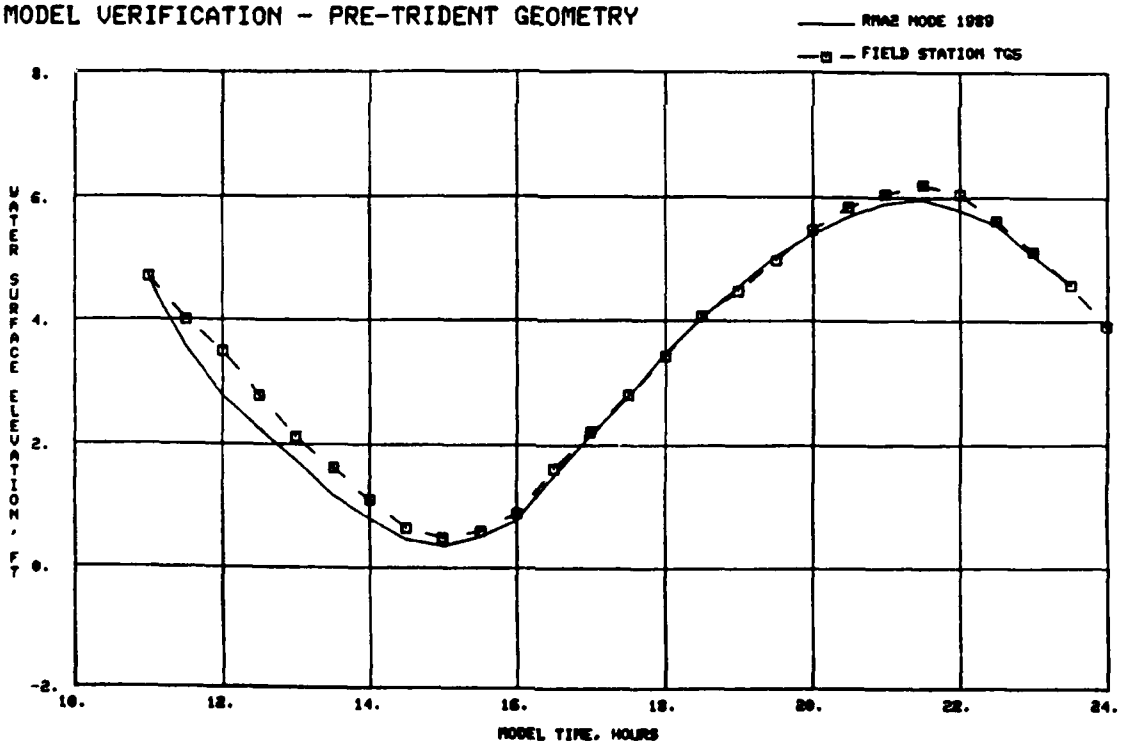

b. St. Marys River

Plate F2. Water-surface elevations, physical and numerical model, for Jolly River and St. Marys River

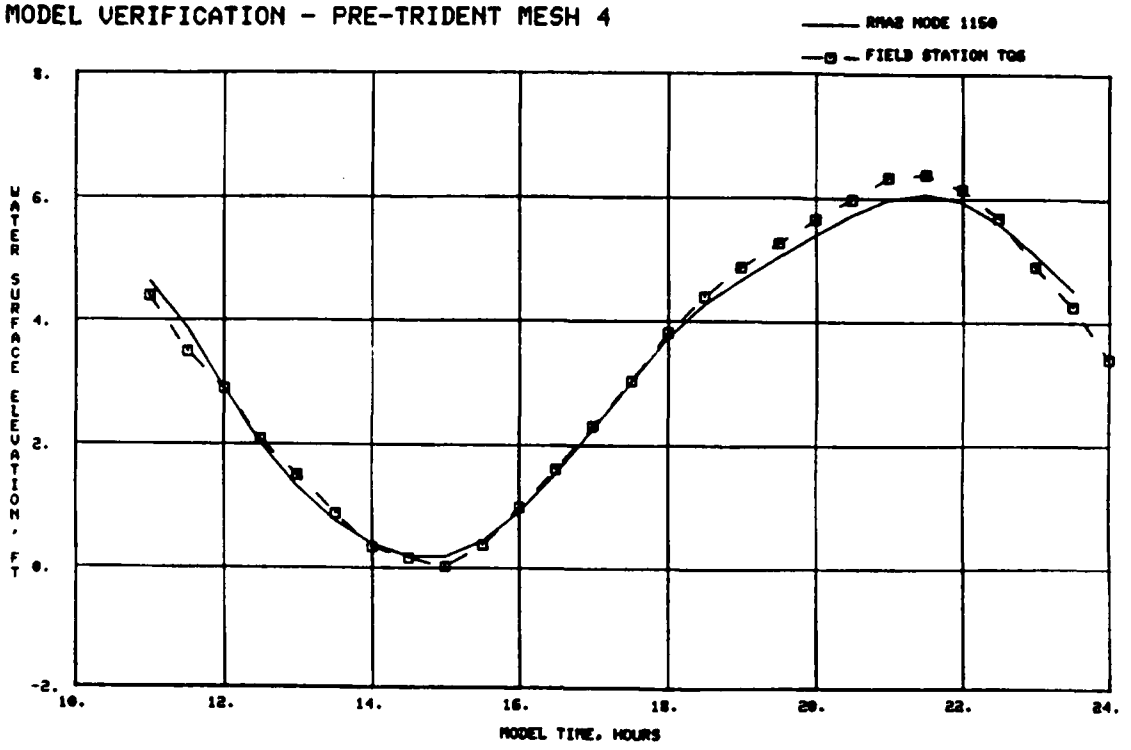

a. Lower Kings Bay

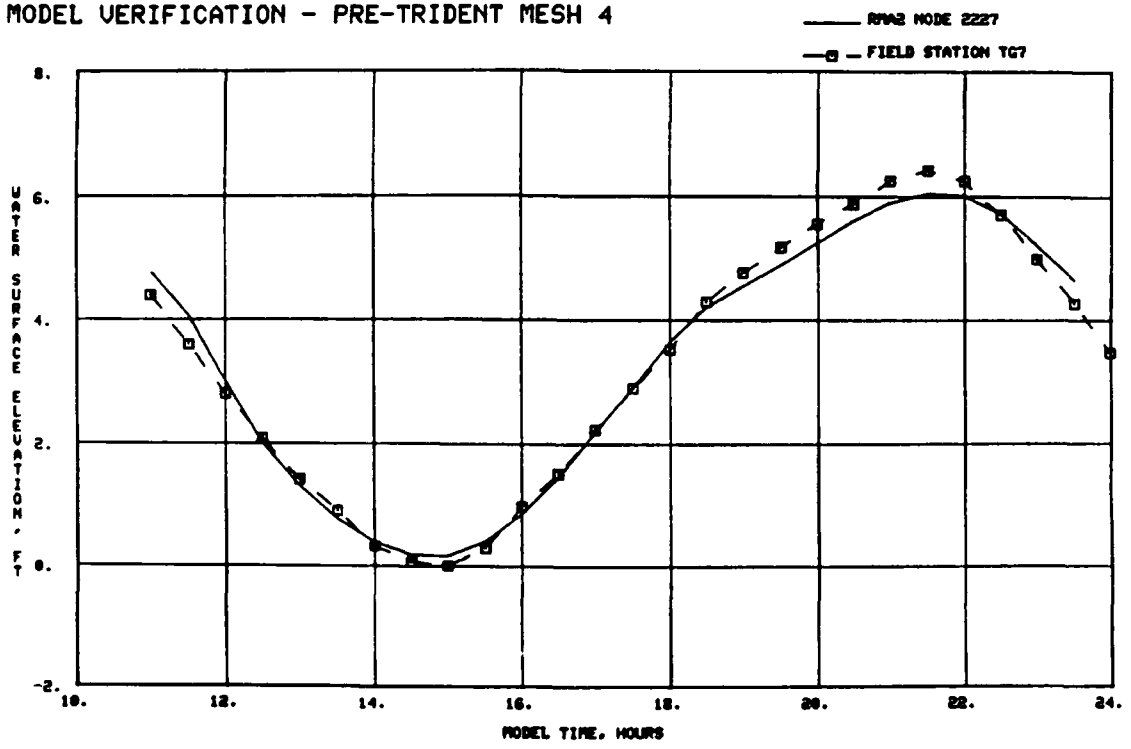

b. Marianna Creek

Plate F3. Water-surface elevations, physical and numerical model, for lower Kings Bay and Marianna Creek

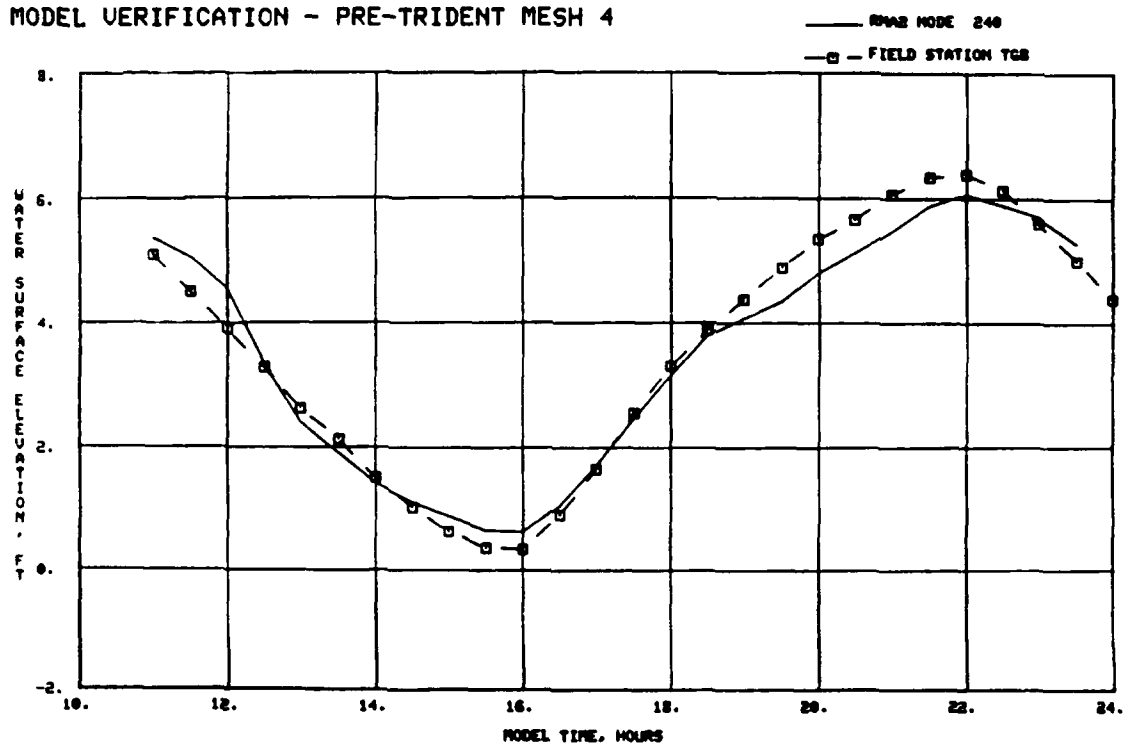

a. Crooked River

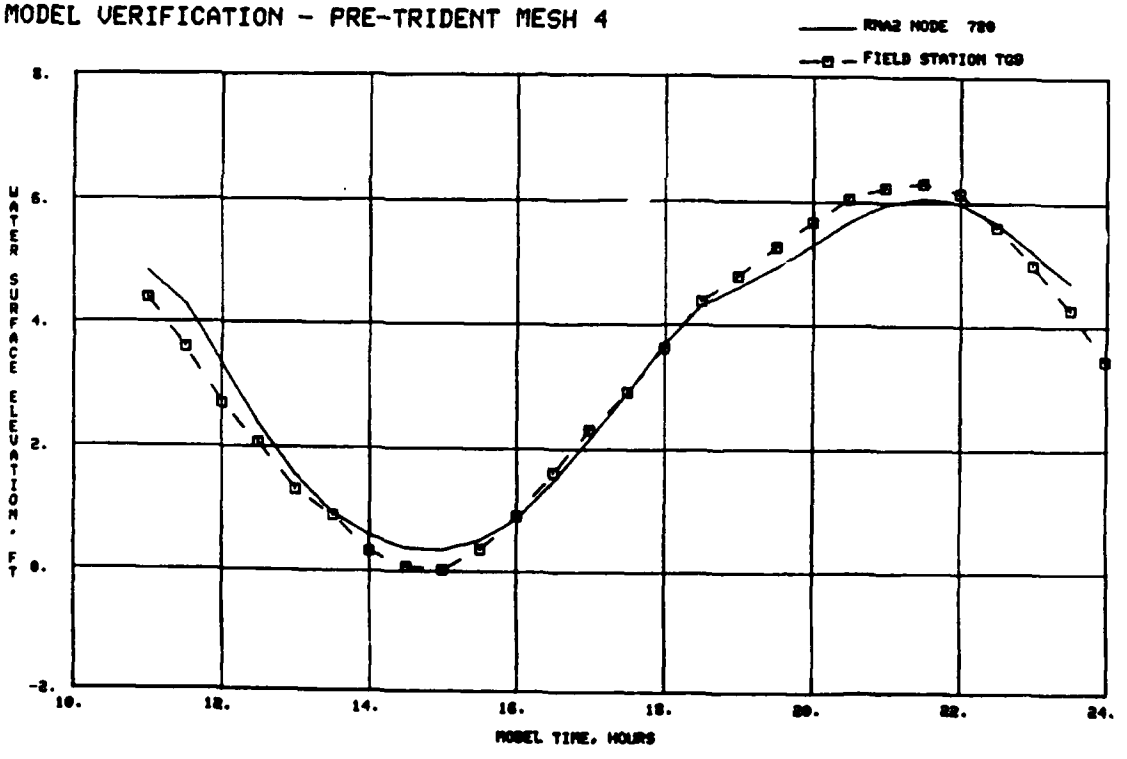

b. Northern Cumberland Sound

Plate F4. Water-surface elevations, physical and numerical model, for Crooked River and northern Cumberland Sound

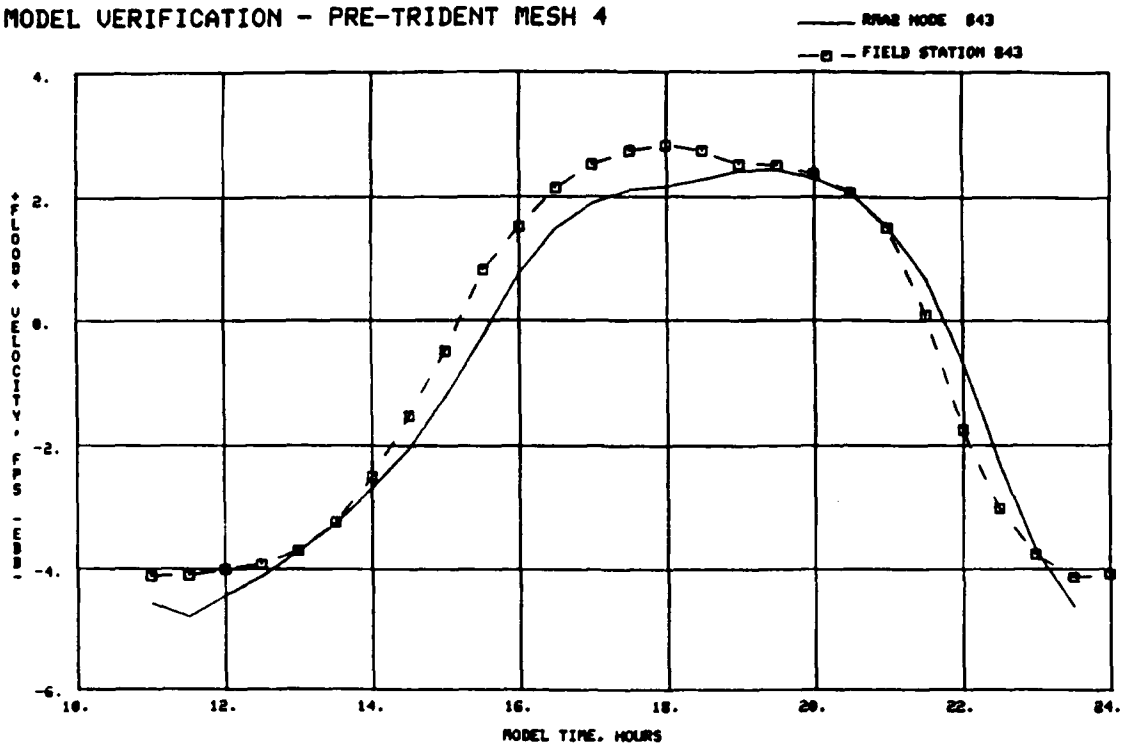

a. Station 843

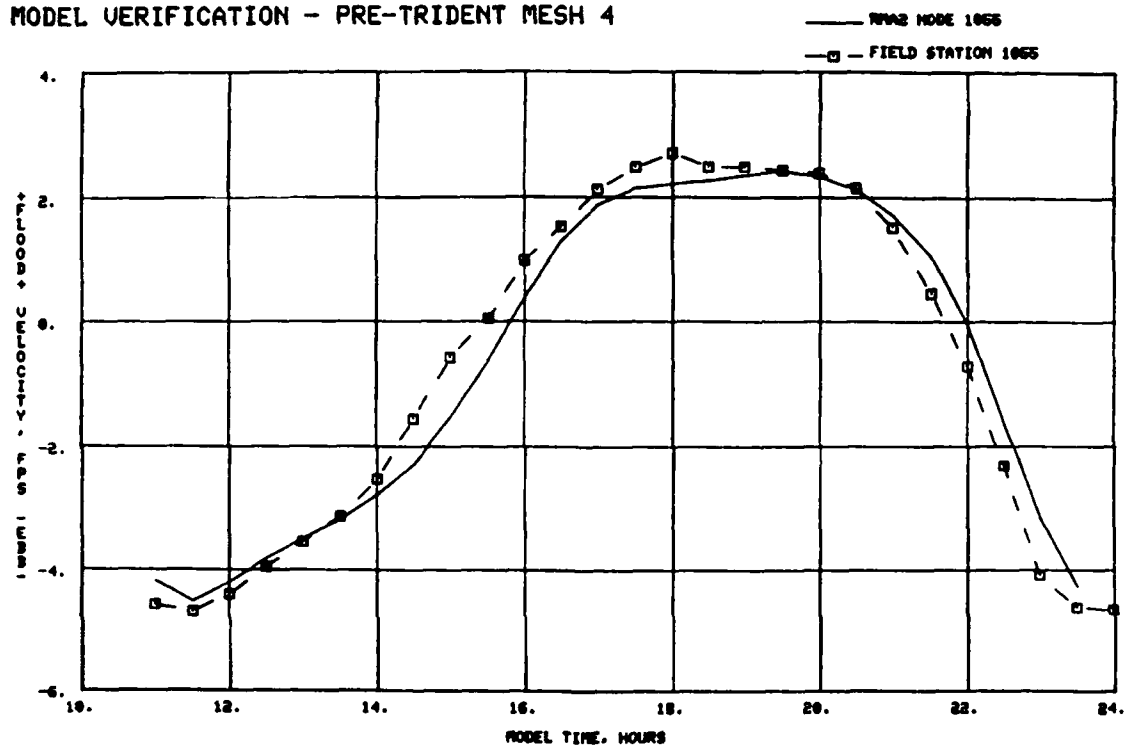

b. Station 1055

Plate F5. Physical and numerical model velocities for stations 843 and 1055

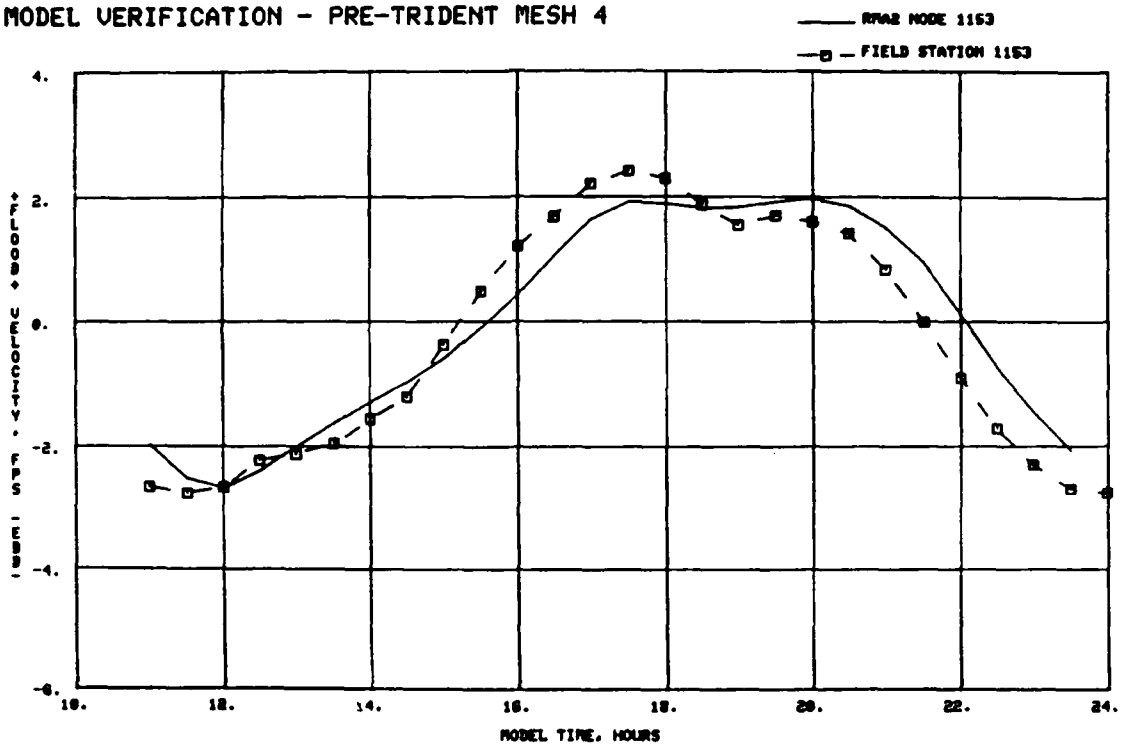

a. Station 1153

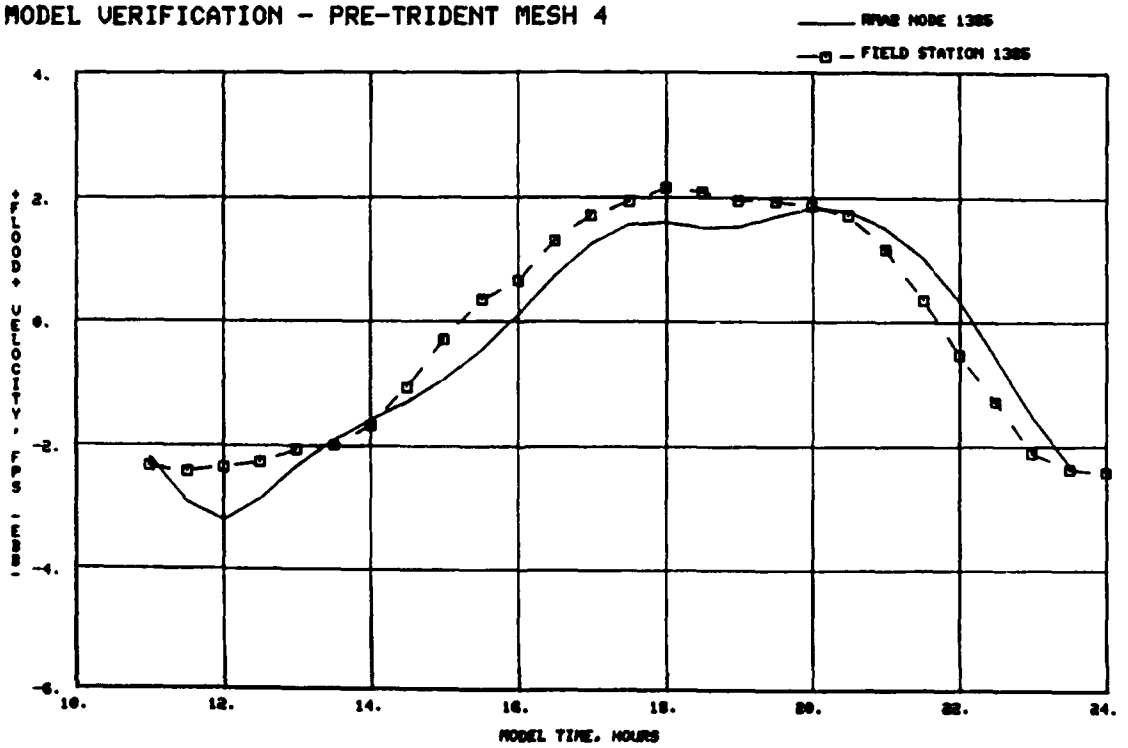

b. Station 1385

Plate F6. Physical and numerical model velocities for stations 1153 and 1385

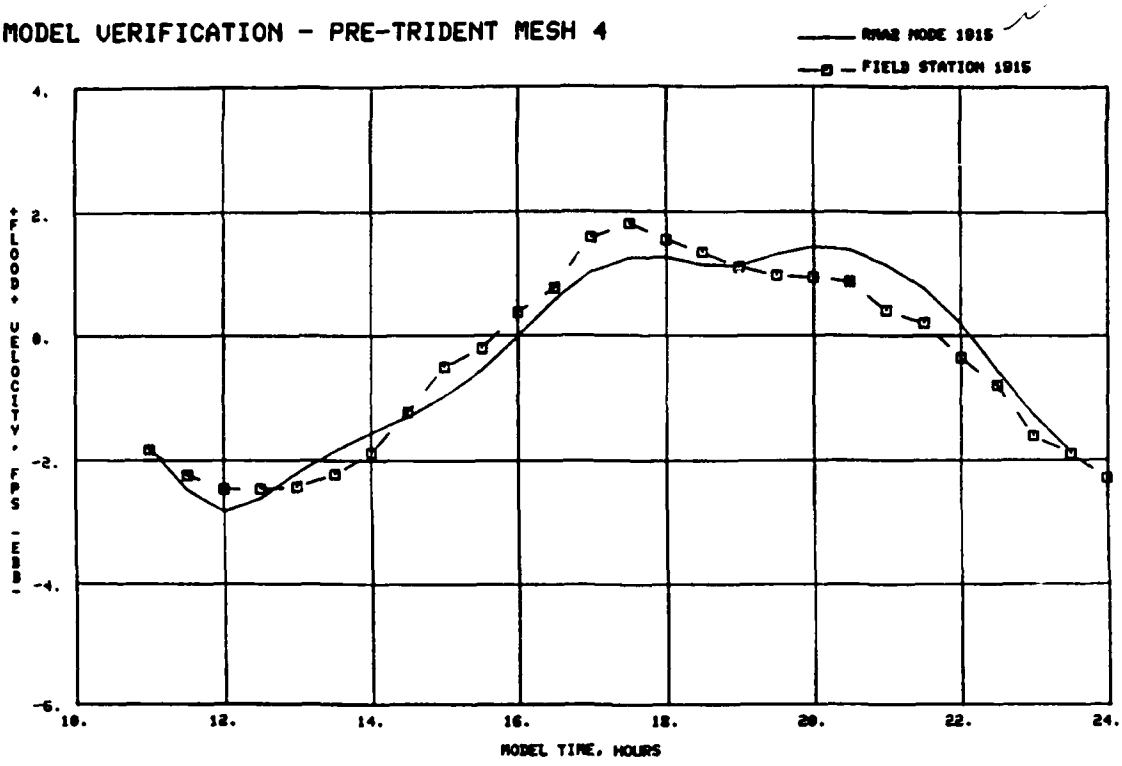

a. Station 1915

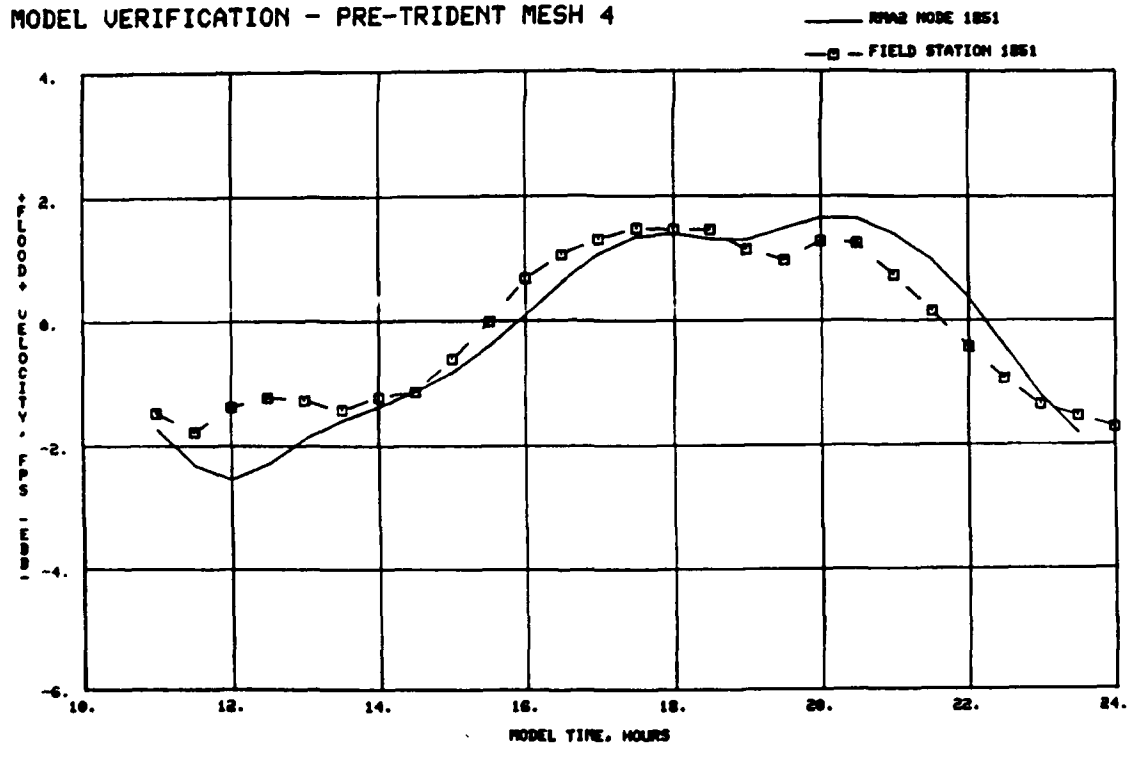

b. Station 1851

Plate F7. Physical and numerical model velocities for stations 1915 and 1851

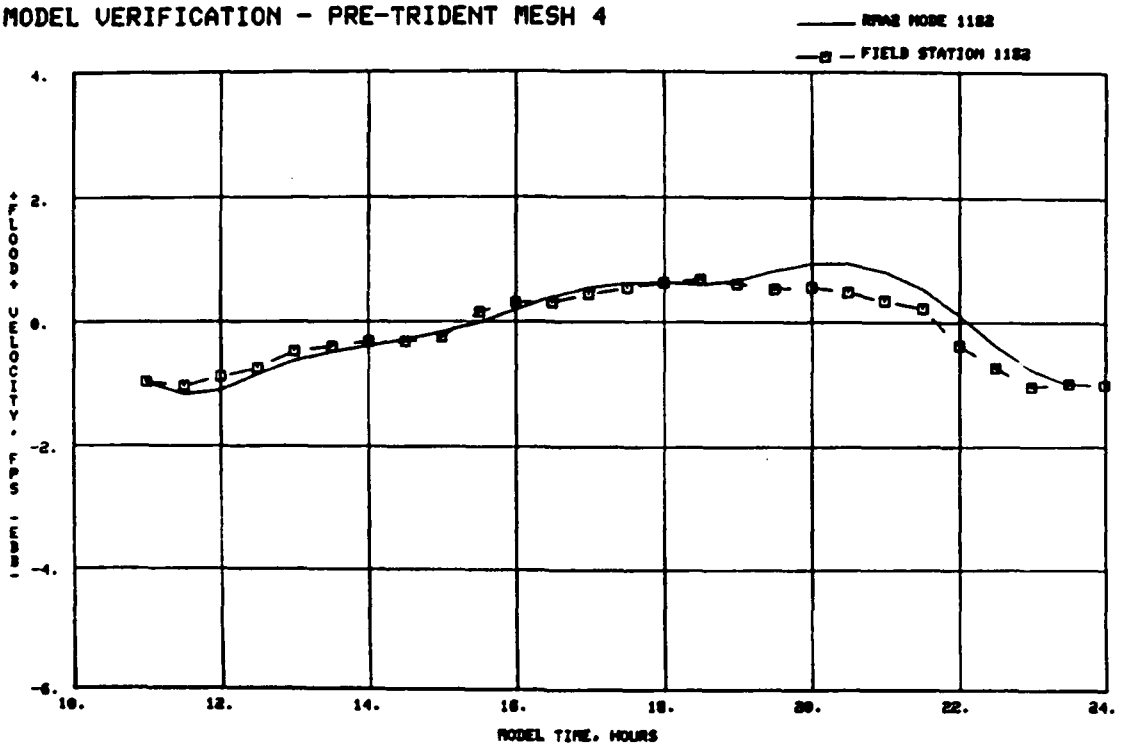

a. Station 1182

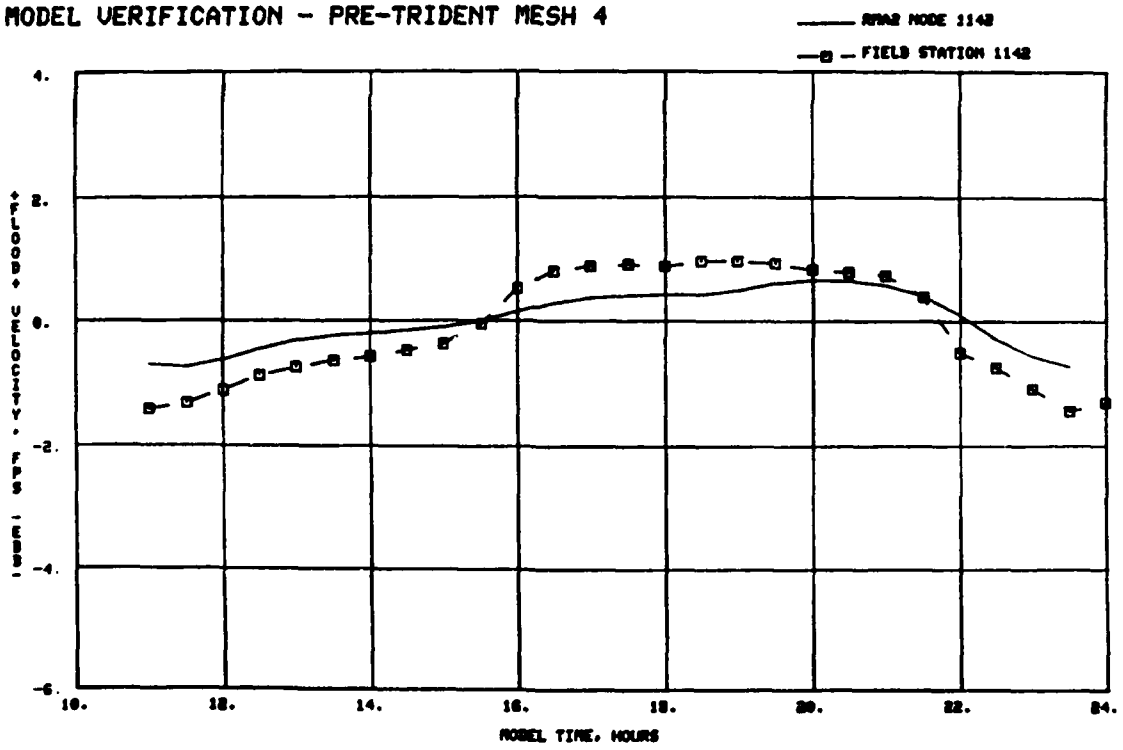

b. Station 1142

Plate F8. Physical and numerical model velocities for stations 1182 and 1142

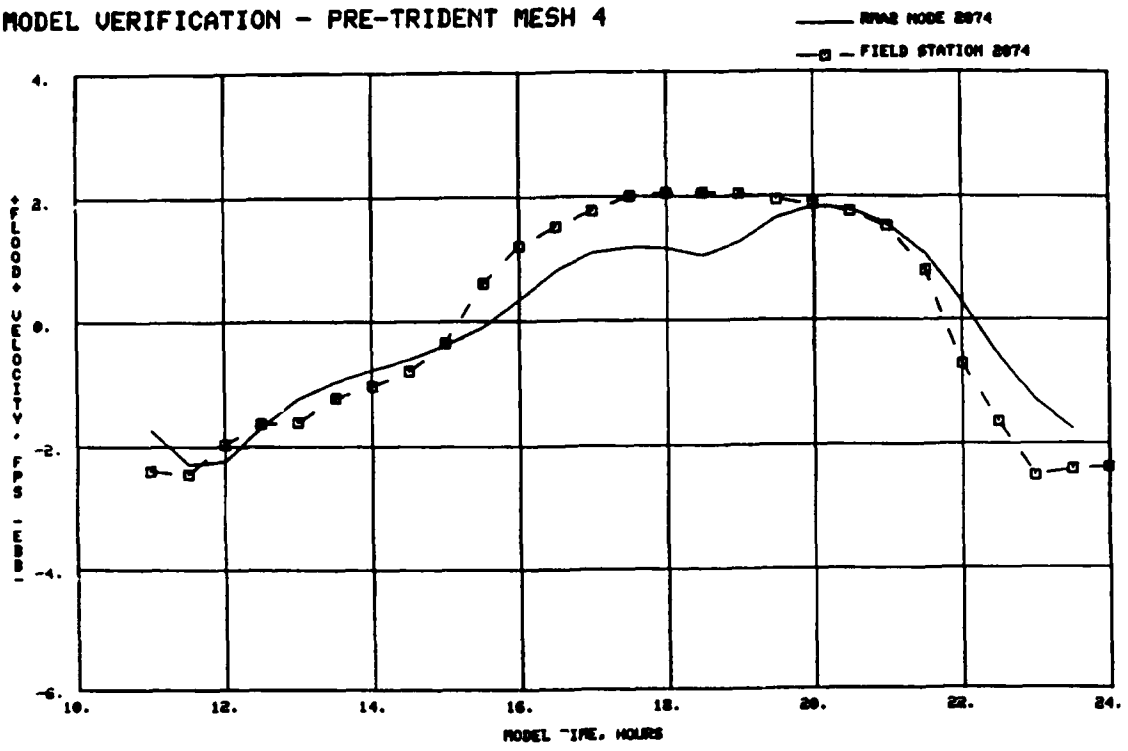

a. Station 2074

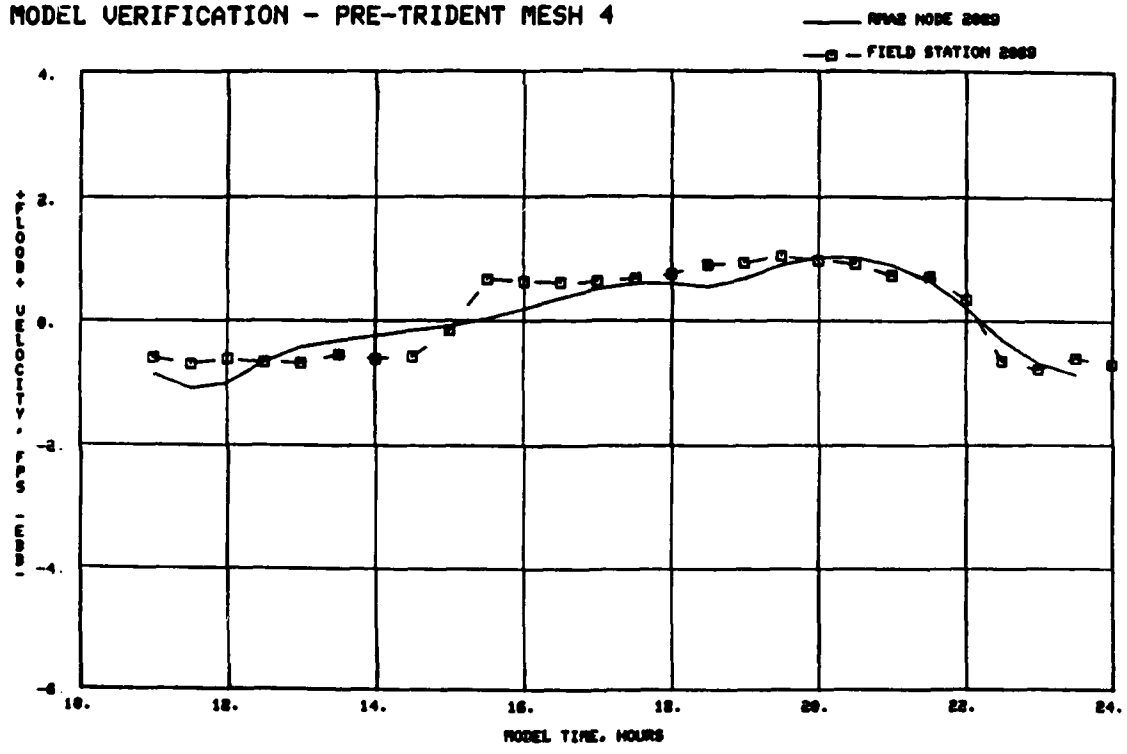

b. Station 2089

Plate F9. Physical and numerical model velocities for stations 2074 and 2089

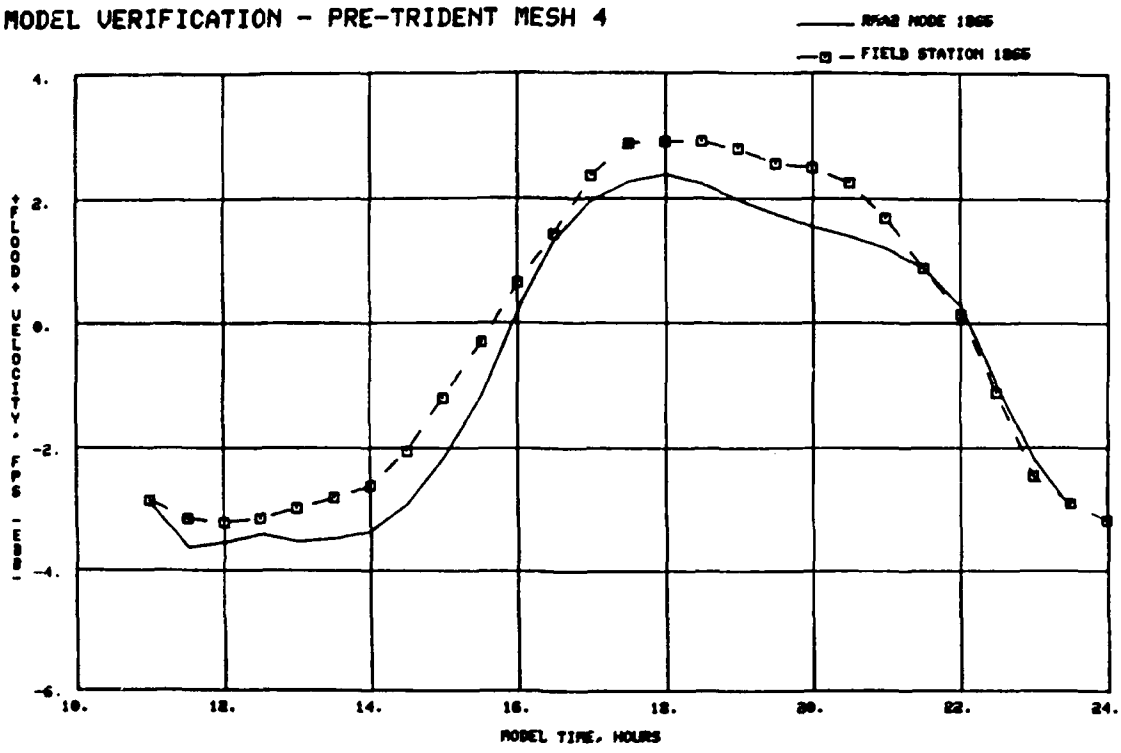

a. Station 1865

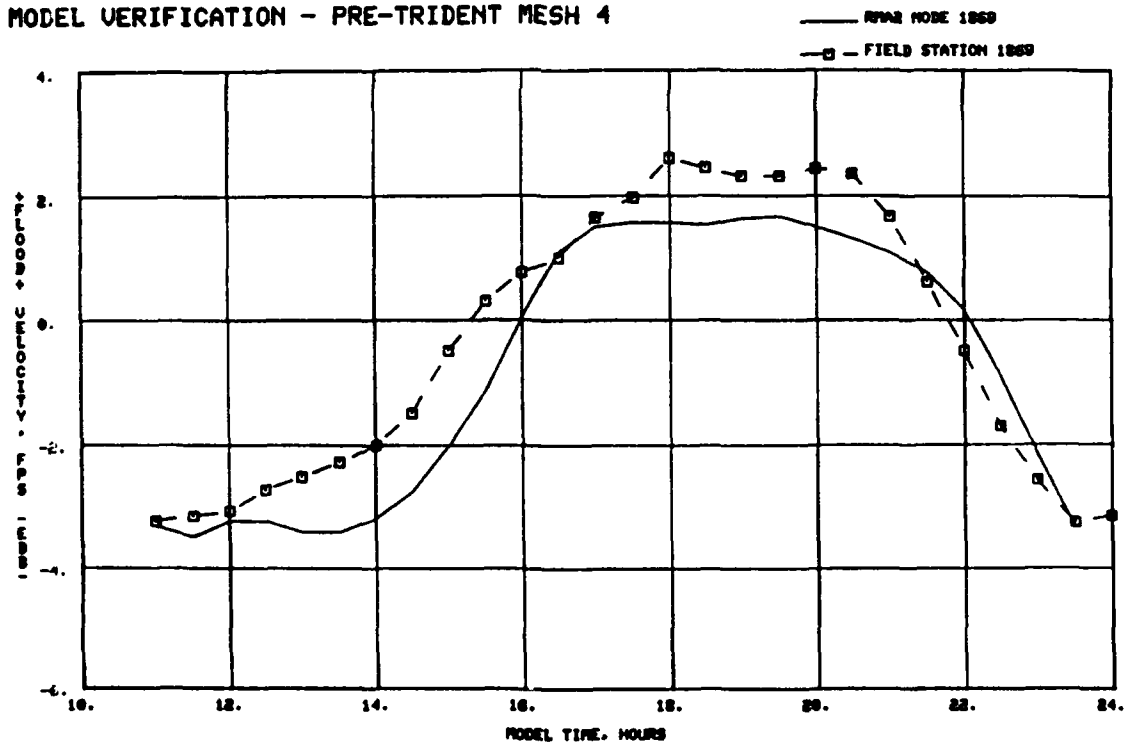

b. Station 1869

Plate F10. Physical and numerical model velocities for stations 1865 and 1869

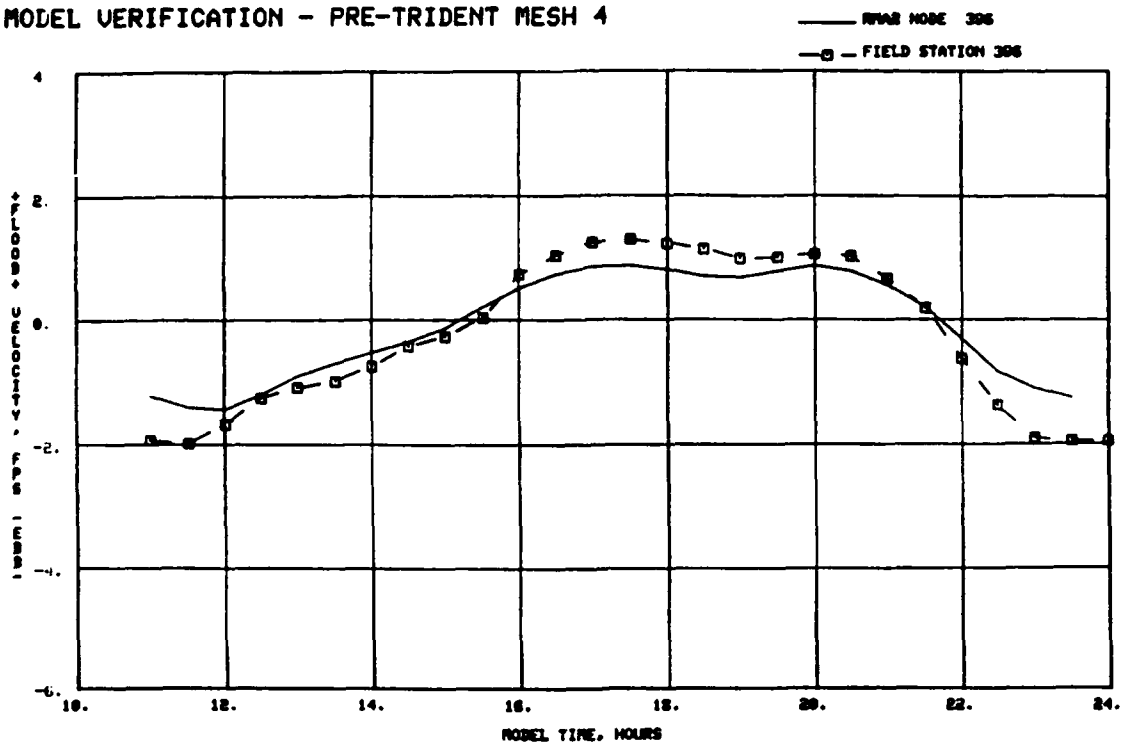

a. Station 396

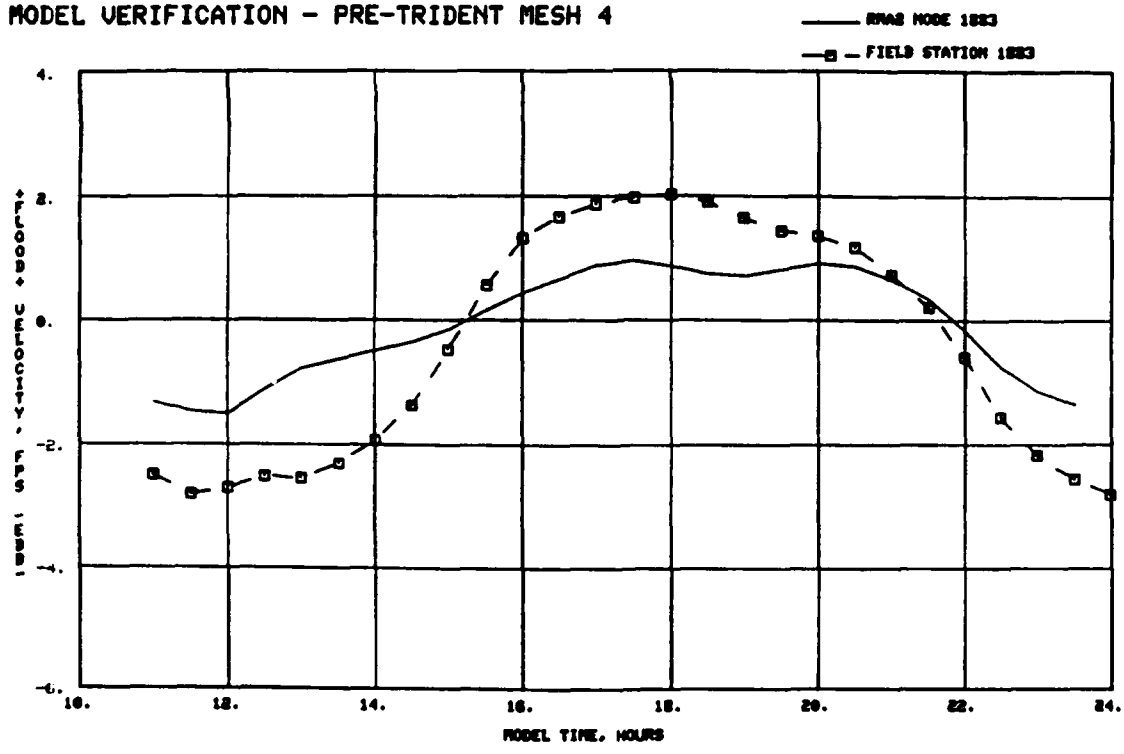

b. Station 1883

Plate F11. Physical and numerical model velocities for Stations 396 and 1883

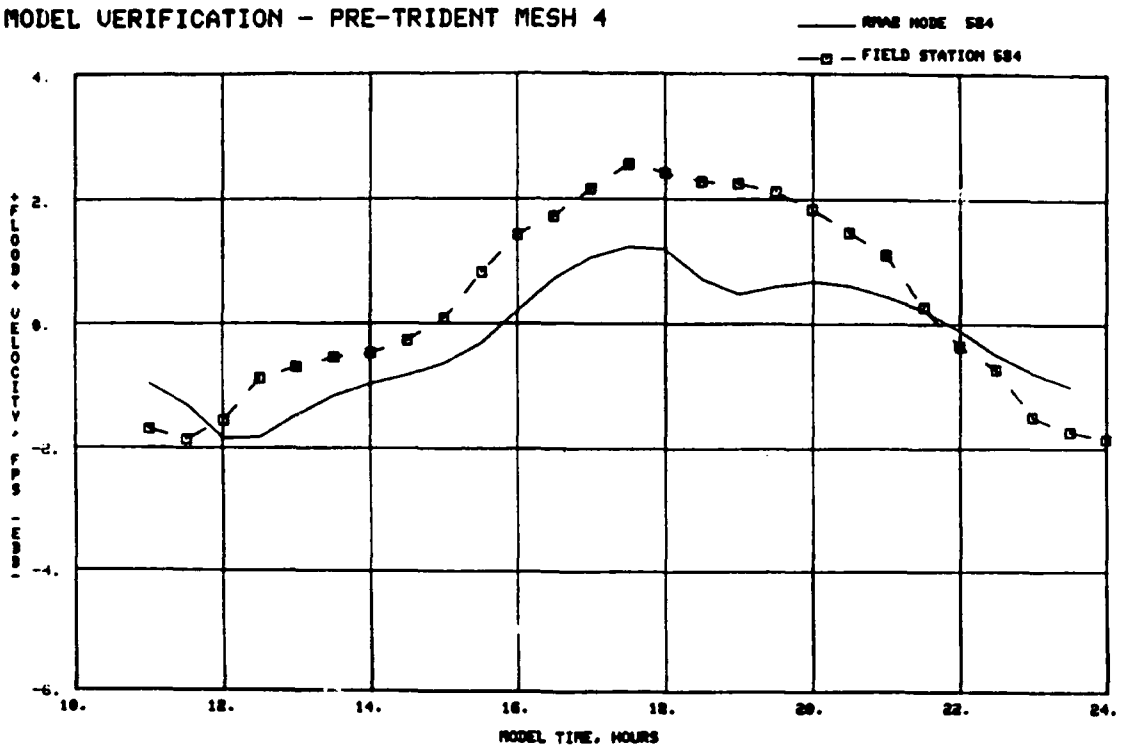

a. Station 584

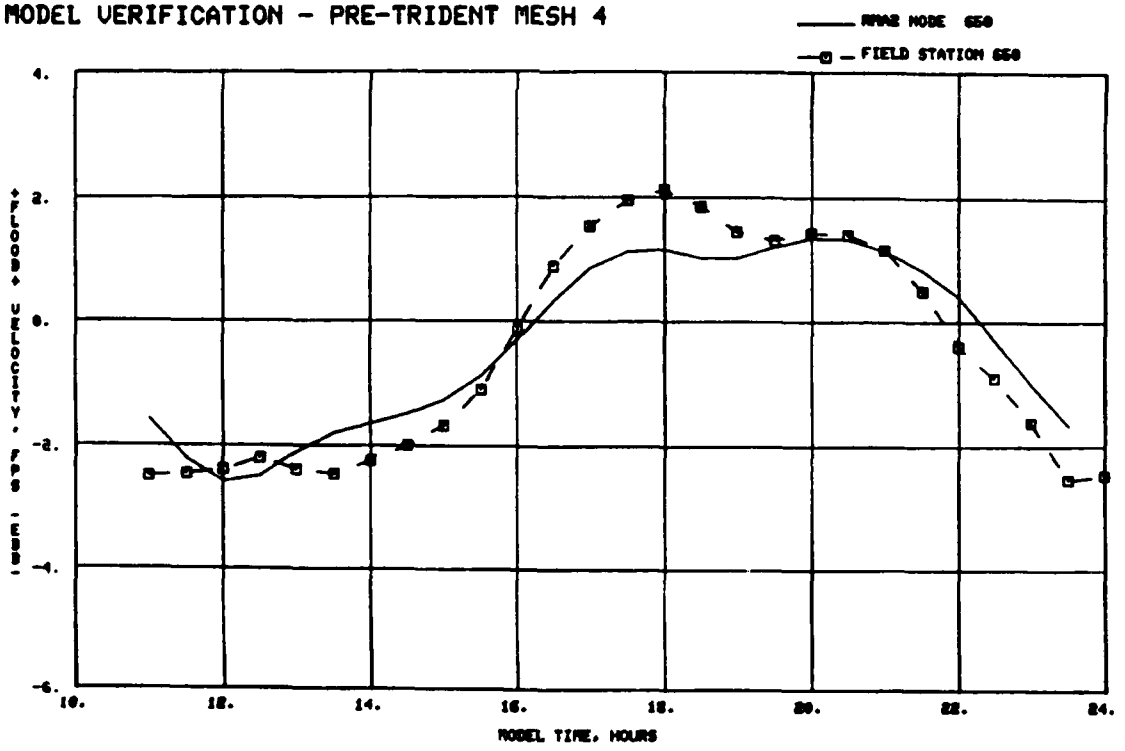

b. Station 650

Plate F12. Physical and numerical model velocities for stations 584 and 650

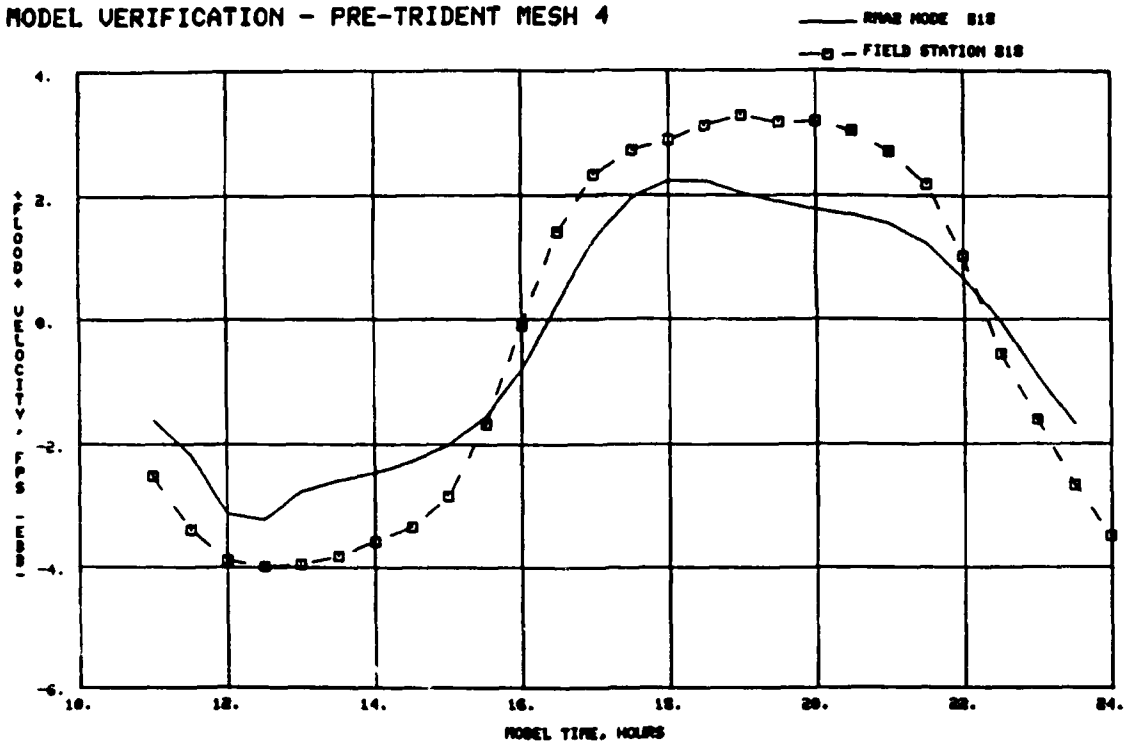

a. Station 818

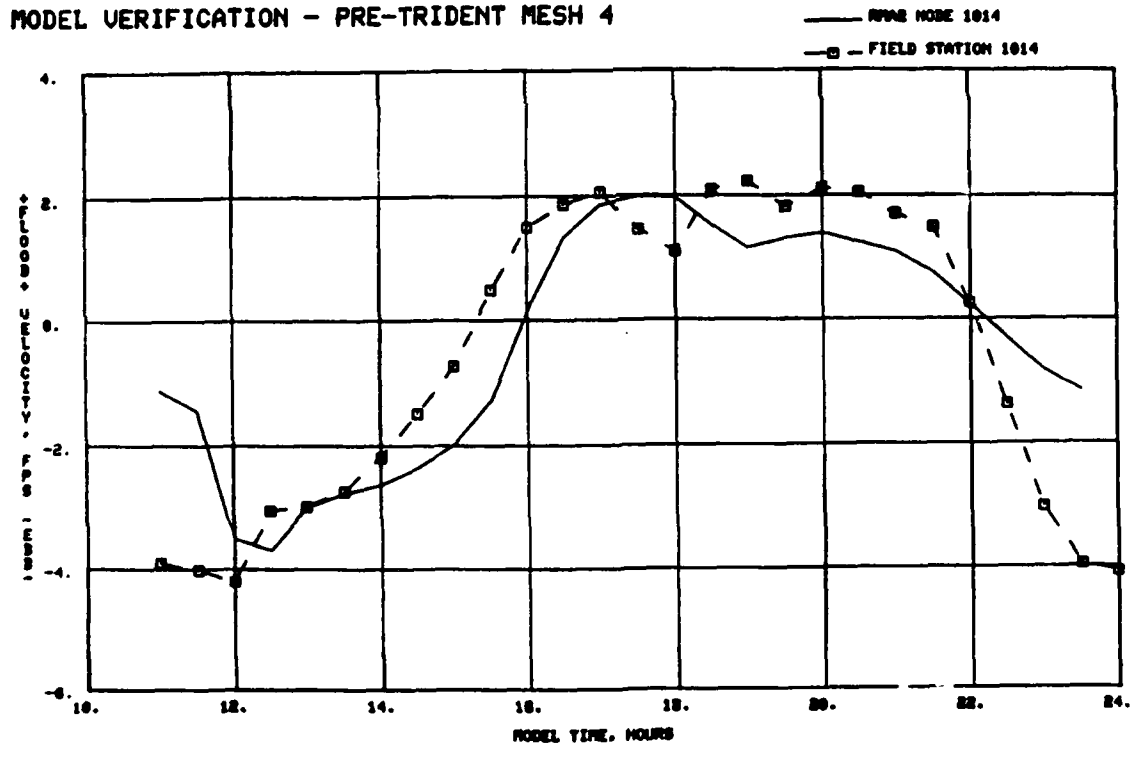

b. Station 1014

Plate F13. Physical and numerical model velocities for stations 818 and 1014

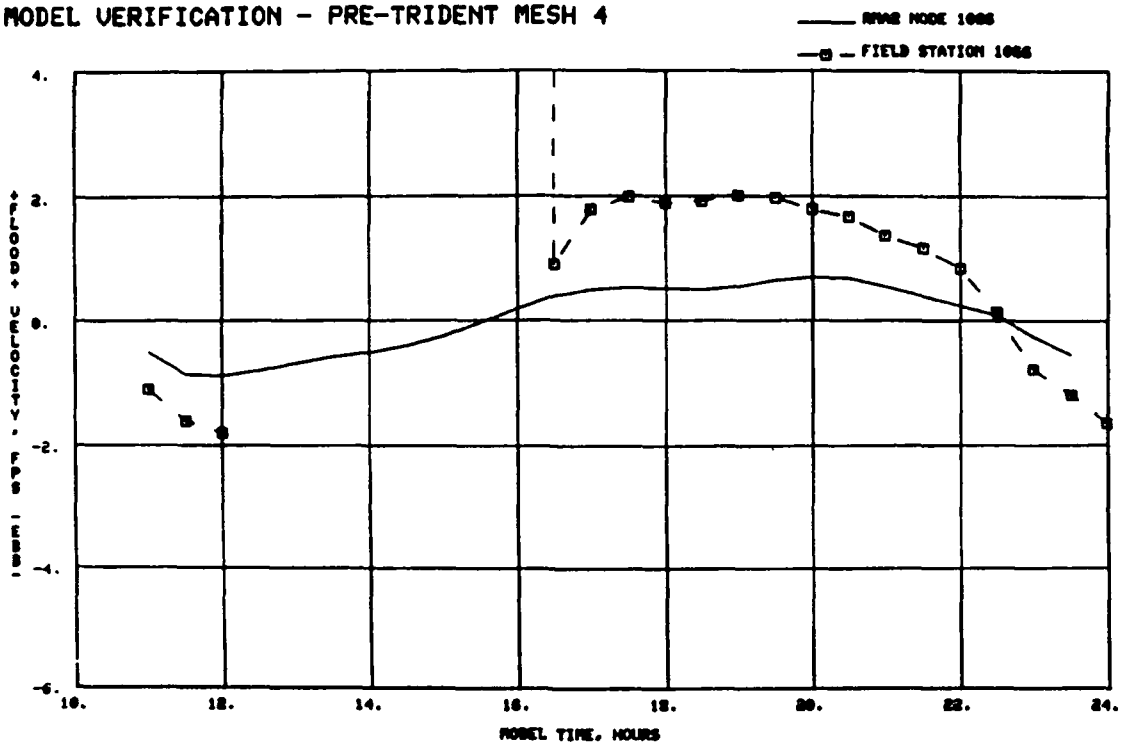

a. Station 1066 (physical model water depths were too shallow for measurements between hours 12.5 and 16.0)

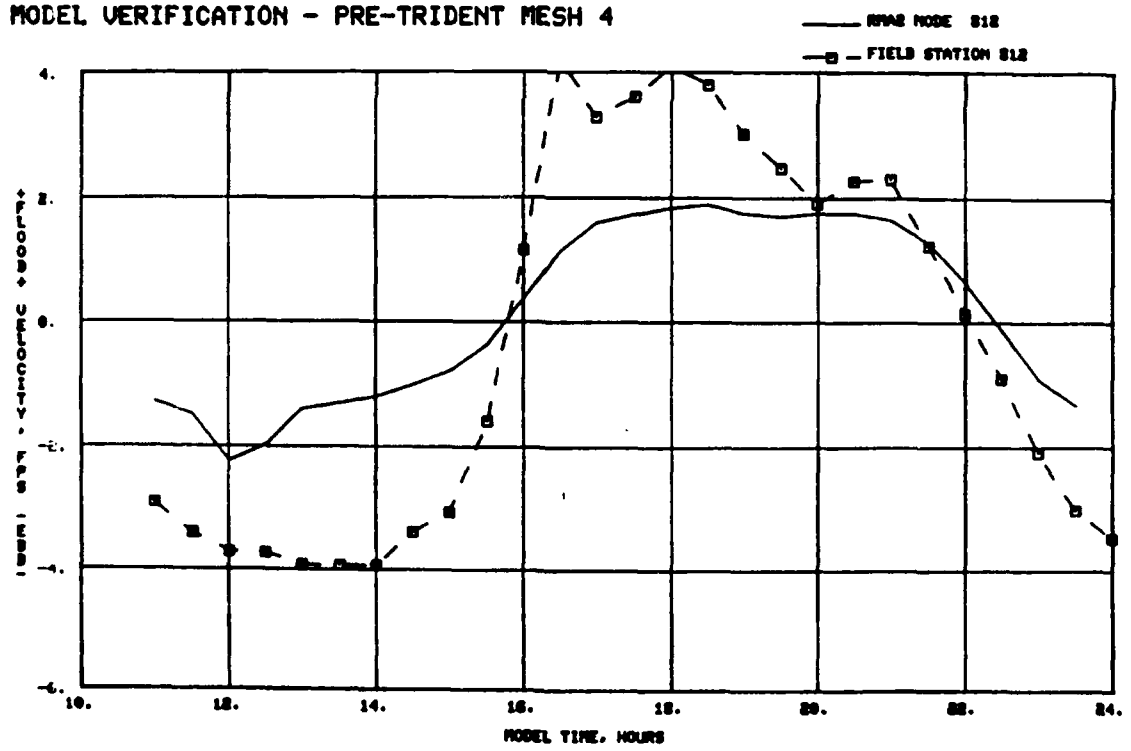

b. Station 812

Plate F14. Physical and numerical model velocities for stations 1066 and 812

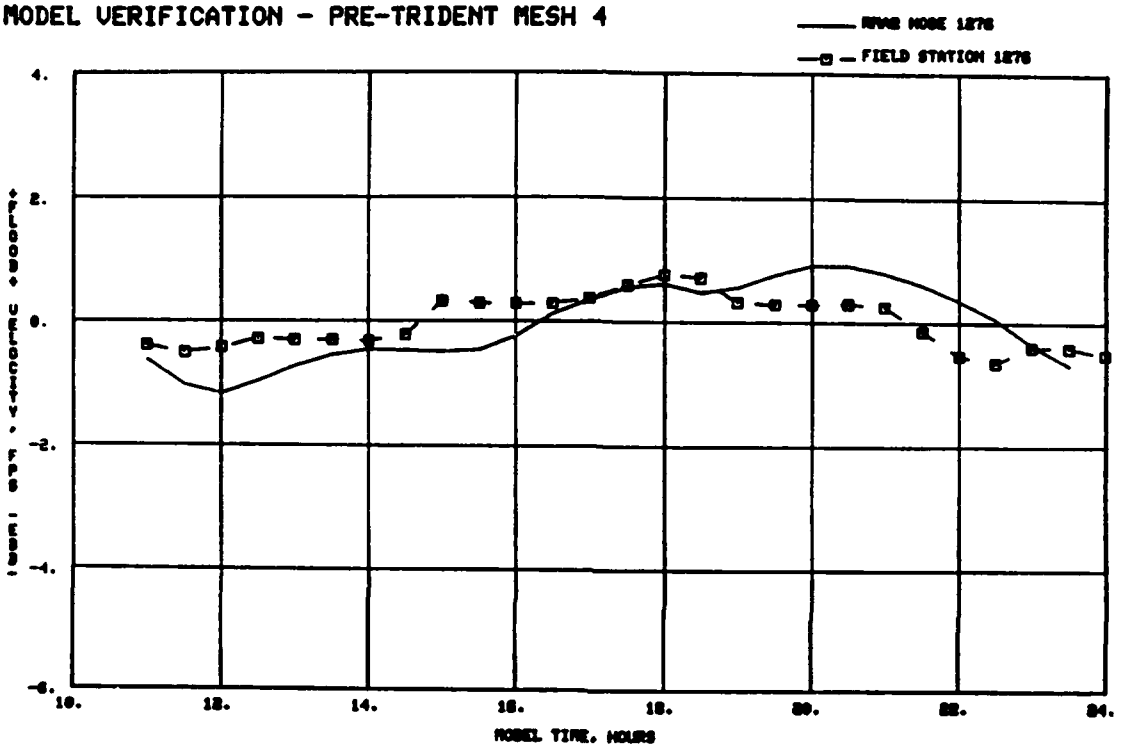

Plate F15. Physical and numerical model velocities for station 1276